2-24-2020 11:00 AM

Synchrophasor Based Islanding & Open phase fault Protection in Distribution Systems

Mansour Jalali, *The University of Western Ontario*

Supervisor: Tarlochan Sidhu, *The University of Western Ontario*

A thesis submitted in partial fulfillment of the requirements for the Doctor of Philosophy degree in Electrical and Computer Engineering

Abstract

With the rapid growth of renewable energy resources, energy efficiency initiatives, electric vehicles, energy storage, etc., distribution systems are becoming more complex such that conventional protection, control, and measurement infrastructure – typically concentrated at the main substation, with little to no access to information along the feeder – cannot maintain the reliability of the system without some sort of additional protection, control and measurement functionalities. As an example, a dedicated communication channel for carrying the transfer trip signal from the substation to the Point of Common Coupling (PCC) to prevent islanding operation of alternative resources, has been a requirement for many utilities. In the transformation of the distribution system from a simple radial system to a bidirectional energy flow network, integration of many intelligent devices and applications will also be required. Thus, this situation calls for investment in communication infrastructure, and augmentation of protection, control, and measurement functionalities.

The value of power system communication technologies such as synchrophasor measurement technology – which includes the Phasor Measurement Unit (measuring and providing voltage and current phasors in the real time via communication), communication infrastructure, and Phasor Data Concentrator (PDC) – is being recognized through large-scale deployments around the world. However, these implementations are predominantly limited to some monitoring-type applications and are being realized primarily in transmission systems and bulk power systems (≥100 kV), where performance requirements are much more stringent compared to distribution systems.

So contrary to transmission systems, the current status of synchrophasor measurement technology can be utilized to its full extent in distribution systems, as shown in current research for anti-islanding and open-phase faults in the distribution feeder protection application, where the number of PMUs and performance required is somewhat lower than the bulk of power energy. Thus, the opportunity to invest in the implementation of synchronized measurement technology in distribution system is timely as it can be coordinated with other investments in feeder modernization, distributed generation (DG)

integration, and infrastructure enhancements that are underway, including “smart grid” initiatives.

In the first use case of this research, the behavior of the major DG types during islanding is studied through accurate transient modeling of utility type distribution systems using PSCAD-EMTDC and MATLAB. The study proposes augmentation of PMU-based solutions to the current passive islanding protection elements, such as voltage and frequency, and improving the non-detection zone of the passive elements by adapting their settings based on normal loading conditions at closest known instant prior to the fault or islanding occurrence. The solution proposes a system architecture that requires one PMU at each PCC bus and in the main substation. The communication aspect is based on the IEC 6850-90-5 report, where the PMU can subscribe directly to the data stream of the remote PMUs such that the need for PDCs in this application is eliminated, yielding better performance.

In the second use case, an open-phase fault – a major concern for distribution utilities from safety of public and equipment perspective – has been studied. Clearing the open-phase fault without identifying the type of fault could result in an attempt by the recloser to reenergize the downed wire; conversely, an undetected open-phase fault could initiate ferro-resonance, thereby stressing equipment and increasing the risk to public safety, both urban and rural. This work discusses comprehensive analysis of symmetrical components of various types of open-phase faults in the distribution feeder with the presence of distributed generators (DGs) and proposes the use of phasor measurement data located at substation and PCC to identify the open-phase fault. The proposed algorithm relies on the rate of change of the various current and voltage sequence components. In the study conducted, the utility type feeder and substation are modeled in PSCAD-EMTDC, and different types of open-phase fault and shunt faults are studied to verify the dependability and security of proposed algorithm.

Keywords

Synchrophasor, PMU, PDC, DG, IEC 61850-90-5, Islanding, Open-phase fault, Breaking conductor.

Summary For Lay Audience

Electricity is a form of energy, and in simple terms it is defined as the flow of electric charges and charge is a property of matter like mass, volume, etc. We produce electricity, from the conversion of other sources of energy, like coal, natural gas, oil, nuclear power, and other natural sources such as Wind and Solar. The system which produces, transfers, and distributes electricity in the cities and rural area is called an electrical grid. The sections of the grid distribute electricity to the consumers is called a distribution system. Distribution systems, historically, only distributed electricity and did not participate in the production. However, with the global warming effect and desire of the society to use a clean carbon free electricity many renewable sources including solar; wind, hydro power, and geothermal are integrated into the distribution systems. Thus, distribution systems now and in the future will have to integrate more resources which add significant complexity and challenges for utilities and asset managers in terms of protection of electrical assets, safety, and quality of power delivered to the consumers. The focus of this work has been on protection of the distribution systems for two specific incidents open phase or broken conductor and islanding operation. These two undesirable situations can cause serious risks and damages to the distribution system. This research proposes new methodology to deal with these types of problems and encourages utilities and regulators to invest in the grid's communication technology infrastructure more real time system data to become readily available. This information can then be utilized for diagnostics and detection of failures and thereby, lower the risk of safety to the public to the system's equipment.

I dedicate this work to my parents, my kids, Zhina and Alan

Acknowledgments

I would like to express my sincere gratitude and appreciation to my supervisor Dr. Tarlochan Singh Sidhu for his invaluable guidance and help throughout the course of this research. His continuous support has helped me in successfully completing my doctoral degree.

I thank my examiners Dr. Bala Venkatesh and Dr. Jing Jiang for their valuable inputs on my work. I thank Dr. Mohammad Dadash-Zadeh for his inputs during the publication of this research.

I thank my parents and my children for their love and affection. Their selfless love and sacrifices have been the eternal fuel for my ambition to achieve greater heights in my academic career. I am thankful to my brothers, sisters, and cousins for their love and affection; it keeps me motivated to pursue higher aspirations in life.

I extend my special thanks to all my other friends and relatives for their moral support.
I am thankful to all the staff members of the electronics shop and administrative staff of the Department of Electrical and Computer Engineering for their support at various stages of my degree programs.

I gratefully acknowledge the financial support provided by Kinectrics Inc. (ex-Ontario Hydro research department). I thank my colleague- Dr. Nafeesa Mehboob, for providing me with an editorial review of some of the chapters.

Thank you.

Table of Contents

List of Tables

List of Figures

List of Appendices

List of Abbreviations

ACSI	Abstract Communication Service Interface
ARPA-A	Advanced Research Projects Agency-Energy
BTMG	Behind the Meter Generation
DER	Distributed Energy Resources
DFIG	Doubly Feed Induction Generator
DFT	Discrete Fourier Transform
DG	Distributed Generation
DoD	Department of Defense (US)
EMT	Electro Magnetic Transient
EMTP	Electro Magnetic Transient Program
EPS	Electrical Power System
ES	Energy Storage
FFT	Fast Fourier Transform
GOOSE	General Object-Oriented Substation Event
GPS	Global Positioning System
GSE	General Substation Event
IEC	International Electrotechnical Commission
IED	Intelligent Electronic Device

IEEE	Institute of Electrical and Electronics Engineers
IRIG-B	Inter Range Instrumentation Group Time Code B
LAN	Local Area Network
LVRT	Low Voltage Ride Through
MG	Microgrid
MPPT	Maximum Power Point Tracking
NASPI	N North American Synchro-Phasor Initiative
NDZ	Non-Detection Zone
NERC	North American Electric Reliability Corporation
NSPP	Negative Sequence Pilot Protection
NTP	Network Time Protocol
OPD	Open Phase Detection
OSI	The Open Systems Interconnection (model)
PCC	Point of Common Coupling
PDC	Phasor Data Concentrator
PLL	Phase Locked Loop
PMU	Phasor Measurement Unit
PPS	Pulse Per Second
PSRC	Power System Relaying Committee (IEEE)

PTP	Precision Time Protocol
PU	Per Unit
SCADA	Supervisory Control and Data Acquisition
SOC	Second-Of-Century
SPS	Standard Positioning Service
SV	Sampled Value
TC57	Technical Committee 57 (IEC)
THD	Total Harmonic Distortion
UG	Under Ground
UTC	Universal Time Clock
VCO	Voltage Controlled Oscillator
VSC	Voltage Source Converter
WAMS	Wide-Area Measurement System
WAN	Wide Area Network).
WT	Wind Turbine

Chapter 1

1 Introduction

In this chapter the needs for the modernization of power systems are briefly reviewed. Specific challenges in the forefront of this modernization in distribution systems is discussed. The research, objective, motivation and structure of this work is presented.

1.1 Power System and Technological Modernization

Electrical power system networks are one of the largest man-made systems in the world. A typical system represents a sizable capital investment that consists of generators, power transformers, substations, overhead lines, along with underground cable, control, measuring, and protection infrastructure. The power system asset oversees the production, transmission, and distribution of the electricity to consumers as per their demand. The electricity must be produced and delivered reliably within the applicable constraints of security. A typical electrical network is shown in Figure 1.1 where generation, transmission, and distribution are well segregated. The past couple of decades have seen a rapid advancement in policies, technology, and standards focused on modernizing the power system network. The most important advancement, however, may well be how the power industry's is thinking has evolved. Today holistic views of the desired goal of grid modernization and how to achieve them are taking a hold. The need to modernize the power grid arises from multiple factors including economic, political, environmental and technical such as aging infrastructure, integration of multiple DER (Distributed Energy Resources), other new technologies, security concern and more influence of the end consumer to the local legislation. In the past power industry investment has favorited the generation and transmission sectors because of their criticality and large amounts of power being transferred. Therefore, it can be observed among many utilities that the generation and transmission systems respectively are much better instrumented for monitoring and control compared to the distribution systems however, the smart grid concept and grid modernization includes the entire grid including distribution system. Utilities and policy makers are recognizing that the distribution system is less prepared for this task and therefore, now is largely focusing on modernization of distribution systems [1].

Traditionally, distribution systems were a simple interface between the end users and rest of the grid with one-way power flow outward system architecture.

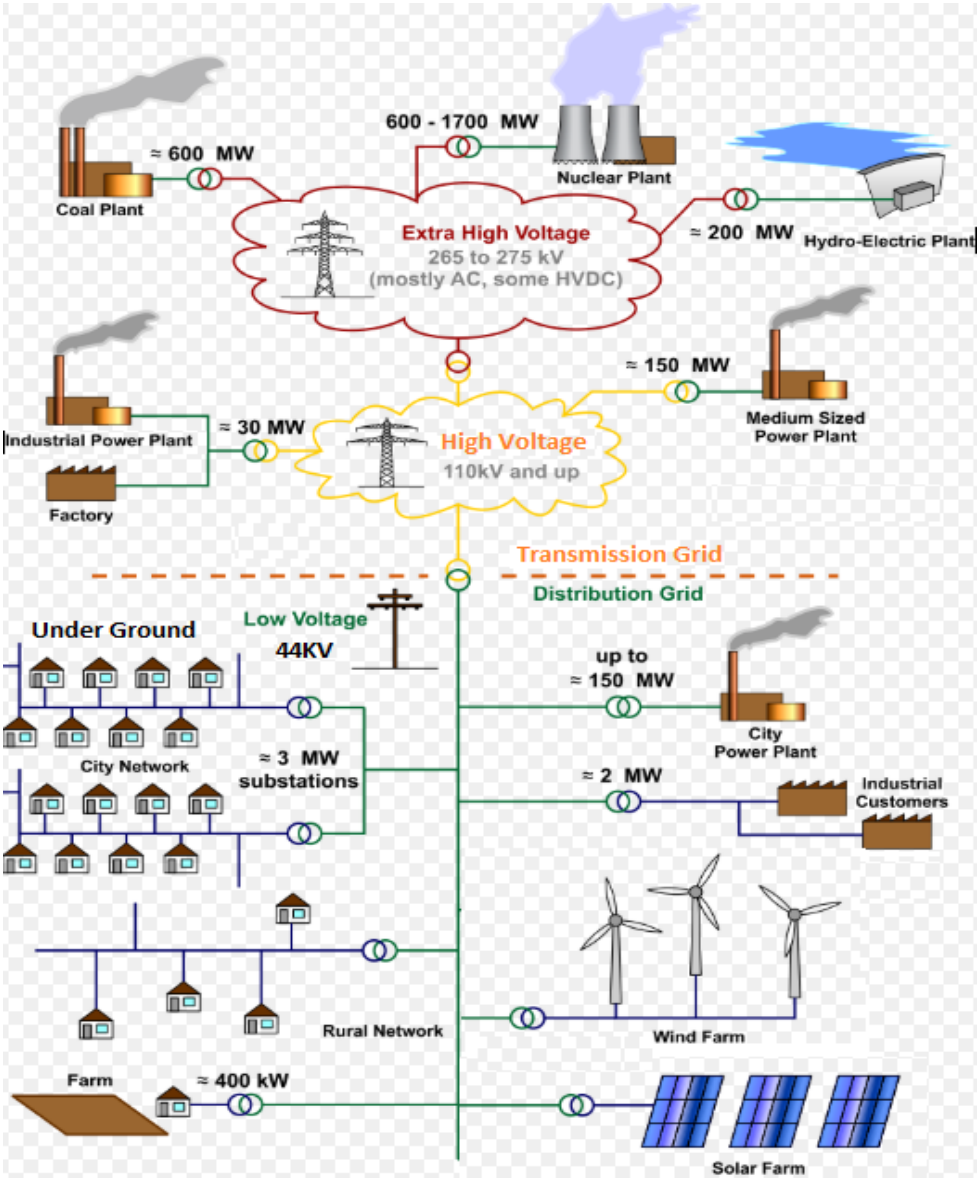

Figure 1.1. Typical Structure of Electrical Network

Distribution feeders were not interconnected and despite this simplistic blueprint yet today this system is facing the following challenges:

1) Need to develop a communication infrastructure
2) Need for the integration of many DERs
3) Need for greater visibility and monitoring of the feeders

4) Need for more automation processes
5) Need for reliable protection and control
6) Need for the renovation of aging infrastructure

Many research studies in the area of communication technology, integration, and application should be completed in order to prepare for the transformation of distribution systems successfully. In fact, this work is motivated to contribute to the required study for the advancement of distribution systems and the integration of communication technology in distribution system protection applications using synchrophasor measurement data.

1.2 Synchrophasor Measurement Technology

Among the many advancements in communication technology used in power systems, synchrophasor measurement technology specifically can be noted for being at the forefront of focus within industries where technology and new standards and applications came together to respond to the needs of those industries. Since the North American blackout of August 2003, phasor measurement technology development has been in high demand by utilities and the US government. The US government supported the North American Synchro-Phasor Initiative (NASPI) that was established to coordinate the research effort in this area in order to improve power system reliability and visibility throughout the grid by fostering the greater use and capability of synchrophasor technology. The synchrophasor measurement uses digital processing of current and voltage waveforms, synchronized to a universal time source GPS (Global Positioning System), to record system conditions at high speeds and provide real-time situational awareness of the electrical grid as shown in Figure 1.2. PMUs (Phasor Measurement Unit) that are installed in the application interested nodes works as a sensor to measure and capture data which can then be reported in real time by as many as 60 measurements per second, which is typically 100 times faster than SCADA (Supervisory Control and Data Acquisition). This real-time monitoring can detect and record events that SCADA misses, enabling much better visibility into the grid conditions for control as well as protection purposes.

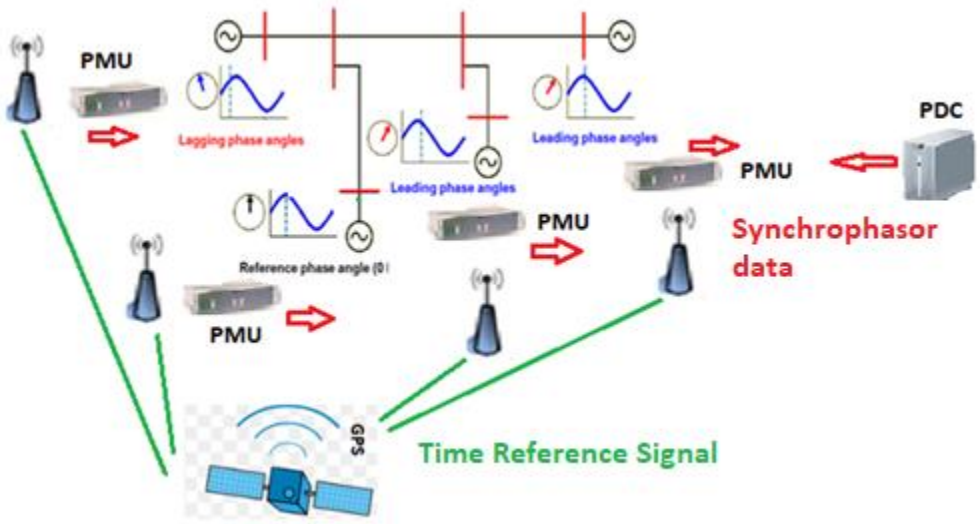

Figure 1.2. Conceptual Synchrophasor Measurement System Architecture

With the publication of various sections of IEC61850 standard starting from 2011 and onward the specification of utilities type protection applications based on communication technology have been formalized and the journey of transformation of the conventional application and prospective of new solutions have been the focus of many researchers and application specialists around the globe. Furthermore, the integration of synchrophasor data to substation automation domain and possibility of PMU using fast peer-to-peer communication services to transfer the data provides more possibility to utilize the PMU data in protection and time critical applications [2]. Background and the state of the art regarding the phasor measurement technology is provided in chapter 3 of this work.

1.3 Phasor Measurement in Distribution System

Traditionally, PMU data is used in transmission applications and it must be noted that the measurable results have been published by NASPI in implementing this technology in transmission grid [3]. As highlighted earlier in this chapter with the shift of focus of power industry and utilities to the concept of smart and modern distribution system the use of

synchrophasor data in this sector have been studied and investigated. Distribution systems are installed in a much smaller geographical area compared to the transmission systems thus, smaller angle differences between the voltage phasors measured by PMUs and much rapid system impedance changes could be expected [4]. In this regard the U.S. Department of Energy's Advanced Research Project Agency funded a US$4 million project to build one of the most precise synchrophasor instruments ever made, with 100 times the resolution of traditional transmission-type PMU's. The μPMU is ideal for research projects that need ultra-precise synchrophasor measurements for investigating stability and impedance questions on distribution grids and microgrids. The current work however proposes the use of synchrophasor data in protection scheme, the open phase fault detection and islanding detection. Further information about background of synchrophasor technology and accuracy required for this work is provided in chapter 3, 4 and 5 of this work

1.4 Protection Philosophy

Some of the constant challenges that electrical networks face are component failure, operation error, and extreme weather conditions such as lightning, wind, and storms. These events directly or indirectly can cause an interruption of the production, transmission, or delivery of electricity in part or entirely. A failure often causes an abnormal operational condition, such as very high short circuit current, extreme high voltage, or abnormal frequency. The impact of these events goes beyond the failed components and can damage other healthy equipment within the network while also posing a safety risk to the personal and public. Therefore, in order to protect the equipment, utility personnel, the general public, and to safeguard the capital invested in the electrical network, utilities deploy protection relays. These devices work to identify the abnormal condition, faulty equipment, and remove it from service as quickly as possible while the balance of the network remains in service as much as possible. Protection relays conventionally rely on local measurement, however, with the significant advancement that has occurred in communication technology over the past decade, they are starting to receive information from remote devices via communication. Thus, communication technology became an essential part of protection functionality. Utilizing measurement data from a synchrophasor in real time for a

protection functionality has started. This is a journey, which will transform the landscape and allow for protection devices to respond to more complex abnormal situations and shift their focus from traditionally protecting network components alone to protecting the network status and operation.

The following properties are defining the different aspects of the protection system performance.

1) **Selectivity:** The concept of protection selectivity refers to the capability of the protection scheme to detect faults on a power system and initiate the opening of switchgear in order to isolate only the faulty part of the system. Good selectivity will maximize service continuity and minimize system outages. The protection must thus be discriminative.
2) **Sensitivity:** Sensitivity refers to the minimum operating level (current, voltage, power, etc.) of protective devices. A relay designed to operate sensitively will be able to detect a fault with a very low value. For example, a sensitive ground fault relay can detect a very small ground fault current.
3) **Reliability (Security and Dependability):** Security and dependability must be evaluated when assessing the reliability of a protection scheme. Dependability refers to the ability of a protection scheme to operate and isolate a fault condition when it is required. Security refers to the ability of the protection system not to operate during any tolerable conditions such as overloading, switching actions, recoverable power swings and faults on other parts of the power system, etc. Failure to operate (loss of dependability) can be extremely damaging and disruptive. False tripping or over-tripping (loss of security) can result in multiple contingencies, unnecessarily disconnecting the healthy power apparatus out of service, and possibly cascading into a widespread blackout. The protection scheme should offer secure and sensitive operation. It should be secure from false operation, not causing de-energization of circuits due to load unbalances, inrush currents, cold load pickup, harmonics, and other transient or steady-state conditions not normally harmful to system components. The equipment in the protection scheme should exhibit enough sensitivity to be able to detect all recognized fault conditions.
4) **Speed:** The function of protection is to isolate faults from the rest of the power system in a very short time. The time in which the fault should be isolated it is an important property of the protection system that is considered for power system stability, relay coordination, and minimization of the damage.

More faults occur on the distribution system than in either the transmission system or in the generating facilities. Distribution systems are widespread and have a relatively high degree of exposure to the environment. Improvements in distribution circuit performance can be achieved by design and by minimizing the number and extent of faults with overcurrent protection systems. Knowledge of the characteristics, i.e., magnitude, duration, and waveform, of distribution faults is essential when applying protection. Fault current calculation methods are fundamental tools for the protection designer. Protection applications require computation of three-phase, line-to-ground, and line-to-line short-circuit currents that are possible within the area of operation of the device.

1.5 Thesis Motivation

This research has focused on the utilization of synchrophasor measurement data in distribution system protection and control application. The research has been developed around two use cases, namely, islanding and open-phase faults. The motivation behind these selections is briefly described here:

a) Why Synchrophasor? Since the blackout of August 2003 in North America, there has been much focus on synchrophasor measurement application by utilities, power system regulators, manufacturers, and researchers. IEEE synchrophasor standards C37.118-1 and C37.118-2 are being updated by specifying the communication requirements and dynamic performance of the synchrophasor measurement unit (PMU). IEC 61850 is a standard that facilitates the implementation of communication technology in protection, control, and measurement in power system application, and integrates the synchrophasor data stream into its data model and communication services. This integration provides the possibility to use the functional and communication infrastructure of substation automation systems to support and reduce the cost of PMU based applications, especially in a smaller area such as a distribution system.

b) The rapid growth of alternative sources of energy in distribution systems is changing the historical role of distribution system as being only a distributor of energy to also being the provider of local generation and manager of small independent grids. This new reality requires modernization of the distribution

system, which most likely will be a very capital-intensive transformation because of its massive size, simplicity of its current core design, and lack of communication infrastructure. With the integration of more alternative resources, many real-time electrical measurements along the feeder will be required for the system to be up to speed for reliable operation.

Installation of synchrophasor units in the distribution system can serve many new and old challenges that this system is encountering and requires much more research in this area.

c) In distribution systems, many overhead lines are built right along roads, streets, and alleys. Because of equipment aging, and more recently extreme weather condition, and car accidents involving the distribution overhead pole, the phase conductor(s) can break and hit the ground creating a hazardous situation for the public. The high impedance ground fault created by this event cannot be detected by any ground fault protection element selectively and hence, the protection in the substation may operate well after its time delay. The uncleared open phase conductor, if the created ground fault is insignificant, can evolve into ferro-resonance which is another added risk to the public and equipment. For many years, utilities and protection manufacturers have worked to develop methods for tripping these hazardous ground faults as quickly as possible. The method proposed in this work describes a new way to identify the open phase conductor selectively with and without DG using the synchrophasor measurement data.

Two use cases in this research are being investigated in a distribution system and with use of synchrophasor data: Islanding detection use case and open phase fault use case.

1.6 Research Objectives

The objective of this research is to investigate the application of synchrophasor measurement data in distribution systems to address some of the challenges related to distribution system protection and control. The research work is divided into three stages:

Stage I – Islanding Detection Scheme: The first objective of the research is to provide a synchrophasor-based islanding detection scheme that can improve the current anti-islanding protection scheme practiced by utilities. In this stage, an Electro-Magnetics Transient (EMT)-based model has been developed for a utility type system, and major types of distribution generators have been studied as individual and aggregated machines using PSCAD/EMTDC, supported through an extensive MATLAB simulation study to formulate and validate the proposed solution.

Stage II – Open-phase fault detection: The scope was to develop a solution that can selectively identify an open-phase and falling conductor fault in a primary distribution system based on the minimum data required from different locations. Customized models in PSCAD/EMTDC have been developed to study this fault and formulate, examine, and validate the proposed solution.

1.7 Methodology

With these motivations, exhaustive research work was conducted to investigate the application of synchrophasor measurement in distribution systems, including islanding detection and open-phase faults. A few alternative models based on utility field data were used to develop a reliable EMT-based model in PSCAD-EMTDC to validate the solution. MATLAB was used for mathematical calculations, result validation or circuit analysis - e.g., load flow for EMT model.

1.8 Thesis Outline

In the first chapter, an introduction to the research objectives, the thesis outline is presented along with the importance and motivation of research in the area of distribution systems, phasor measurement systems, and the need for more research work in the specific application that has been targeted in this work.

In Chapter 2, fundamentals of the distribution feeder related to this work are studied. The integration of distributed energy resources (DER), including the history of different types of distributed generation (DG), is reviewed and discussed. The modeling aspect of the DGs is studied. The history of IEEE 1547 in DG operation requirement and unintentional islanding is reviewed.

In Chapter 3, fundamentals of synchrophasor phasor measurement, history, phasor and frequency estimation, standard application, system architecture, performance, and state-of-the-art technology is studied and reviewed. The use of alternative communication standard IEC61850 and its advantage to the conventional C37.118 communication is proposed and reviewed. The cost-effective system architecture adequate for the studied applications is proposed.

In Chapter 4, background of unintentional islanding operation in distribution feeder with integrated DG is reviewed and major islanding detection is categorically reviewed. A new proposed solution is formulated. EMT modeling of utility-based distribution system is described in PSCAD/EMTDC. A new solution with mathematical formulation is proposed. EMT modeling in PSCAD/EMTDC is presented. The number of cases studied, and the simulation results obtained, are presented and discussed in this chapter.

In Chapter 5, the background of open-phase faults, single-phase, double-phase with and without ground in power system distribution feeder is studied. Existing detection methods are reviewed. The new solution with the mathematical formulation is proposed, and EMT modeling in PSCAD/EMTDC is presented. The number of cases studied, and the simulation results obtained, are also discussed in this chapter.

In Chapter 6, the conclusion and summary are provided, and further research topics are suggested. The reference document list is provided, and appendices contain additional model parameterization to enable reproduction of this work and further simulation.

1.9 Summary

A brief introduction to the research and its importance to the area of power system protection is provided in this chapter. The challenges and need to modernize the power

system and distribution systems is reviewed. The application of phasor measurement technology and the driver behind the need for the implementation of this technology in transmission and distribution is reviewed and discussed. The fundamental characteristics of distribution power system protection are described. The research objectives and a detailed outline of the organization of the thesis is presented. The research motivation to focus on phasor measurement applications in distribution systems is discussed. The specific use cases that have been studied in this work is also introduced. And the fundamentals of distribution feeder structure, plus an introduction to the Distributed Energy Resources (DER) and thire EMTP modeling, will be discussed in the next chapter.

Chapter 2

2 Introduction to Distribution Systems

Historically, electrical distribution networks have been the consumer interfaces with the power plants and transmission systems where electricity, which is normally produced far away from the center of load, is being transferred, delivered, and consumed. Although interruption in the distribution services or failure in the distribution equipment directly affects the end user, and the reliability and quality of the service, compared to the other sector of energy distribution system it has been less technologically advanced. However, in recent years with the rapid growth of alternative energy resources and the necessity for the integration of many new devices such as Distributed Generations (DG), microgrids, electric vehicles, etc., the distribution system is transforming to be at the forefront of the renovation of electrical grids. It is very important to note that because of the massive infrastructure of distribution systems, it is very capital and labor intensive [5], and therefore, simplification and cost awareness have to be considered as chief characteristics that will be demanded from researchers and solution providers. In this chapter, the background of distribution system, with focus on the North American grid and some of the challenges it is facing relevant to the current work, is presented.

2.1 Primary Feeder Structure

From a structural point of view, the distribution system can be considered a connection of substation, primary, and secondary feeders. The topology and configuration of the system can vary depending on the location where the distribution system is serving its customer; as an example, downtown core, urban, rural, industrial, or a commercial area. The major voltage classes used in the primary network are typically in the following range 4-5 KV; 7-8 KV;15-27.6 KV; and 35-44 KV. The most prevalent voltages in Ontario are 4.16, 13.8, 27.6 and 44 KV. Figure 2.1 shows typical voltage ranges for a vertically integrated electrical power system. The secondary network voltage range at which electricity is delivered to the meter is in the range of 120-600 V.

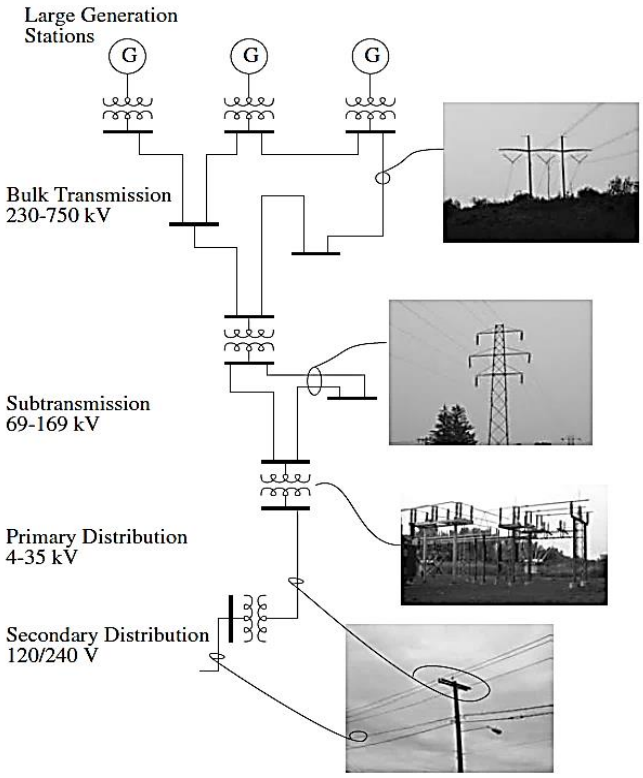

Figure 2.1. Conventional Vertical Power Grid Infrastructure **[6]**

The most common primary feeder configuration used by north American utilities is the four-wire three-phase power multi-grounded neutral system. There are other types of feeder configurations as well but generally, radial characteristics are very common between primaries and secondaries. A distribution primary feeder can come in a variety of shapes and forms, depending on the geometry of the area that a feeder is covering. For example, the shape of the area and the layout of the streets will heavily impact the number and size of the branches and overall form of the feeder. Figure 2.2 shows an arbitrary overhead line primary feeder with a number of single-phase and three-phase laterals taped off from the main circuit. As shown in this circuit here, the radial distribution feeder is normally provided with the possibility to be connected to one or more adjacent feeders through the open tie. This will improve the reliability of the circuit to be able to supply whole or part of feeder load by closing the tie with the adjacent feeders. The distribution feeder can be subjected to accommodate an integration with the DER(s) at one or more Point of Common Coupling (PCC) which will be determined by utilities along the main circuits. The

integration of DGs imposes a new set of functionalities that should be provided by both the utility and DG owner to maintain the safe operation of the feeder with the new generation(s).

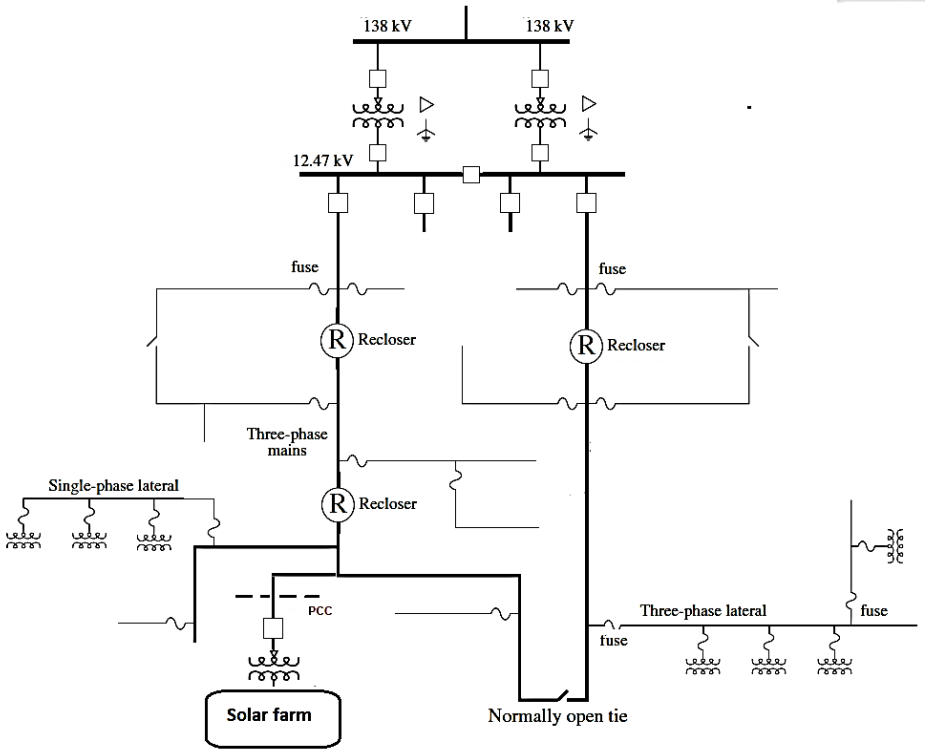

Figure 2.2. Typical Two Primary Radial Feeders with Open Loop

2.2 Under Ground Network

Often, in locations, such as urban area or downtown cores, underground networks are replacing the overhead lines. Under Ground (UG) feeders normally daisy-chain all the distribution transformers that are feeding secondary networks; these transformers are known as a network transformer that are intended to supply the secondary network. The secondary of underground UG network in the urban areas are interconnected. The transformer, primary switch, and, network protector is in the underground vault across the streets. Figure 2.3 illustrates the simplified one-line diagram of three UG feeders with their

connection to the secondary grid. The network protector provides the following functionality:

a. It prevents back feeding of the primary circuit by secondary grid during a primary fault by tripping the circuit. Network protector is equipped with reverse power protection element.
b. It trips the circuit and disconnects from the secondary grid when primary feeder is deenergized.
c. It closes the circuit automatically when the primary feeder is energized.

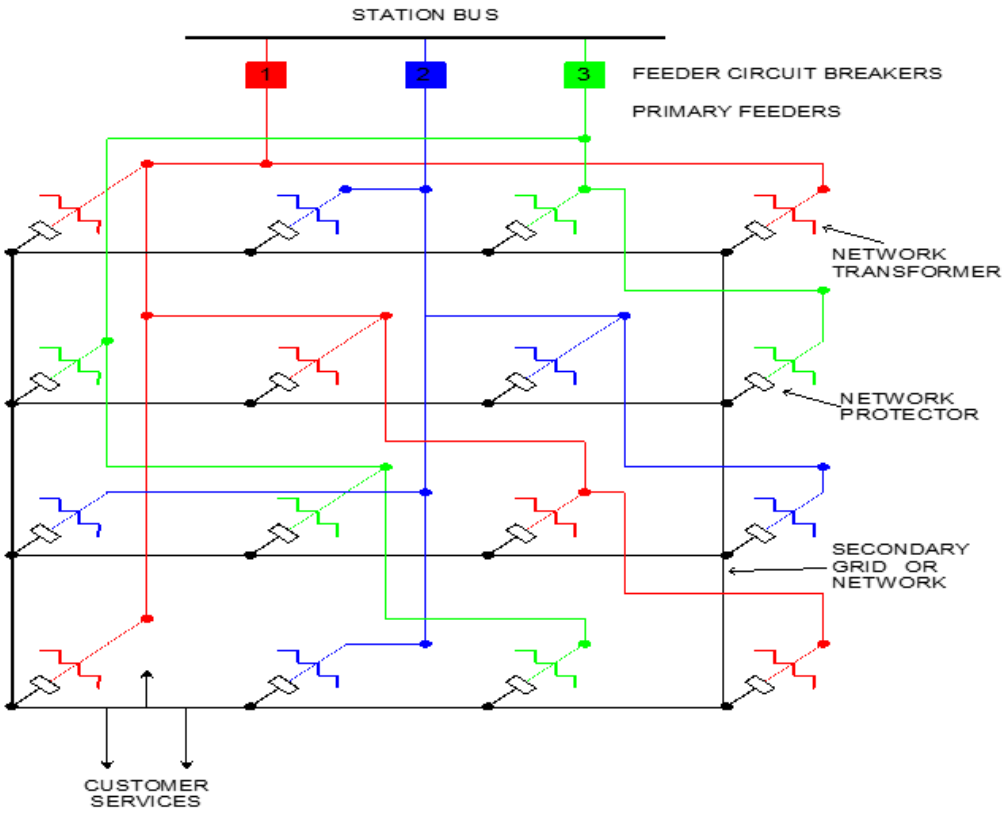

Figure 2.3. Underground Distribution Network (Courtesy of Toronto Hydro)

The schematic of a network vault with two network transformers is presented in Figure 2.4. The primary switch is used to connect the transformer to the primary feeder as well as provides the ground at the location of the vault for the primary circuit. The meters are also located at the secondary of the network transformer.

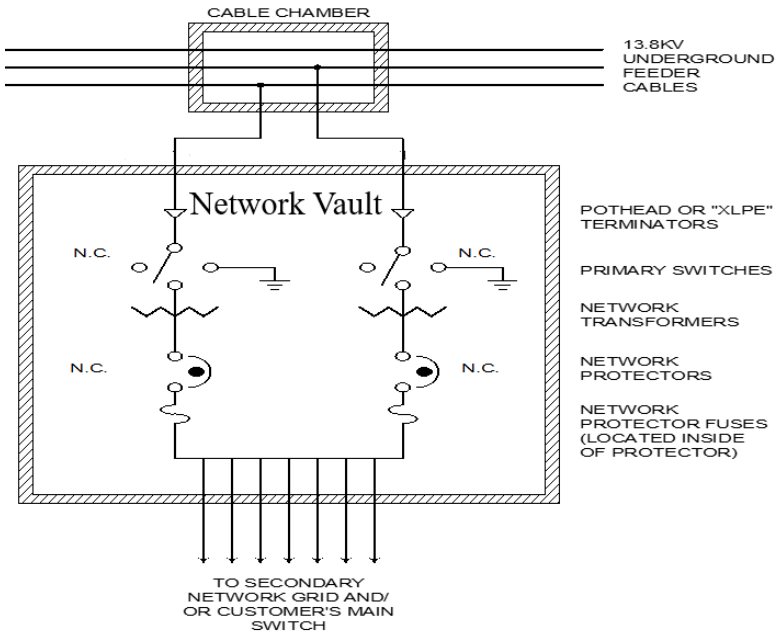

Figure 2.4. Network Vault One-line Diagram (Courtesy of Toronto Hydro)

2.3 Feeder Protection in Distribution Network

The objective of protection for generation, transmission, and distribution systems are similar. The main requirement of reliable system protection is that all points in the system fall within one or more protected zones, so that there are no blind spots in the overall protected system as shown in Figure 2.5 In distribution system several natural zones that require a dedicated protection can be identified.

a. Transformers,
b. Buses,
c. Lines/feeders (transmission, subtransmission, distribution),
d. Utilization equipment (motors, static loads, etc.),
e. Capacitor and/or reactor banks
f. DER

Protection with a boundary defined by measuring devices such as current transformers is referred to as closed-zone Protection. Differential relaying is a typical example of closed-

zone protection that can detect a fault within the protected zone with high selectivity and security. Protective relays with the protected zone defined by their “reach” are referred to as an open zone. The open zone is not bonded by the measuring devices and operates when the measured quantity exceeds the pre-set threshold. Correct operation of open-zone protection heavily relies on the protective element setting. Performance of an open-zone protection scheme is usually a trade-off between security and dependability.

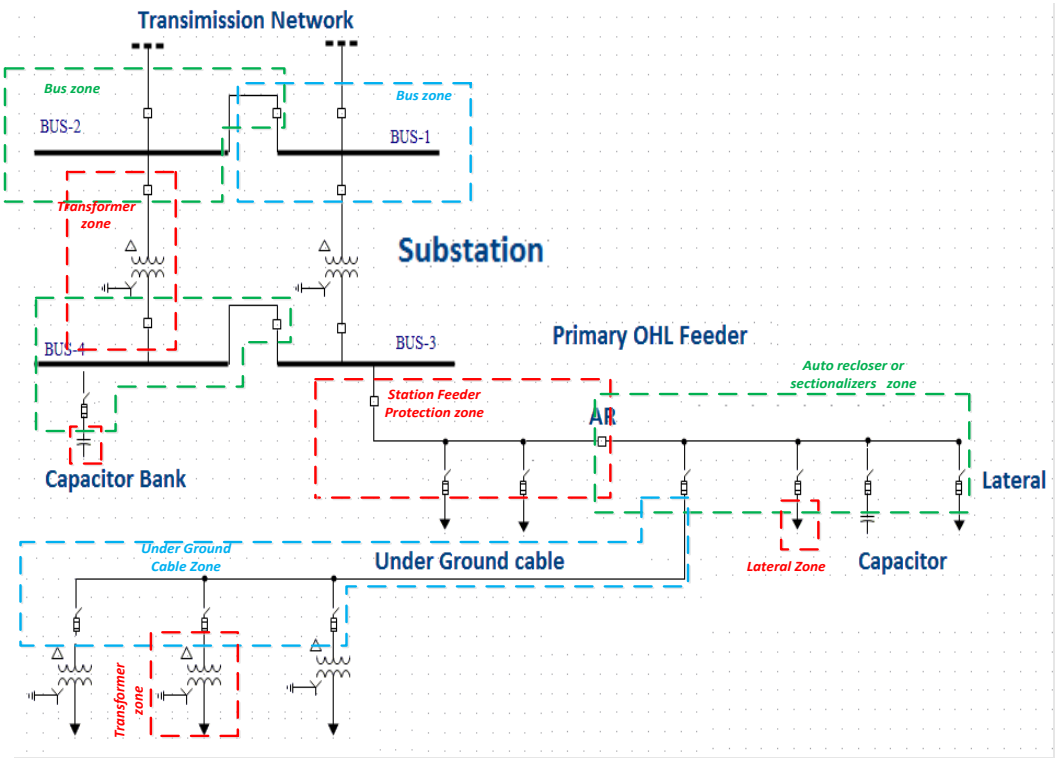

Figure 2.5. Typical Protection Zone in Distribution Network

Reach in protection literatures refers to the locus of the most remote prospective fault locations for which a specific protective device is capable to detect and clear. All points electrically inside this frontier are considered to be within the zone of that protection device. Typical example of protective devices with the clear reach are Distance and over current relays. Distance relay can provide directional impedance measurement based on the current and voltage of the network at the relay location. The reach in this relay relatively stable and immune to the system condition. Overcurrent relay reach however, is a highly

variable and the ability of the relay to detect the fault within its reach will expand and contract with variations in fault types and system conditions.

Table 2-1 presents the result of IEEE Power System Relay committee (PSRC) survey for the practices on distribution system feeder protection. The results of the survey show by far the over current relay phase and ground are the main protection schemes implemented in distribution primary feeders.

Table 2-1. IEEE Survey Results for Protection Schemes in Distribution Systems [7]

Type of Protection	Number of utilities responded	Percentage implemented
Circuit recloser (79)	31	73%
Phase overcurrent (50,51)	42	100%
Ground overcurrent (50N,51N)	41	97%
Negative sequence over current (46)	4	5%
High impedance Detection device (Broken conductor)	2	0.05%
Distance (21)	4	5%
Directional over current (67, 67N)	1	0.02%

Figure 2.6 presents the most common protection schemes that have been used in distribution feeders across the North American grid. The circuit recloser (79) that is frequently used is another over current based protection that is capable to clear the fault in its downstream location and is utilized to isolate the transient fault and reenergize the circuit without the permanent outage. The circuit recloser can provide a very fast or a slow response to the fault. The number of closing attempts and fast or slow tripping can be programmed. It is common practice for utilities to use the circuit recloser in the fuse saving or fuse blown schemes which are intended to save or blown the fuse respectively during the transient faults. It can be noted that the high impedance ground fault protection which is used to detect the broken conductor when it comes in touch with the ground is used less

than 0.05 % among the utilities that responded to survey. The feeders with integrated DER are often equipped with protection transfer trip when the main is lost in order to prevent the DER to supply the feeder consumers when the feeder circuit breaker is open.

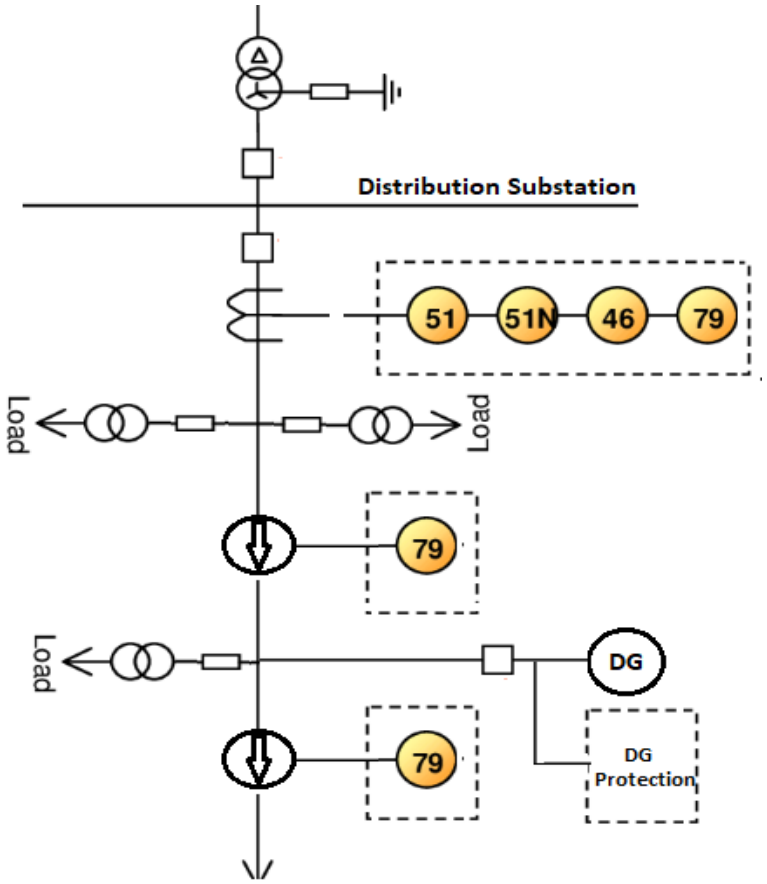

Figure 2.6. Typical Feeder Protection in Distribution Network

Figure 2.7 shows a typical interface protection requirement for the DER owner. The anti-islanding protection as shown here often is a point to point transfer trip (block 3) plus the frequency and voltage protection elements (27, 59, and 81) that are installed at the PCC. The anti- islanding protection can be further equipped with frequency rate of change (81R) and loss of synchronism or out of step (78) protection elements.

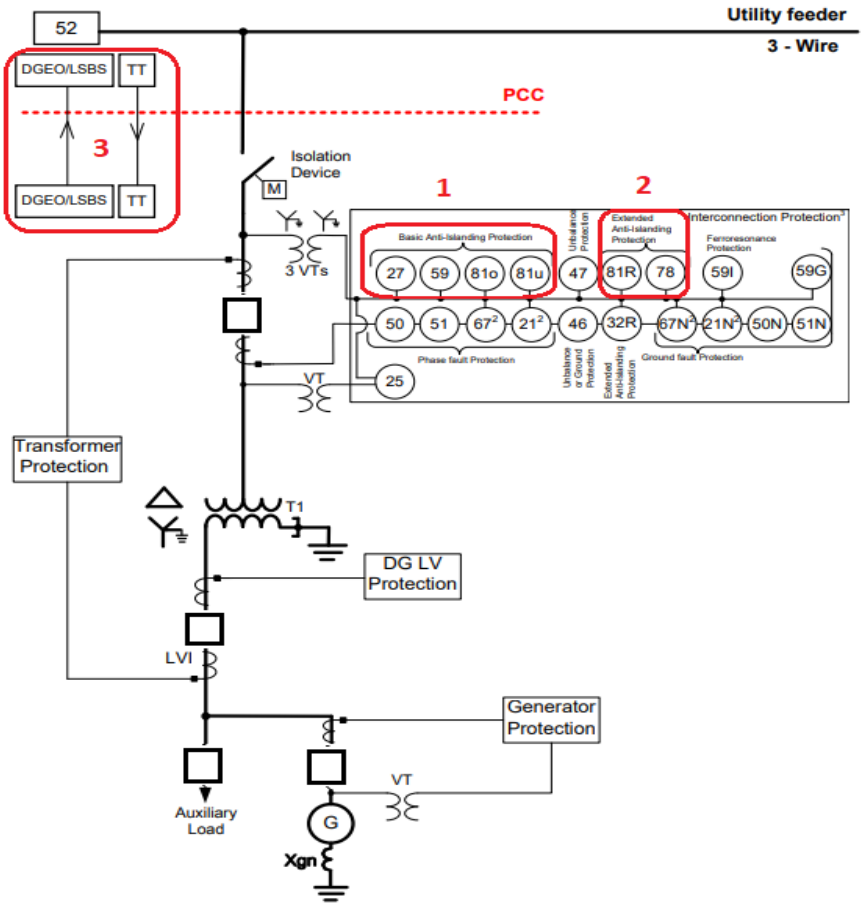

Figure 2.7. Utility Type Anti-Islanding Protection [8]

2.4 Conventional Distribution System Properties

Some of the important design characteristic of the existing primary distribution system that is a focus of this work and is common among different types of networks (overhead and underground) and feeder configurations can be summarized as follows:

a. The feeder is designed based on one-way load flow.
b. Measuring devices are mainly installed at the substation and often no sensors are available along the feeder.
c. For the main primary circuit, the main protection is mainly over current element(s) located at the substation, and alongside of the main circuit there may be other over current elements, such as recloser, especially for overhead type feeder, that provides sectionalized protection.

d. In the overhead circuit, the laterals tapped off from the main circuit through the fuses to protect laterals selectively, as shown in Figure 2.2.
e. The simplicity of the design is the main property of the existing system that ties to the fact that distribution system, because of its size, is a very capital-intensive business.
f. The anti- islanding protection that is shown in Figure 2.7 often is a point to point transfer trip.
g. Often, no dedicated protection for an open phase fault is implemented.

Considering the status quo and backbone of electrical distribution system as some of the properties summarized above, with the direction that has been taken by utilities and government for production of clean energy, distribution grids with minimum hardware preparation, is at the forefront of transformation to a new and smart gird. Integration of rapid growth of DER, new solutions such as Microgrids, and energy storage etc. to support reliability of system [9], [10] [11] from one side and advancement of communication technology has provided an opportunity to many researchers and solution providers to work towards addressing many of distribution system issue as a whole and facilitate the transformation [12]. In the current work, the use of phasor measurement unit is proposed to provide an advanced solution for addressing legacy issues, such as open phase fault, and looking into the detection of DER operation in an unintended islanding operation.

2.5 Distributed Energy Resources

Distributed Energy Resources (DERs) are small scale electricity-producing resources that contrary to the centralized conventional plant are distributed and directly connected to a local distribution system. NERC (North American Electric Reliability Corporation) considers any resource on the distribution system that produces electricity and is not otherwise included in the formal NERC definition of the Bulk Electric System (BES) as DER. BES from NERC's point of view includes all Transmission Elements operated at 100 kV or higher and Real Power and Reactive Power resources connected at 100 kV or higher [13].Therefore, DER includes the following [14]:

Distributed Generation (DG): Any single or multiple generating units at a single location owned and/or operated by the distribution utility a merchant entity. This includes Solar and Wind Turbine generation.

Behind the Meter Generation (BTMG): A generating unit or multiple generating units at a single location (regardless of ownership), of any nameplate size, on the customer's side of the retail meter that serve all or part of the customer's retail load with electric energy.

Energy Storage Facility (ES): An energy storage device or multiple devices at a single location (regardless of ownership), on either the utility side or the customer's side of the retail meter. This may include various technologies, including electric vehicle (EV) charging stations.

Microgrid (MG): An aggregation of multiple DER types behind the customer meter at a single point of interconnection that has the capability to island.

Cogeneration: Production of electricity from steam, heat, or other forms of energy produced as a byproduct of another process.

Figure 2.8 presents major DER categories that have been integrated into the distribution system so far. Among the different type of DERs, the renewable devices, such as wind and solar, are the most frequently installed and integrated into the distribution system. In the current study, wind and solar DGs are considered in the modeling wherever DER presence has been required.

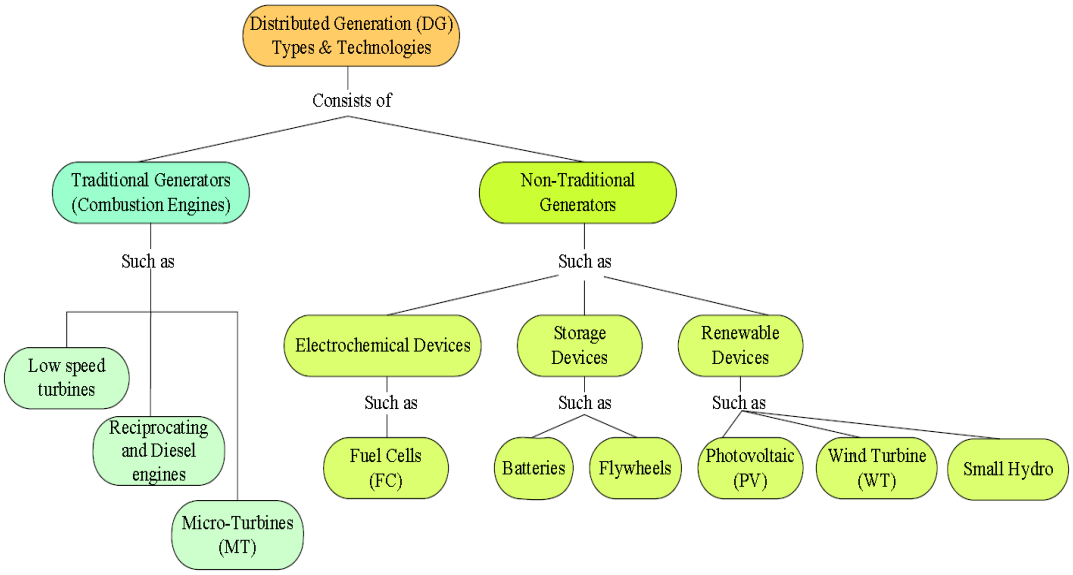

Figure 2.8. DER Category Conventional and Non-conventional

2.5.1 Renewable DER Frequency and Voltage Control

Renewable DGs even in the same category as an example Wind Turbines it may have different features as a result of their constructions. The prime mover is a mechanism that produces energy and determines if the DG is dispatchable, i.e., if the production of electricity can be scheduled as per the utility's needs. The grid interface; however, have a direct impact on how the voltage and reactive power could be controlled (for example, generator versus inverter). IEEE PES [15] recognizes a few types of wind turbine configurations, which will be reviewed briefly in this subsection and are differentiated based on their network interfaces.

2.5.2 Induction Machine Type 1 and 2

Figure 2.9 presents the block diagram of the wind turbine type 1. The grid interface in this type of system is an induction generator with squirrel cage rotor. During the operation, this machine will be connected directly to the grid. The speed of this machine is almost fixed and is around the frequency of the grid. In contrary to any synchronous machine, induction machine used in type 1 does not have an independent excitation system and therefore, is not capable of producing energy without presence of the grid. An independent source of voltage will be required to provide the reactive power needed to generate and maintain the

magnetizing field of this machine. This is also the reason why capacitor banks are often required to support the economical operation of this type of machine. From islanding operation perspective, type 1 machine cannot support the unintentional islanding and supply the load alone. The type 1 belongs to the early generation of wind turbine; the size of this machine is in the range of 10 to 100 KW, and lack of speed regulation makes this type of machine undesirable with today's available technology.

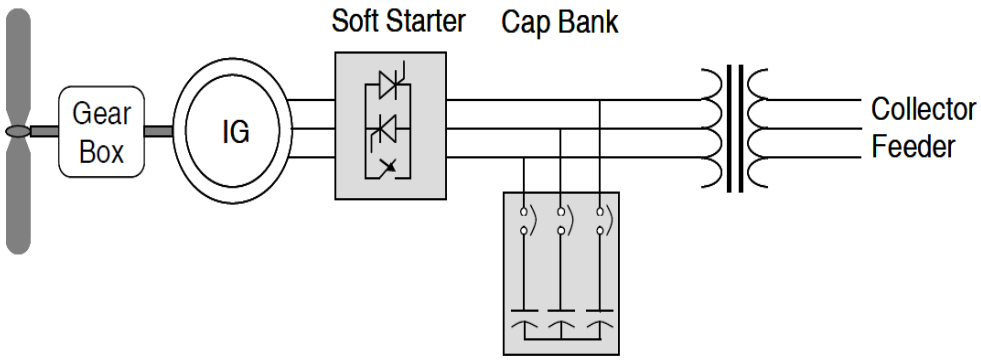

Figure 2.9. Induction Wind Turbine Type 1

Figure 2.10 presents the result of different fault type for wind turbine machine type 1 developed in PSCAD EMTDC. Prior to the short circuit instance at t= 4 sec machines were supplying 1 per unit load. The time of the fault is an arbitrary one and the asymmetrical current is not maximized based on the moment of the fault. The generator is shorted at the collector prior to the point of common coupling transformer. It can be observed that the type 1 machines are able to contribute a significant fault current to the grid depending on the time of the short circuit. The contribution of the initial cycle of the fault (asymmetrical current) can be as high as seven times the rated current and more. As the fault persists, the contribution decreases in magnitude. By its nature, an induction machines consumes reactive power both in the generating and motoring operation. The reactive power consumption increases significantly as the output power increases.

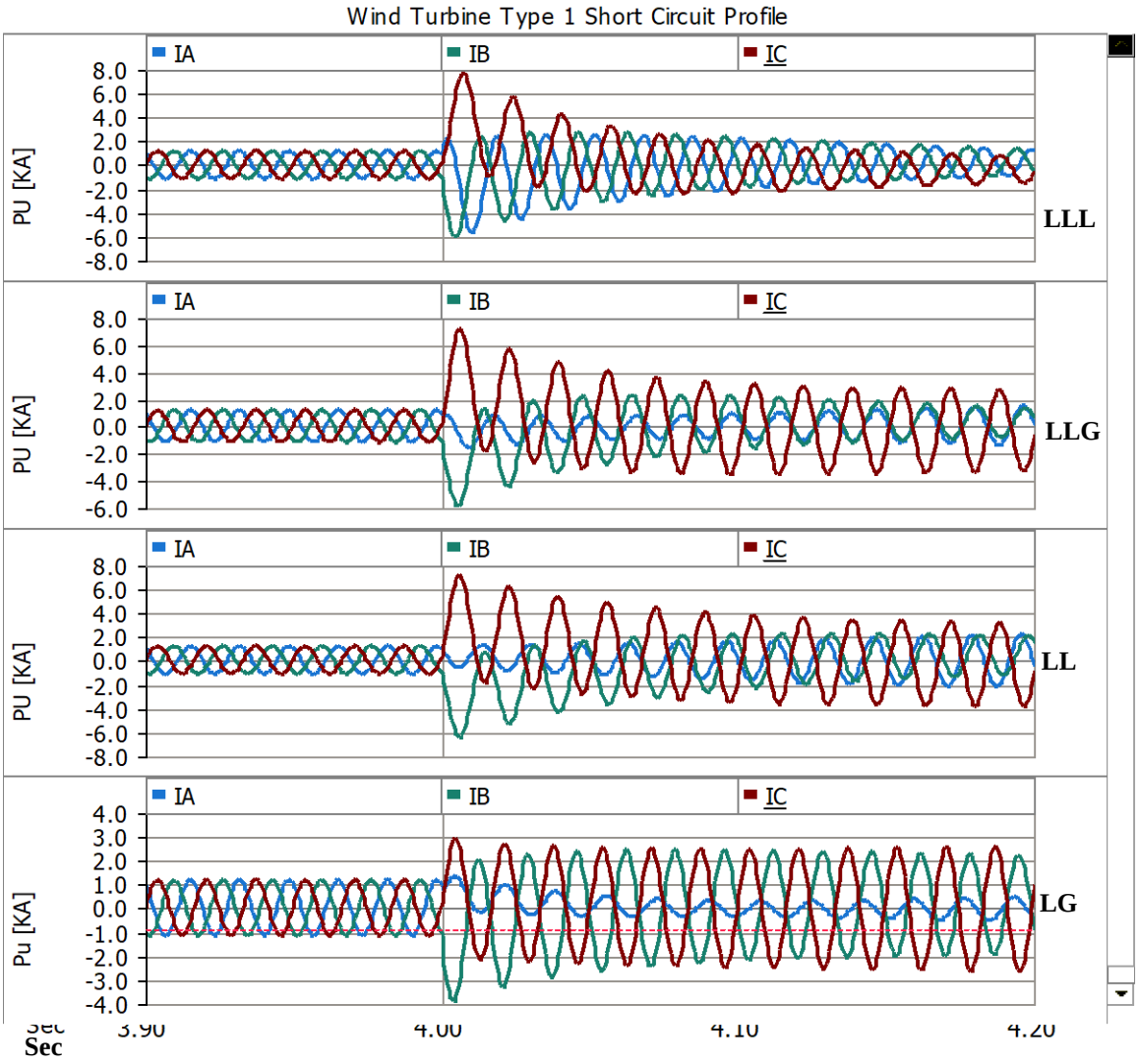

Figure 2.10. Induction Wind Turbine Type 1 Short Circuit Profile

In the type 2 wind turbine, shown in Figure 2.11, the induction generator used is a wound rotor. There are no major differences between type 1 and type 2 turbines. They both have almost fixed speed control. Type 2 has a better possibility for speed regulation by adding resistance to the rotor circuit, and the real power curve can be “stretched” to the higher slip and higher speed ranges. That is to say that the turbine will have to spin faster to create the same output power, for an added rotor resistance.

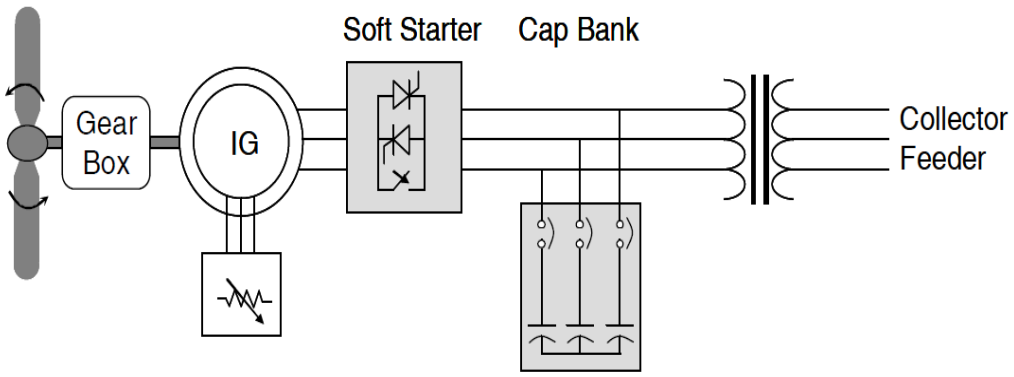

Figure 2.11. Induction Wind Turbine Type 2

The short circuit characteristics of a wind turbine type 2 is similar to a type 1. When the external rotor resistance is not added to the rotor or shorted, the short circuit current is not different with the squirrel-cage induction generator. Figure 2.12 shows the short circuit simulation carried out in PSCAD EMTDC for the type 2 wind turbine for different types of fault. The simulation is carried out with one external rotor resistance. The external resistance in the rotor circuit will affect the value of the short circuit contribution negatively. Prior to the short circuit instance at t=4 sec the machine is suppling a rating value. The moment of short circuit is arbitrary and asymmetrical current is not maximize based on the instance of the short circuit. It can be noted in this simulation that the type 2 machine can contribute significantly to the short circuit in the grid 4 to 5 per unit in the initial cycle.

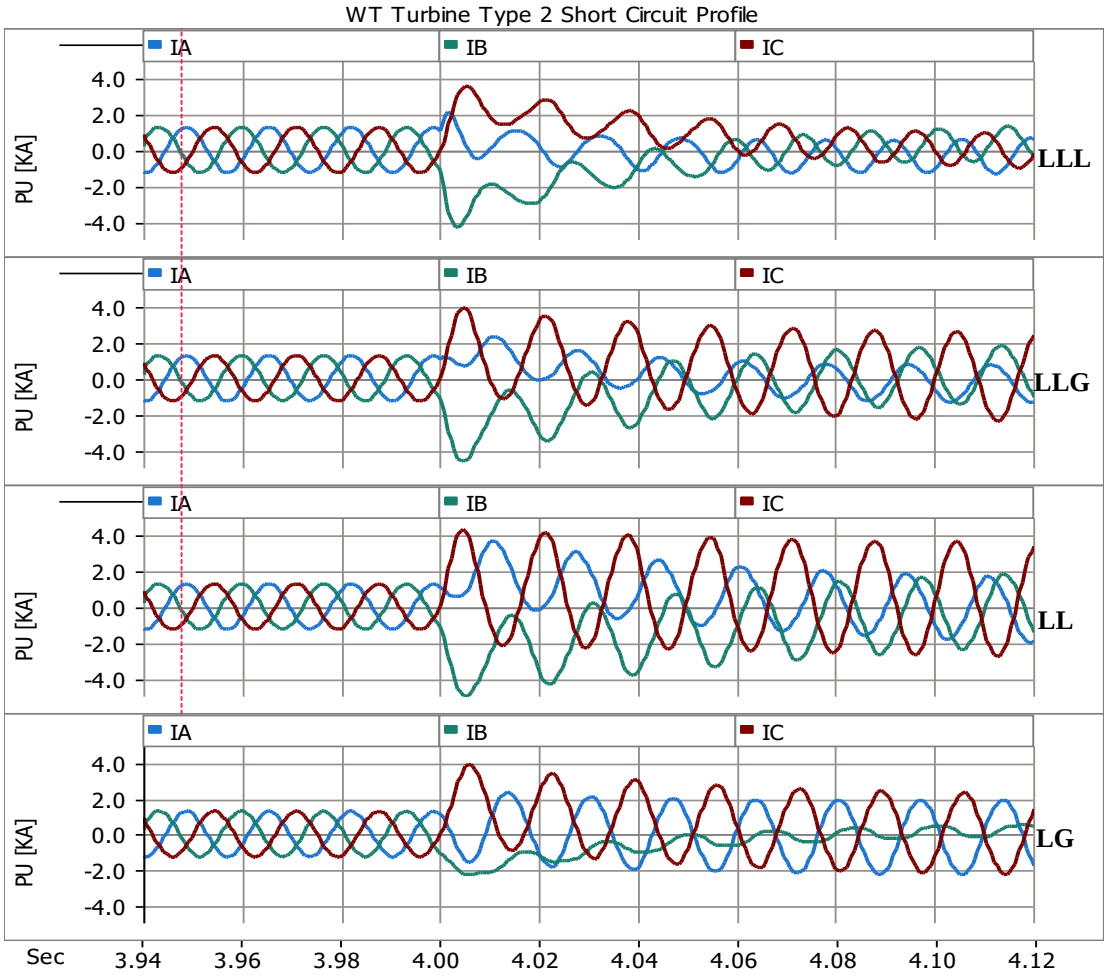

Figure 2.12. Induction Wind Turbine Type 2 Short Circuit Profile

Type 1 and type 2 are often equipped with a smooth starter where the induction machine is supplied with variable frequency and reduced voltage and to run the machine until bring the machine up to the rating voltage and speed.

Figure 2.13 shows a simple simulation of induction machine start up in PSCAD. The recorded graphs are active power, reactive power, speed, and generator terminal voltage. At the start, the voltage and frequency are gradually increased, and the machine absorbs active and reactive power. When speed and voltage reach the value of network, the smooth starter is bypassed, and the wind turbine is directly connected to the grid. From this moment onward, as shown in this simulation, the induction machine generates real power (P) when the turbine shaft rotates faster than the grid frequency.

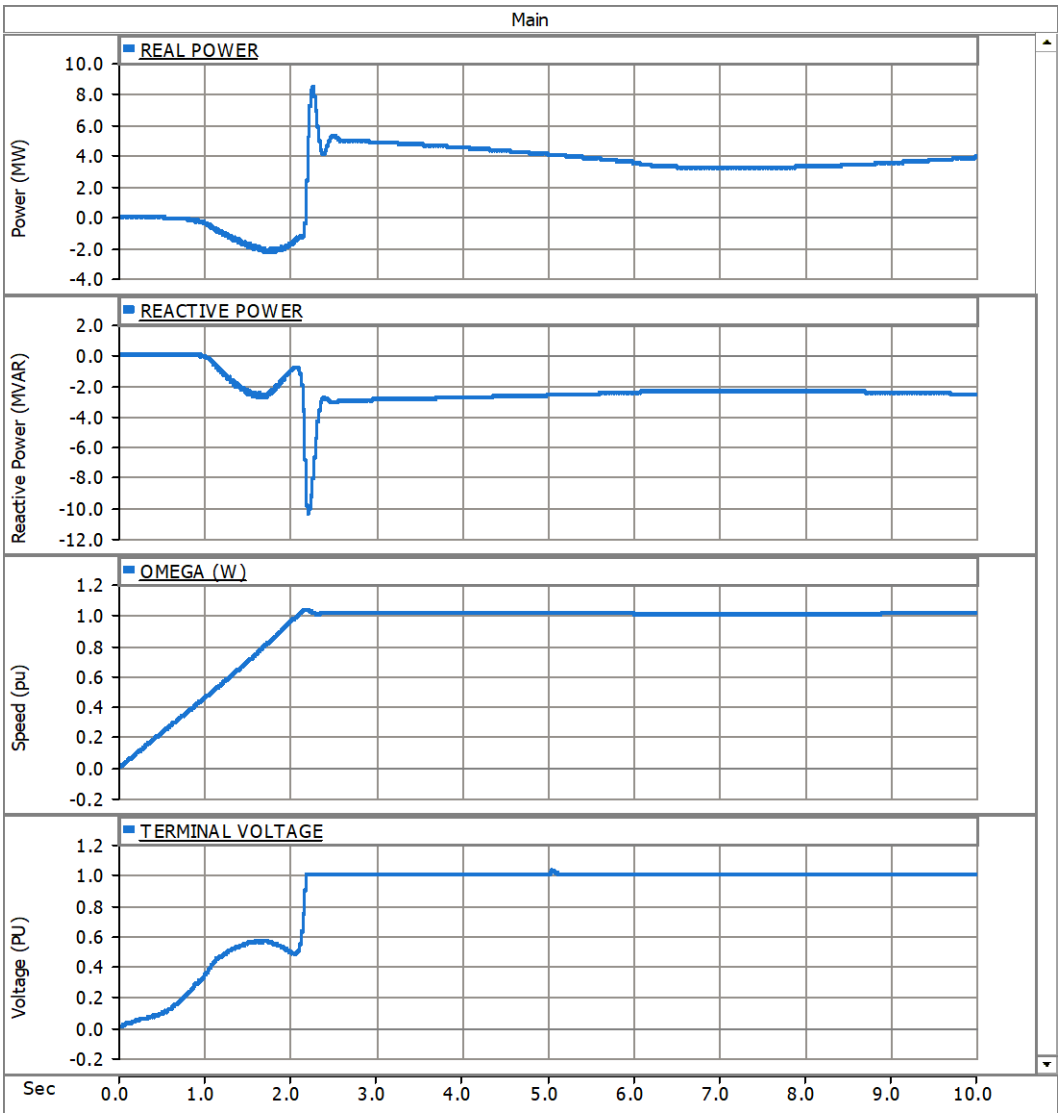

Figure 2.13. Induction Wind Turbine Smooth Start up

2.5.3 Induction Machine Type 3 (DFIG)

Variable-speed generator drives enable the wind turbine control system to adapt the rotational speed of the rotor to the instantaneous wind speed over a relatively wide range. The electrical system has a fixed frequency though. A generator drive connecting a variable-speed mechanical system to a fixed frequency electrical system must, therefore,

contain some kind of a slip or decoupling mechanism between the two systems. In variable-speed wind turbine Doubly Fed Induction Generator (DFIG), the rotor circuit is fed from a converter with variable frequency, as shown in Figure 2.14.

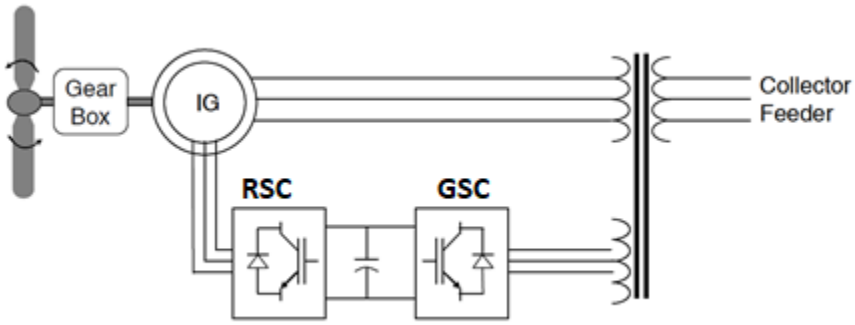

Figure 2.14. Induction Wind Turbine Type 3

Thus, the angular velocity of stator rotary field can be written as follows:

$$\frac{\omega_s}{p_s} = \omega_{mech} \pm \frac{\omega_r}{p_r} \tag{2.1}$$

$$s = \frac{n_s - n_r}{n_s},$$

Where p_s and p_r denote the number of stator and rotor poles respectively, ω_s is the power system frequency which is equal to the sum of the angular velocity of mechanical rotation (ω_{mech}), and rotor current frequency (ω_r). Depending on the direction of the supply frequency, this machine can operate in over or under synchronous speed and has much more flexibility to work over a wider range of wind speeds. For the simplification of power and torque equations, assuming $P_s = P_r = 1$, then the following can be stated from the basic asynchronous machine model:

$$\omega_m = (1 - S)\omega_s$$

$$P_{mech} = 3|i_r|^2\left(\frac{1-s}{2}\right) R_r \tag{2.2}$$

$$T_{mech} = 3|i'_r|^2\left(\frac{1-s}{s}\right)\frac{R'_r}{\omega_m} = 3\Psi_m|i'_r| \quad (2.3)$$

Where Ψ_m stator core magnetizing flux and prim indicates reflection of current and rotor value to the stator side.

$$\Psi_m = L_m i_m = \frac{V_s}{\omega_s}$$

Unlike type 1 and type 2 wind turbine machines, type 3 can provide reactive power to participate in voltage regulation and when is connected to the grid. Figure 2.15 shows a simulation that was carried out with the normal loading condition at t around 1.4 seconds; the grid voltage is reduced by 6%, and thus, instantly the wind turbine in the absorbing reactive power condition of (-0.4 PU) is changed to generating plus 0.4 PU to compensate for loss of reactive power and reduction of voltage.

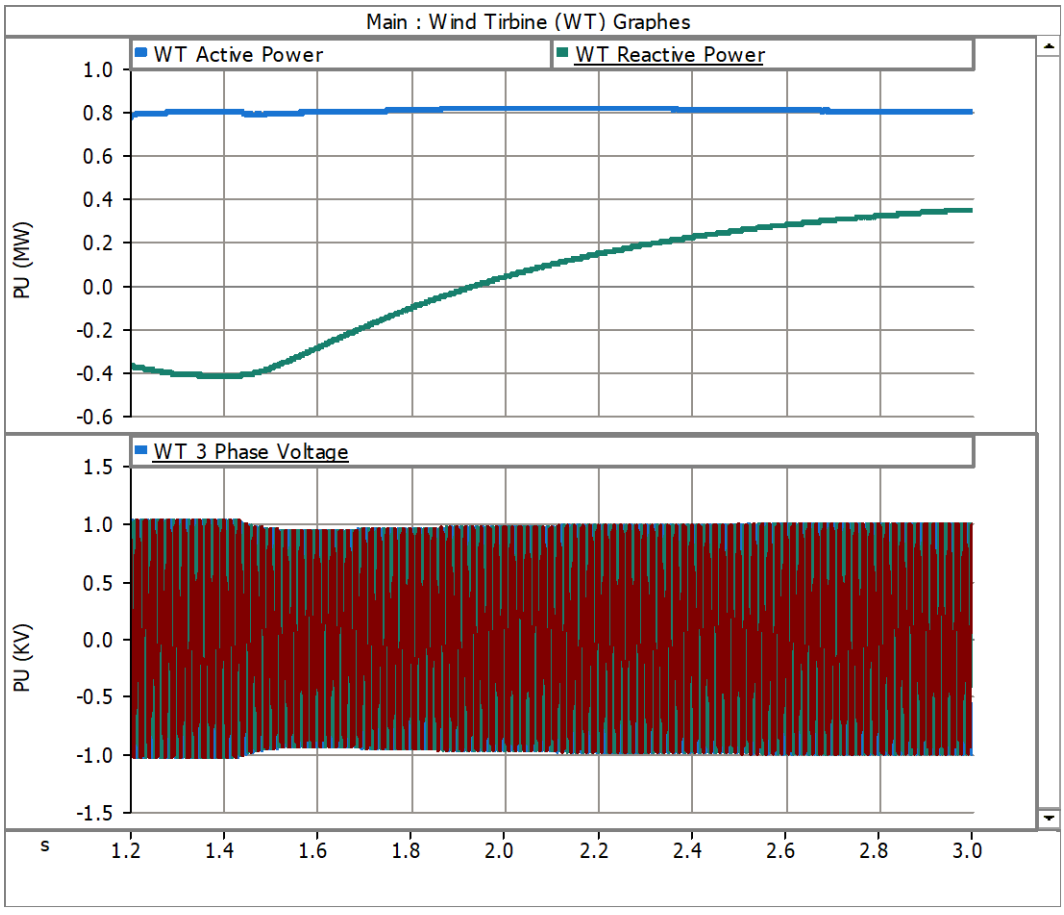

Figure 2.15. Wind Turbine Type 3 Reactive Power Regulation

Similar to what is presented for the earlier wind turbine in this chapter, Figure 2.16 shows the short circuit simulation for the type 3 machine carried out in PSCAD EMTDS. The short circuit contribution for three-phase fault is shown to have the shortest decay time with the peak current around 4 per unit. The phase to-phase -to-ground fault gives about the same short circuit magnitude as the three-phase faults, but the decay time is longer. The single line-to-ground fault produces the lowest peak current of about 5 per unit and it also decays longer than the three-phase fault. From the short circuit waveforms, it can be recognized that the symmetrical component analysis for the unbalanced short circuit is not producing the same result as a conventional machine.

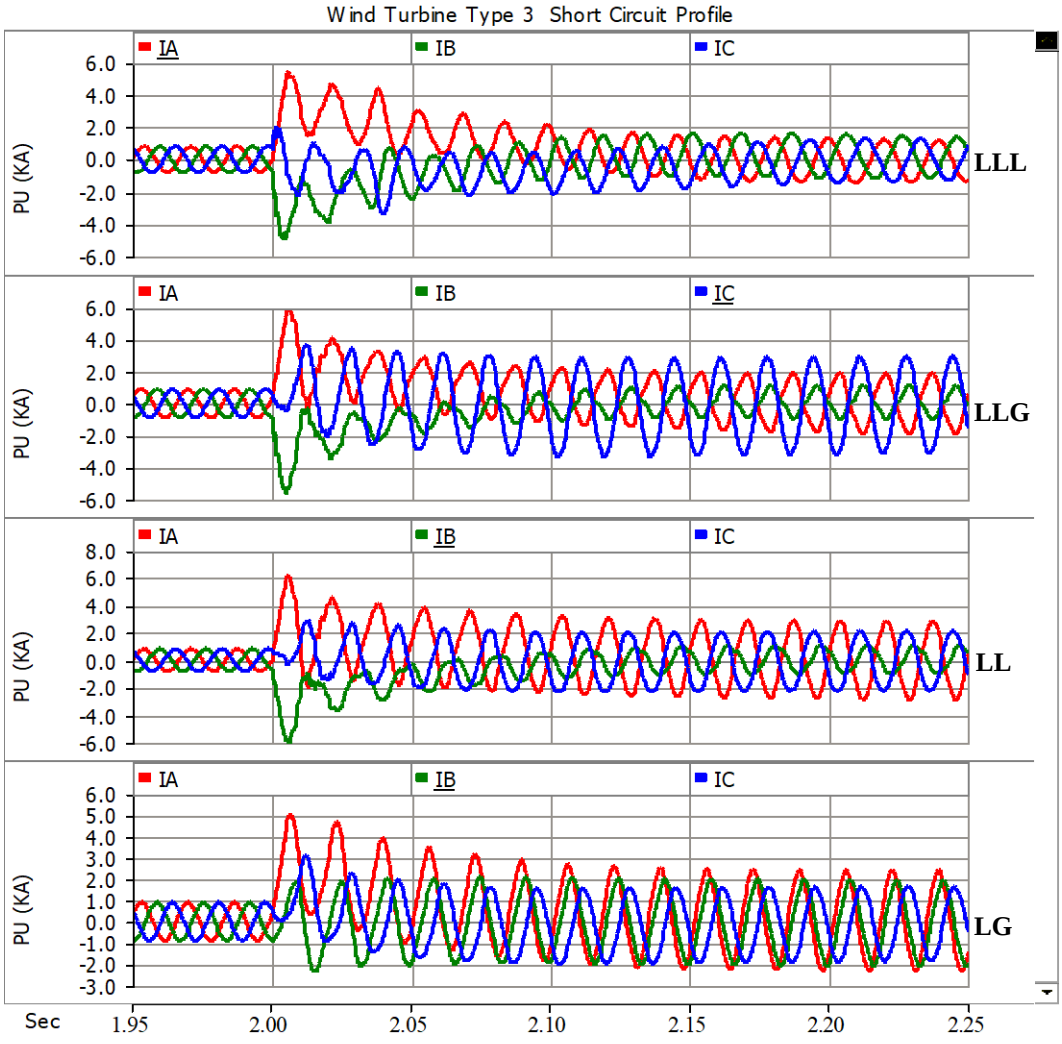

Figure 2.16. Wind Turbine Type 3 Short Circuit Profile

The complete active power, reactive power, and frequency control of DFIG for this work is developed and customized in “dq” control using PSCAD. The overview of the PSCAD model is reported in the Appendix C.

Figure 2.17 shows a type 4 full-fledged back-to-back inverter-based machine. The grid interface can be an induction or synchronous generator. This type of wind turbine is most frequently implemented around the world. Type 4 can provide an independent active and reactive power control loop and therefore, it can participate effectively in the grid feeder voltage regulation. This type of configuration offers a great deal of flexibility in operation

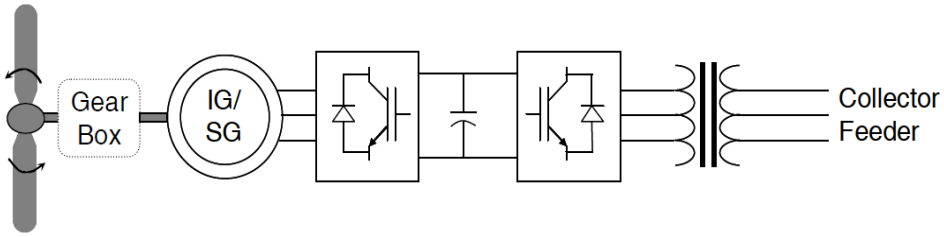

Figure 2.17. Typical Wind Turbine Type 4

since there is no direct connection between the generator and the grid. The turbine is allowed to rotate at its optimal aerodynamic speed, and the power output can still be adjusted to the grid frequency. The dq control model customized for this study and its parametrization is reported in the Wind Turbine Model Type 4.

Similar to type 3 this machine is capable of providing reactive power to participate in voltage regulation when it is connected to the grid. Figure 2.18 shows the simulation that was carried out with the normal loading condition at t around 3 seconds. The grid voltage is reduced by 10%, thus, instantly the wind turbine in the absorbing reactive power condition of (-0.1 PU) is changed to generating plus 0.3 PU to compensate for the loss of reactive power and the reduction of voltage.

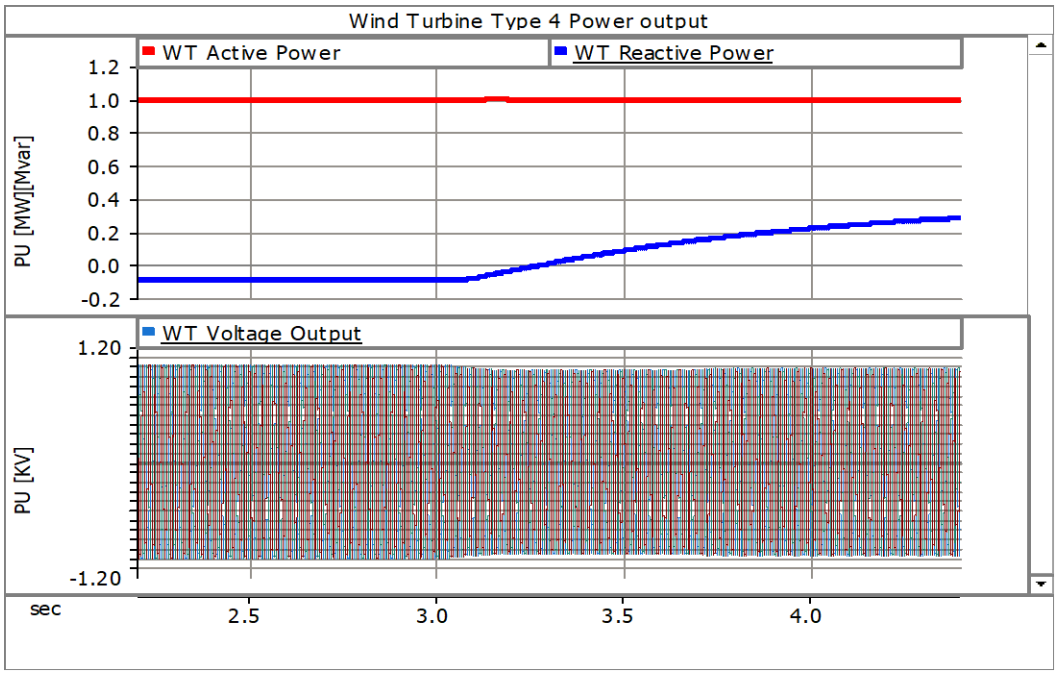

Figure 2.18. Wind Turbine Type 4 Reactive Power Contribution

Figure 2.19 presents the short circuit contribution of wind turbine type 4 for a different type of fault. It can be noted that a short circuit current even for a three-phase fault is limited to the rated current or a little above the machine rated current. The type 4 machine, depending on the design of inverter it can support some 10% to 20%. The generator in this type of machine is not connected directly to the grid therefore, during the fault in the grid the generator can still be running with the connection to the machine side converter and power will be delivered by the grid side converter with reduced amount of voltage and current.

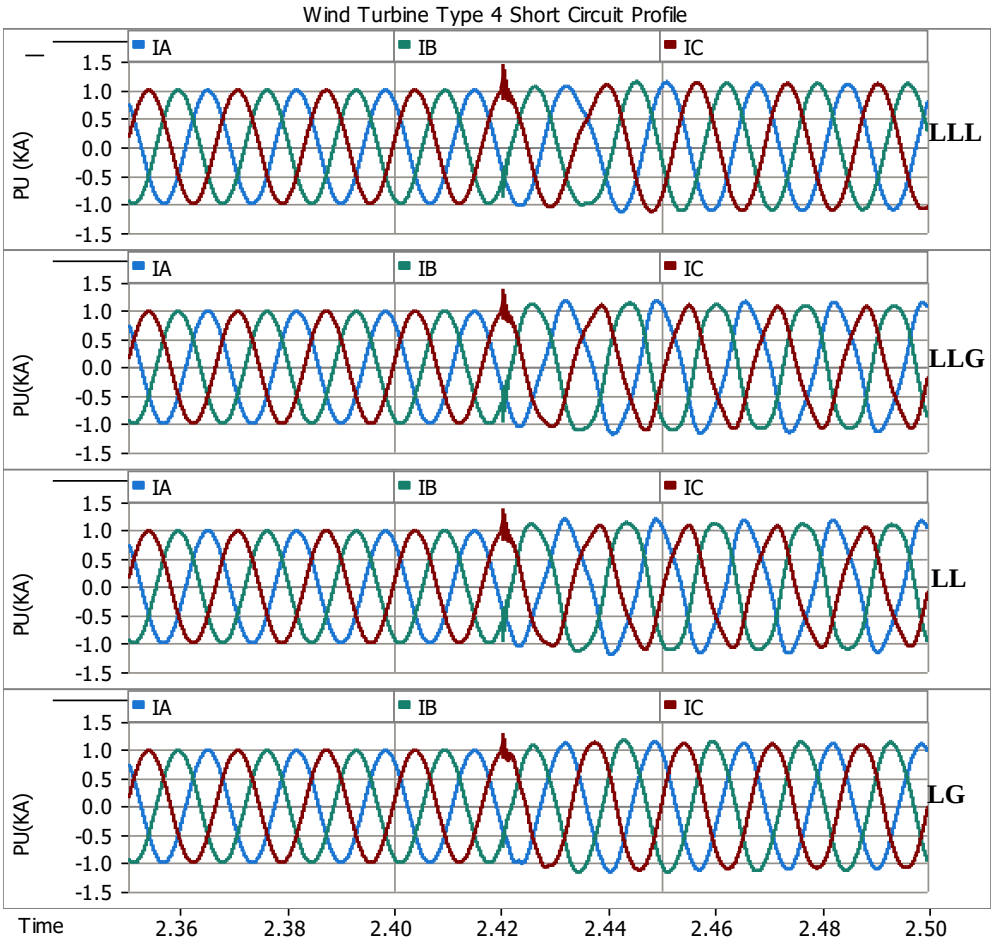

Figure 2.19. Wind Turbine Type 4 Short Circuit Profile

2.5.4 Photo Voltaic

In distribution systems, because of the limitation of renewal capacity that can be integrated into the primary feeder, the connection of solar farms is the most prevalent compared to other types of DER. Figure 2.20 presents a conceptual block diagram of a utility grade solar farm. At the DC side, the number of PV panels are normally in series and parallel to make up for the current and power that is required to be connected to the DC/AC grid-connected type of inverter. The AC voltage in the output of inverter will then be raised to the collector voltage level which is often in the range of distribution class voltage and may integrate more similar units to the main substation and common point of coupling (PCC) through another transformer or directly.

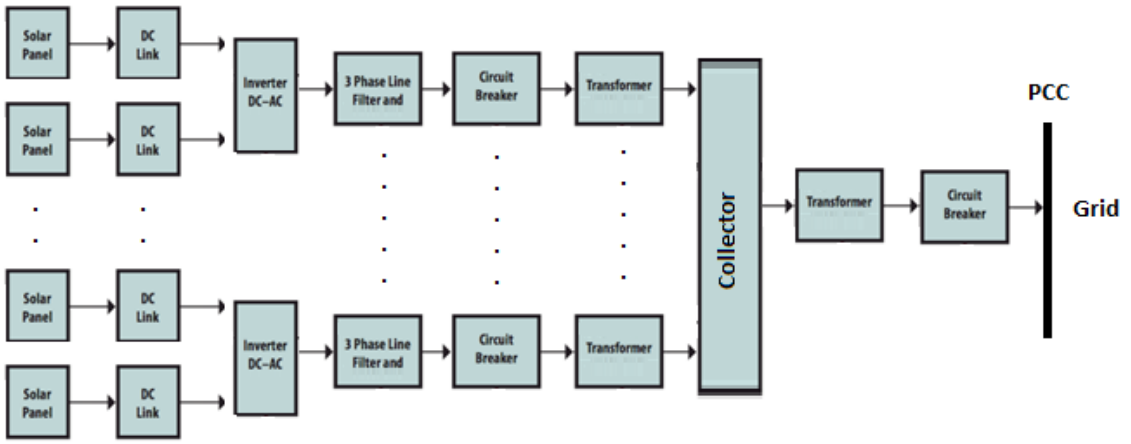

Figure 2.20. Typical Solar Farm Block Diagram

For the purpose of this work and study of unintended islanding, an integrated model of the PV solar in PSCAD presented in Figure 2.21 is considered.

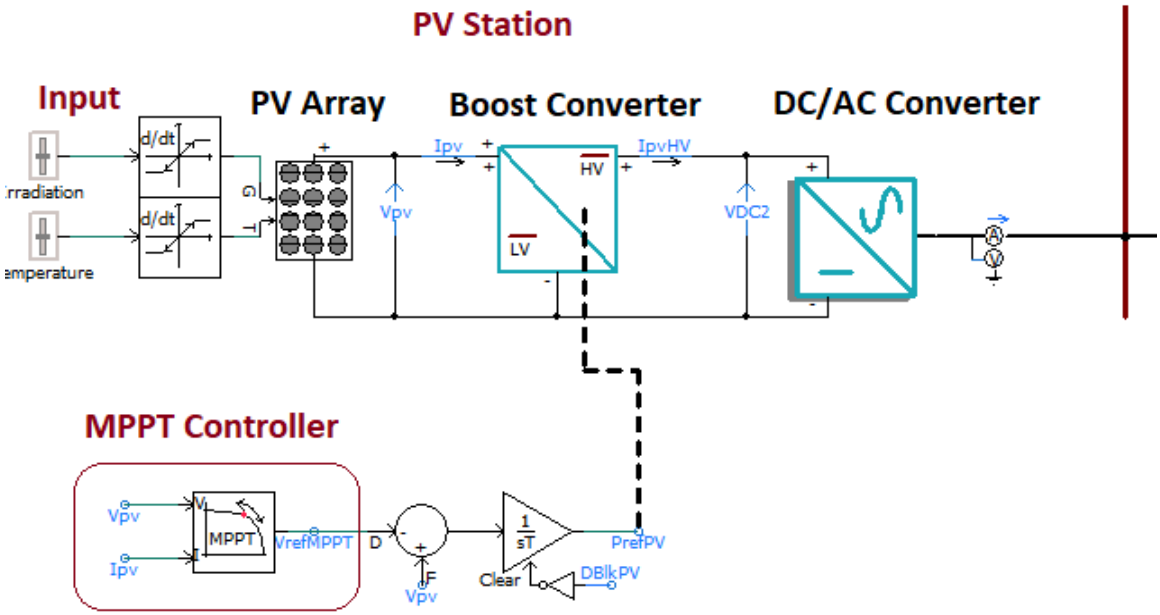

Figure 2.21. Grid Connected PV Model

The amount of power that can be taken from a solar cell depends on the operating point of I_V cure which is maximum at the keen point of this curve as shown in the model. MPPT (Maximum Power Point Tracking) is a power electronic DC-DC converter implemented to

ensure that the PV cell operated at maximum power point. Figure 2.22 presents the short circuit contribution of PV array for a different type of fault. The contribution of the short circuit current even for the three-phase fault is limited and in the instance of the fault is very close to the load. However, the short circuit current if the fault persisted in the next cycles could reach to 2 PU to 3 PU. The PV similar to type 3 and 4 wind turbines can supply the grid with reactive power.

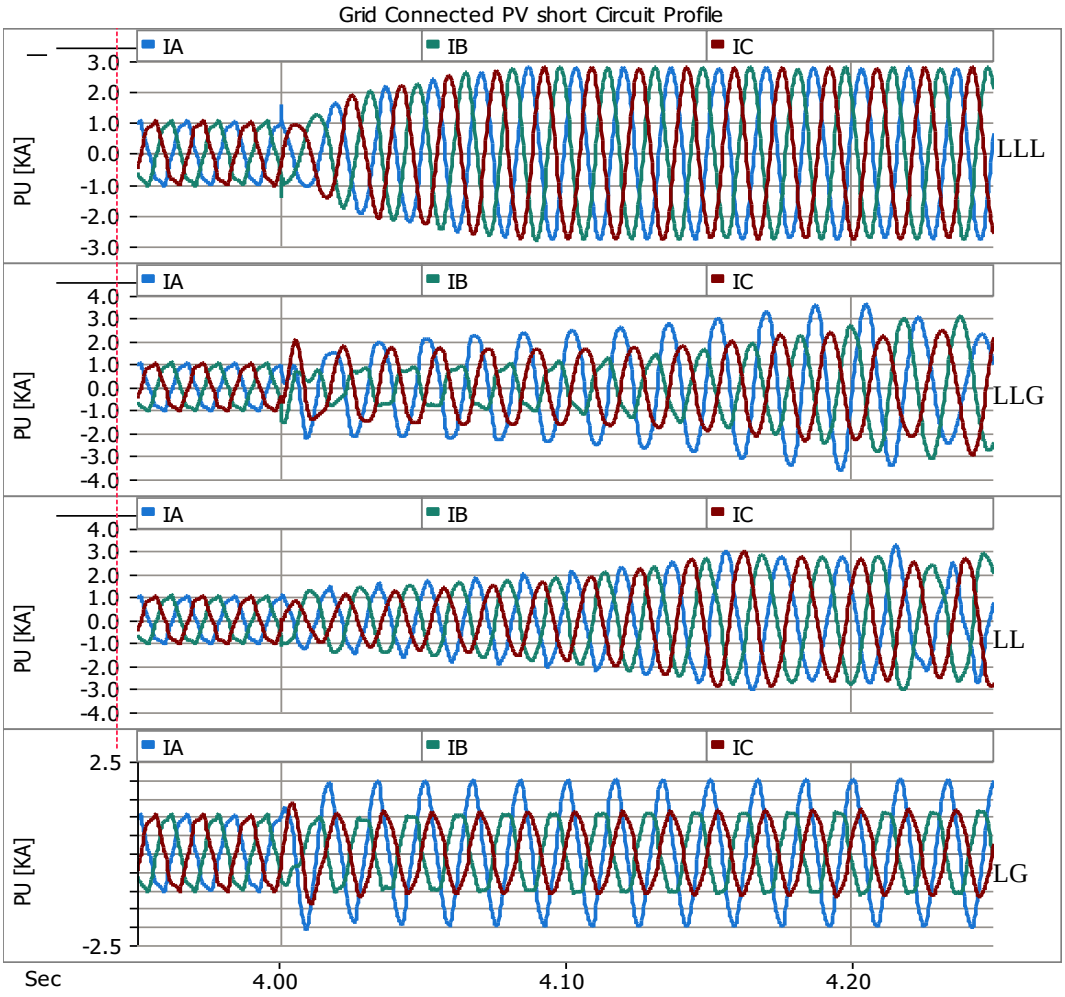

Figure 2.22. Grid Connected Solar Farm Short Circuit Profile

2.5.5 DER Model Developed for Islanding Application

Three EMT models including wind turbine type 3, type 4, and PV, are developed and customized for studying the islanding application in this work. The islanding application

background and state-of-the-art solutions will be discussed in chapter four. In this section, the overview and principle of the models used for DER modeling are presented.

The models developed for DER are based on the space phasor on αβ, and dq frames. A three-phase positive rotation system can be shown as a single space phasor $\vec{f}(t)$.

$$F_a(t) = f_{max}\cos(\omega t + \theta_0)$$

$$F_b(t) = f_{max}\cos\left(\omega t + \theta_0 - \frac{2\pi}{3}\right) \quad (2.4)$$

$$F_c(t) = f_{max}\cos\left(\omega t + \theta_0 + \frac{2\pi}{3}\right)$$

$$\vec{F}(t) = \frac{2}{3}\left[e^{j0}f_a(t) + e^{j\frac{2\pi}{3}}f_b(t) + e^{j\frac{4\pi}{3}}f_c(t)\right] \quad (2.5)$$

Where θ_0, is the arbitrary initial angle of the three-phase system with the time origin.

Knowing,

$$E^{j0} + e^{j\frac{2\pi}{3}} + e^{j\frac{4\pi}{3}} = 0$$

$$\cos\theta = \frac{1}{2}\left(e^{j\theta} + e^{-j\theta}\right)$$

Therefore,

$$\vec{f}(t) = \left(f_{max}e^{j\theta 0}\right)e^{j\omega t}$$

Figure 2.23 presents the space phasor representation of a 3 phase AC system in the αβ and dq frame.

$$\vec{F}(t) = f_\alpha + jf_\beta = \left(f_d + jf_q\right)e^{-j\omega t} = \left(f_d + jf_q\right)e^{j\rho t}$$

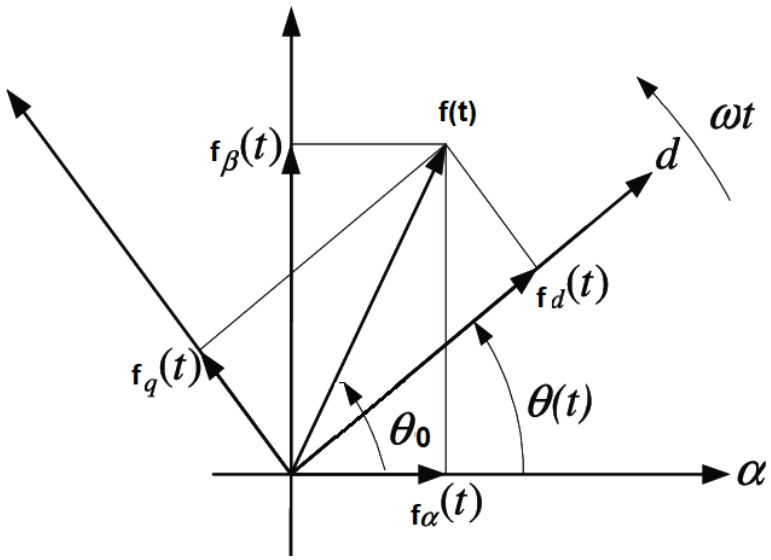

Figure 2.23. Representation of Space Phasor in dq Frame

While $\alpha\beta$ frame is static and is not rotating, dq frame is locked with the rotation of space phasor $\vec{f}(t)$ and therefore, the component in these frames is similar to the DC type quantity. In (2.6) and (2.7), the dq quantities from three phase "abc" and vice versa are calculated respectively. These calculations are known as the Park's transformation.

$$\begin{bmatrix} fd \\ fq \\ 0 \end{bmatrix} = \frac{2}{3}\begin{bmatrix} \cos\theta & \cos\left(\theta - \frac{2\pi}{3}\right) & \cos\left(\theta + \frac{2\pi}{3}\right) \\ \sin\theta & \sin\left(\theta - \frac{2\pi}{3}\right) & \sin\left(\theta + \frac{2\pi}{3}\right) \\ \frac{1}{2} & \frac{1}{2} & \frac{1}{2} \end{bmatrix}\begin{bmatrix} fa \\ fb \\ fc \end{bmatrix} \tag{2.6}$$

$$\begin{bmatrix} fa \\ fb \\ fc \end{bmatrix} = \begin{bmatrix} \cos\theta & \sin\theta & 1 \\ \cos\left(\theta - \frac{2\pi}{3}\right) & \sin\left(\theta - \frac{2\pi}{3}\right) & 1 \\ \cos\left(\theta + \frac{2\pi}{3}\right) & \sin\left(\theta + \frac{2\pi}{3}\right) & 1 \end{bmatrix}\begin{bmatrix} fd \\ fq \\ 0 \end{bmatrix} \tag{2.7}$$

The angle Θ(t) in the above transformation is estimated based on the angular velocity of the grid by Phase Locked Loop (PLL) function. The function block diagram of PLL is shown in Figure 2.24. Voltage Controlled Oscillator (VCO) in this diagram works as a resettable integrator between 0 and 360 degrees. It will reset the value of Θ(t) when it reaches 360 degree. In Figure 2.23, if PLL forces fq to zero at any given time, the "d" axis in the "dq" frame will be in the same position of f(t) and therefore, the "dq" frame

will be locked to the space phasor rotation which generally represents the desired frequency that should be measured.

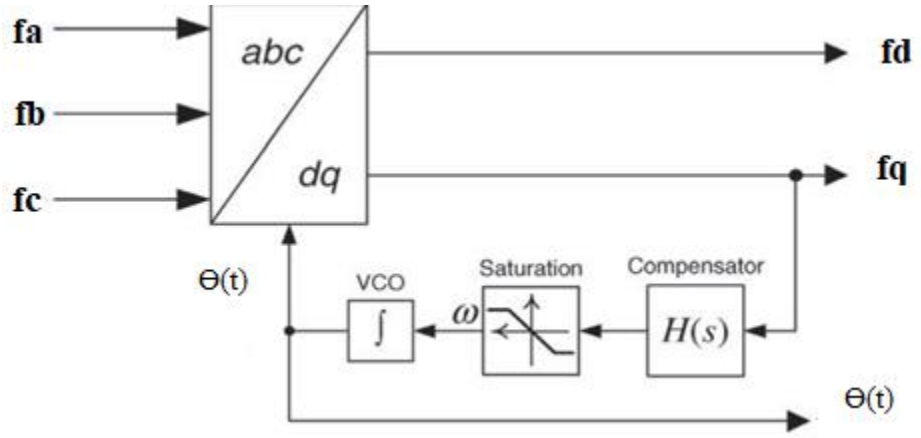

Figure 2.24. Phase Looked Loop Block Diagram

Figure 2.25 shows the conceptual control block diagram of grid-imposed Voltage Source Converter (VSC) illustrating the basic concept of the control of power models. The DC source (VDC) in the case of type 3 and type 4 wind turbines is a simplified representation of machine side convertor and in the case of a solar farm, represents a PV panel. The control based on the dq frame is decoupled, i.e., there is a separate control loop for active and reactive power. The estimation of grid frequency is an essential part of the conversion of three phase AC system to the "dq0" stationary axis rotating with the angular frequency of the grid source voltage $\theta(t)$. In addition to "dq0"conversion, $\Theta(t)$ is used to adjust the frequency of the grid side converter output. In simple terms, for the type 3 type 4 wind turbines, and the PV solar farm, if there are no provisions for the islanding operation where DER can supply the load in an islanded feeder, for the grid-imposed voltage source converter without presence of an active source, the islanding mode cannot be sustained.

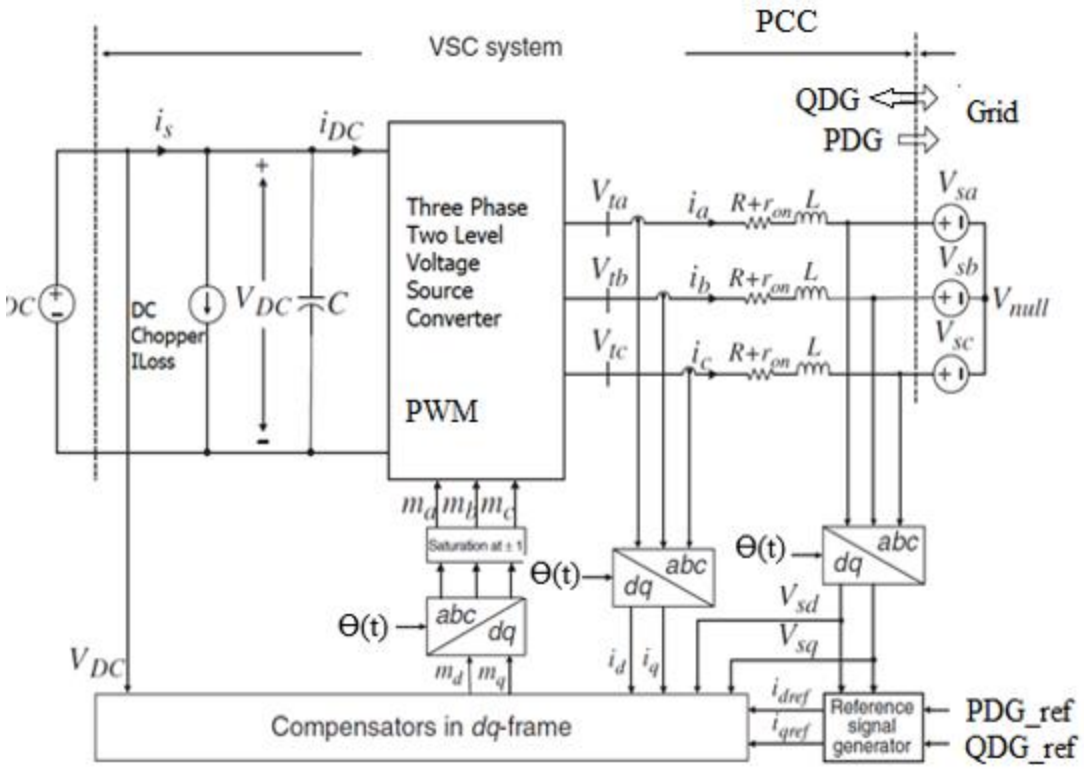

Figure 2.25. Real and Reactive- Power Control of Grid Imposed VSC

Figure 2.26 shows the simulations carried out for the generic PLL grid used for this study. The first graph Θ(t) in degrees is the output of VCO, and the second graph is a derivative of the first graph ($\frac{d\theta(t)}{dt}$) without any limitation on the output value. The grid frequency at $t = 1.5\ sec$ changes gradually to 58 Hz and at $t = 1.6\ sec$, the frequency is restored to its original value of 60 Hz. The simulation is carried out for the grid side PLL used for type 4 machine.

The information related to the actual EMT models for DER used in this study are presented in the Appendix C and Appendix D.

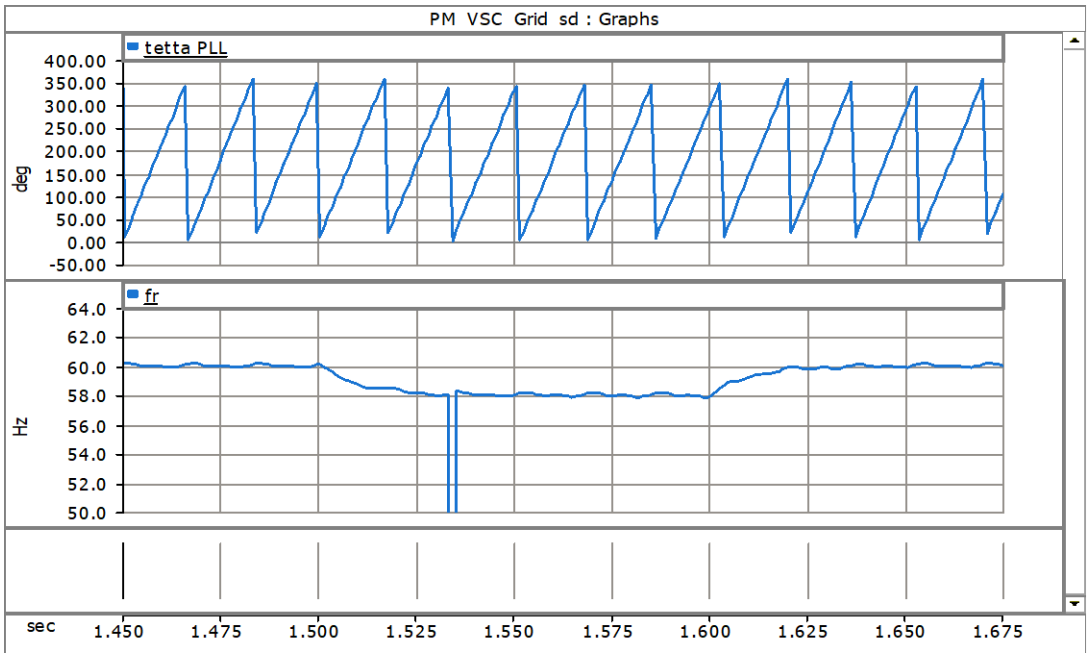

Figure 2.26. Phase Looked Loop Simulation

2.6 Regulatory Requirements for DERs

Since the publication of IEEE 1547 “DER interconnection standard” in 2003, this standard has gone through a major rework and revision which in a way reflects the state-of-the-art in DER technology. Figure 2.27 presents the revision history of IEEE 1547 with highlights of the major changes in the DER power network support.

The contributions of DER in the regulation of voltage, reactive power; frequency, and network inertia are the major changes that can been seen from the earlier version of the standard. In the early generations of DERs, they were mostly unable to support islanding operation since there was no capacity to generate var and to regulate the voltage and frequency without an additional control circuit that supports this operation. With DER getting the functionality that can support grid operation, IEEE 1547 scope has changed from focusing only on a distribution network to covering both distribution and bulk energy systems.

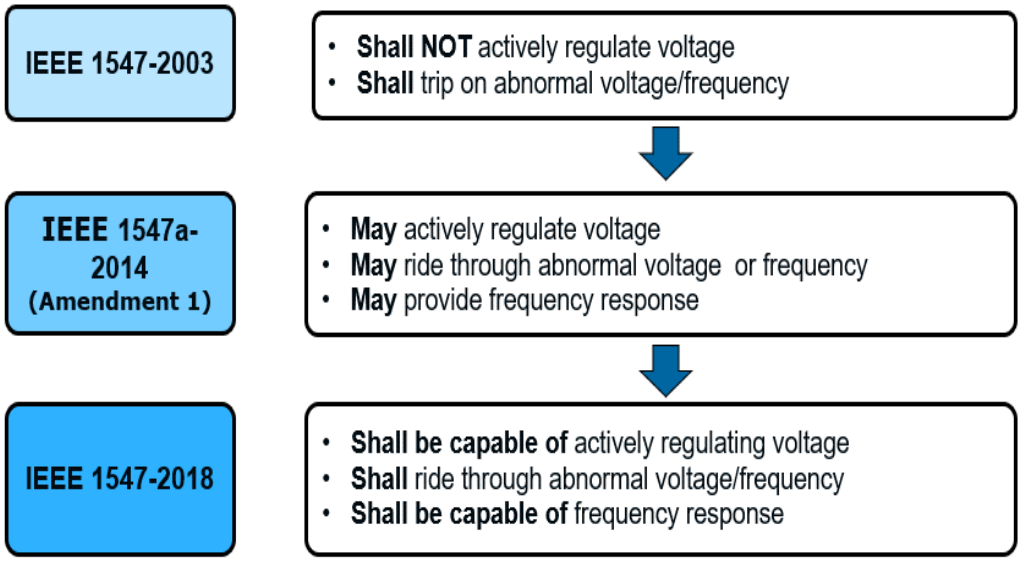

Figure 2.27. IEEE 1547 Grid Support Function History [Courtesy of IEEE 1547 WG]

In this regard, the standard has defined DER categories (Cat A, B) for the voltage capabilities based on reactive power generation as a percentage of the power capacity of DER for individual as well as aggregated units. The performance of the DER for an abnormal operating condition have also been categorized (cat I, II, III), where Cat III is specifically indented for bulk power systems.

DER Islanding in IEEE 1547-2018 standard

Following are the main highlights related to islanding in the latest version of the standard and have taken into consideration the following:

- An island condition is defined as an operation in which a portion of an Area Electrical Power System (EPS) is energized solely by one or more DER alone and utility source is disconnected.
- AN unintentional island is one that is not planned and the DER must detect, **trip, and clear within 2 seconds** –same as IEEE 1547-2003. Area EPS Operator (utility) can extend this to 5 seconds.

- Intentional island: one that is planned such that DER can carry a specific load (e.g., microgrid, emergency/standby power supply). 1547-2018 now addresses intentional islands.

2.7 Summary

A brief review of the conventional role of a distribution system as a power system interface to the load center is discussed. It was shown that because of distribution system size, which makes it a very capital- and labor-intensive business, and simplified functionality, which was expected from this redial system, the technological disadvantage of the distribution system infrastructure in comparison to the other sector of power systems was ignored by utilities and system owners. Communication technology typically has not been part of the solutions and research that have been offered. It is also discussed that distribution system became the forefront of the green energy and smart grid initiative around the globe which is transforming this system to be more technologically advanced, and hence, requires more research and solutions similar to this work.

In this chapter, a background of distribution systems from a structural point of view is studied with focus on the North American network. The voltage class, primary feeder topology, distribution in urban and rural areas, and underground network in the city core is discussed. A background and fundamental and main characteristic of feeder protection in distribution systems more specifically related to the islanding and open phase fault which is a focus of this work is reviewed and the summary of conventional distribution system properties is developed.

A brief introduction to DER and their classification, as applicable to the distribution system, is reviewed. The schematics and control model of the main type of DER that is used in this work is studied. The short circuit contribution of different DER is model and simulated. The contribution of DER into voltage and reactive power generation is verified and studied. The summary of changes in IEEE standard for DER integration are outlined. The generic control concept based on the space phasor and “dq” frame is studied. The control frequency for the grid-imposed voltage source converter and Phase locked loop (PLL) functionality is studied and the generic PLL model developed for this study is

presented. The detailed EMT models DERs used in this work are presented in Appendix D. In the next chapter, synchronized phasor measurement technique, signal processing, phasor and frequency estimation, possible applications, and optimized system architecture for the use cases studied in this work are presented.

Chapter 3

3 Phasor Measurements

With the many advancements in communication, hardware processors, and information technology in the industry, these technologies are finding their way into power system applications. Although reliability and performance remain the leading requirement for power system applications for any new technology, in recent years, it can be observed that the phasor measurement system has become a technique of choice for electric power system utilities. The phasor measurement is a hardware of choice for this work which is discussed in this chapter.

3.1 Fundamental of Synchrophasor Measurement

The idea of computing synchronized measurement of the power system network in different remote locations has been around even before the technology was able to support it. Understanding the behavior of interconnected electrical grids with the objective of controlling and protecting such a network created the need for simultaneous measurement of voltage and current with the common time references to meaningfully compare both magnitude and phase angle of the measurements. Figure 3.1 shows a simple structure of synchrophasor network consisting of Phasor Measurement Units (PMUs) and Phasor Data Concentrator (PDC).

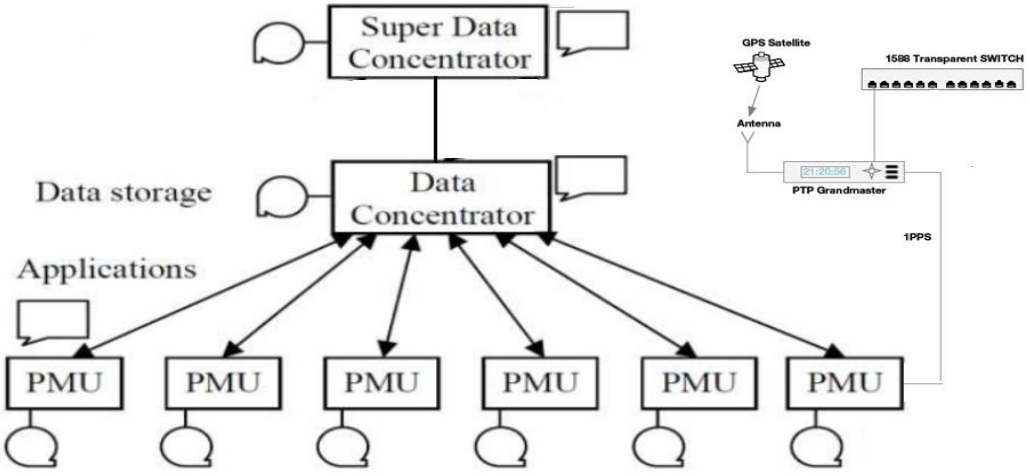

Figure 3.1. Phase Angle Reference in Interconnected Grid

The minimum structure that is required for preparing the synchrophasor data for specific applications consist of the following:

Phasor Measurement Unit (PMU): PMUs is a function or logical device that provides synchrophasor and system frequency estimates, as well as other optional information such as calculated megawatts (MW) and megavars (MVAR), sampled measurements, and Boolean status words. The PMU can provide synchrophasor estimates from one or more voltage or current waveforms [16]. The PMU can be realized as a stand-alone physical device or as part of a multifunctional device, such as a protective relay, DFR, or meter. The number of PMUs and locations where the PMU measures the electrical signal can vary depending on the application requirement.

The introduction of PMU, which nowadays is heavily standardized in the industry, goes back to the mid-1980s [17]. Since then, with the advancement in hardware computation power, communication media, and availability of GPS around the globe (see Figure 3.2), it became possible to use PMU as a standalone device or as a low-cost integrated function in protection and control of Intelligent Electronic Devices (IEDs) by utilities in many control, supervisory, and backup protection applications.

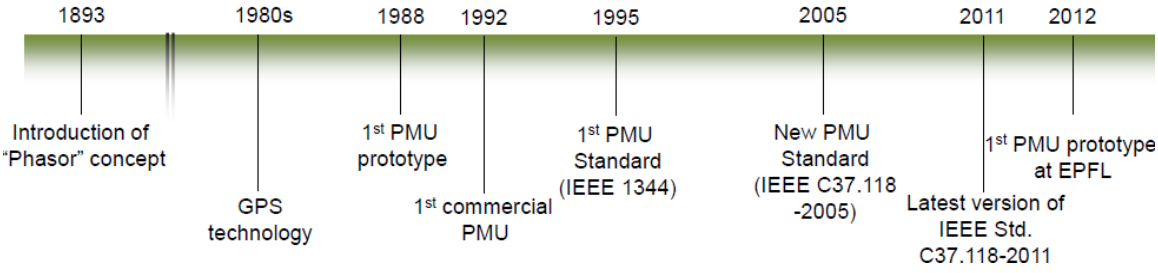

Figure 3.2. PMU History Time Line [18]

Time reference: The samples obtained by the PMU must be synchronized to a common timing reference, so the angles of the phasors computed at different locations will be comparable. As such, the electrical phasor which represents the analogue waveform of current or voltage at different locations of the power system are synchronized by means of Global Positioning System (GPS) to the Universal Time Clock (UTC) through communication.

Synchronized clocks, providing precise timestamps for events, and data acquisition applications on electric power systems. One way to provide precise time values is to use a dedicated GPS receiver for every single device. But this is a costly solution. Alternatively, time distribution mechanisms via dedicated buses or, for newer IEDs using Ethernet connectivity can be implemented in practice. Each time synchronization method has its own advantages and disadvantages and not all of them are optimal for use in substation applications. Table 3-1 below, the most common time synchronization methods available in the industry are compared for typical accuracy, data indication capability, dedicated cabling requirements, cost effective implementation, and scalability. The methods are briefly described here:

IRG-B- Inter Range Instrumentation Group time codes, also known as IRIG time codes, are standard formats for transmitting time information. The original code formats were described in IRIG document 104-60, and later revised several times over the years, with the latest version being the IRIG Standard 200-04. IRIG codes B (IRIG-B time-codes) is the industry standard for distributing synchronized time signals to IEDs. For time code transmission, IRIG-B requires an external time source, such as a GPS receiver and a dedicated twisted pair, coaxial cable or - fiber links. Therefore, this is not a low-cost solution for time synchronization.

Pulse-Per-Second (1PPS): The 1 Pulse –per-Second waveform, which is a digital-bit transmitted every second, with a pulse width of 10 milliseconds. A one pulse per second (1PPS) signal provides better accuracy than the 100 ns (on-time mark), but does not provide any indication of the date or time of day. 1 PPS is sent to every IED over separate lines and is typically used in a substation application in conjunction with other synchronization methods, such as IRIG-B. Because of this limitation, and the fact that the hardware requirements and performance are similar to those for an unmodulated IRIG-B code, IRIG-B has generally supplanted 1 PPS for substation use.

Network Time Protocol (NTP): NTP represents a software mechanism for transferring the time between computers using a communication network, such as the Internet, and is defined in RFC-1305. It generally provides moderate accuracy (1-10ms) depending on how the NTP clients and server are interconnected and also on the performance of the

communication software. NTP is very robust, widely deployed throughout the Internet, and well tested over the years and is generally regarded as state of the art in distributed time synchronization protocols for unreliable networks. It can reduce synchronization offsets to a few milliseconds over the public Internet and sub-millisecond levels over local area networks. For best accuracy, the logical connection between the clients and servers should be as short as possible.

IEEE 1588 V2: The IEEE 1588 Standard defines the Precision Time Protocol (PTP) for packet-based networked systems. The time synchronization of IEEE 1588 protocol is achieved by send message between master and slave docks. The clocks in the network are divided into master and slave. Version 1 of the protocol was initially released in 2002 and in 2008, was revised as Version 2. The first version does not support transparent clocks or industry profiles and has larger packets that generate more traffic than the second version. These two versions are not compatible. [19]

Table 3-1. Accuracy for Time Synchronization Methods [20]

Method	**Typical Accuracy in substation with given method**	**Provides date and time of day indication**	**Dedicated cabling not required**	**Fulfills IEEE C37.118 Synchrophasor Data requirements**
IRIG-B	100 µs	x		
1PPS	1µs			x
Built in GPS	1µs	x		x
NTP	1-10 ms	x	x	
IEEE 1588	1µs	x	x	x

Phasor Data Concentrator (PDC): The phasor measurements are real time measurements streamed by PMUs to the other devices, conventionally to the PDC, that work as a node in a communication network where synchrophasor data from a few PMUs or other PDCs is correlated and fed out as a single stream to the higher level PDCs and/or applications. The PDC correlates synchrophasor data using a time tag to create a system wide measurement set.

Communication Media: The Synchrophasor measurement system requires a communication media where PMU, GPS, and PDC data steam from different location can be exchanged or send to the higher-level application hierarchy devices. The performance of communication media from reliability, speed and security has at most impact on the application functionality.

GPS Timing: The Global Positioning System (GPS) is a space-based, radio-navigation system that enables extremely accurate positioning, navigation and timing. Originally designed as a 24-satellite constellation, GPS is currently comprised of 31 satellites (Oct 2018). The system is owned and operated by the U.S. Government as a national resource. The U.S. Department of Defense (DoD) is the "steward" of GPS and responsible for operating the system in accordance with the IS-GPS-200H system specification and, by U.S. law, the Standard Positioning Service (SPS) and Precise Positioning System (PPS) Performance Standards. The PMUs are required to be synchronized tot eh GPS timing so any data analysis and comparison between measurement of PMUs in different location will be possible.

3.2 Formal Phasor Definition

In short, the synchrophasor representation of the time domain signal x(t) in equation (3.1) is the value X in (3.3), where φ is the instantaneous phase angle relative to a cosine function at the nominal system frequency synchronized to UTC.

$$\mathbf{x(t) = X_m(t)\cos(\omega t + \emptyset)} \qquad (3.1)$$

Equation (3.1) can be written also as (3.2) in the exponential format.

$$\mathbf{x}(t) = \mathrm{Re}\{(X_m(t))e^{j(\omega t+\emptyset)}\} = \mathrm{Re}[\{e^{j(\omega t)}\}X_m e^{j\emptyset}] \quad (3.2)$$

The term $e^{j(\omega t)}$ will be suppressed knowing that ω is the frequency of the power system and therefore, the sinusoidal is commonly shown as the phasor equation of:

$$X = \left(\frac{Xm}{\sqrt{2}}\right)e^{J\emptyset} = \left(\frac{Xm}{\sqrt{2}}\right)[Cos\emptyset + Jsin\emptyset] \quad (3.3)$$

Under this definition, φ is the offset from a cosine function at the nominal system frequency synchronized to UTC. A cosine has a maximum at t = 0, so the synchrophasor angle is 0 degrees when the maximum of x(t) occurs at the UTC second rollover (1 PPS time signal), and –90 degrees when the positive zero crossing occurs at the UTC second rollover (sine waveform). Figure 3.3 shows the phase angle/UTC time relationship.

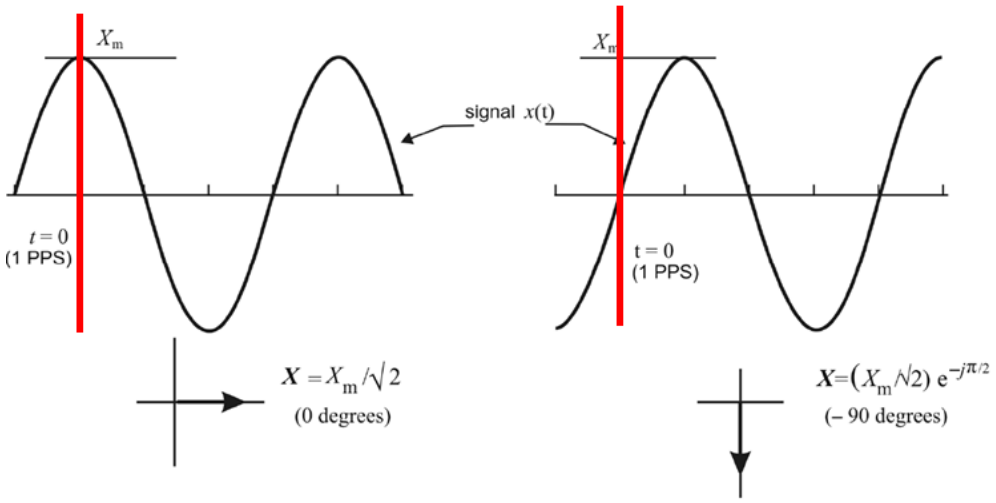

Figure 3.3. Convention for Synchrophasor Representation

In the real world, however, the power system frequency will vary in time, and the current and voltage are not an ideal sinusoidal waveform. Therefore, a more comprehensive transformation from a pure sinusoidal signal to phasor representation, as the one discussed

earlier from frequency, amplitude, and waveform point of view will be discussed in this chapter briefly.

3.2.1 Phasor Representation of Non-Sinusoidal Waveform

In power systems, the current and voltage often have other frequency components, and in order to represent them in the phasor form, it is necessary to extract the single frequency component (fundamental frequency component) from the measured signal. The Fourier Transformation or filter is conventionally used to extract the main frequency component from the corrupted sinusoidal signal.

Fourier transformation is used to break the measured signal into an alternate representation characterized by summation of series sine and cosine. Equation (3.4) illustrates how an arbitrary signal or measurement f(t) can be split into sine and cosine components using Fourier transformation [21]:

$$f(t) = \frac{a_0}{2} + \sum_{k=1}^{\infty}[(a_k \cos\left(\frac{2\pi kt}{T}\right) + b_k \sin\left(\frac{2\pi kt}{T}\right))] \quad (3.4)$$

where a_k and b_k are constant given by

$$a_k = \frac{2}{T}\int_{-\frac{T}{2}}^{+\frac{T}{2}} f(t)\cos\left(\frac{2\pi kt}{T}\right)dt, K = 0,1,2,,\ldots \quad (3.5)$$

$$b_k = \frac{2}{T}\int_{-\frac{T}{2}}^{+\frac{T}{2}} f(t)\sin\left(\frac{2\pi kt}{T}\right)dt, K = 0,1,2,,\ldots \quad (3.6)$$

Figure 3.4 illustrates the same concept where the squared waveform signal with variable frequency is transformed into Fourier components. The main components with fundamental frequency in this transformation, i.e., the red color signal will be considered if representation of such a signal into the phasor form is required.

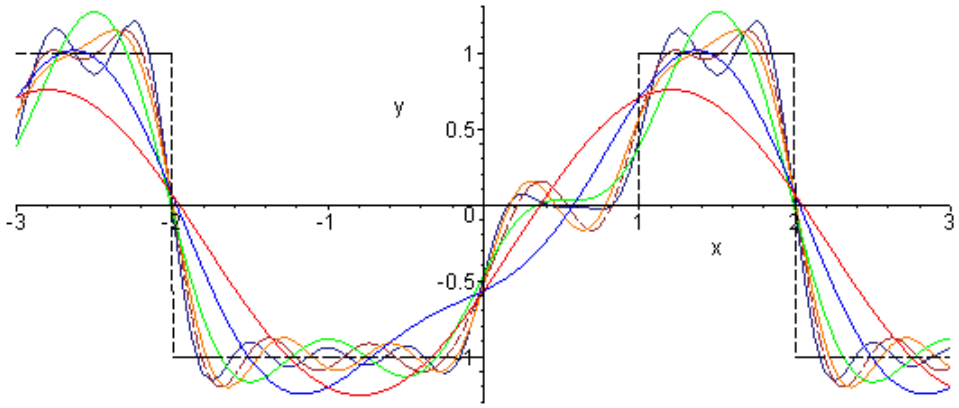

Figure 3.4. Fourier Transformation of Squared Waveform

3.2.2 Off Nominal Frequency

In synchrophasor application the current and voltage of power system must be represented in the real time with the consideration of frequency variation. (3.7) and (3.8) in which the corresponding phasor will rotate at the uniform rate of Δf, i.e., is illustrating the difference between the actual and nominal frequency .

$$x(t) = X_m(t)\cos(\omega t + \emptyset) = X_m(t)\cos(2\pi(f_0 + \Delta f)t + \emptyset) \quad (3.7)$$

$$x(t) = \mathrm{Re}\{(X_m(t))e^{j(\omega t+\emptyset)}\} = \mathrm{Re}[\{e^{j(\omega t)}\}X_m e^{j\emptyset}] \quad (3.8)$$

This concept is illustrated in Figure 3.5 where the analogue waveform has been shown in real time at intervals {0, T0, 2T0, 3T0,..,nT0, …}, where T0= 1/ f0 (the nominal power system period) and the sequence corresponding phasor of these measurement are {X0, X1, X2, X3, … Xn, …}.

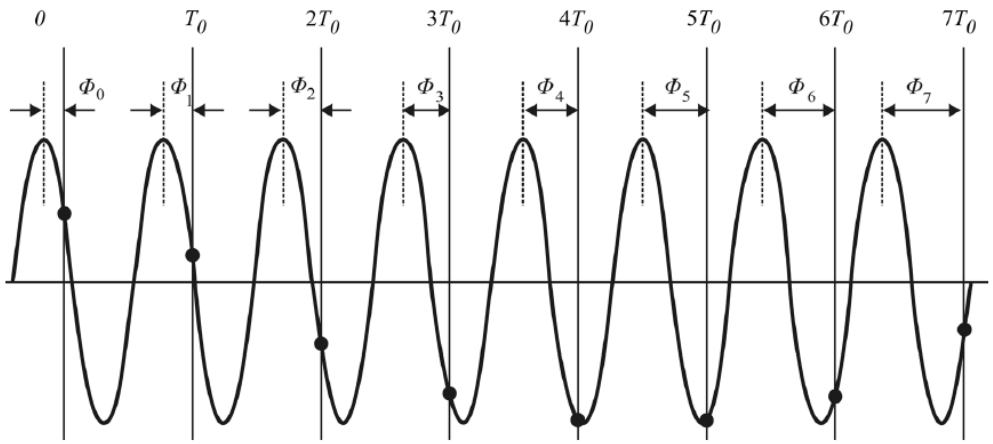

Figure 3.5. Waveform with Positive $\Delta f > 0$ ($f > f0$)

If the phasor magnitude is constant, the phase angles of the sequence of phasors {X0, X1, X2, X3, … Xn, …} will change at a constant angular velocity proportional to $2\pi\Delta f/T0$. Assuming these values are reported in real time, the phase angle will increase continuously until it reaches 180 degrees where these would wrap around to –180 degrees, and continue to increase, as shown in Figure 3.6. It should be noted that in synchrophasors, the angles commonly reported are from –180 degrees to +180 degrees rather than 0 to 360 degrees.

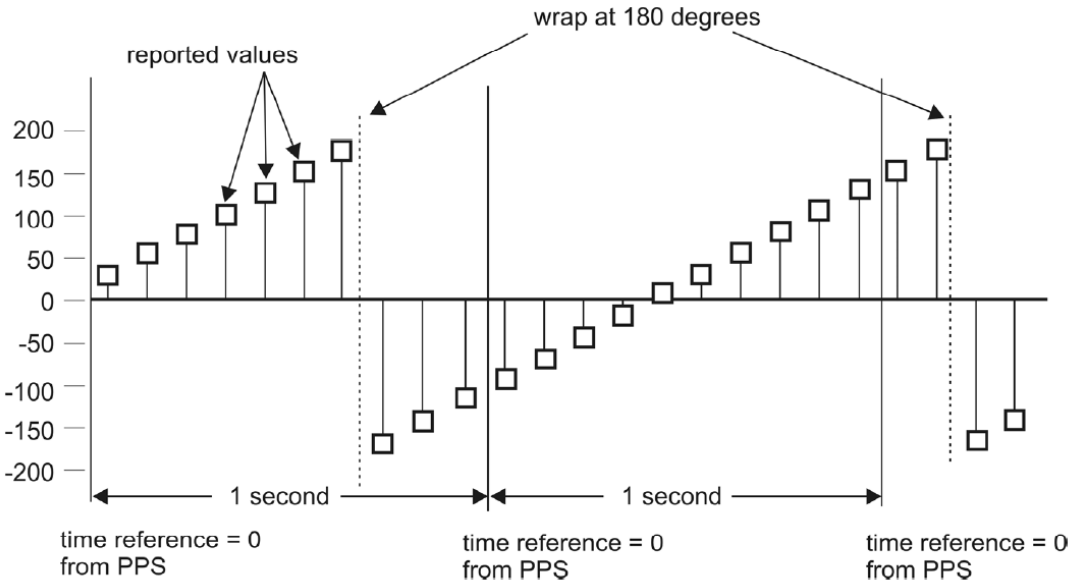

Figure 3.6. Off Nominal Power Frequency Sampling

3.3 Signal Processing

Figure 3.7 shows a simplified functional block diagram of a typical PMU. Before the phasor to be computed, the analog signal must go through the conversion. In the numerical process, the analogue signal is measured though several sampled values per cycle of the original signal. This part of PMU functionality is like any IED or digital fault recorder device where the analog signal must be measured based on sequential samples over the time.

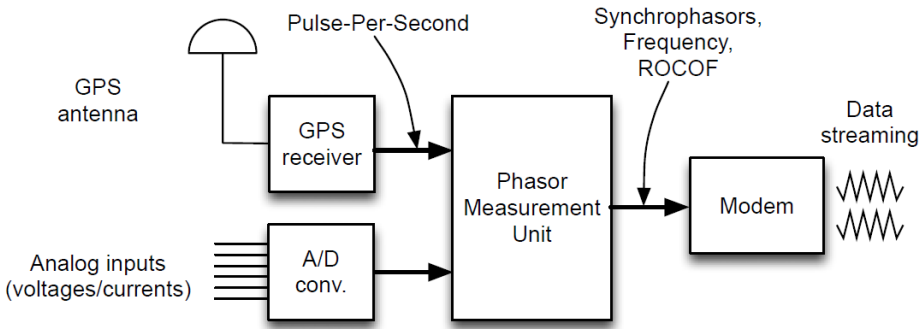

Figure 3.7. Typical PMU Configuration

The phasor of the main frequency component is estimated by use of Discrete Fourier Transform (DFT) or Fast Fourier Transform (FFT).

The DFT is the equivalent of the continuous Fourier transform for signals known by only N instants separated by sample time of ΔT. If f(t) is an arbitrary analog (continuous) input signal which is the source of the data and f[0], f[2], …,f[N-1] are the N samples. The Fourier transform of signal f(t) can be written as follows:

$$F(j\omega) = \int_{-\infty}^{\infty} f(t)e^{-j\omega t}dt \qquad (3.9)$$

If we regard each sample as an impulse having area f[k] which is f(k)*ΔT, then, (3.9) can exist only at the sample points:

$$F(j\omega) = f[0]e^{-j0} + f[1]e^{-j\omega\Delta T} + \cdots + f[N-1]e^{-j\omega(N-1)\Delta T}$$

$$F(j\omega) = \sum_{K=0}^{N-1} f[K]e^{-j\omega K\Delta T} \qquad (3.10)$$

For fundamental frequency and its harmonic (including the DC components ($\boldsymbol{\omega}$=0) of the original signal),

$$\Omega = 0, \frac{2\pi}{NT}, 2\ \frac{2\pi}{NT} \dots, (N-1)\frac{2\pi}{NT}$$

$$F(n) = \sum_{K=0}^{N-1} f[K] e^{-j\frac{2\pi}{N}nK} \quad (n = 0 : N-1)$$

In principle, (3.10) can be used for any $\boldsymbol{\omega}$ with only N samples. Sampling data from the input signal is the start of the process to estimate the phasor. Over the years, several considerations and techniques have been developed to digitalize the analog signal for precise representation, which is described briefly in this section.

3.3.1 Nyquist Frequency and Anti-Aliasing Filter

An analog signal is acquired by PMU or any IED through the Analog to Digital conversion where the analog signal sample is taken based on a sampling rate. The aliasing concept is totally dependent on this sampling rate. If the sampling rate is not sufficient, aliasing problems occur during the reconstruction of the sampled signal while converting the digital signal into the analog signal. According to Nyquist's sampling theorem, the sampling rate must be at least twice the bandwidth of the analog signal at the beginning of the sampling procedure to be able to reconstruct the sampled signal. In other words, if the analog signal is a periodic signal, at least two points must be sampled in one period. Figure 3.8 shows the impact of the sampling rate in capturing the information of the input signal. As shown, the sample rate must be greater than or equal to two times of highest frequency component in the input signal. The limit where the maximum frequency component in a sampled data system can accurately be handled is known as the Nyquist limit.

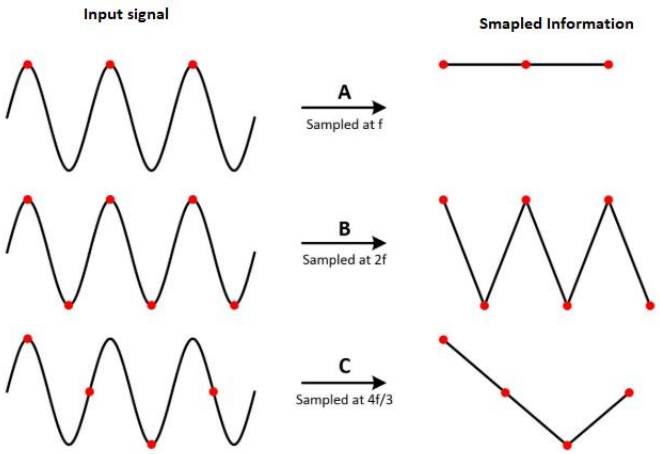

Figure 3.8. Impact of Signal Sampling Rate On A/D Conversion

In the actual devices the high frequency components of the input signal that are not within the Nyquist limit will be cut off during the signal processing by anti-aliasing filter.

3.4 Phasor and Frequency Estimation

As presented earlier, phasor "V" is a representation of sine waves whose amplitude (A), phase (φ), and angular frequency (***ω***) is time variable.

$$V(t) = A.\cos(\omega t + \varphi) = A.\mathrm{Re}\{e^{j(\omega t+\varphi)}\} \tag{3.11}$$

$$V = A\measuredangle\varphi$$

In power systems, however, amplitude (A), phase (φ), and angular frequency (***ω***) are time-based variables. Therefore, the phasors for power systems should be estimated in time-based processed signals, such as voltage and current, which will be estimated for a window in a time-based manner and the estimation will be updated, as shown in Figure 3.9.

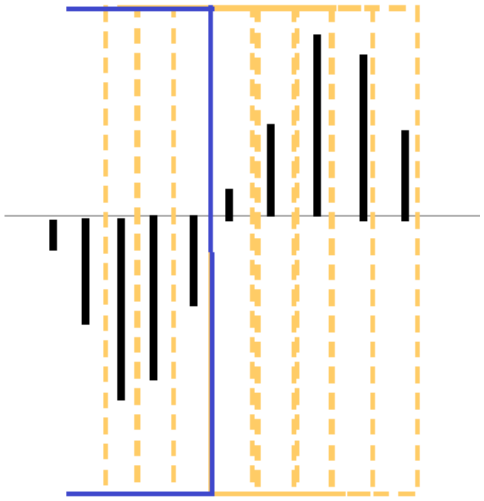

Figure 3.9. Phasor Estimation Windows

A few numbers of techniques have been developed over the years related to real time phasor estimation. The short and long windows for phasor estimation are the main categories that are known in this area. The short windows algorithm, such as Miki and Mikano, Mann and Morrison, Rockefeller and Urden, and long windows algorithm, such as DFT, LES, can be noted.

3.4.1 Short Windows Phasor Estimation

Short windows-based estimation has a fast-transient response and fewer computations; however, when the input signal contains harmonics, DC, and noise, it tends to impact the performance of the short windows-based estimation. Figure 3.10 illustrates Miki and Mikano short-window phasor data windows with two samples.

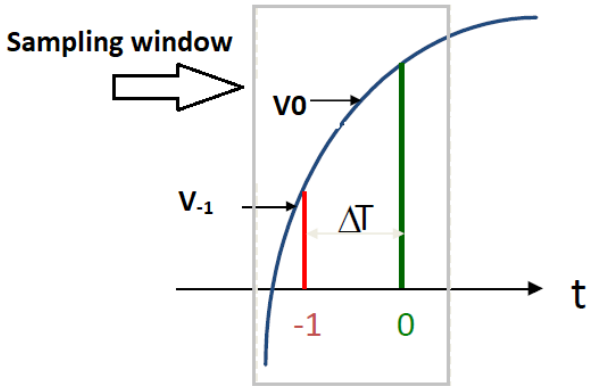

Figure 3.10. Phasor Estimation

At time t= 0 and t= -1, the following can be formulated:

$$V_0 = V_p \cos(\emptyset) \tag{3.12}$$

$$V_{-1} = V_p \cos(-\omega\Delta T + \emptyset)$$

$$V_{-1} = V_p \{\cos(\omega\Delta T)\cos(\emptyset) - \sin(\omega\Delta T)\sin(\emptyset)\}$$

$$V_p \sin(\emptyset) = \frac{[V_{-1} - V_0 \cos(\omega\Delta T)]}{\sin(\omega\Delta T)} \tag{3.13}$$

From equation (3.12) and (3.13), real and imaginary parts of the phasor can be calculated, and accordingly, their magnitude and angle :

$$V_p = \sqrt{V_0^2 + \left[\frac{V_{-1} - V_0 \cos(-\omega\Delta T)}{\sin(-\omega\Delta T)}\right]^2} \tag{3.14}$$

$$\emptyset = \tan^{-1} \frac{\sin(\omega\Delta T)}{V_0} \tag{3.15}$$

3.4.2 Long Windows Phasor Estimation

For the long window-based estimation using DFT, the phasor can be formulated based on sample data measured from the input signal for any sampled value using (3.17) or fundamental frequency using (3.19) which is of prime interest in phasor measurement.

$$X_k = \frac{2}{N}\sum_{n=0}^{N-1} X[n] e^{\frac{j2\pi}{N}kn} \qquad k = 0,..,N-1 \qquad (3.16)$$

$$X[n] = \sum_{n=0}^{N-1} X_k e^{\frac{j2\pi}{N}kn} \qquad n = 0,..,N-1$$

$$A_k = X_k = \sqrt{Re(X_k)^2 + Im(X_k)^2} \qquad k = 0,..,N-1 \qquad (3.17)$$

$$\Phi_k = \tan^{-1}(X_k)$$

And phasor for fundamental frequency can be simplified as follows:

$$X_1 = \frac{2}{N}\sum_{n=0}^{N-1} X_n e^{\frac{j2\pi}{N}n} \qquad k = 0,..,N-1 \qquad (3.18)$$

$$X_1 = \frac{1}{N}\sum_{n=0}^{N-1} X_n \cos\left(\frac{2\pi}{N}n\right) + j\frac{1}{N}\sum_{0}^{N-1} X_n \sin\left(\frac{2\pi}{N}n\right) \qquad n = 0,..,N-1$$

$$A_1 = \sqrt{\left\{\frac{1}{N}\sum_{n=0}^{N-1} X_n \cos\left(\frac{2\pi}{N}n\right)\right\}^2 + \left\{j\frac{1}{N}\sum_{n=0}^{N-1} X_n \sin\left(\frac{2\pi}{N}n\right)\right\}^2} \qquad n = 0,..,N-1 \qquad (3.19)$$

$$\emptyset_1 = \tan^{-1}\left(\sum_{n=0}^{N-1} X_n \cos\left(\frac{2\pi}{N}n\right) + j\sum_{0}^{N-1} X_n \sin\left(\frac{2\pi}{N}n\right)\right) \qquad n = 0,..,N-1$$

In recent years, much research has been done to improve phasor estimation and how the estimation should be updated for the real time application. The windows of data acquisition must move forward with the objective of using phasor-based measurement for transient study, fast power system phenomenon, such as protection. In [22], the authors propose an improved DFT to immunize the accuracy of DFT phasor estimation from the presence of DC component (short circuits scenarios). In [23], a dynamic current phasor measurement is presented to deal with the noise in current signals. In [24], a method to estimate the phasor for off-frequency based on Taylor series is proposed. In [25], [26], and [27] more studies have been done to present phasor estimation for protection and time critical application.

3.5 Frequency Estimation

The PMU is required to measure instantaneous voltage, current, and estimate phase angle frequency and rate of change of frequency of voltage & current signals. One of the main

reasons behind the estimation of frequency is the fact that if the frequency is not known, the phasor estimation itself is not accurate.

LES-based Frequency Estimation: The Least Square Frequency Estimation technique is an accurate when the deviation of the frequency is small from the rated frequency; however, it is sensitive to harmonic components.

Zero Crossing: This method monitors timing between the wave from zero crossing in the negative and positive half wave in order to estimate the frequency of the phasor in the predetermined time interval.

3.6 Communication and Reporting the Data

PMUs are capable of reporting phasor data from nominal and off-nominal frequency by providing single-phase and multi-phase data at multiples and submultiples of rated frequency, which must be supported by the PMU. The rate will be selected by user, and higher and lower rate will also be permitted depending on the need of the application. Table 3-2 presents the reporting rate that is identified by the standard [28] that must be supported by the PMU. The rate will be selected by the user, and higher and lower rates will also be permitted depending on the need of the application.

Table 3-2. PMU Reporting Rates

System Frequency	50 Hz			60Hz					
Reporting rates (F_s—Frame per second)	10	25	50	10	12	15	20	30	60

The essence of synchrophasor measurements is to gather PMU information from different nodes in the power system that are far from each other and to be able compare the information. Figure 3.11 presents the conventional communication system architecture for wide area application. IEEE C37.118.2 standard specifies a method that a synchronized phasor measurement data between PMU and PDC with any suitable protocol for real-time communication can be used. It also defines the message types, contents, and data formats, as well as communication options and requirements.

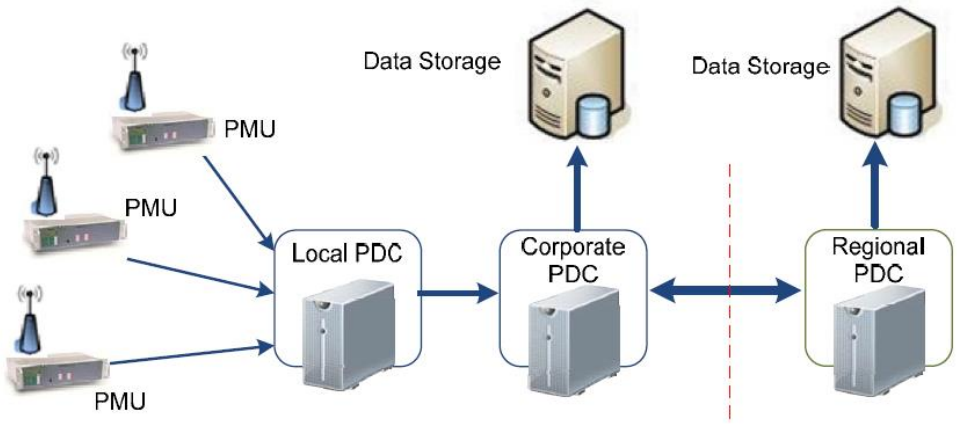

Figure 3.11. Conventional Phasor Measurement Communication Architecture [29]

All message frames start with a 2-byte SYNC word followed by a 2-byte FRAMESIZE word, a 2-byte IDCODE, a time stamp consisting of a 4-byte Second-Of-Century (SOC), and 4-byte FRACSEC, which includes a 24-bit FRACSEC integer and an 8-bit Time Quality flag. All frames are transmitted exactly as described with no delimiters. Figure 3.12 illustrates this frame transmission order. The SYNC word is transmitted first and CHECK word last.

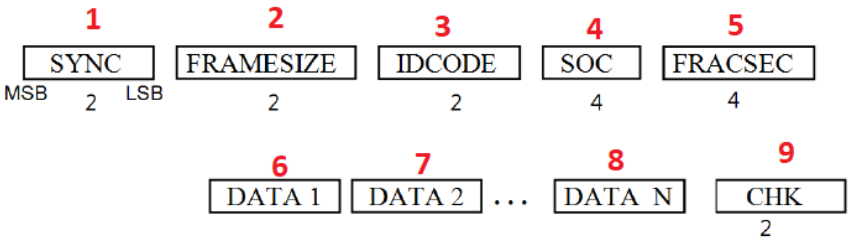

Figure 3.12. Communication Example C37.118-2 Frame

For time critical applications, time delay and device performance are important.

Table 3-3 presents the typical range of time delay in processing and communication that can be expected for typical PMU based applications.

Table 3-3. Typical Delay Range for PMU Application [28]

Cause of delay	**Typical range of delay**
Sampling window (delay of ½ windows)	17 ms to 100 ms
Measuring filtering	8 ms to 100 ms
PMU processing	0.02ms to 30 ms
PDC processing and alignment	2 ms to2 sec
Serializing output	0.05 ms to 20 ms
Communication system I/O	0.05 ms to 30 ms
Communication distance	3.4 $\frac{\mu s}{km}$ to 6 $\frac{\mu s}{km}$
Communication system buffering and error correction	0.05 ms to 8 sec
Application input	0.05 ms to 5 ms

In line with hardware advancements that have been made in the last couple of decades in terms of how the PMU and PDC perform, the communication media, such as LAN (Local Area Network), Ethernet-based communication with speed of 1.00GB/sec or faster, have replaced serial type communication in utilities-based applications. In this regard compliance of Phasor measurement data with IEC IEC61850-90-5 standard created the possibility of using time critical communication services, such as GOOSE message (General Object-Oriented Substation Event) and Sample Value (SV), that is defined by this standard series and managed IEC Technical Committee 57 (TC57) to be available for time critical application such as protection in substation . IEC/TR 61850-90-5 [30] provides a way of exchanging synchrophasor data between PMUs, PDCs WAMPAC (Wide Area Monitoring, Protection, and Control), and between control center applications. The data,

to the extent covered in IEEE C37.118-2005, is transported in a way that is compliant with the concepts of IEC 61850. However, given the primary scope and use cases, this document also provides routable profiles for IEC 61850-8-1 GOOSE [31] and IEC 61850-9-2 SV [32] packets which can be used to transfer synchrophasor data using GOOSE (General Object-Oriented Substation Event) message over WAN (Wide Area Network). To summarize the rule and relation of IEC and IEEE standard in the context of synchrophasor measurement and application IEEE C37.118.1 remains the global standard for defining the measurement technology for synchrophasor while IEEE C37.118.2 is the IEEE protocol to address current system requirements enabling IEC TR 61850-90-5 to be the basis for a more scalable, and secure, protocol to meet application requirements.

Figure 3.13 shows the synchrophasor communication architecture based on IEC61850-90-5. As shown here, the communication relation between PMUs and PDC is based on publishing and subscribing relationship over the Wide Area Network. The first advantage of being able to use time critical communication services of IEC61850, such as SV or GOOSE, is the availability of PMU data streams in the entire network when it is published, with no requirement for intermediate devices. This design especially benefits the performance and elimination of PDC for small applications which is proposed by the current research.

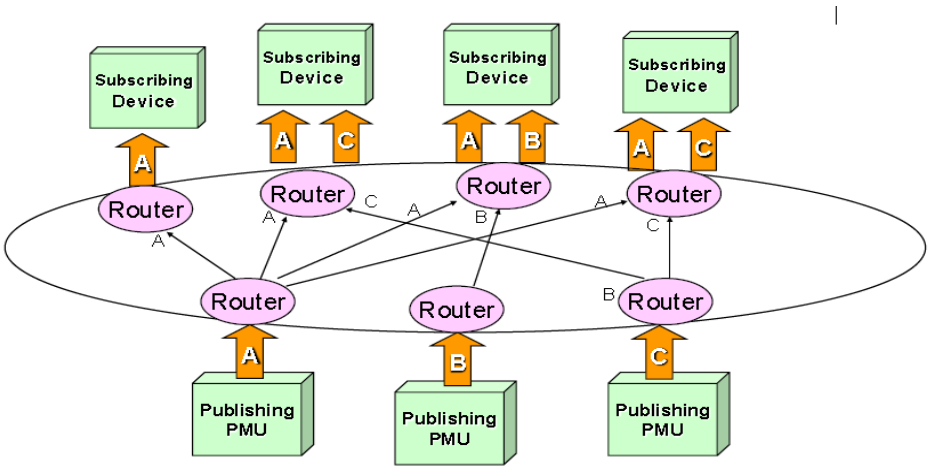

Figure 3.13. Synchrophasor IEC61850-90-5 Based System Architecture

In Appendix B more information related to the peer to peer communication services in IEC61850 standard is described.

3.7 PMU Applications in Distribution Systems

Historically, synchrophasor measurements were implemented in bulk power applications in transmission system with conventional generation. In recent years, and shortly after August 2003 North American blackout [33] and some more in Europe [34], more attention and research work was drawn to the field of Wide-Area Measurement System (WAMS) with the objective of serving and improving monitoring, protection, and control of power networks [35]. Primarily, PMU is used for power system state estimation [36]; however, a lot of research is still expected for the large-scale systems and accurate estimation. Most research has been focused in the area of time critical applications, such as protection. [37]. Use of synchrophasor measurement in some of the distribution applications, which is the focus of this work is gradually getting more attention from researchers and technology providers

Conventionally, the distribution systems were assumed to be simple and posed little need to be observed with granularity in space and time. The measuring sensors implemented in the feeder almost uniquely were limited to the substation location only. Most of the control and protection applications have been developed based on the accessibility of measurements only back at the substation. However, with the transformation of the energy sector and rapid growth in deployment of distributed energy resources, bi-directional electricity flows, and new devices, such as electric vehicles, there is a growing interest and requirement for observation tools along the feeder for significantly impacted distribution feeders. Therefore, PMU, as an integrated function in IED, can play an important role in redefining many distribution management system functionalities which were based on limited data. In the current work, islanding, and open phase fault in the distribution overhead line are targeted and developed.

3.7.1 Micro-PMU Development

PMUs specifically designed for use in distribution systems are sometimes referred to as D-PMUs, or as micro-PMUs (μPMUs) [38]. It should be noted that the term μPMU is not a

trademark and is originated by Advanced Research Projects Agency-Energy (ARPA-E) led by the University of California Berkeley and funded by the US Department of Energy. The μPMU is a generic term used for extremely high precision power disturbance recorder adapted for making voltage phase angle or synchrophasor measurements, capable of storing, analyzing and communicating data live. The resolution of this device is roughly 100 times more than the IEEE PMU and the phase angle accuracy is 0.01 degrees versus 1 degree. The motivation for developing such a device can be summarize as follows:

1) In distribution systems, because of the direct interface to loads, there are many more branches, short lines, and a high density of electronics have a more elevated noise-to-signal ratio compared to the transmission system. Thus, higher resolution measurement will be useful in distribution systems.
2) To determine the small power flow in distribution systems, more precise angle measurement will be required.
3) Unlike the transmission grid, where reactance value (X) is dominated the impedance, in distribution feeders resistance (R) value is significant and in some parts even the parallel capacitance due to underground cables cannot be neglected, therefore, a more complex representation of the impedance will be required to have a visibility over the network.
4) Generally, the change of voltage angle along the distribution system is small thus, being able to measure tenth of degree can support some applications.

Not all the applications in distribution system required the high-performance PMU application. In this work islanding and open phase is studied in chapter 4 and chapter 5. The proposed islanding method has considered the limitation of IEEE PMU. While the proposed open phase is not requiring the voltage or current phase angle measurement the minimum requirement phase angle measurement for islanding for the stable measurement is considered to be one degree. Table 3-4 presents some application class for distribution PMU with the high accuracy and resolution.

Table 3-4. Expected Data Requirement for μPMU Application [39]

Application	Measurement quantity	Time resolution	Accuracy	Note

Voltage Magnitude profile	Voltage magnitude	1 sec	0.5 %	Voltage phase angle useful for understanding tap changes
Real time load awareness	Current magnitude	1 cycle	0.5 %	
Outgas management	Voltage and current magnitude	1 sec	1%	
State estimation	Voltage phasor	Time synchronization is critical	Very high accuracy required 0.00001 PU	
Micro-grid islanding	Voltage phase angle	1 cycle	0.01 degree	
Model validation	Voltage and current phasor	Time synchronization is critical	0.5 %	

The availability of PMU data with the higher resolution can potentially increase the sensitivity of the proposed solutions however, the amount of data that must be transferred cannot be handled by the current available market devices and communication infrastructure. The islanding application in this work is intended to be used by utilities as backup for the local islanding protection scheme and to replace the transfer trip. Therefor this application is not intended for Microgrid or small size DG applications (2MW and above) and as such the high-resolution PMU will not provide its full benefit.

3.8 Summary

The fundamentals of synchronized phasor measurement system architecture were presented in this chapter. The functionality of phasor measurement unit (PMU), data

concentrator, and GPS were discussed, and the history of the early PMU and advancement of phasor measurement technology was presented. It was shown that along with IEEE C37.118 restructuring in recent years, the technology as well as the standard, are more prepared to support the real time application of control and protection.

The flow of analogue signal and its process in PMU hardware was also studied in this chapter. Various phasor and frequency estimation techniques were looked. The communication aspect of synchronized phasor measurement unit and phasor data concentrator was studied. The new communication standard of IEC61850-90-5 and the possibility of the integration of the synchrophasor data stream with the substation automation data was presented. The implication of using of IEC61850-90-5 and GOOSE messages in peer to peer communication between the PMUs and the elimination of PDC, especially in the distribution systems, was discussed. Measurement was discussed in this chapter as well. The motivation behind the call for use of synchrophasor data (by this work) in the distribution protection application using substation automation infrastructure was presented.

The development of μPMU with high accuracy and high resolution was reviewed, along with the difficulty of measurement in distribution systems and the accuracy required for them. The possible conceptual application of high performance synchrophasor is reviewed. In the next chapter, the islanding detection use case for distribution feeder, including the background, critical review of the state of the art, issue formulation, development of a solution, and modeling and test system will be discussed.

Chapter 4

4 Adaptive Islanding Scheme

In this chapter, the proposed islanding detection method for distribution system is presented.

4.1 Introduction

Utilities' main concern behind islanding operations in the distribution network is safety and the lack of adequate infrastructure that can monitor and control the operation of DGs within the islands in a reliable manner. Thus, in the current stage of distribution modernization, it is broadly taken for granted that the island is an unregulated power system that has behaves unpredictably. Voltage and frequency in the islanded area can significantly deviate from the acceptable range since utilities have no means to curb the power mismatch between the DG production capacity and the load(s) connected to the island.

One of the most commonly used passive islanding methods consists of detection of under-, over-, and rate of frequency variations. The primary concerns and limitations of the local passive detection methods are that these methods cause an operating region where, in that specific region, islanding conditions cannot be found or detected in a timely manner. This region is known as the Non-Detection Zone (NDZ). Similar NDZ regions can be identified among many passive detection techniques which have been the topic of much research. There is no single passive method that can be effective in all scenarios and the Power Systems Community is undecided on what type of islanding detection should be used. For example, IEEE standards 1547-2003 and 929-2000 specify the performance characteristics of the islanding detection methods with detailed test circuits that can be used to validate the method considered. Issues related to the passive islanding techniques can be summarized as follows:

1) The Non-Detection Zone is a major concern in deploying a passive scheme; there is no single passive method which can work in all scenarios. Hence, evaluation of the NDZ region and the probability of island occurrence need to be verified.

2) Broadly speaking, the performance of passive islanding methods shows a dependency on the type of DG installed in the distribution network. Therefore, dependability and the security of an island detection scheme may vary from one application to another.

3) Most of the work in this area has been conducted around low DG penetration or single DG island detection cases, while higher DG penetration cases can further enlarge the NDZ and affect the security and dependability of the schemes.

4.2 Islanding

Prior to reviewing islanding detection techniques and their significance, it is appropriate to define the term islanding. Islanding is a generic term used to describe a scenario in which a section of a transmission, or distribution network (which contains DG) is separated from the rest of the grid. This separation is often caused by the action of the protective relays to clear and isolate the electrical fault. Subsequent to this separation, the DG restarts or continues to power the loads trapped within the island [40]. Figure 4.1 illustrates a typical North American distribution feeder with a few DGs, a step-down substation with several outgoing distribution feeders, and one of the outgoing distribution feeders shown in detail.

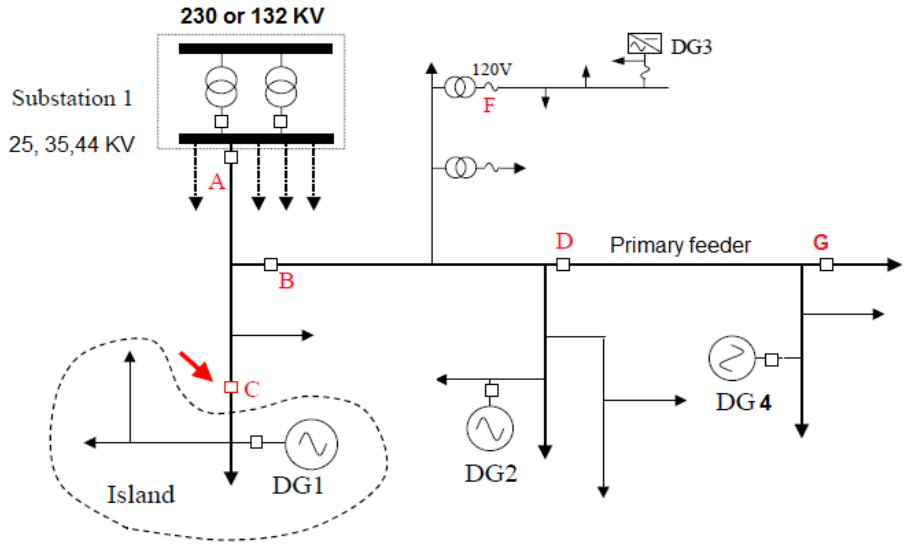

Figure 4.1. Typical Primary Distribution Feeder Topology in North America

An islanding situation occurs, for instance, when recloser C opens while DG1 is still feeding the load and an island is created as a result of the recloser operation. The utility's main concern behind the islanding operation in the distribution network is safety and the lack of adequate infrastructure which can monitor and control the operation of DGs within the islands in a reliable manner. Thus, in the current stage of distribution modernization, it is broadly taken for granted that the island is an unregulated power system. Its behavior is unpredictable and voltage and frequency in the islanded area can significantly deviate from the acceptable range, since utilities have no means to curb the power mismatch between DG production capacity and load connected to the island. The main concern for such an operation among utilities can be listed as follows [41]:

1) The quality of power fed to an islanding portion of feeder may be lower compared to when the power is supplied by the utility. The range of voltage and frequency in the islanded portion of the feeder is a main concern since the supply utility is no longer controlling the voltage and frequency delivered to their customers and any excursion from expected boundaries of voltage and frequency can cause considerable damage to customers' equipment within the island.
2) An islanding operation may also create a hazard for line-workers or the public by causing a line to remain energized that may have been assumed to be disconnected from all energy sources.
3) The likelihood of the islanded portion not being in phase with the network voltage and phases, at the instant when the islanded portion is reconnected through reclosing or an automation, is a real concern. This can damage the generating equipment and DGs in the island. Ultimately, such an attempt of restoration may fail.
4) Islanding may interfere with the manual or automatic restoration of feeder or cause issues for neighboring customers and can complicate loop operation of feeders.

4.3 Review of Current Islanding Detection Techniques

As depicted in Figure 4.2, islanding detection techniques developed so far can be fundamentally split into two categories according to their working principles. The first type consists of communication-based schemes and the second type consists of non-communication-based schemes, which also is known as a local based scheme.

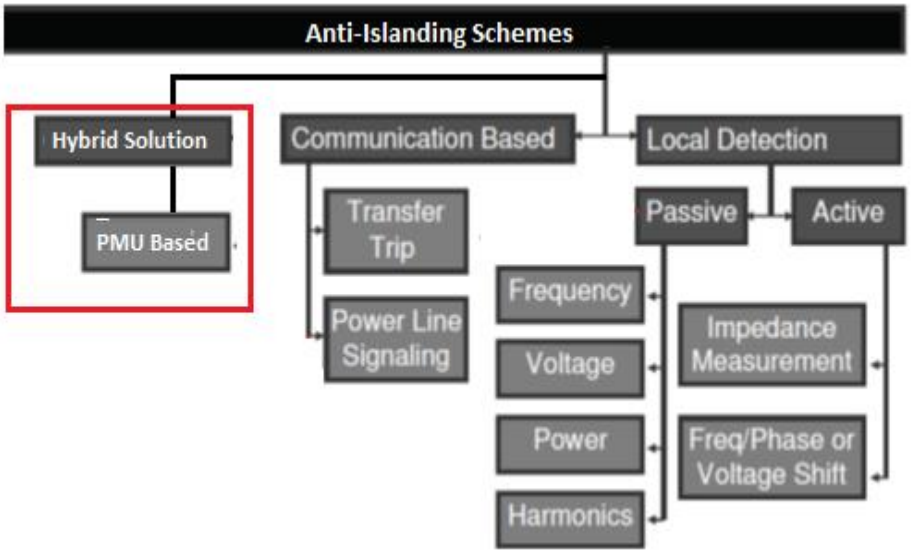

Figure 4.2. Classification of Islanding Detection Scheme **[42]**

The PMU based islanding proposed by this work is a hybrid solution which does not fit in one category since it uses combination of techniques, as follows:

- The measurement in this solution is a passive type and active power and frequency are monitored.
- The measurement process relies on the local PCCs and remote communication therefore communication is an important part of this solution.

4.4 Communication Based Schemes

Communication based schemes rely on telecommunication data transfer in order to detect the islanding and trip DGs when islands are formed. The performance of these methods is generally independent of the type of distributed generators integrated into the feeder.

4.4.1 Transfer Trip

The transfer trip scheme is very simple in concept and is considered a utility preferred choice for simple feeder topology and a large farm. This method requires all circuit breakers and reclosers (which can island the DG) to be monitored and linked to the central unit, as shown in Figure 4.3. When disconnection (CB open status) is detected, the central algorithm determines the islanded area and sends a trip signal to the appropriate DG to shut down the unintended island. Issues related to this method are reported in a few papers [41], [43], [44] and can be summarized as follows:

1) The method requires an extensive communication network in the distribution system. Traditionally, such an infrastructure does not exist and therefore, the cost factor needs to be considered.
2) The method is based on feeder topology and determining the islanded area by monitoring all the switching points, which can get very complicated, especially if loop operation along with neighboring feeders is permitted. On the other hand, flexible operation of the feeder, which will most likely be a future requirement of the smart grid and advanced distribution network, will be very hard to achieve with this method.

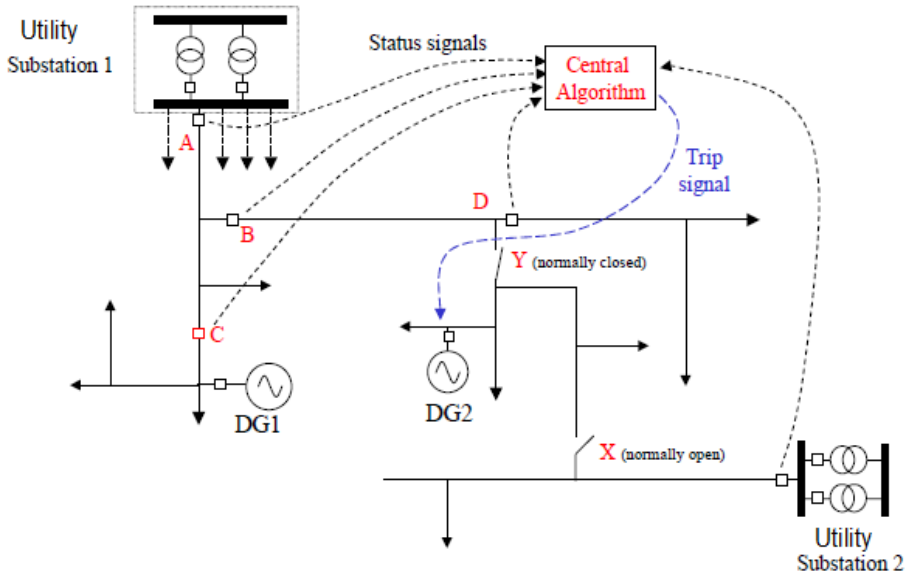

Figure 4.3. Transfer Trip Concept [45]

4.4.2 PLC Signaling

As presented in Figure 4.4, the signal generator located at the utility substation is continuously broadcasting a patterned signal to the signal detectors of all distributed generators. When islanding occurs, the signal will no longer be available to DGs and subsequently, a local trip will be issued to shut down the generator.

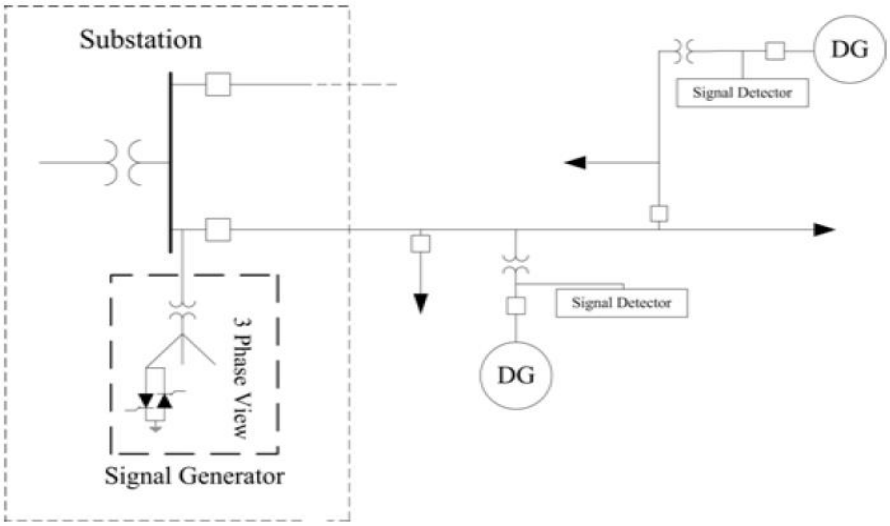

Figure 4.4. Power Line Signal Islanding

Issues related to this method are reported in various literature and can be summarized as follows:

1) Cost is the major concern here, as the Power Line signal must be transmitted in all three phases in order to detect single phase islanding.
2) The transmitted signal must be re-attenuated along the way if the distances from the station to the DG or Point of Common Coupling (PCC), are longer than 15 Km [46].
3) The reliability of this method, with the presence of inter-circuit harmonic pollution, is another concern which is solicited in different research work.

4.5 Local Detection

Local refers to the DG and PCC side, and local detection schemes detect the occurrence of islanding based on frequency, power, and current signals available from the DG. As shown earlier in Figure 4.2, the local detection group is further split into two sub-groups. One is known as a passive detection method, which arrives at decisions based on electrical signals measurements (V, I, F, etc.). The second group is known as the active detection method. These methods inject an electrical signal into the supply system and detect islanding conditions based on system responses measured locally at the PCC.

4.5.1 Passive Detection Methods

The passive method detects islanding based on monitoring the current, voltage, or other properties of the electrical signal such as frequency, harmonic, etc. available on the DG side. One of the most commonly used passive islanding methods consists of under-, over- and rate of alteration of frequency-based detection. The primary concern and limitation with the local passive detection methods is that these methods cause an operating region where, in that region, an islanding condition cannot be found or cannot be detected in a timely manner. This region is known as the Non-Detection Zone (NDZ). As an example, Figure 4.5 shows the area where if the power mismatch between an arbitrary synchronous type DG and the load is not greater than a certain value, the frequency-based islanding scheme will not work.

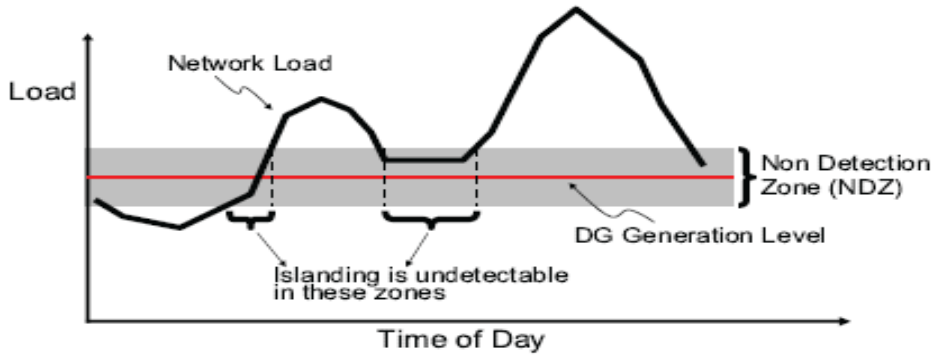

Figure 4.5. None Detection Zone Based Daily Profile Variation

The generation profile of the DG varies during the day and in many operational instances, the islanding scheme will not work. Besides frequency, other power quantities can also be used to help detect island situations such as:

1) Voltage based detection
2) Power factor (P/Q)
3) Change of active power
4) Change of reactive power
5) Change of total harmonic distortion (THD)
6) Built in inverter-based islanding techniques

Reference [47] proposes the use of reactive power rate of change to detect the islanding. The method can be useful for relatively when a large amount of DG is integrated to grid and issue of NDZ has not much of importance. In recent years many hybrid methods based on combination of the passive techniques mostly integrated into the inverter-based devices are developed. [48] proposes monitoring of voltage and current magnitude together with current and voltage THD at PCC.

Among the above-mentioned schemes, the voltage-based detection method is most commonly used in the industry. The relay operates on the principle of reactive power mismatch in an island. Excessive reactive power will drive up the system voltage and deficit reactive power will result in voltage decline. By determining the change or rate of change of the voltage at the DG terminal, it is possible to detect islanding conditions that cannot be detected by frequency-based relays.

4.6 Active Detection Method

Active detection schemes rely on injecting disturbances into the supply system to detect the islanding situation. The mainstream active methods studied in the industry can be listed as follows:

a) Impedance measurement
b) Impedance measurement at specific frequency
c) Frequency ship mode
d) Frequency bias or AFD
e) Sandia frequency and voltage shift
f) Current injection methods

Many technical problems need to be solved before one can use them with confidence. Some of the issues related to active methods are reported in various literature [40], [46], and are as follows:

1) One of the main problems of the active methods is the interference of disturbances introduced by multiple DGs. Not much research has been conducted on such issues.
2) The type of active islanding detection method which can be deployed is very much dependent on the type of DG installed in the network. The design of a universal active method solution which can cover a range of installations is very difficult if not impossible. Therefore, this scheme generally has low adaptability.
3) Generally active methods can have a negative impact on the grid power quality compare to the passive methods.

4.7 Grid Tied Inverter Anti-Islanding Consideration

With the many advancements in the design and manufacturing of the grid tied inverters, state of the art technology today comes with anti-islanding, Low Voltage Ride Through (LVRT), and Maximum Power Point Tracking (MPPT) embedded functionalities. Some of the techniques that are used to develop anti-islanding are public information. As an example, [49] suggests that islanding can be detected, if the inverter output voltage or inverter output frequency is driven outside of the normal range. In [50], frequency profile of non-islanding events is identified as an oscillating event in nature, whereas islanding

event frequency profile is monotonically increasing or decreasing. This particular property is used to develop anti-islanding protection scheme. In [51], the rate of frequency is used to detect the islanding event. It should be noted that inverters are part of the DER system and they are mainly the property of the market participants (DER owner), The focus of this work, however, is to provide the utility based solution that can be used as main or back up protection in order to assure that utility costumer and assets will be protected by the system owned and maintained by them.

4.8 Proposed Islanding Detection Method

The proposed method in this paper relies on measuring the active power (P), reactive power (Q), bus voltages (Vrms), voltage phase angle (phi), and frequency measurement from any Point of Common Coupling (PCC) where distributed generation is installed along the feeder and station bus which is supplying the feeder from the grid, as shown in Figure 4.6. The PMU functions as a standalone device or as a function incorporated in the protection or control Intelligent Electronic Devices (IED). The PMU will be used to provide a data stream of above-mentioned values that will serve to calculate a required setting sensitivity for the 81, 59, and 27 protection elements and the voltage phase angle rate of change to detect an islanding event. The measurement and calculation are performed prior to the islanding event and the IED’s protection setting can be adapted to the new setting if it is required.

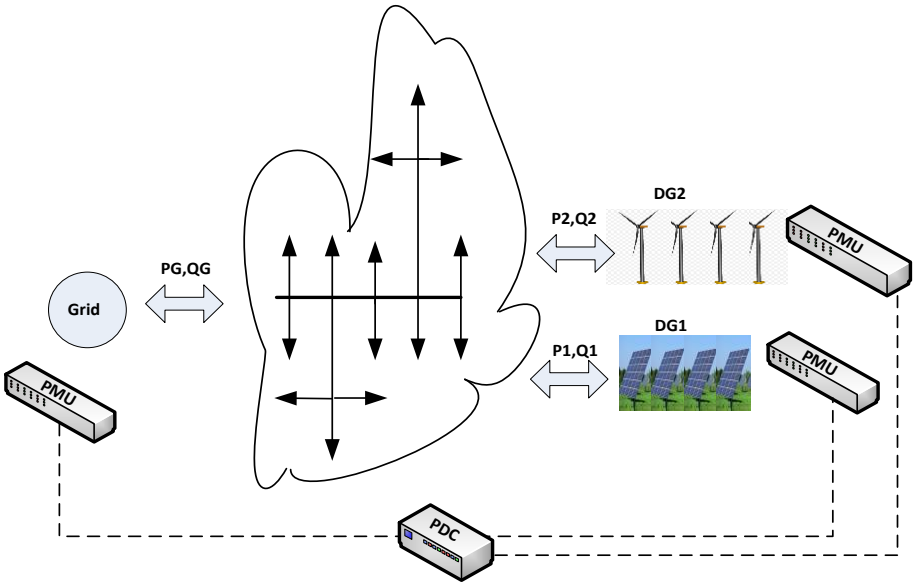

Figure 4.6. Conceptual PMU Based Islanding Detection Architecture

The islanding event is modeled as a small power perturbation where the primary feeder losses the grid supply and the feeders are then supplied power by the DGs.

Table 4-1. Parameter and Unit for Power Mismatch Scenarios

Symbol	**Quantity**	**UNIT [SI]**
D	Damping constant expressed as percentage change in load for one percent change in frequency	PU typical value 1-2%
f	Power system frequency	PU (Hz)
Δfss	steady state frequency deviation	PU (Hz)
H	machine Inertia constant	sec
P_{DG}	DG active power	PU (MW)

P_{Grid}	Grid active power	PU (MW)
Q_{DG}	DG reactive power	PU (MVar))
Q_{GRID}	Grid reactive power	PU (MVar)
T	Electrical torque	PU (MW/rpm)
Tm	Mechanical torque	Pu (MW/rpm)
tss	Settling time	sec
w	Angular velocity	PU (rpm)
S	Laplace operator	

The proposed method uses continuous measurement of active and reactive power at the substation (supply by grid) and the distributed generation (supply by DGs) prior to the islanding event to determine the power mismatch between the load of the feeder and generation located at the feeder. Based on this information, the sensitivity of the aforementioned protection elements that detect the islanding will be adapted accordingly. If we consider the power loss as a part of the feeder load change, the following can be stated at the instance of islanding event, $\mathbf{P_{Grid} = 0}$ considering the generator response to speed change equation (4.1) as follows:

$$\Delta T_m - \Delta T_e = \frac{1}{2HS}\omega \quad (4.1)$$

$$P_{DG} = P_{Load} - P_{Grid} \quad (4.2)$$

$$P_{DG} = \Delta P_{Load} - \Delta P_{Grid} \quad (4.3)$$

$$P_{DG} = P_{DG0} + \Delta P_{DG} = (\omega_0 + \Delta\omega)(T_0 + \Delta T) \quad (4.4)$$

$$\Delta P_{DG} \approx (\omega_0 \Delta T + \Delta\omega)(T_0 + \Delta T) \quad (4.5)$$

$$\Delta P_{mDG} - \Delta P_{DG} = \omega_0(\Delta T_m - \Delta T_e) + \omega(\Delta T_{m0} - \Delta T_{e0}) \quad (4.6)$$

In the steady state, $\omega_0 = 1$ pu , $T_m = T_e$, and in the absence of speed governor $\mathbf{\Delta P_{mDG} = 0}$ and it is assumed that the feeder load is constant during the islanding event $\mathbf{\Delta P_{Load} = 0}$.

Therefore, the system response to load change ($\mathbf{P_{Grid} = 0}$) is determined by the machine inertia constant.

$$\Delta P_{mDG} - \Delta P_{DG} = \Delta P_{Load} - \Delta P_{Grid} \quad (4.7)$$

$$-\Delta P_{DG} = (\Delta P_{Load} - \Delta P_{Grid}) + D\Delta\omega \quad (4.8)$$

For the load step load change equal to equal to $-\Delta P_{Grid}$ and from (4.1) and (4.8)

$$-(-\Delta P_{Grid}) = \left(\frac{1}{2HS+D}\right)\Delta\omega \quad (4.9)$$

$$\Delta\omega_{ss} = \frac{\Delta P_{Grid}}{D}, \qquad \tau = \frac{2H}{D} \quad (4.10)$$

$$\frac{df}{dt} \approx\geq\ 0.632\frac{\Delta f_{ss}}{\tau} \quad (4.11)$$

From (4.10) and (4.11), the final frequency deviation and time of the transient and the transient change during the islanding event can be estimated. For a group of DGs, the same can be concluded, except that H must represent the total feeder inertia. For the inverter-based type DGs, such as type 3, type 4, and PV, where no inertia is connected to the grid, the voltage and reactive power mismatch must be taken into consideration. Similarly, for reactive power, following can be stated:

$$Q_{Grid} + Q_{DG1} + Q_{DG2} + \cdots + Q_{DGn} + Q_{Load} = 0 \quad (4.12)$$

$$\Delta P = 0 \quad (4.13)$$

$$\sum_{i=1}^{n} Q_{DGi} + Q_{Load} = \Delta Q \quad (4.14)$$

$$\Delta\, V_{Pcc} \cong f(\Delta Q) \quad (4.15)$$

For completely balanced islanding, where prior to the islanding event no power mismatch is measured, the sensitive change of voltage angle differences with some security measures are considered. The phase angle differences are used to shrink the NDZ where the sensitivity of the 27, 59, and 81 elements are not adequate to detect the separation of the primary feeder when there is no power mismatch.

$$\frac{\Delta\varphi}{\Delta t} = \frac{\Delta\left(\measuredangle V_{pcc} - \measuredangle V_{Grid}\right)}{\Delta t} \quad (4.16)$$

$\Delta P \approx 0,$

$$\Delta Q \approx 0 \quad (4.17)$$

In addition to the initial static conditions, mentioned in (4.10) and (4.11), to enable the phase angle supervision, the dynamic conditions of such a supervision must also be taken into consideration. It is important to note that any electrical fault, load, or capacitor bank switching may trigger a sensitive phase angle supervision; therefore, at the instance of islanding detection, the feeder must be mostly free of any switching and changes.

$$\frac{\Delta I_2}{\Delta t} \cong 0 \quad (4.18)$$

Where I_2 is the negative sequence component for both grid and DGs.

4.9 Test System

Figure 4.7 presents the simplified one-line diagram of the utility type distribution feeder with a nominal voltage of 27.6 kV which has been used for this case study. The feeder and 115 kV upstream substation are modeled using PSCAD EMTC. The primary feeder and all the laterals are modeled as an overhead line pi model. In the primary feeder, two locations were examined as Point of Common Couplings (PCCs) with the connection of different type of DGs that are most relevant to this study. The complex time domain model of PSCAD EMTC is used for type 3 DG, type 4 DG, and conventional machine with a modified Hydro governor. The parameterizations of each case are reported with the calculation results of each case study. The detailed one-line diagram of the system with the its equipment data is reported in the Appendix A.

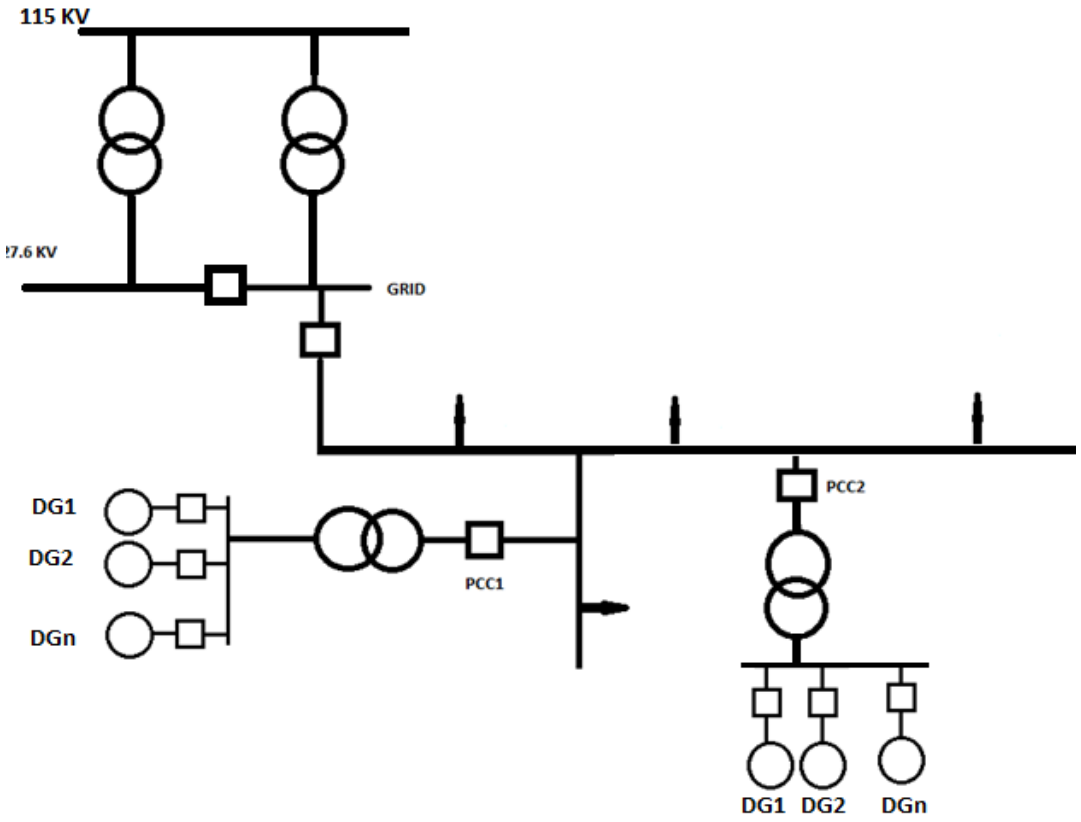

Figure 4.7. Simplified One Line Diagram of System Under Study

4.10 Simulation Scenarios

Although the islanding condition is defined independent of the type of installed DGs in the feeder, the responses and the behavior of the different types of DG vary after the islanding event. Hence, in this work, to examine the performance and generalize the concept of the proposed approach, many cases, with the most relevant DGs, are considered to verify the performance of the proposed islanding detection technique. It should be noted that distribution systems are not interconnected networks therefore; utility feeder is the full-scale system for this work to be considered for testing. This has been the motivation behind developing the model for 27.6 KV 50 MW utility type feeder. The cases that have been studied are the following:

a) **Scenario 1:** In this scenario, a constant speed type DG and generator, which includes conventional synchronous machine, wind turbine type 1, and wind turbine type 2, are studied. These units are connected to the grid directly without inverter

interface and they add to the inertia of the system. It should also be noted that a mixed generation (inverter based and synchronous machines) is considered in this category. Inverter-based machines will follow the synchronous machine frequency response during the islanding. Three cases in this scenario is reported.

b) **Scenario 2:** In this scenario, the variable speed (inverter based) DGs are being studied. These units are connected to the grid through the inverter, wind turbine as follow:
    a) Wind turbine type 3: case 1 and case 2
    b) Wind turbine type 4: case 1 and case 2
    c) PV solar: case 1 and case 2
c) **Scenario 3:** In this scenario, the effectiveness of proposed solutions in non-detection zone where the power mismatch is almost zero is considered.

4.10.1 Scenario 1-Case 1-3 (Synchronous machine)

In this scenario, the connected DGs are aggregated at one point and generators are participating in the total generation inertia mass. Three cases are simulated with the parameters shown in Table 4-2:

Table 4-2. Parameter for Conventional Machine

No	Symbol	Description	Unit
1	S_{DG}	Installed DG Power	30 MVA
2	H	Total Inertia	5.83 sec
3	D	Load damping constant	1.126%
4		Mechanical loss	0.001 PU

Figure 4-8 presents the results of three cases where islanding is performed with the different active power mismatch at t=40 sec. It is assumed that for any given simulation that the generator cannot deliver more power than what it is already providing. The governor gate valve is set to the maximum of its opening to limit the reaction of frequency load compensation. The plot presents DG frequency (f_{DG}), DG active power (PDG), grid active power (PGRID), DG reactive, power (QDG), and grid reactive power (QGrid). Feeder load is the same for all the three cases simulated while contribution of DGs in supplying active and reactive power are different.

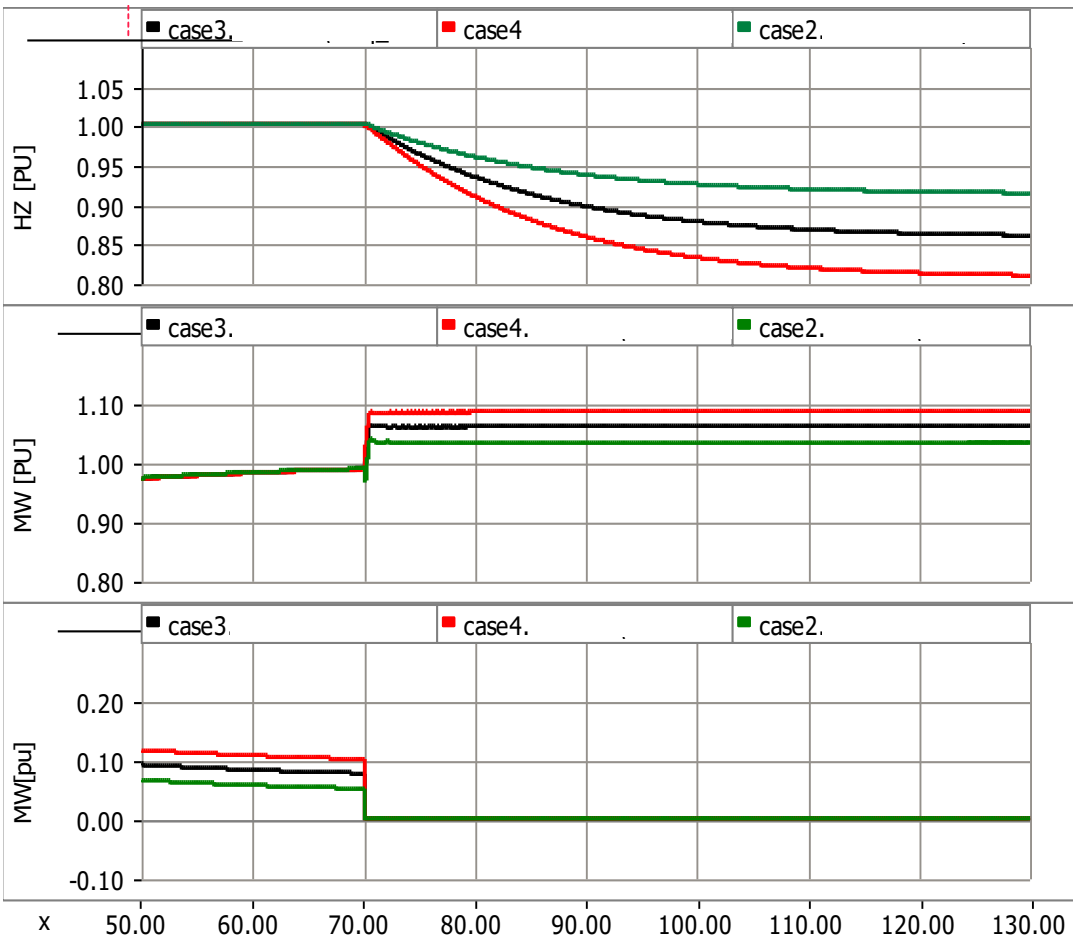

Figure 4.8. Islanding Scenario of Synchronous Machine

Table 4-3 presents the on-line estimation of $\Delta \mathbf{f_{ss}}$ and $\boldsymbol{\tau}$ based on (4.11) and power mismatch measured during the simulation. The frequency rate of change $\frac{\mathbf{dfG}}{\mathbf{dt}}$ can be directly calculated from the value estimated for each simulation and linearization of the change during the interval of one time constant.

$$\frac{\mathbf{dfG}}{\mathbf{dt}} \cong \frac{\mathbf{0.632\ \Delta fG_{ss}}}{\boldsymbol{\tau}} \tag{4.19}$$

where the Δf_{Gss} is a steady state value of frequency deviation. It should be noted that online estimation is only valid prior to the islanding event. If the D value is known or estimated correctly, online estimation will generate an accurate result that can serve to set the frequency element(s) of islanding detection system. Table 4-3 shows the results of the frequency deviation and time constant of the frequency settlement for the cases that have

been simulated based on the concept of the active power mismatch presented earlier. The ratio of $\frac{dfG}{dt}$ estimated based on the power mismatch prior to the islanding and can be compared with the actual average values of $\frac{dfG}{dt}$ measured. The results in all the cases shows that estimation value is more conservative than the actual rate of the change and protection frequency element which adapted to this estimation, can trip for such a rate of the change in all the cases.

Table 4-3. Frequency Rate of Change Estimation

Case	Symbol	Estimated	Actual	Error
2	Δf_{ss}	-5.34 Hz	-5.28 Hz	1.1%
	τ	22.20 sec	23.4 s	5.4%
	$\frac{df}{dt}$	-0.15 Hz/s	-0.14 Hz/s	6.6%
3	Δf_{ss}	-8.74 Hz	-8.64 Hz	1.1%
	τ	22.20 Sec	23.4 sec	5.4%
	$\frac{df}{dt}$	-0.248 Hz/s	-0.233 Hz/s	6.04%
4	Δf_G	-22.8 Hz	-23.01 Hz	1.03%
	τ	22.2 sec	23.4 sec	5.4%
	$\frac{df}{dt}$	-0.331 Hz/s	-0.317 Hz/s	4.04%

In any protection adaptive setting, the setting should be changed only within the predefined limitation that has to be set up based on the actual application data.

4.10.2 Scenario 2 – (WT type3)

Figure 4.9 and Figure 4.10 present the results of simulations of two islanding cases (case1 and case 2) of a group of 10 type 3 wind turbines connected to the feeder at one location. Table 4-4 presents the data of machine sued in these cases.

Table 4-4. Wind Turbine Type 3 Model Data

Parameter	Description	Value
S [MVA]	Apparent power	2.5
Pt [MW]	Turbine power	2
H [sec]	Inertia	3

For the purpose of simulation, it was assumed that pitch control was at its optimal position and remained unmoved after the initial model activation, that maximum power was obtained from the wind, and that the wind speed remained constant during the simulations. Prior to the islanding instant at t =2 sec, the load active power is totally compensated by the wind turbine and the contribution of the grid for the active load is almost zero. This should have created a most favorable situation to sustain the islanding operation by wind turbine. In case 1, the wind turbines are in under-excitation mode and are consuming reactive power while in case 2 the wind turbine is in over-excitation mode and is generating the reactive power.

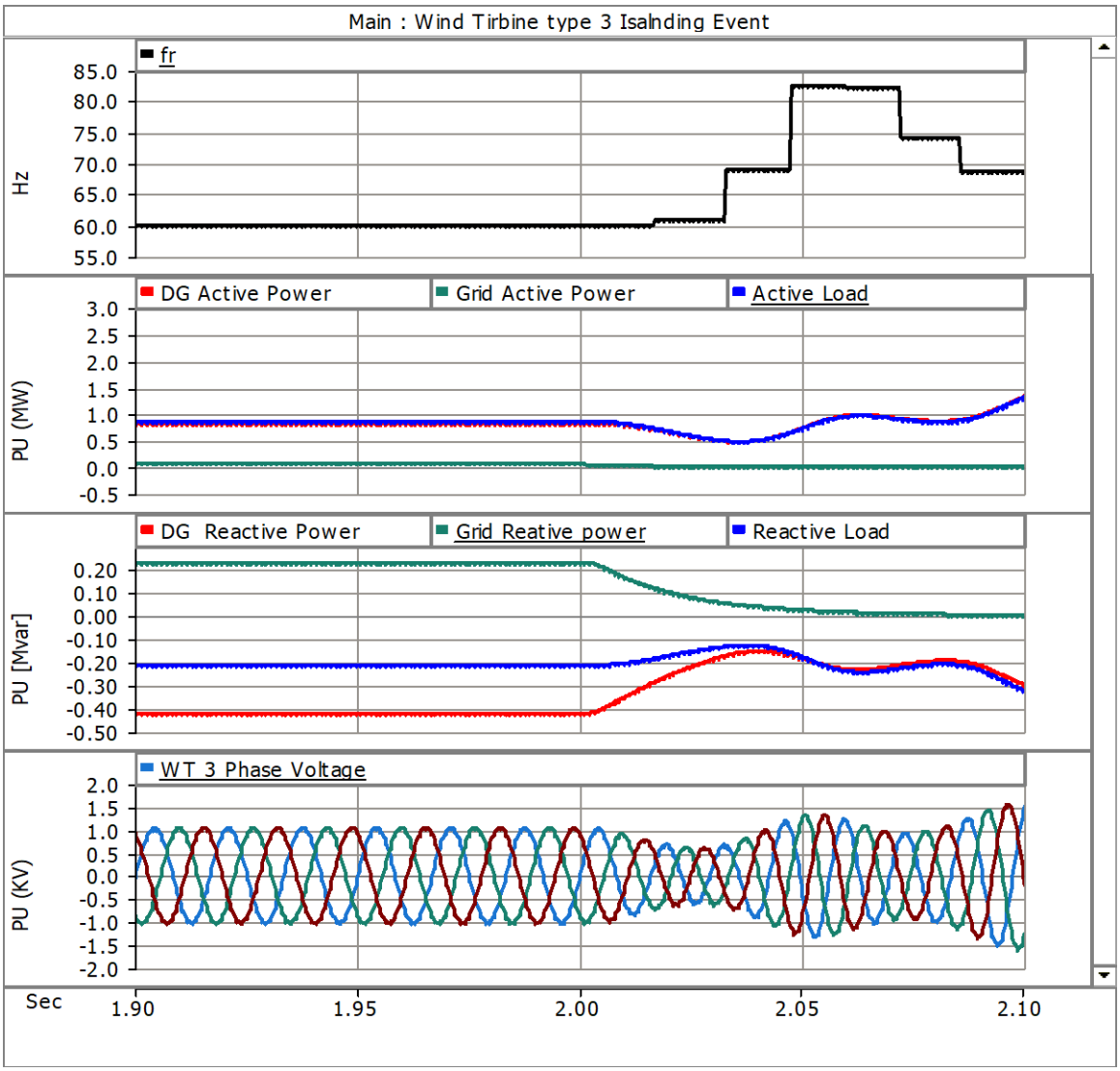

Figure 4.9. Wind Turbine Type 3 Islanding Event with Balance of Power Case 1

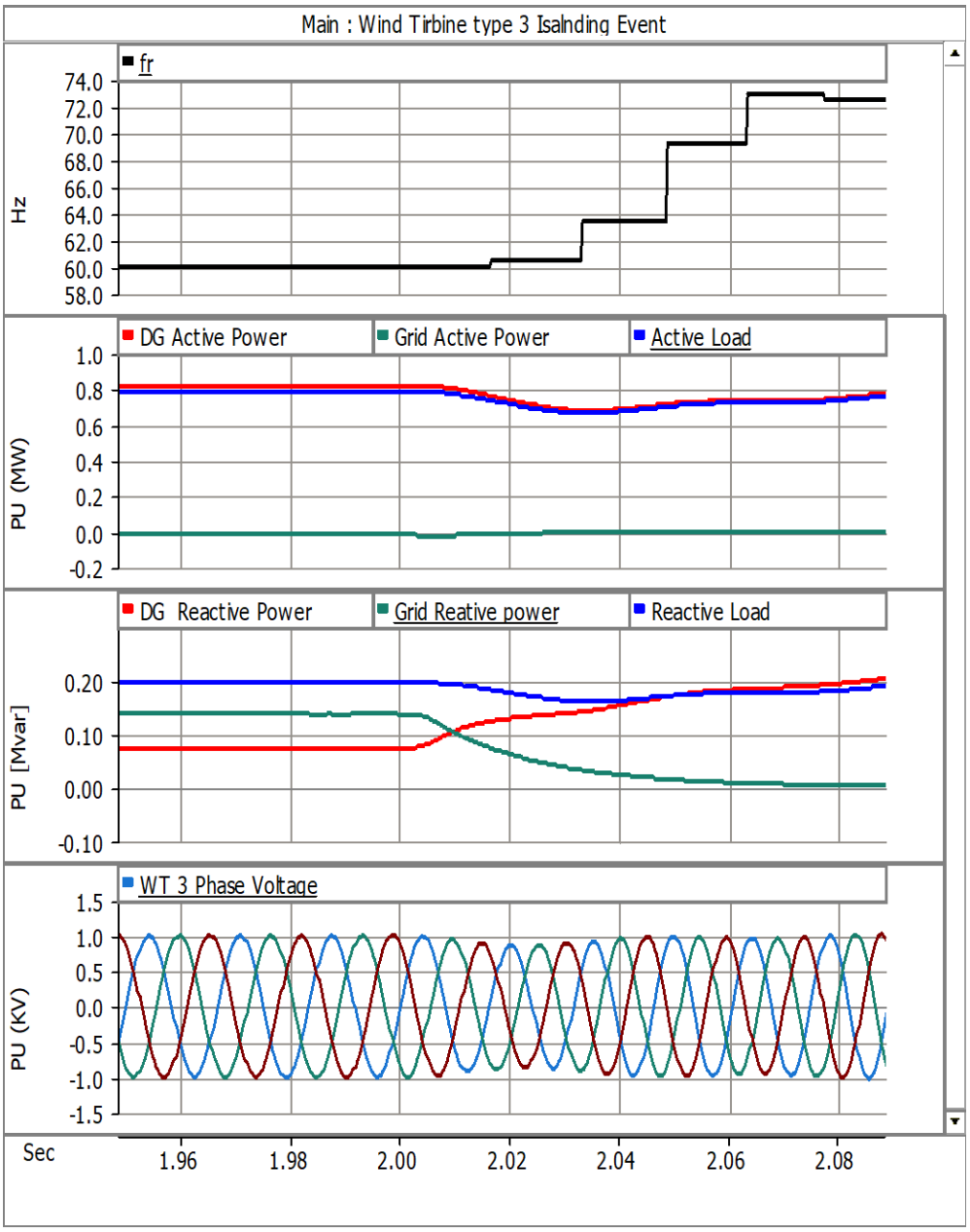

Figure 4.10. Wind Turbine Type 3 Islanding Event with Balance of Power Case 2

The simulation results show that with the loss of a self-regulated power frequency source (grid), the phase locked loop control that controls the DG frequency by following the grid frequency becomes unstable and enters to a self-excited and unstable loop resulting in a major deviation from the grid frequency. The study also reveals that even a zero-power

mismatch can lead to significant power frequency deviation (Δf). A greater power mismatch than the balance of power also cannot be sustained by a type 3 machine and the island will be detected up by voltage and frequency elements at PCC or by the machine's internal protection.

4.10.3 Scenario 2 -Case 2 (WT type 4)

Among the variable speed wind turbine, the type 4 wind turbine, also known as a full back-to-back inverter, is used as a representative for this type of machine in this work. The simplified one-line diagram of this model is presented earlier in Figure 2.17. Figure 4.11 shows the actual one-line diagram of the machine and grid source inverter used for this study. Generally, the DC link in this type of machine plays an important role between the machine and the grid source converter in understanding the dynamic of type 4. In this model, we have used both an aggregated model where the group of machines is shown with one model and the output of a single machine is linearly matched with the number of units involved in the study, as well as an individual model that is used to study the dynamics between the individual machines in one site.

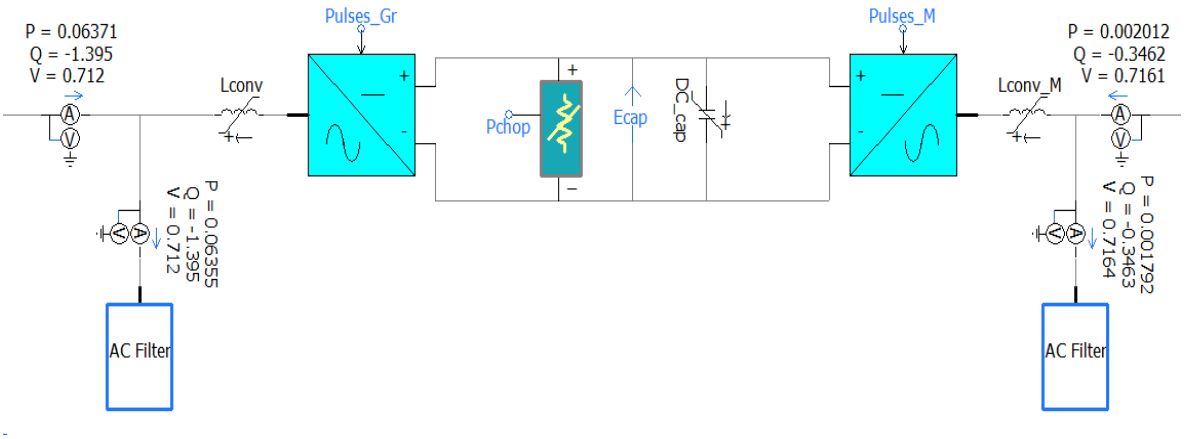

Figure 4.11. Type 4 Wind Turbine Model Block Diagram

Among that many cases which have been studied, the following two cases in Figure 4.12 and Figure 4.13 serving as the representative cases. Table 4-5 shows machine data for the type 4 wind turbine used in this study.

Table 4-5. Wind Turbine Type 4 Model Data

Parameter	Description	Value
S [MVA]	Apparent power	2.5
Pt [MW]	Turbine power	2
H [sec]	Inertia	2

For the purposes of simulation, it was assumed that pitch control was at its optimal position and remained unmoved after initial model activation, that maximum power was obtained from the wind, and that the wind speed remained constant during the simulations. Figure 4.12 and Figure 4.13 present the results of the simulations for a group of 10 type 4 wind turbines connected to the feeder at one location. The islanding occurs at t= 2 sec. The power mismatch in both cases is very small and wind turbines were able to sustain the load after islanding provided that the Phase Locked Loop (PLL) was designed for islanding operation. The simulation results show that with the loss of a self-regulated power frequency source (grid), the phase locked loop control that controls the DG frequency by following the grid frequency becomes unstable and enters into a self-excited and unstable loop resulting in a major deviation from the grid frequency. The study also reveals that even a small or no power mismatch can lead to significant power frequency deviations (Δf). A greater power mismatches cannot be sustained by a type 4 machine and island it will be picked up by voltage and frequency elements at PCC or by the machine's internal protection. In case 1, the wind turbines were in under-excitation mode, while in case 2 they are in over-excitation mode. In both cases, the active power mismatch is near zero. The deviation from the rating frequency is very large and in a few cycles after the instant of islanding takes place.

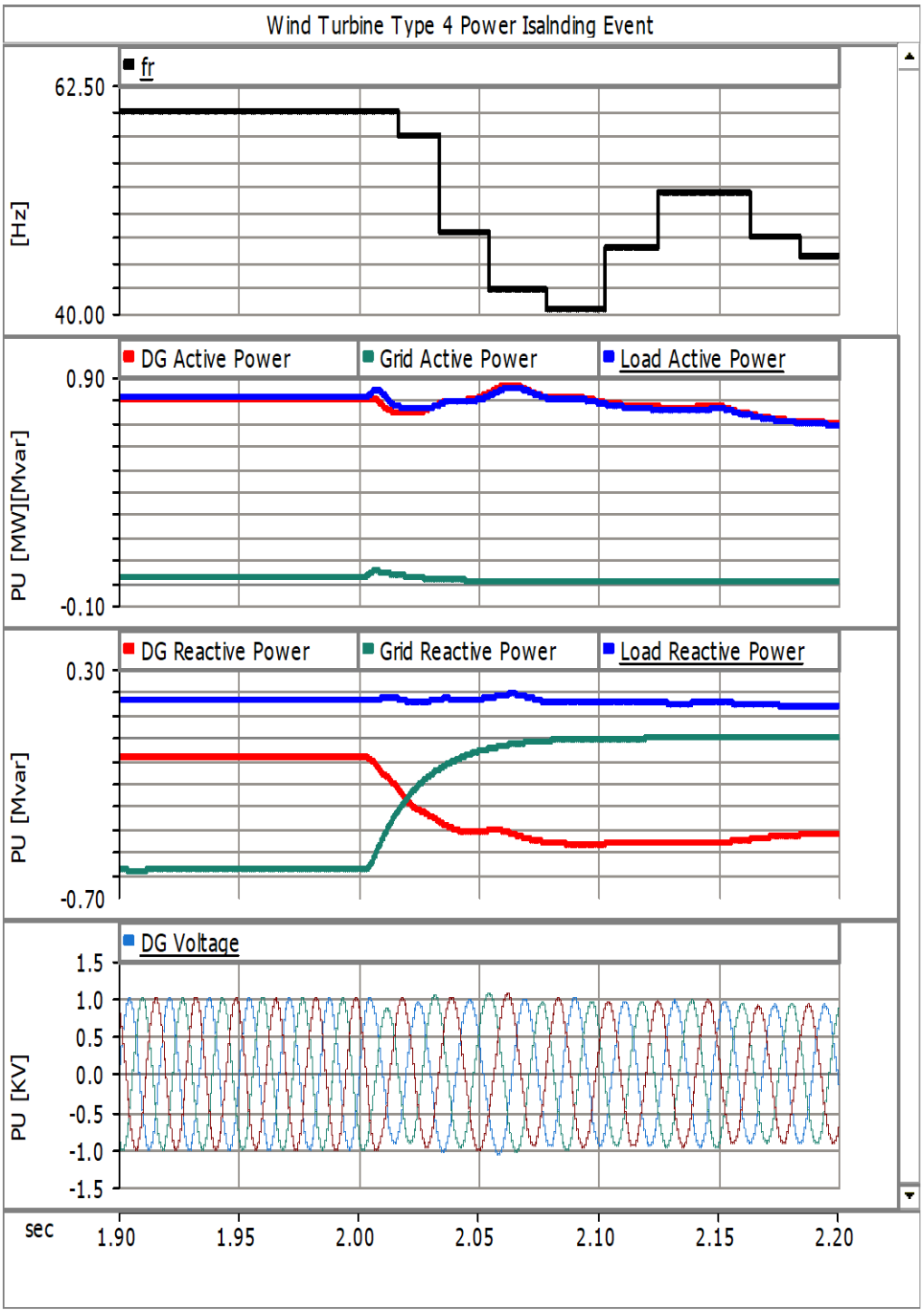

Figure 4.12. Wind Turbine Type 4 Islanding Case 1

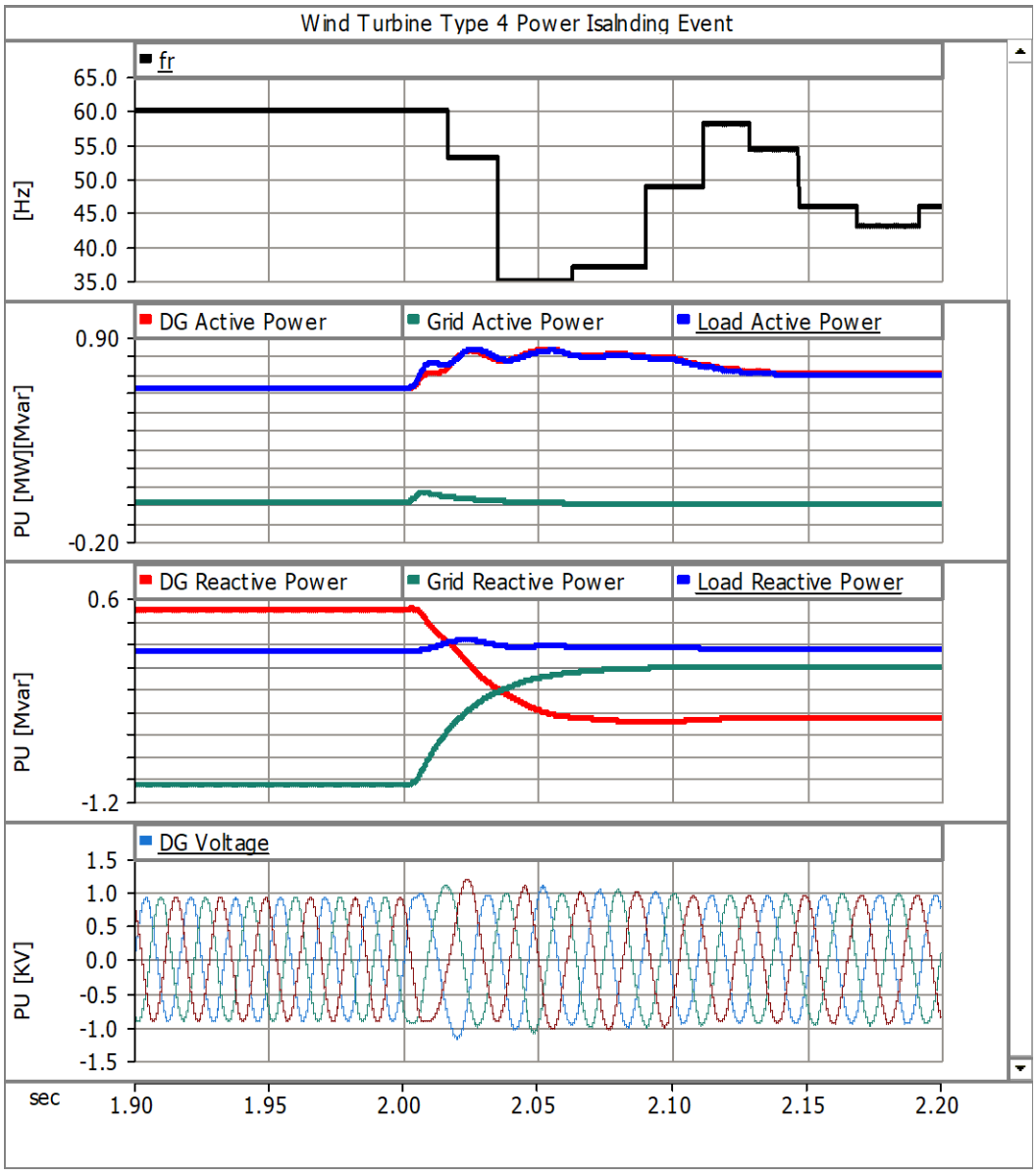

Figure 4.13. Type 4 Islanding Case 2

4.10.4 Scenario 2-Case3 (PV solar)

The solar farm has been modeled with the number of parallel and series PV arrays. The results of 2 simulated cases with different reactive power mismatches are presented in Figure 4.14. and Figure 4.15. For both cases, it was assumed that the temperature of the cells and sun radiation remained constant. The islanding event occurs at t=5 sec. The results show that PV generation does not provide any frequency response to the islanding active power mismatch. The frequency collapses even for a small power mismatch. The cases are

very similar with very small differences in power mismatches prior to the islanding event. When solar PV is not prepared for the islanding operation as discussed earlier, in the case of wind turbine Type 3 and Type 4, the PLL does not sense any independent frequency after unintentional islanding, and frequency becomes unstable.

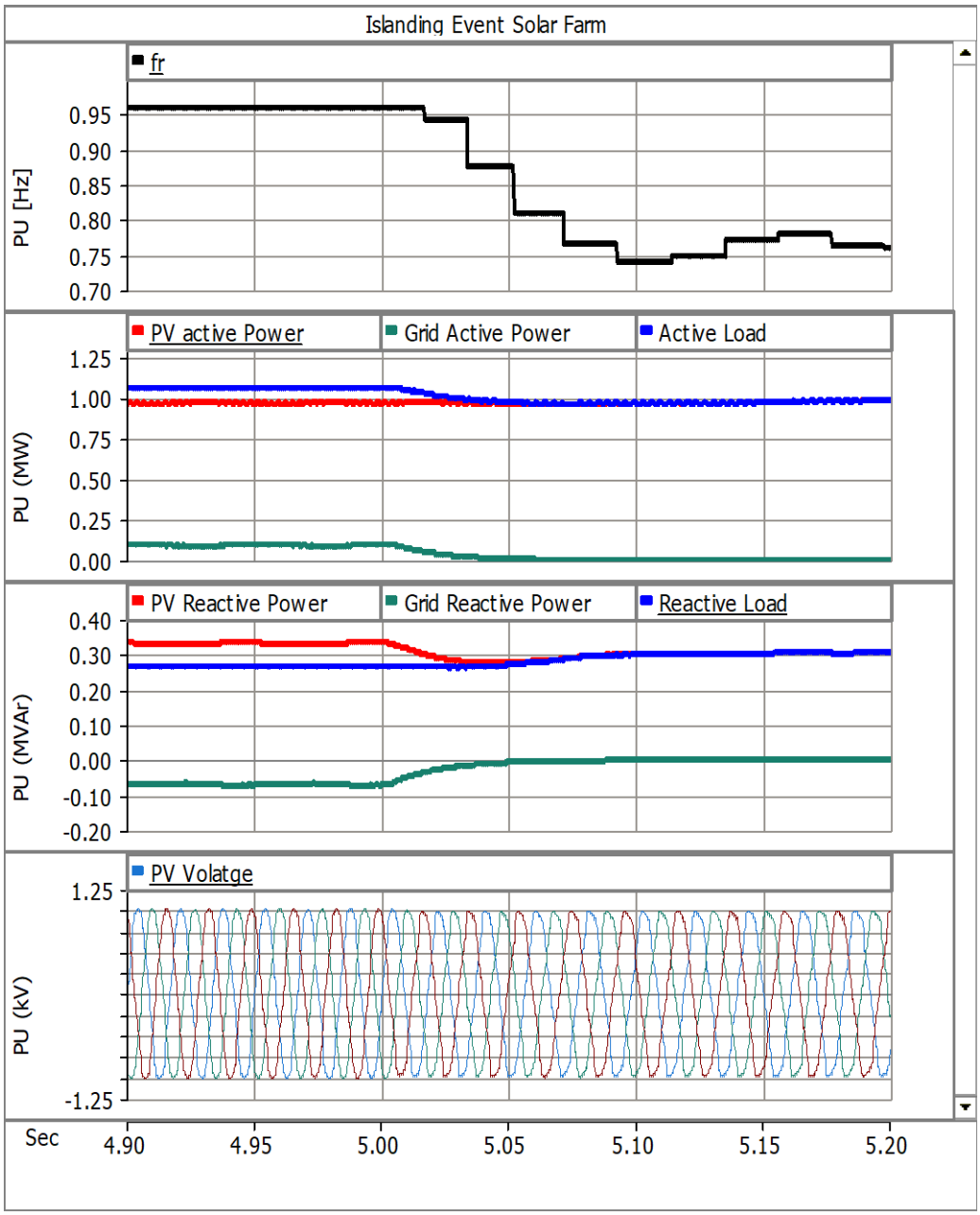

Figure 4.14. PV Islanding Scenario Case1

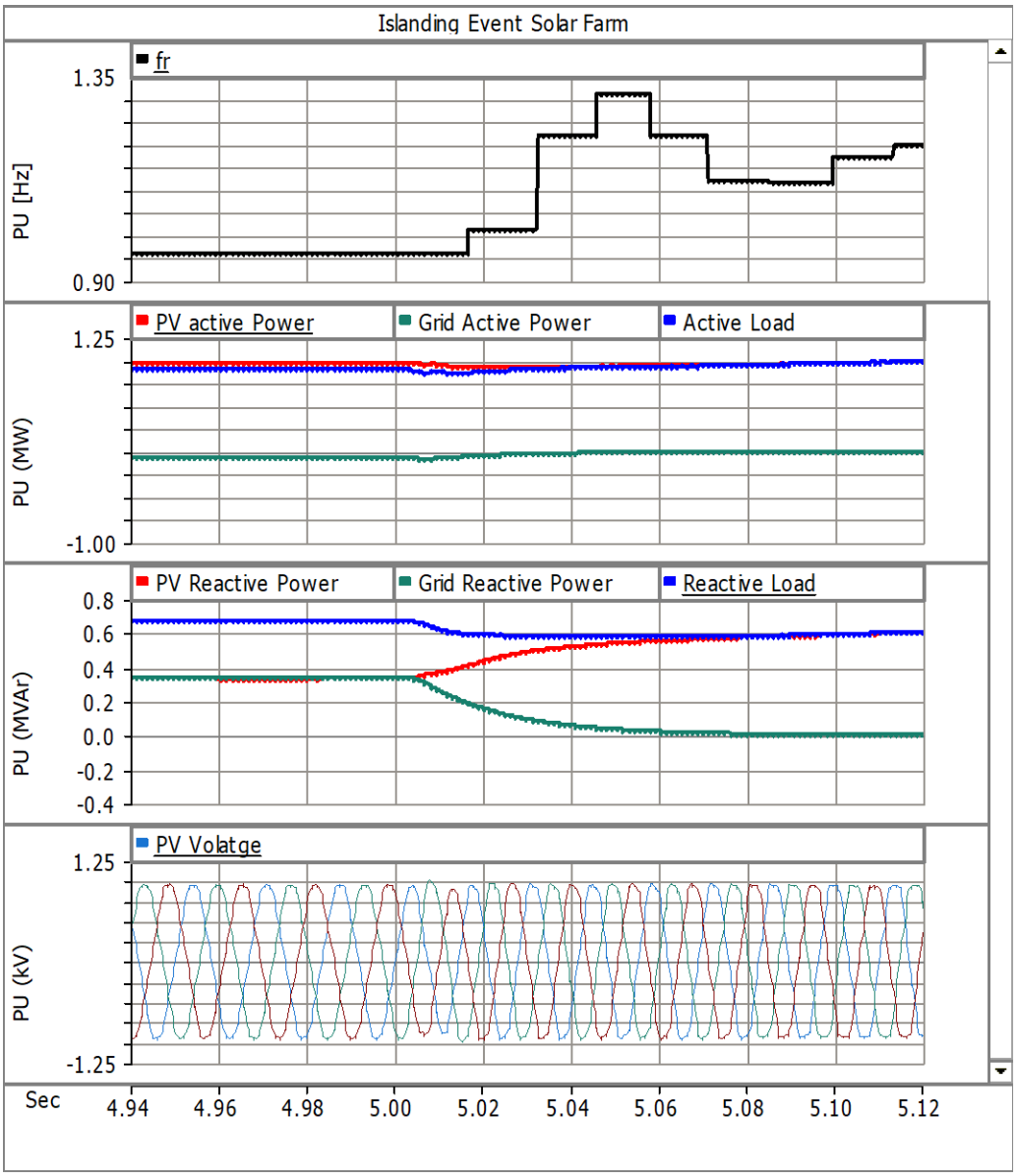

Figure 4.15. PV Islanding Scenario Case 2

4.10.5 Scenario 3- (Balance of power)

Balance power islanding refers to scenarios where nearly no power mismatches are measured prior to the islanding detection, as shown in Figure 4.16. The DG is supplying all the load of the feeder and islanding event, which in this case occurs at t=4 sec. For all three simulations, it occurs smoothly with no significant impact on the frequency and power of the load. As described earlier, the angle of voltage supervision between the PCC and substation is used to detect the separation of the feeder from the grid.

$$\Delta\varphi = \measuredangle V_{Grid} - \measuredangle V_{PCC}$$

This supervision can shrink the NDZ which commonly exists for all passive islanding detection methods. The high sensitivity of this function is the essence of utilizing this supervision in NDZ. Cases 1 to 3 are highly balanced scenarios where the voltage angles differences 2 seconds after the islanding events, change by a very small value.

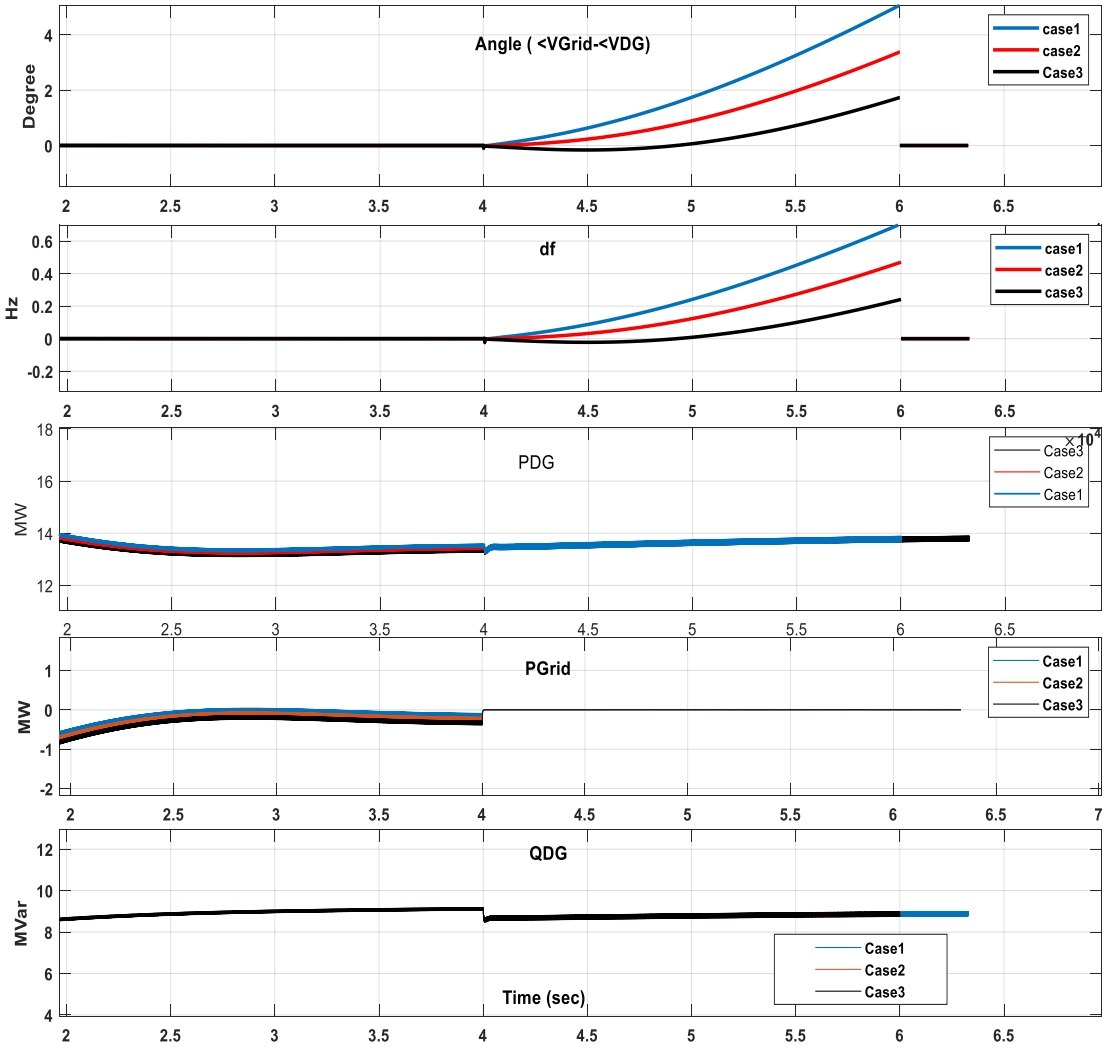

Figure 4.16. Islanding Simulation with Balance of Power

The simulation results are shown in Table 4-6. The power mismatch is expressed as a percentage of feeder real time load. The negative value of power mismatch means that the DG, in addition to supplying the feeder load, is also exporting small amount of power to

the grid. With the setting of 2 degrees for the voltage angle supervision between PCC and substation, the time required to detect the islanding for each case are shown. The results of this study show that NDZ area, with the given supervision setting, can be reduced to maximum 1.5% (case 2) of the feeder load. The islanding for case 3, is detected after 2 seconds which does not meet the IEEE 1547 requirement. The phase angle supervision, like any other sensitive function in the field of protection, may provide good dependability; however, it always lacks good security performance. The reliable scheme, however, is a right balance of two properties dependability and security. Therefore, (4.22) and (4.23) are the security condition that must be considered to activate the supervision function to ensure that during the transient (fault, switching, etc.) where the phase angle can change this function is disabled. The following can be formulated as the sensitivity limit in terms of frequency for the proposed solution and the cases studied:

$$\Delta\varphi = \measuredangle V_{Grid} - \measuredangle V_{PCC} = 2^{\circ} \tag{4.20}$$

$$\Delta f = \frac{2}{360} = 2.78 \text{ mHz} \tag{4.21}$$

$$\frac{dv_{2DG}}{dt} \cong 0 \tag{4.22}$$

$$\frac{dI_{2DG}}{dt} \cong 0 \tag{4.23}$$

Table 4-6. Balance of Power Case Study Results

Case	P_{DG} (MW)	P_{Grid} (MW)	Q_{Grid} (Mvar)	$\Delta\emptyset_{set}$ (degree)	Detection time	$\Delta P\% = \frac{P_{Grid}}{P_{DG} + P_{DG}}$
1	13.56	-0.38	8.5	2	1.0 sec	-2.8%
2	13.38	-0.21	8.5	2	1.50 sec	-1.5%
3	13.27	-0.19	8.5	2	2.2 sec	-1.4%

It is important to highlight that the sensitive islanding detection solution proposed in this section relies on IEEE PMU with a 1-degree phase angle resolution. Thus, if we assume μPMU or high resolution PMU is used, the limit, proposed in (4.20) and (4.21) can

theoretically be reduced. For example, considering 0.01° phase angle resolution and hypotheses of selecting 0.5 degree as angle supervisions setting, the results of the previous cases will change to what is shown in

Table 4-7. The more sensitive phase angle measurement and threshold theoretically can improve the sensitivity bottom line. As an example, case 3 which was not detectable in previous evaluation within 2 seconds (IEEE 1547 requirement) now it can be detected within 1.363 seconds.

Table 4-7. Balance of Power Case Study Results with $\boldsymbol{\mu}$PMU

Case	P_{DG} (MW)	P_{Grid} (MW)	Q_{Grid} (Mvar)	$\Delta\emptyset_{set}$ (degree)	Detection time	$\Delta P\% = \frac{P_{Grid}}{P_{DG} + P_{DG}}$
1	13.56	-0.38	8.5	0.5	0.426 sec	-2.8%
2	13.38	-0.21	8.5	0.5	0.750 sec	-1.5%
3	13.27	-0.19	8.5	0.5	1.363 sec	-1.4%

With lower and more sensitive setting for phase angle measurement, supervision to maintain the security of the proposed solution will be much harder to maintain if it is not impossible. It should be noted that (4.20) and (4.21) are not the only precondition for the activation of phase angle supervision. This condition should be maintained during the entire islanding detection process. Figure 4.17 shows the impact of the transient three-phase short circuit on the voltage phase angle measurement at the adjacent feeder at t= 30 sec. As suggested in (4.22) and (4.23) and shown here, negative sequence component of the DG current and voltage can be used to inhibit the phase islanding detection based on voltage phase angle. Therefore, it must point out that the sensitive islanding detection method cannot be reliably used without a period of stabilizing where no fault and switching operation in the feeder is detected. Furthermore, this condition must be present during the entire islanding detection process. The phase angle supervisions setting, it may differ from on feeder to another depend the load minimum feeder and DG size.

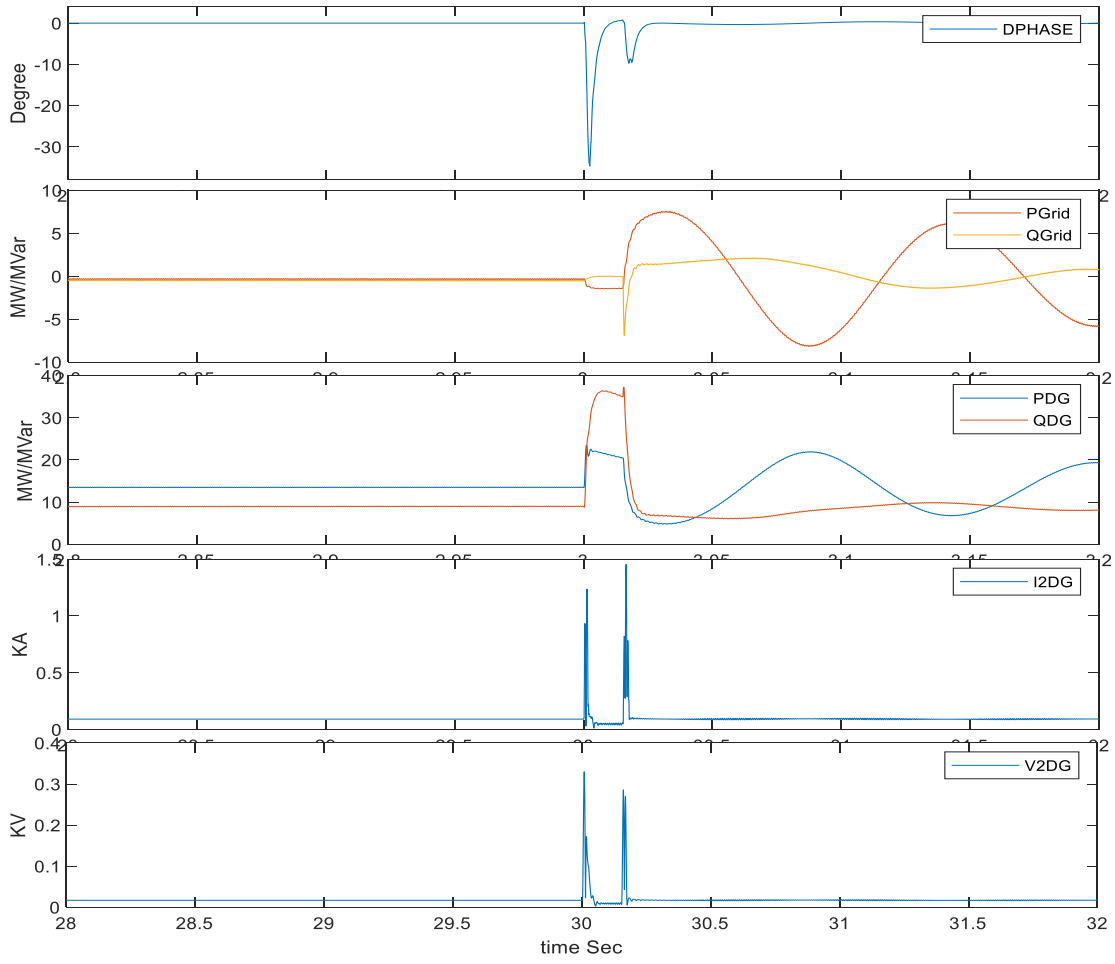

Figure 4.17. Adjacent Feeder Fault

4.11 Conceptual Implementation Consideration

The major studies using PMU so far have been focused on the wide area of the power transmission network and bulk energy power system. Although the proposed solution focuses on islanding in a distribution network, the same principle can be applied in any network by taking advantage of the PMU data stream phasor measurements that make sets of current and voltage phasors available on a real time basis at any PCC. The availability of PMU functionality in mainstream IEDs from protection and control manufacturers does not impose any significant additional cost except for the communication medium. The main goal of the system is to estimate a more sensitive setting for the conventional anti-islanding protection as described in various simulations. The base settings must remain unchanged

when a more sensitive set of settings cannot be calculated. The communication system architecture for the proposed solution is illustrated in Figure 4.6. The utilization of PDC, particularly for the size of suggested application, using IEC61850-90-5 where the PMUs can directly use the data stream from each other with GOOSE PDU can be eliminated. This can further improve the time performance of the proposed solution. This paper presented some comprehensive islanding scenarios with their relevant analysis of active and reactive power mismatches and a smooth balance power islanding in the distribution type feeder. The EMT-based detailed modeling using PSCAD of PV, type 4, and synchronous machine is used to study the transient of this phenomenon in an actual utility type feeder, load, and network.

It is important to note that the proposed solution works in conjunction with passive local islanding detection, i.e., protection elements such as 81 and 27 located at PCC (local anti-islanding elements). The proposed solution will adapt the setting of frequency elements from a base setting, considered to be the utility standard setting, to the more sensitive one based on the power measured during the operation. The power measurement will only be considered if it has been measured during a no-fault situation. For this reason, the moving average of the power mismatch between the grid and summation of all the DGs within a selected time interval must be measured and continuously updated until the fault is detected. During the fault, the moving average must not be updated and if this fault results in an islanding event, then the last moving average of the power mismatch must be used for this solution.

The PMU communication protocol is based either on IEEE C37.118-2 or IEC61850-90-5 standards that support binary data transfer, which means that the transfer trip based on substation trip beaker status can be directly transferred to the PCCs. This feature can always be used as a backup for the solution provided here, which is intended to be response-based solution and not event-based solution (transfer trip).

4.12 Summary

In this chapter, the first use case for detecting unintentional islanding operation in distribution systems with DER using the synchrophasor data was studied.

The issue related to the islanding operation was discussed, and the state-of-the-art detection methods were critically reviewed. Then, an adaptive detection solution was proposed to augment the exiting anti islanding protection scheme. The solution was formulated and presented. The concept of the proposed solution is based on measuring the power mismatch between the grid and DG in non-critical time and prepare the setting or response in real time.

The provision of the solution for zero power mismatch and non-detection zone was analyzed and proposed. The proposed method was further developed to include a feeder with multiple integrated PCCs.

The mathematical formulation was developed and presented. The test system was developed by detailed modeling of the utility type distribution feeder and the complex modeling of aggerated DG type 3, type 4, and PV in EMT using PSCAD/EMTDC software.

The test scenario to examine the reliability of the proposed solution was developed with emphasis on dependability and security. From the many simulations that were carried out, selected representative cases were reported and analyzed.

The conceptual implementation for the proposed solution with consideration of the marked available hardware and software was also proposed.

The next chapter will study the second use case using the synchrophasor data to detect the open phase fault in the distribution feeder.

Chapter 5

5 Open Phase Fault Detection

In this chapter, the summary of research and analysis leading to the proposal of selective detection of the open phase fault as well as the results of EMT modeling and simulation are presented.

5.1 Introduction

With the prospect of integration of many Distributed Energy Resources (DERs) into the electrical grid, especially in the distribution network, coupled with the concept of smart grid, there is a necessity for more investment in communication infrastructure to operate such a system while maintaining the safety and reliability of the grid. Even though the use of Intelligent Electronic Devices (IEDs) enhances the reliability of protection and control by improving dependability, i.e., the ability to detect the fault, security, and differentiate a normal situation from the fault.

A typical distribution network has many miles of overhead lines, still protected by fuses. The protection relays are installed in the substation and their algorithm and performance relies mainly on local measurements. In this chapter, in line with the distribution network transformation and requirement of grid modernization for communication infrastructure, open phase fault detection method based on phasor measurement data from the substation and every Point of Common Coupling (PCC) in the feeder (where the DER is connected to the distribution feeder) is presented.

The open-phase or broken conductor fault is a challenging fault for utilities to detect, as there is no dedicated protection element to identify this fault. Open phase fault often coincides with a broken and downed conductor to earth, which is a public safety risk. If this event develops into a ground fault, (a high impedance fault with a very low current), it becomes hard to detect. Most importantly, for the distribution feeder with an auto-recloser, without identifying this type of fault as an open phase, and therefore, blocking the recloser attempts, the feeder may get reenergized and intensify the risk of electrification to the public.

The undetected open phase during a light load condition can cause ferro resonance and an increase in transient voltage in the feeder. Figure 5.1 presents a conceptual architecture of proposed solution which shows a set of three-phase current and voltage phasor data from a feeder breaker at a substation and point of common couplings (PCC1 and PCC2) obtained from PMU 1 to PMU3 (Phasor Measurement Unit), respectively.

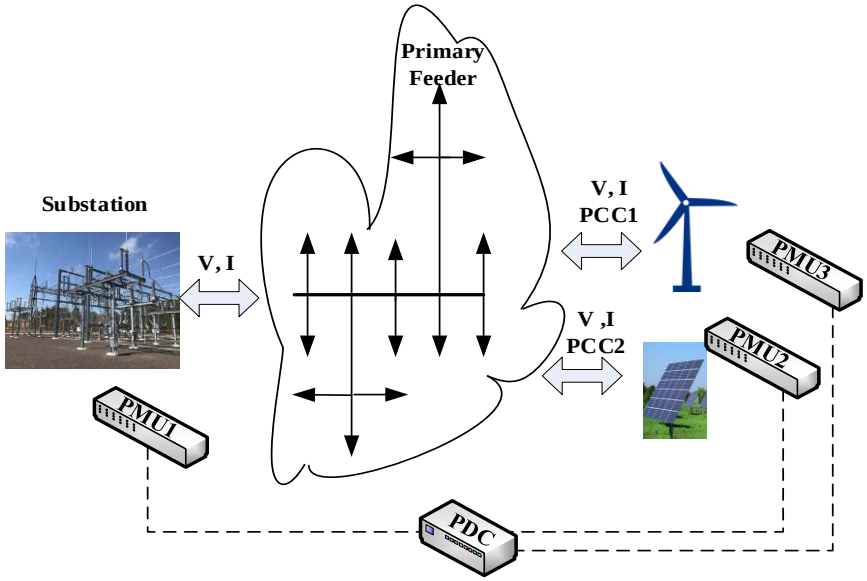

Figure 5.1. Conceptual System Architecture of the Proposed Solution

The data from the PMUs can be processed in Phasor Data Concentrator (PDC) as shown here, assuming a conventional C37.118 communication is used. Here, the PMU data stream needs to be aligned in the PDC before being used by application.

5.2 Review of Open Phase Detection Techniques

Detecting and clearing the open phase fault in the distribution network has not been the subject of much research in recent years. In this section, the most relevant research to this work is reviewed. In [52], the open phase fault and fallen conductor are recognized as a major public safety issue and a problem for cases of open phase conductor, and when a downed wire is addressed by adding a mechanical accessory to the line pole. The applicability, however, may be limited. In [53], a good conceptual idea is published with the suggestion to use the voltage phasor data in the modern substation environment to catch the open phase before touching the ground. Use of current phasor data, especially when

there is no other voltage source in the feeder, is essential for any algorithm development. In [54], [55], and [56], the impact of open phase fault in distribution and sub-transmission network, Temporary Over Voltage (TOV) and possibility of resonance circuit in resonantly grounding system is verified. The open phase fault can be very detrimental to the health of the equipment. In [57], the vulnerability of a Negative Sequence Pilot Protection (NSPP) scheme for a very long transmission line is verified and a compensation method based on the open phase symmetrical component analysis is introduced. In [58], it is proposed that the zero-sequence voltage be measured by electric field sensors alongside of feeder. The criteria for detection are relying on the fact that unbalanced voltage after the fault will be much higher than the normal unbalanced operation of the feeder. This model has been verified in the field; however, open phase detection in the presence of DG will not have the same signature, and therefore, a decision-making algorithm may not apply to a feeder with DG. In [59], the focus is on detecting the high impedance fault in distribution feeder caused by a broken or downed conductor. The characteristic of this fault with consideration to the harmonic content and the current waveform is verified. In [60], the rule-based fault detection method, including the open phase fault, is compared with the Artificial Neural Network (ANN). In [61] and, [62], the use of computer-based modeling of open phase and fault analysis has been reported.

5.3 Open Phase Fault Signature

5.3.1 Single Open Phase Fault without Ground

Figure 5.2 shows the open phase fault in phase “a” between the P (bus side) and Q (line side). The voltage and current relationship can be summarized as follows:

$$V_a^{PQ} = V_a^P - V_a^Q \neq 0$$

$$V_b^{PQ} = V_b^P - V_b^Q = 0$$

$$V_c^{PQ} = V_c^P - V_c^Q = 0$$

$$I_a = 0, I_b \neq 0, I_c \neq 0$$

Where V_a^{PQ}, I_b, and I_c,represent the voltage across the P and Q and phase currents respectively.

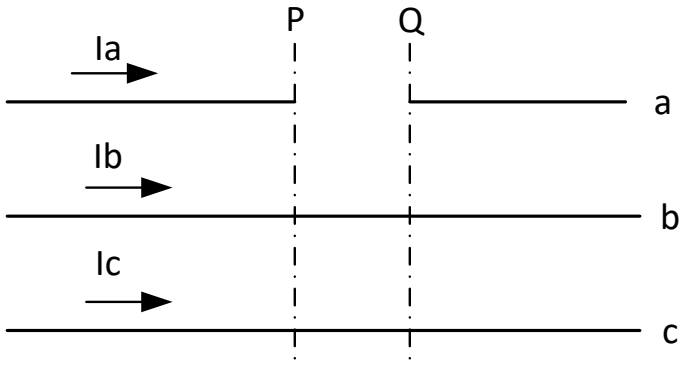

Figure 5.2. Open Phase Fault in Phase "a" at P-Q

The symmetrical component of the above circuit and group equation can be summarized as follows:

$$V_1^{PQ} = 1/3(V_a^{PQ} + aV_b^{PQ} + a^2V_c^{PQ}) \quad (5.1)$$

$$V_2^{PQ} = 1/3(V_a^{PQ} + a^2V_b^{PQ} + aV_c^{PQ}) \quad (5.2)$$

$$V_0^{PQ} = 1/3(V_a^{PQ} + V_b^{PQ} + V_c^{PQ})$$

Therefore,

$$V_1^{PQ} = V_2^{PQ} = V_0^{PQ} = \frac{1}{3V_a^{PQ}} \quad (5.3)$$

Similarly, the symmetrical component of the current can be summarized as:

$$I_a = 0, I_b \neq 0, I_c \neq 0$$

$$I_1 = {}^1\!/_3\,[I_a + aI_b + a^2I_c] = {}^1\!/_3\,(aI_b + a^2I_c)$$

$$I_2 = {}^1\!/_3\,[I_a + a^2I_b + aI_c] = {}^1\!/_3\,(a^2I_b + aI_c)$$

$$I_0 = {}^1\!/_3\,[I_a + I_b + I_c] = {}^1\!/_3\,(I_b + I_c)$$

$$(1 + a + a^2) = 0$$

$$I_1 = I_2 + I_0 \quad (5.4)$$

Considering (5.1) to (5.4) , the equivalent circuit for the open phase fault is shown in

Figure 5.3.

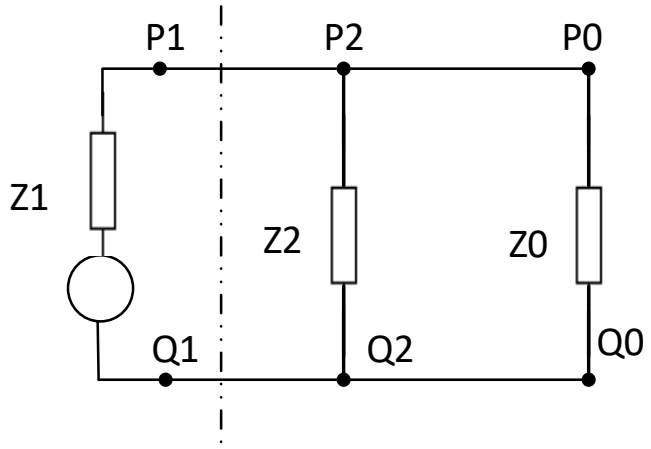

Figure 5.3. Symmetrical Component Circuit of Open Phase Fault

5.3.2 Single Open Phase Fault with Ground

Similar to the analysis described in the previous section, the open phase with the downed wire on the "Q" side of the circuit, as shown in Figure 5.4, is considered. In order to generalize the case for the ground fault, it has been assumed that the system is not radial, and a ground fault can be supplied by either side of the line. The P side is where the phase is opened, and Q is the side where the phase wire is down, and the ground fault occurs.

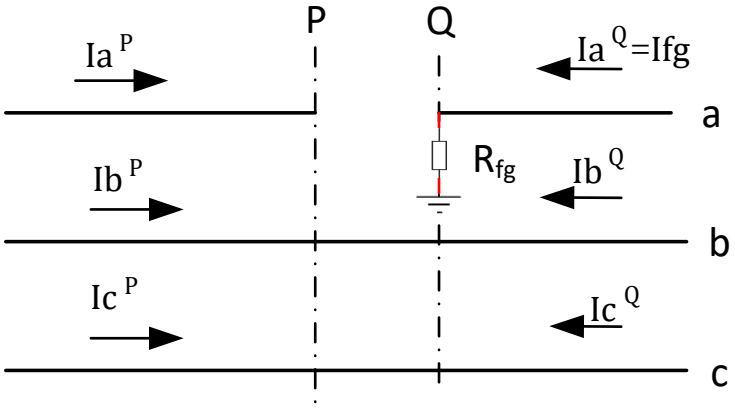

Figure 5.4. Open Phase Fault with Downed Wire

The following can be stated for voltage and current in P and Q side.

$$I_a = 0$$

$$I_a = I_{a1} + I_{a2} + I_{a0} = 0$$

$$V_b^{PQ} = V_b^P - V_b^Q = 0$$

$$V_c^{PQ} = V_c^P - V_c^Q = 0$$

The following symmetrical component can be stated for P and Q

$$V_b^P = a^2 V_{a1}^P + a V_{a2}^P + V_{a0}^P$$

$$V_b^Q = a^2 V_{a1}^Q + a V_{a2}^Q + V_{a0}^Q$$

$$V_c^P = a V_{a1}^P + a^2 V_{a2}^P + V_{a0}^P$$

$$V_c^Q = a V_{a1}^Q + a^2 V_{a2}^Q + V_{a0}^Q$$

$$V_b^{PQ} = V_b^P - V_b^Q = a^2\left(V_{a1}^P - V_{a1}^Q\right) + a\left(V_{a2}^P - V_{a2}^Q\right) + \left(V_{a0}^P - V_{a0}^Q\right) = 0 \quad (5.5)$$

$$V_c^{PQ} = V_c^P - V_c^Q = a\left(V_{a1}^P - V_{a1}^Q\right) + a^2\left(V_{a2}^P - V_{a2}^Q\right) + \left(V_{a0}^P - V_{a0}^Q\right) = 0 \quad (5.6)$$

We know that

$$a^2 + a + 1 = 0 \quad (5.7)$$

Therefore, from (5.17), (5.6) and (5.7), the following can be concluded:

$$\left(V_{a1}^P - V_{a1}^Q\right) = \left(V_{a2}^P - V_{a2}^Q\right) = \left(V_{a0}^P - V_{a0}^Q\right) \quad (5.8)$$

Eq. (5.8) can be also developed for the healthy phases “b” and “c”:

$$I_b^{PQ} = I_b^P - I_b^Q = 0$$

$$I_c^{PQ} = I_c^P - I_c^Q = 0$$

$$I_b^{PQ} = I_b^P - I_b^Q = a^2\left(I_{a1}^P - I_{a1}^Q\right) + a\left(I_{a2}^P - I_{a2}^Q\right) + \left(I_{a0}^P - I_{a0}^Q\right) = 0 \quad (5.9)$$

$$I_c^{PQ} = I_c^P - I_c^Q = a\left(I_{a1}^P - I_{a1}^Q\right) + a^2\left(I_{a2}^P - I_{a2}^Q\right) + \left(I_{a0}^P - I_{a0}^Q\right) = 0 \quad (5.10)$$

Eq. (5.11) similar to (5.16) can be extracted from (5.9) and (5.10).

$$\left(I_{a1}^P - I_{a1}^Q\right) = \left(I_{a2}^P - I_{a2}^Q\right) = \left(I_{a0}^P - I_{a0}^Q\right) = \frac{1}{3} I_{fg} \quad (5.11)$$

Based on (4.20) and (5.11), the equivalent circuit of the single open phase fault with a downed wire to ground in the interconnected network (source in both side of the fault) is shown in Figure 5.5. The zero-sequence component of current caused by the ground fault at Q is shown by use of an ideal 1:1 ratio interpose transformer connecting the sequence component circuits together. The ground fault resistance (R_{fg}) in real cases most likely will be a high impedance. Eq. (5.11) is representing the ground fault zero sequence component.

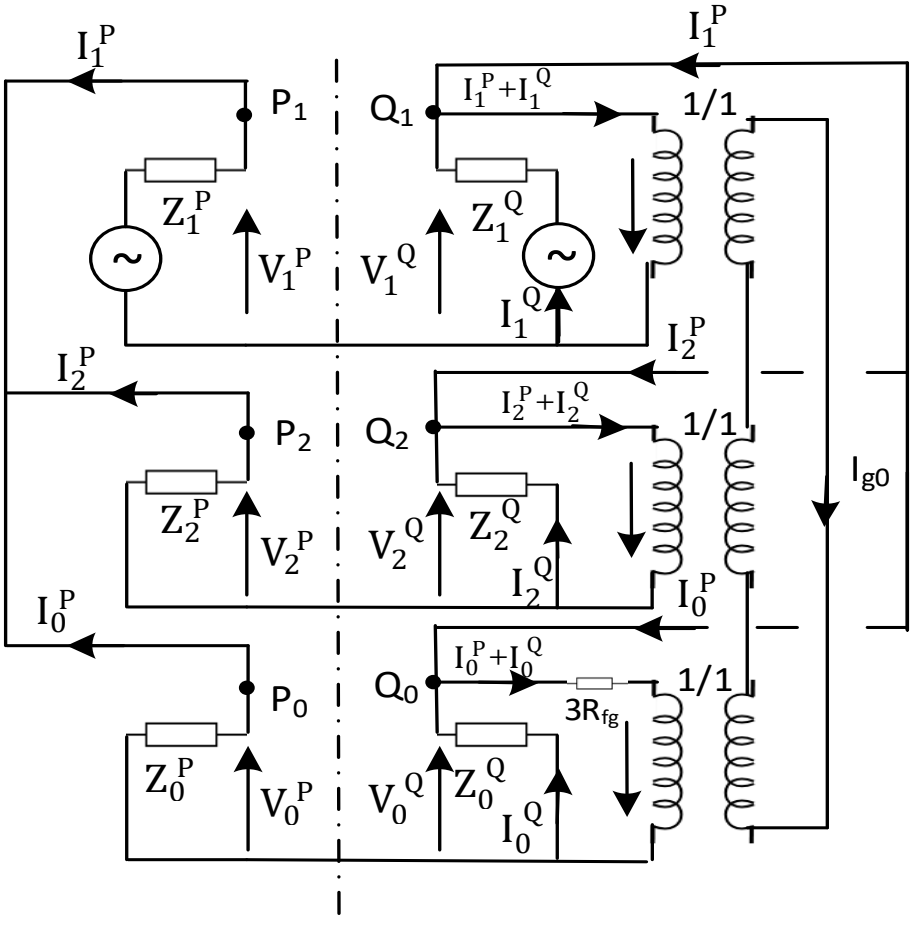

Figure 5.5. Symmetrical Component Circuit of Open Phase with Ground

The circuit can be simplified further if we consider the radial system presented in Figure 5.2. Such cases can frequently occur in the distribution feeder and thus, it is worthwhile that the summary of the analysis is presented as an equivalent circuit with the ground fault at the source side (bus side), as shown in Figure 5.6.

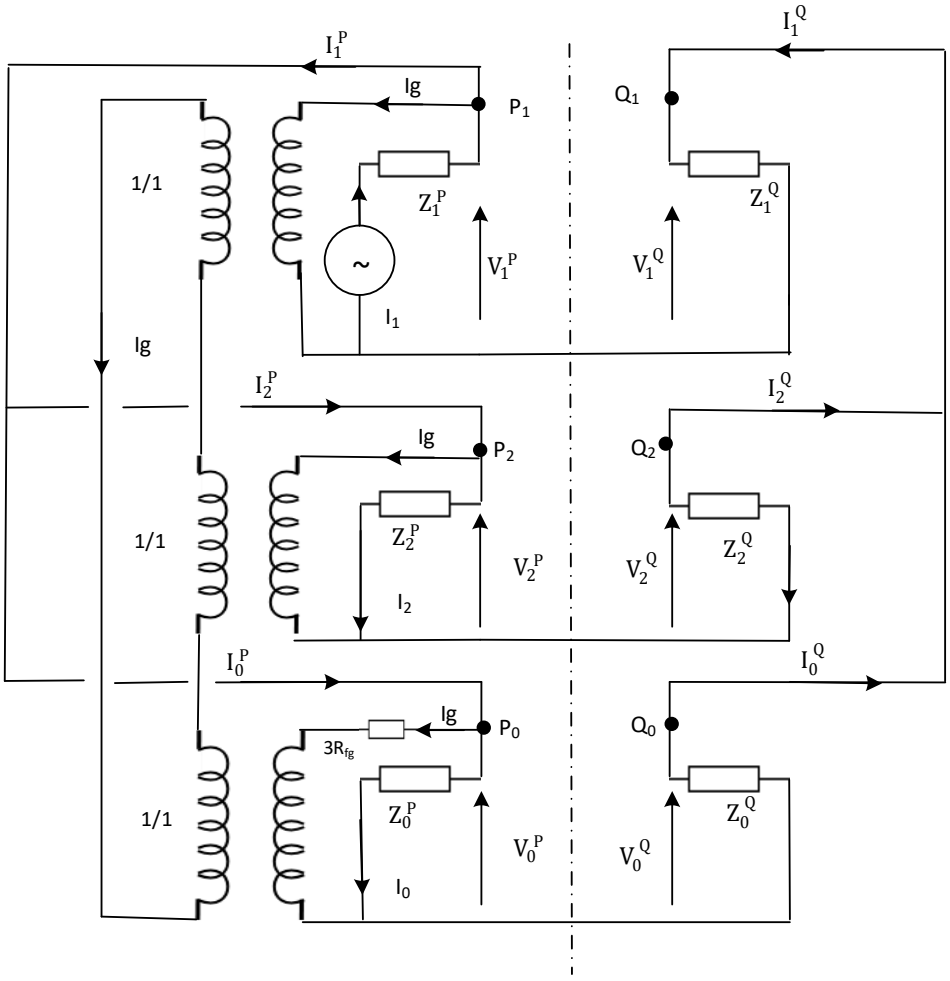

Figure 5.6. Open Phase Fault with Ground at the Source Side

A similar relationship between current and voltage can be developed for an open phase and the downed wire at “Q” side (load side) of the circuit. In this case, the 1/1 ratio interpose transformer, which is used to represent the zero-sequence current caused by the ground fault, must be moved to the load side (Q side) of the circuit.

5.3.3 Double Open Phase Fault with No Ground

Figure 5.7 shows the open phase fault circuit for two phases - b and c. The current and voltage equation can be written as follows:

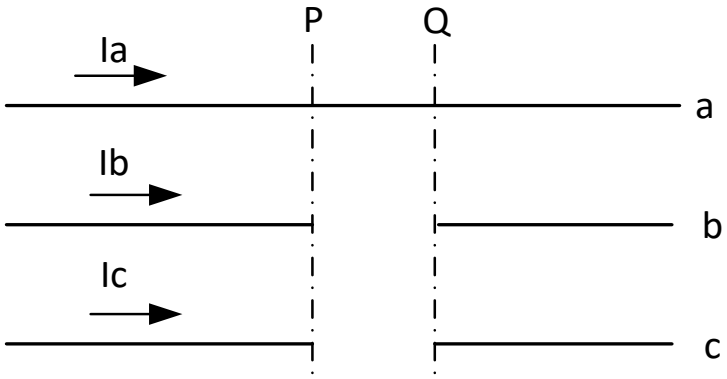

Figure 5.7. Symmetrical Component Circuit of Double Open Phase Fault

Updating (5.1), (5.3), (5.4) and (5.11) from single open phase to double open phase, the following can be stated for voltage, current, and sequence components:

$$V_a^{PQ} = V_a^P - V_a^Q = 0$$

$$V_b^{PQ} = V_b^P - V_b^Q \neq 0 \qquad (5.12)$$

$$V_c^{PQ} = V_c^P - V_c^Q \neq 0$$

$$V_1^{PQ} = 1/3(V_a^{PQ} + aV_b^{PQ} + a^2V_c^{PQ}) = 1/3(aV_b^{PQ} + a^2V_c^{PQ}) \qquad (5.13)$$

$$V_2^{PQ} = 1/3(V_a^{PQ} + a^2V_b^{PQ} + aV_c^{PQ}) = 1/3(a^2V_b^{PQ} + aV_c^{PQ}) \qquad (5.14)$$

$$V_0^{PQ} = 1/3(V_a^{PQ} + V_b^{PQ} + V_c^{PQ}) = 1/3(V_b^{PQ} + V_c^{PQ}) \qquad (5.15)$$

Adding both sides of (5.13), (5.14), and (5.15), we get:

$$V_1^{PQ} + V_2^{PQ} + V_0^{PQ} = \frac{1}{3}(1 + a + a^2)\left(V_b^{PQ} + V_b^{PQ}\right)$$

We know $(1 + a + a^2) = 0$ thus, (5.16) can be concluded.

$$V_1^{PQ} + V_2^{PQ} + V_0^{PQ} = 0 \qquad (5.16)$$

Eq. (5.17) shows the similar relation between the current sequence components presented on (5.16) for the fault of broken wire in two phases.

$$I_a^{PQ} \neq 0\ ,\ I_b^{PQ} = 0,\ I_c^{PQ} = 0$$

$$I_1^{PQ} = 1/3(I_a^{PQ} + aI_b^{PQ} + a^2 I_c^{PQ}) = \frac{1}{3} I_a^{PQ}$$

$$I_2^{PQ} = 1/3(I_a^{PQ} + a^2 I_b^{PQ} + aI_c^{PQ}) = \frac{1}{3} I_a^{PQ}$$

$$I_0^{PQ} = 1/3(I_a^{PQ} + I_b^{PQ} + I_c^{PQ}) = \frac{1}{3} I_a^{PQ}$$

$$I_1^{PQ} = I_2^{PQ} = I_0^{PQ} = \qquad (5.17)$$

Eq. (5.16) and (5.17) shows that the sequence component circuit of double open phase are in series as shown in Figure 5.8.

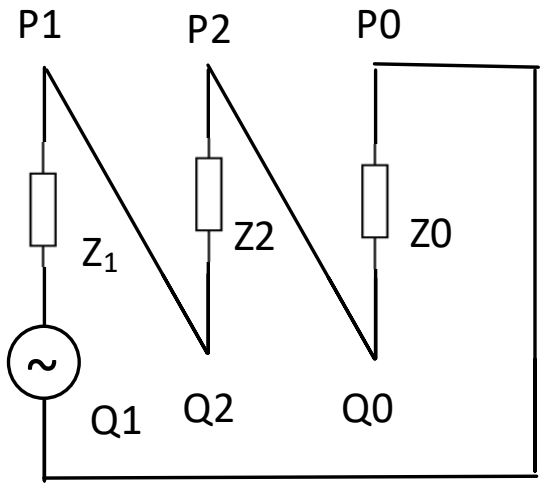

Figure 5.8. Double open phase fault equivalent circuit

The double open phase fault with downed wire(s) most likely will extend to a phase-to-phase short circuit fault, which will be detected with the conventional protection scheme.

5.4 Proposed Open Phase Fault Detection Criteria

As shown in the previous section, the symmetrical component analysis of an open phase fault around faulty point provides a set of discriminative criteria to detect an open phase incident. However, these criteria are not applicable to any distribution feeder where the current and voltage along the feeder are different from the measurement available to protection and control devices, located at substation and point of common coupling. The proposed solution detects an open phase by analyzing the dynamic characteristics of the current sequence components of power sources during the fault transition. It depends on the number of PCCs where DGs are connected to the distribution feeder the proposed solution considering the use of PMU in substation and PCCs. For conventional feeders where no DGs are integrated in the feeder, one point of measurement at substation without PMU will be enough. The available data in substation and PCC partially contains the open phase signature. To overcome this issue, the average rate of changes of the current component in the phasor data, which shows significant similarity with the open phase fault characteristics measured at the fault location, is considered. Therefore, (5.4) is developed based on the information of the location of the fault and can be restated for other measuring points, such as substation or PCC, where PMUs are located as a group of inequality equations which must be considered all together.

$$(\Delta \mathrm{I}_i = \mathrm{I}_i^{\mathrm{af}} - \mathrm{I}_i^{\mathrm{bf}}),\ i = 0,1,2$$

$$\frac{\Delta \mathrm{I1}}{\Delta \mathrm{t}} < 0\ \ ,\left(\frac{\Delta \mathrm{I2}}{\Delta \mathrm{t}}\right) > 0,\ \left(\frac{\Delta \mathrm{I0}}{\Delta \mathrm{t}}\right) > 0 \qquad (5.18)$$

$$\left(\frac{\Delta \mathrm{I1}}{\Delta \mathrm{t}}\right).\left(\frac{\Delta \mathrm{I2}}{\Delta \mathrm{t}} + \frac{\Delta \mathrm{I0}}{\Delta \mathrm{t}}\right) < 0$$

$$\mathrm{Max}\ (\mathrm{I}_1, \mathrm{I}_2, \mathrm{I}_0) << \mathrm{Isc} \qquad \Delta \mathrm{V1} \simeq 0$$

Where $\mathrm{I}_i^{\mathrm{af}}$ and $\mathrm{I}_i^{\mathrm{bf}}$ represents the sequence current component before and after the fault. The inequality of the short circuit and ($\Delta \mathrm{V1} \simeq 0$) shows that the open phase fault is not generating any short circuit current that can be compared with any type of the parallel faults and therefore the positive voltage at the PCC and the substation almost remain intact. It also should be noted the inequality (5.18) has no threshold to control the sensitivity of

the detection logic thus, in order to immunize the detection logic against fuse failure or feeder unbalance, zero and negative sequence components must be greater than user defined threshold (Min set1, Min set2 or Min set3) in order to activate the detection logic.

$$\frac{\Delta I1}{\Delta t} \geq \text{Min set1} \ , \ \frac{\Delta I2}{\Delta t} \geq \text{Min set2} \ , \ \frac{\Delta I0}{\Delta t} \geq \text{Min set3} \qquad (5.19)$$

Not all the three thresholds in (5.19) is required to control the sensitivity of the open phase fault detection logic. The voltage at the substation and PCC will have no significant change for an open phase fault contrary to a parallel type of fault in the feeder. Thus, $\Delta V1 \simeq 0$ is added to the above-mentioned conditions. When there is more than one source in the feeder, the inequality equations of (5.19) must be considered for the sources that feeding the load behind the fault point. In the following section, this concept will be developed adequately. In this regard, an arbitrary distribution feeder with DG is shown in Figure 5.9.

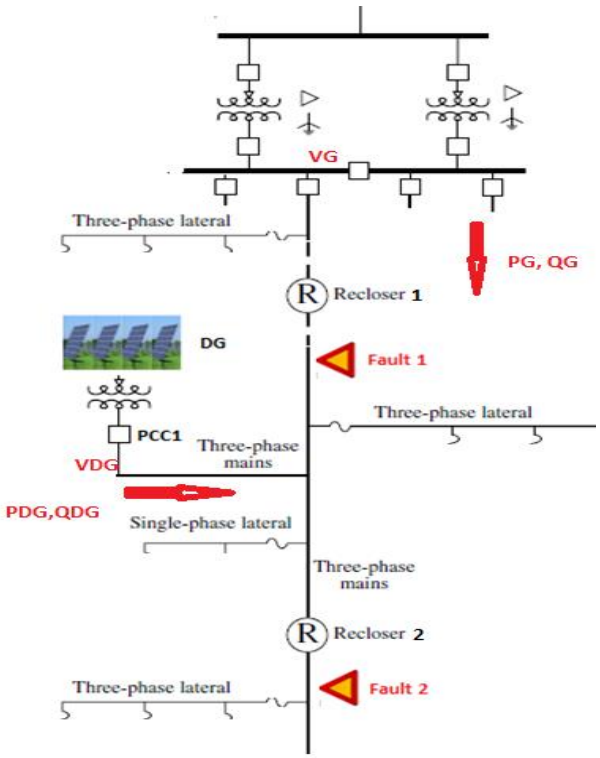

Figure 5.9. Typical Distribution Feeder with DG

In order to formulate the detection criterion for the open phase fault, two locations of the faults at point 1 (fault1) and at point 2 (fault 2) is considered that represent an open fault between the two sources and a fault on the same side of the sources, respectively. The location of the fault, with respect to the power sources, is required to develop different set of conditions that must be recognized at the early stage of the fault detection process. It must be noted that the proposed criteria (5.18) and (5.19) are current based and therefore, in order for this algorithm to work, the open phase fault should expose minimum load of the feeder to the fault. This means a minimum load required to go through the fault point which can be as low as 2% of the feeder load. The sensitivity detection will be determined by greater value of (5.19) or the minimum required load being exposed to open phase fault. Table 5-1, the rate of change of the current symmetrical components for different type of faults and switching operations is compared with the proposed solution for the open phase fault. The "↑" sign represents the positive rate of the change and the ↓sign shoes the negative rate of the change. The results of many simulations shows that dependability criteria introduced in (5.18) and (5.19) presents a unique characteristic which can be discriminated with the open phase fault from all other type of the faults. The representative simulation for each fault or operation is shown in Appendix E.

Table 5-1. Current Rate of Change for Parallel Faults

No.	Fault or switching type	$\frac{\Delta I1}{\Delta t}$	$\frac{\Delta I2}{\Delta t}$	$\frac{\Delta I0}{\Delta t}$	$\frac{\Delta V1}{\Delta t}$	Figure No.
1	Three phase fault	↑	NA	NA	-	Figure E2
2	Two phase fault	↑	↑	NA	-	Figure E4
3	Two phase to ground	↑	↑	↑	-	Figure E6
4	Ground fault	↑	↑	↑	-	Figure E8
5	Energizing unbalance load	↑	↑↓	↑↓	NA	Figure E9

6	De-energizing unbalance load	↓	↑↓	↑↓	NA	Figure E12

The case 6 of in the above table “de-energizing the unbalance load” in some cases when the load of the feeder is balanced can leave the same signature as the open phase fault formulated in (5.18). The constrained introduced in (5.19) must be used to desensitized the proposed open phase algorithm against the unbalanced load that could occur in normal operation. This case will be further discussed in the sensitivity section in this chapter.

Table 5-2 presents the variables and their units which is used to analyze cases with more power sources.

Table 5-2. Variable Used for Case Study

Symbol	**DESCRIPTION**	**UNIT [SI]**
ViG i=1,2,0	Substation voltage	KV (rms)
ViDG i=1,2,0	PCC voltage	KV (rms)
IiG i=1,2,0	Substation current	KA (rms)
IiDG i=1,2,0	PCC current	KA (rms)
PG	Active power station	MW (ave)
PDG	Active power PCC	MW (ave)
QG	Reactive power station	MVar (ave)
QDG	Reactive power PCC	MVar (ave)
I0	Zero sequence current ground fault	KA
Rfg	Grong fault resistance	Ω

5.5 Single Open Phase Fault Between Two Sources

The single open phase fault at point 1 in Figure 5.9 is considered. This fault is located between the two sources of DG and the distribution grid. Therefore, in the instance of an open phase fault, active power for the two sources changes in direction at the station and at the PCC. It is assumed that if load distribution fault $P_{DG} \uparrow$ increases to compensate for the portion of the load which is no longer being supplied from the grid $P_{Grid} \downarrow$ decreases. For simplicity, it is assumed that losses are part of the load, and redistribution of the open phase load after the fault does not cause a significant change in the losses. If the grid and DG supply $K\%$, $(1-K)\%$ of the load, respectively, and "N" represents the portion of the load in the open phase (phase "b" in this case), which will be discontinued from the grid after the fault. The index Zero (0) in the equations represents the power before the fault, and ΔP_x represents the change in power after the fault.

$0 < K < 1$, and, $N \leq K$

$$P_{DG0} + P_{Grid0} = P_{load0} = P_{lA0} + P_{lB0} + P_{lC0} \tag{5.20}$$

$P_{load0} \approx P_{load}$

$$P_{Grid0} = K\,P_{load} = K(P_{lA} + P_{lB} + KP_{lC}) \tag{5.21}$$

$$P_{DG0} = (1-K)P_{load} = (1-K)((P_{lA} + P_{lB} + KP_{lC}) \tag{5.22}$$

$P_{Grid} = K\,P_{load} = KP_{lA} + (K-N)P_{lB} + KP_{lC} = K(P_{lA}+P_{lB}+P_{lC}) - NP_{lB}$

$P_{DG} = (1-K)P_{load} = (1-K)(P_{lA} + P_{lB} + P_{lC}) + NP_{lB}$

$\Delta P_{Grid} = P_{Grid0} - P_{Grid} = -NKP_{lB}$

$\Delta P_{DG=} P_{DG0} - P_{DG} = NP_{lB}$

$$\frac{\Delta P_{Grid}}{\Delta P_{DG}} \leq -1 \tag{5.23}$$

When the grid is supplying the load behind the open phase, (5.19) is considered as follows:

$$\left(\frac{\Delta I1G}{\Delta t}\right).\left(\frac{\Delta I2G}{\Delta t}+\frac{\Delta I0G}{\Delta t}\right)<0$$

5.5.1 Fault in a Feeder with More Than Two Sources

The open phase detection criteria can be extended for the feeder with more than two sources of energy. $P_{source1}$ and $P_{source2}$ represent the group of generation, including the grid, located on the both sides of the fault

$$P_{source1}=P_{Grid}+\sum_{i=1}^{m}DG_i$$

$$P_{source2}=\sum_{i=m}^{z}DG_i$$

$$P_{source1_0}+P_{source20}=P_{load0}=P_{lA0}+P_{lB0}+P_{lC0}$$

$$P_{source1_0}=K\,P_{load}=K(P_{lA}+P_{lB}+KP_{lC}) \tag{5.24}$$

$$P_{source2_0}=(1-K)P_{load}=(1-K)((P_{lA}+P_{lB}+KP_{lC}) \tag{5.25}$$

$$\Delta P_{source1}=P_{source1_0}-P_{source1}=-NKP_{lB}$$

$$\Delta P_{source2}=\Delta P_{source2_0}-\Delta P_{source2}=NP_{lB}$$

$$\frac{\Delta P_{source1}}{\Delta P_{source2}}\leq -1 \tag{5.26}$$

$$\left(\frac{\sum\Delta I1Source1}{\Delta t}\right).\left(\frac{\sum\Delta I2Source1}{\Delta t}+\frac{\sum\Delta I0Source1}{\Delta t}\right)<0$$

5.5.2 Open Phase Fault with the Ground Fault

As mentioned earlier in this chapter, when an overhead electric power distribution circuit conductor breaks—for example, when a car strikes a pole, or a splice or clamp fails—the energized conductor falls to the ground. The resulting high-impedance ground fault and its impact on the open phase fault is shown in Figure 5.4 and Figure 5.5 and the following can be concluded:

- High impedance ground fault caused by broken conductor and downed wire, i.e., from an overhead tower to the ground, takes some time (in the order of seconds). This

sequence is recognizable by PMU measurement. Therefore, the signature of an open phase fault, which is the backbone of the proposed algorithm, remains intact, and an open phase fault prior to becoming a ground fault can be identified. This is also a very desirable response to prevent any public hazards caused by energized wires at the ground level.

- High impedance ground fault constitutes a very small portion of the current fault which most likely is not a measurable at the station level but, nonetheless, the positive rate of change can be measured, if the ground fault occurs after the open phase in the sequence described previously. From (5.10), (5.11), and (5.19), the ground fault current can be calculated. It is assumed that at $t1$, the open phase fault occurs and at $t2$, the ground wire touching ground occurs, and I0 is a high impedance ground fault.

$$\mathrm{Ia1} - \mathrm{Ia'1} = \mathrm{Ia2} - \mathrm{Ia'2} = \mathrm{Ia0} - \mathrm{Ia'0} = \mathrm{I0}$$

$$[(\Delta \mathrm{IxG})_{t2} - (\Delta \mathrm{IxG})_{t1}] > 0 \qquad (\mathrm{x}=0,1,2) \qquad (5.27)$$

$$[(\Delta \mathrm{IxDG})_{t2} - (\Delta \mathrm{IxDG})_{t1}] > 0 \qquad (\mathrm{x}=0,1,2) \qquad (5.28)$$

The above equations, developed for the point in time that an open phase fault occurs, are valid when the ground fault is at the grid or DG side, respectively. Similar to what was described for the open phase fault criteria, the PMUs measuring devices are at the substation and PCCs. Hence, the above equation cannot be directly verified since the location of the fault also unknown. However, for the high impedance ground fault which is expected to be less than 50 A on the primary, reduces the unbalance of the system caused by interruption of one phase load and thus, the following behavior can be measured by PMUs at the instant the high impedance ground fault develops from an open phase fault.

$$\begin{bmatrix} \left(\frac{\Delta \mathrm{I1G}}{\Delta \mathrm{t}}\right) > 0 \\ \left(\frac{\Delta \mathrm{I2G}}{\Delta \mathrm{t}}\right) < 0 \\ \left(\frac{\Delta \mathrm{I0G}}{\Delta \mathrm{t}}\right) < 0 \end{bmatrix} \qquad (5.29)$$

Similar inequality equations can be verified by grid side PMU, if the high impedance ground fault is supplied from the grid.

5.6 Open Phase Fault at the Same Side of the Sources

In this section, an open phase fault recognition criterion at point 2 in Figure 5.9 is considered. This fault is located on the same side of the two sources of DG and distribution grid. In the instance of a fault, active power for the two sources changes in the same direction at the station and at the PCC. In contrary to the previous case, for a fault on the same side of the sources, in the instant the fault occurs, active power for the two sources changes in the same direction at the station and at the DG. Both $P_{DG} \downarrow$ and $P_{Grid} \downarrow$ decrease due to the loss of portion of the load in phase "b". For simplicity, we have assumed that the losses are part of the load. The grid and DG supply $K\%$, $(1-K)\%$ of the load in all three phases (P_{lA}, P_{lB}, P_{lC}), and "N" is representing the portion of the load in phase "b" which is deenergized after fault occurs. The index Zero (0) in the equations represents the power before the fault and ΔP_x represents the change of power due to the fault.

$0 < K < 1$, and, $N \leq K$

$$P_{DG} + P_{Grid} = P_{load} = P_{lA} + P_{lB} + P_{lC} \tag{5.30}$$

$$P_{Grid0} = K\,P_{load} = K(P_{lA} + P_{lB} + KP_{lC}) \tag{5.31}$$

$$P_{DG0} = (1-K)P_{load} = (1-K)((P_{lA} + P_{lB} + KP_{lC}) \tag{5.32}$$

$$P_{Grid} = K\,P_{load} = K(P_{lA}+P_{lB}+P_{lC} - NP_{lB})$$

$$P_{DG} = (1-K)P_{load} = (1-K)((P_{lA} + P_{lB} + KP_{lC} - NP_{lB})$$

$$\Delta P_{Grid} = P_{Grid0} - P_{Grid} = -NKKP_{lB}$$

$$\Delta P_{DG=} P_{DG0} - P_{DG} = -N(1-K)P_{lB}$$

$$0 \leq \frac{\Delta P_{Grid}}{\Delta P_{DG}} \cong \frac{K}{1-K} \tag{5.33}$$

In this case, both grid and DG are supplying the load behind the open phase and therefore, the inequality equations (5.18) can be considered for both power sources.

$$\left(\frac{\Delta I1G}{\Delta t}\right).\left(\frac{\Delta I2G}{\Delta t}+\frac{\Delta I0G}{\Delta t}\right)<0$$

$$\left(\frac{\Delta I1DG}{\Delta t}\right).\left(\frac{\Delta I2DG}{\Delta t}+\frac{\Delta I0DG}{\Delta t}\right)<0$$

5.6.1 Fault in a Feeder with More Than Two Sources

The open phase detection criteria in this case can also be extended to the feeder with more than two sources of energy. $P_{source1}$ and $P_{source2}$ represent the group of generation sources, including the grid that is integrated to the feeder.

$$P_{source1}=P_{Grid}+\sum_{i=1}^{m}DG_i$$

$$P_{source2}=\sum_{i=m}^{z}DG_i$$

$$P_{source1_0}+P_{source20}=P_{load0}=P_{lA0}+P_{lB0}+P_{lC0}$$

$$P_{source1_0}=K\,P_{load}=K(P_{lA}+P_{lB}+KP_{lC})$$

$$P_{source2_0}=(1-K)P_{load}=(1-K)((P_{lA}+P_{lB}+KP_{lC})$$

$$\Delta P_{source1}=P_{source1_0}-P_{source1}=-KNKP_{lB}$$

$$\Delta P_{source2}=\Delta P_{source2_0}-\Delta P_{source2}=-(1+K))NP_{lB}$$

$$0\leq\frac{\Delta P_{source1}}{\Delta P_{source2}}\cong\frac{K}{1-K} \qquad (5.34)$$

$$\left(\frac{\sum\Delta I1Source1}{\Delta t}\right).\left(\frac{\sum\Delta I2Source1}{\Delta t}+\frac{\sum\Delta I0Source1}{\Delta t}\right)<0$$

$$\left(\frac{\sum\Delta I1Source2}{\Delta t}\right).\left(\frac{\sum\Delta I2Source2}{\Delta t}+\frac{\sum\Delta I0Source2}{\Delta t}\right)<0$$

5.6.2 Open Phase Fault with Ground

The ground fault impact on the open phase fault between the two sources is verified in 5.5.2. The only notable difference with the current case is a ground fault will be supplied

by both sources rather than one of them, therefore (5.27) and are to be updated as follows:

$$[(\Delta \mathrm{IxG})_{t2} - (\Delta \mathrm{IxG})_{t1}] + [(\Delta \mathrm{IxDG})_{t2} - (\Delta \mathrm{IxDG})_{t1}] > 0 \qquad (x=0,1,2) \qquad (5.35)$$

However, as discussed in 5.5.2, the high impedance ground fault reduces the load unbalance of the system caused by interruption of one phase and thus, the following behavior can be measured by PMUs at the instant of a high impedance ground fault develops from an open phase fault.

$$\begin{bmatrix} \left(\frac{\Delta \mathrm{I1G}}{\Delta t}\right) > 0 \\ \left(\frac{\Delta \mathrm{I2G}}{\Delta t}\right) < 0 \\ \left(\frac{\Delta \mathrm{I0G}}{\Delta t}\right) < 0 \end{bmatrix} \qquad (5.36)$$

$$\begin{bmatrix} \left(\frac{\Delta \mathrm{I1DG}}{\Delta t}\right) > 0 \\ \left(\frac{\Delta \mathrm{I2DG}}{\Delta t}\right) < 0 \\ \left(\frac{\Delta \mathrm{I0DG}}{\Delta t}\right) < 0 \end{bmatrix} \qquad (5.37)$$

5.7 Test System

The base of this case study relies on 27.6 KV grounded utility distribution feeder with integrated wind machine type 4. Figure 5.9 shows the simplified one-line diagram of the feeder modeled using PSCAD/EMTDC Electromagnetic Transient-based software. The feeder contains single- and three- phase laterals and therefore, will have some degree of voltage and current imbalances. The detailed feeder is presented in Appendix A.

5.8 Test Scenarios

The two representative scenarios of a single open phase fault with the following cases are studied:

1) Scenario 1: fault located between the DG and the grid (point 1)

    a. Case 1: Single open phase fault with no ground

b. Case 2: single open phase with downed wire (high impedance ground)

2) Scenario 2: fault between the same side of DG and grid (point 2)

a. Case 1: single open phase with no ground

b. Case 2: single open phase with the downed wire (high impedance ground)

c. Case 3: single open phase with the solid ground fault

3) Scenario 3: Sensitivity & security limitation

5.8.1 Scenario 1 Case 1

The single open phase fault without ground is simulated at point 1, and at t=2.5, second (phase "b" is opened) of the feeder is shown in Figure 5.9. The results of simulation are shown in Figure 5.10 and Figure 5.11. In Figure 5.10, active power, reactive power, and magnitude of symmetrical component voltage of DG and grid are shown. In Figure 5.11, the magnitude of the symmetrical component currents is shown. It is assumed that the measurement is performed by two PMUs located at the PCC and the substation. In Figure 5.10, the opposite rate of change in power of the two sources reveals that the fault is located between the DG and the grid. Since after the fault, $P_{Grid} \downarrow$ decreases $P_{DG} \uparrow$ increases, and the direction of power flow is from the grid to the faulty point, the following equations will identify the fault:

$$\frac{\Delta P_{Grid}}{\Delta P_{DG}} = \frac{-2.20}{1.5} = -1.46 \leq -1$$

The above result reveals that the fault is between the two sources and is being fed by the grid.

$$\left(\frac{\Delta I1G}{\Delta t}\right) < 0 \quad \frac{\Delta I0G}{\Delta t} > 0$$

$$\left(\frac{\Delta I1G}{\Delta t}\right).\left(\frac{\Delta I2G}{\Delta t} + \frac{\Delta I0G}{\Delta t}\right) < 0$$

The validity of the above inequality reveals that the fault is an open phase fed by the grid.

$$\Delta V1G = \Delta V1DG \simeq 0$$

The rate of positive sequence voltage change shows that no parallel fault is detected during the simulation.

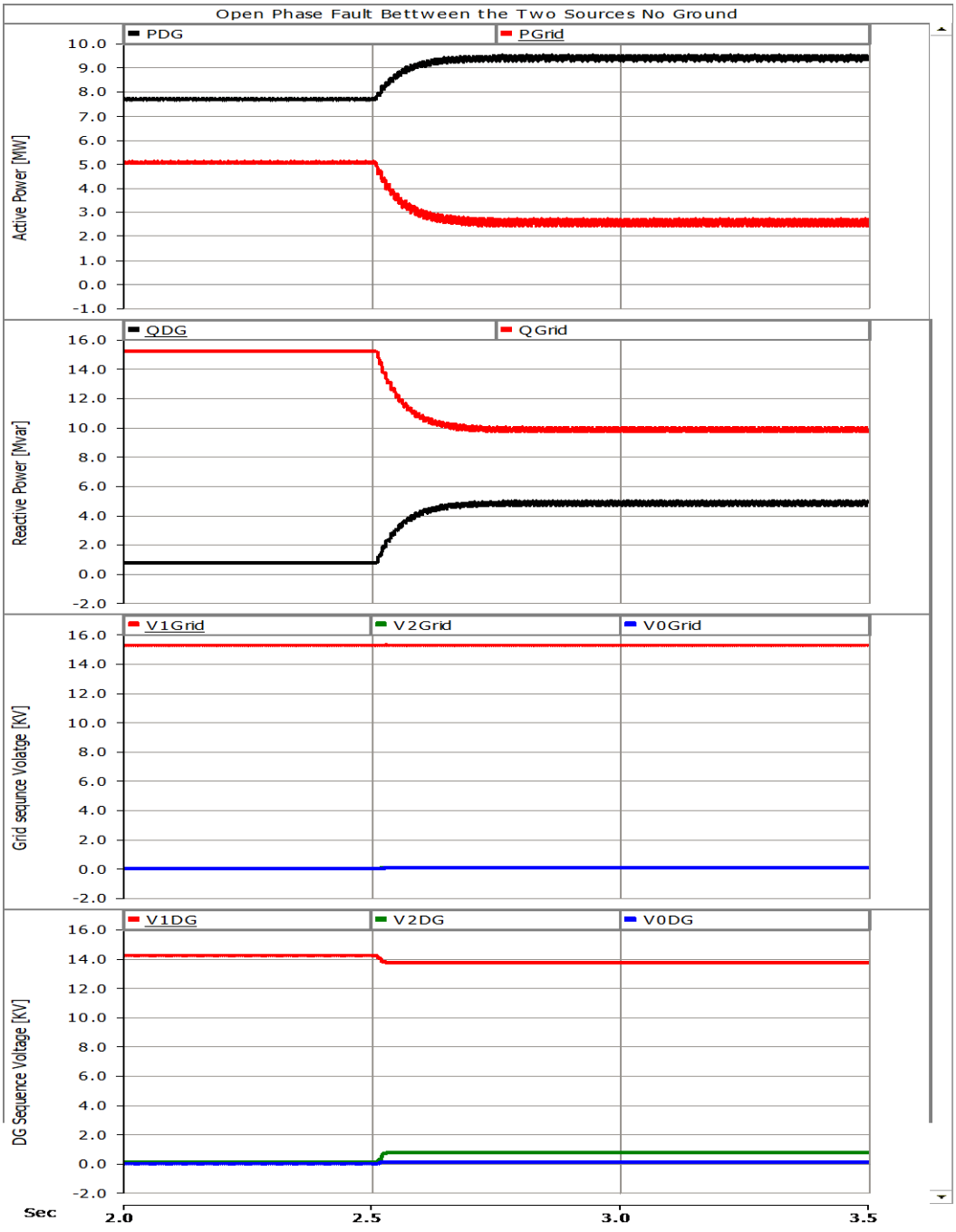

Figure 5.10. Open Phase Fault Scenario 1-Case 1-Power & Voltage

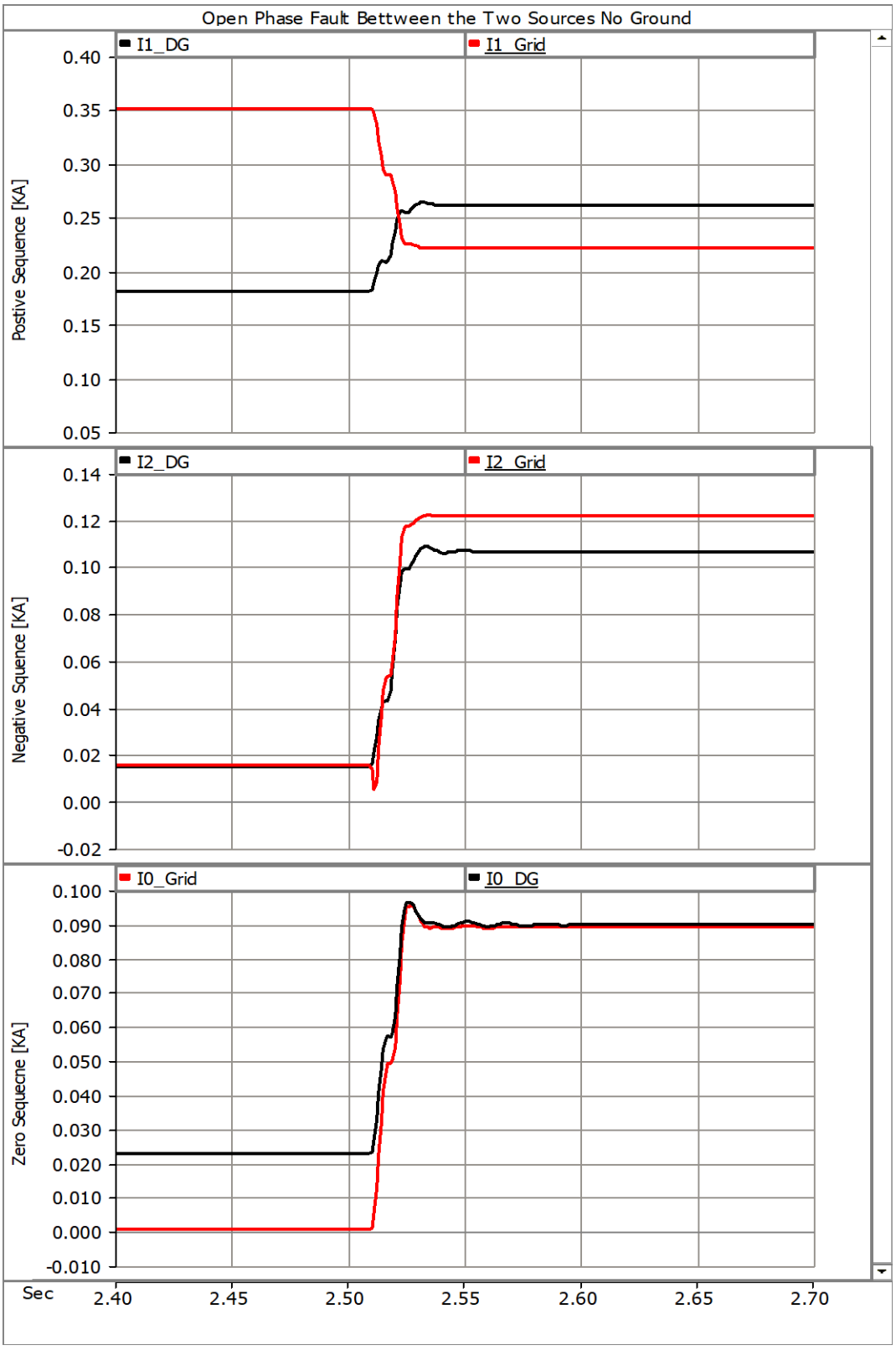

Figure 5.11. Open Phase Fault Scenario 1-Case 1-Current

5.8.2 Scenario 1 Case 2

The single open phase fault with ground is simulated at point 1 and at t=2.5 second (phase "b" is opened) of the feeder, as shown earlier in Figure 5.9. The fault extended to an open phase fault with high impedance ground at t=4 sec at the grid side of the open phase. The results of simulation are shown in Figure 5.12 and Figure 5.13. In Figure 5.12 active power, reactive power, and magnitude of symmetrical component voltage of DG and grid are shown. In Figure 5.13, the magnitude of the symmetrical component currents is shown. It is assumed that the measurement is performed by two PMUs located at the PCC and the substation. For the time between $2.5 \leq t \leq 3$, is very similar to sequence that has shown in the previous case (scenario 1- case 1).

$$\frac{\Delta P_{Grid}}{\Delta P_{DG}} \leq -1$$

The above result shows that the fault is between the two sources and is fed by the grid.

$$\left(\frac{\Delta I1G}{\Delta t}\right) < 0$$

$$\left(\frac{\Delta I2G}{\Delta t}\right) > 0$$

$$\frac{\Delta I0G}{\Delta t} > 0$$

$$\left(\frac{\Delta I1G}{\Delta t}\right).\left(\frac{\Delta I2G}{\Delta t} + \frac{\Delta I0G}{\Delta t}\right) < 0$$

The validity of the above inequality reveals that the fault is an open phase type and confirms that it is being fed by the grid. At $t = 3.00$ sec, the high impedance ground fault with a resistance of 200 ohms has been added to the circuit. The changes in the signature of the open phase fault with high impedance ground fault is negligible, as expected.

$$\Delta V1G = \Delta V1DG \simeq 0$$

The rate of change of positive sequence impedance shows that no parallel fault is detected.

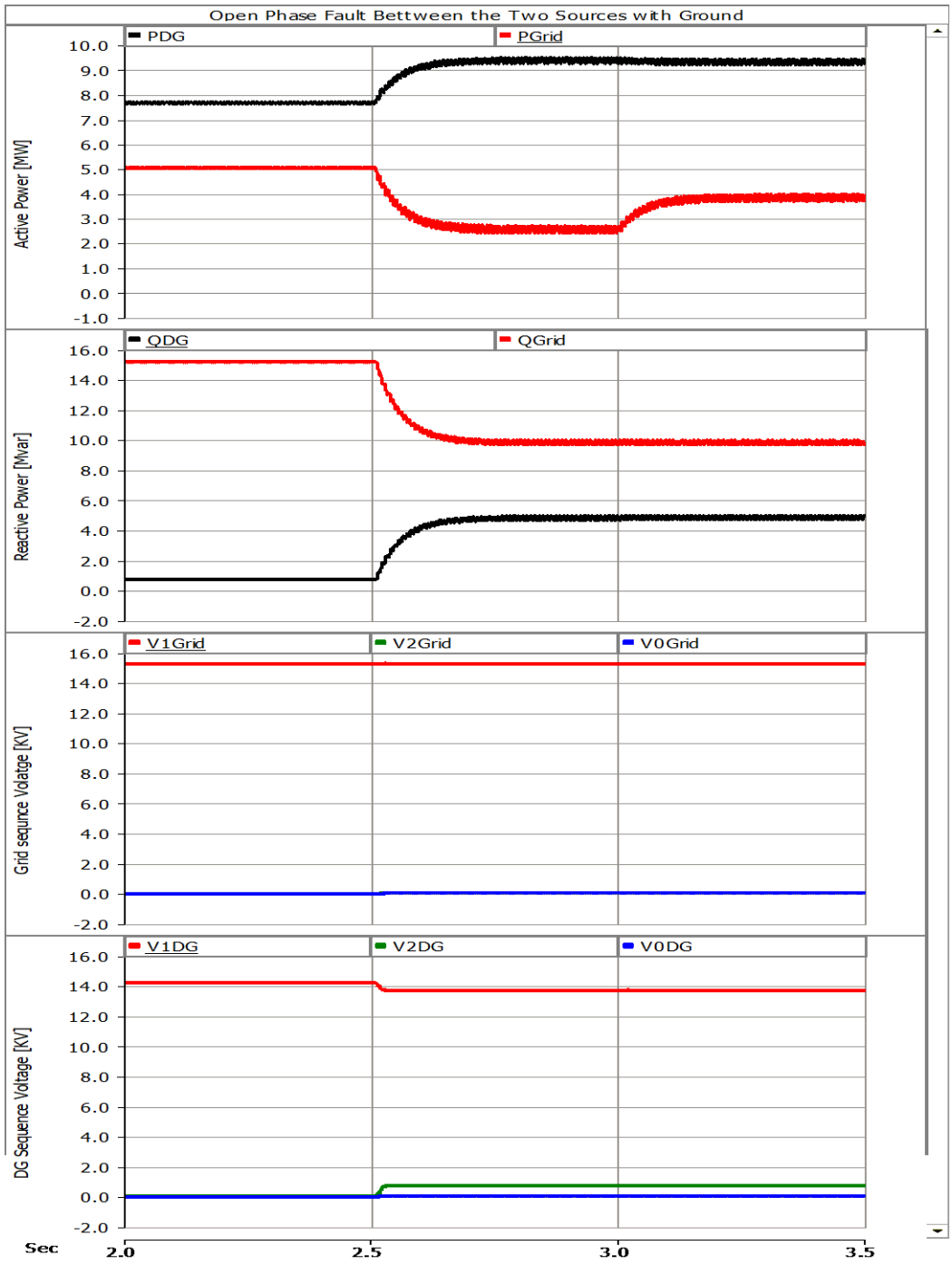

Figure 5.12. Open Phase Fault Scenario 1-Case 2

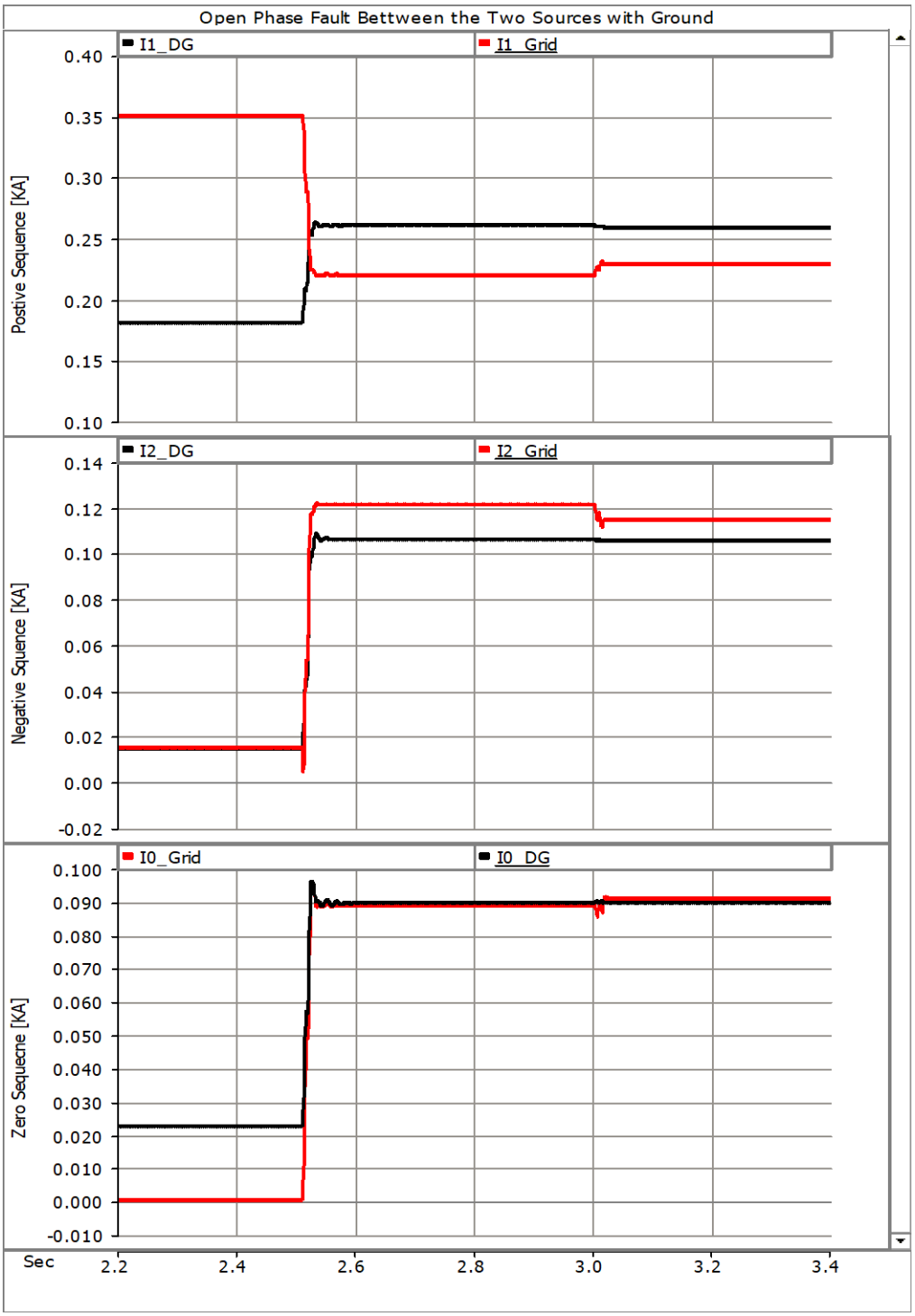

Figure 5.13. Open Phase Fault Scenario 1-Case 2

5.8.3 Scenario 2 Case 1

The single open phase fault without ground is simulated at point 2 and at t=2.5 second (phase "b" is opened) of the feeder shown earlier in Figure 5.9. The open phase is located on the same side of both sources. The result of this simulation is shown in Figure 5.14 and Figure 5.15. In contrary to the previous simulation, for the fault on the same side of the sources, at the instant of the fault, active power for the two sources changes in the same direction at the station and DG. Both $P_{DG} \downarrow$ and $P_{Grid} \downarrow$ decrease due to the loss of portion of the load in the phase "b".

$$\frac{\Delta P_{Grid}}{\Delta P_{DG}} > 0$$

The above result shows that the fault is between the two sources and is fed by the grid.

$$\left(\frac{\Delta I1G}{\Delta t}\right) < 0 \qquad \left(\frac{\Delta I1DG}{\Delta t}\right) < 0$$

$$\left(\frac{\Delta I2G}{\Delta t}\right) > 0 \qquad \left(\frac{\Delta I2DG}{\Delta t}\right) > 0$$

$$\left(\frac{\Delta I0G}{\Delta t}\right) > 0 \qquad \left(\frac{\Delta I0DG}{\Delta t}\right) > 0$$

$$\left(\frac{\Delta I1G}{\Delta t}\right).\left(\frac{\Delta I2G}{\Delta t} + \frac{\Delta I0G}{\Delta t}\right) < 0 \qquad \left(\frac{\Delta I1DG}{\Delta t}\right).\left(\frac{\Delta I2DG}{\Delta t} + \frac{\Delta I0DG}{\Delta t}\right) < 0$$

The validity of above inequality reveals the that fault is open phase and confirms that it is being fed by grid.

$$\Delta V1G = \Delta V1DG \simeq 0$$

The rate of change of the voltage shows that during the simulation no parallel fault is detected.

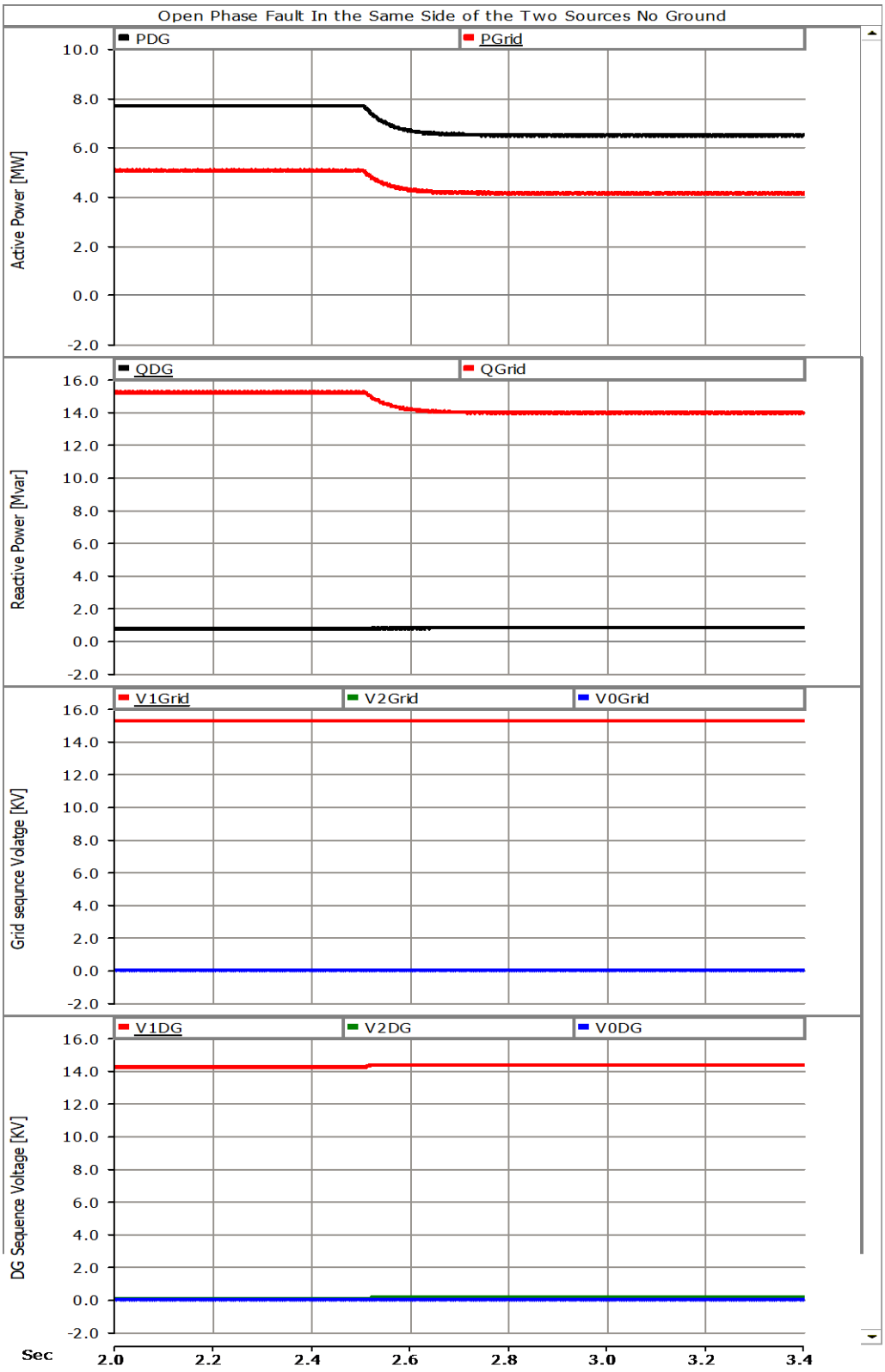

Figure 5.14. Single Open Phase Fault (phase b)- Current

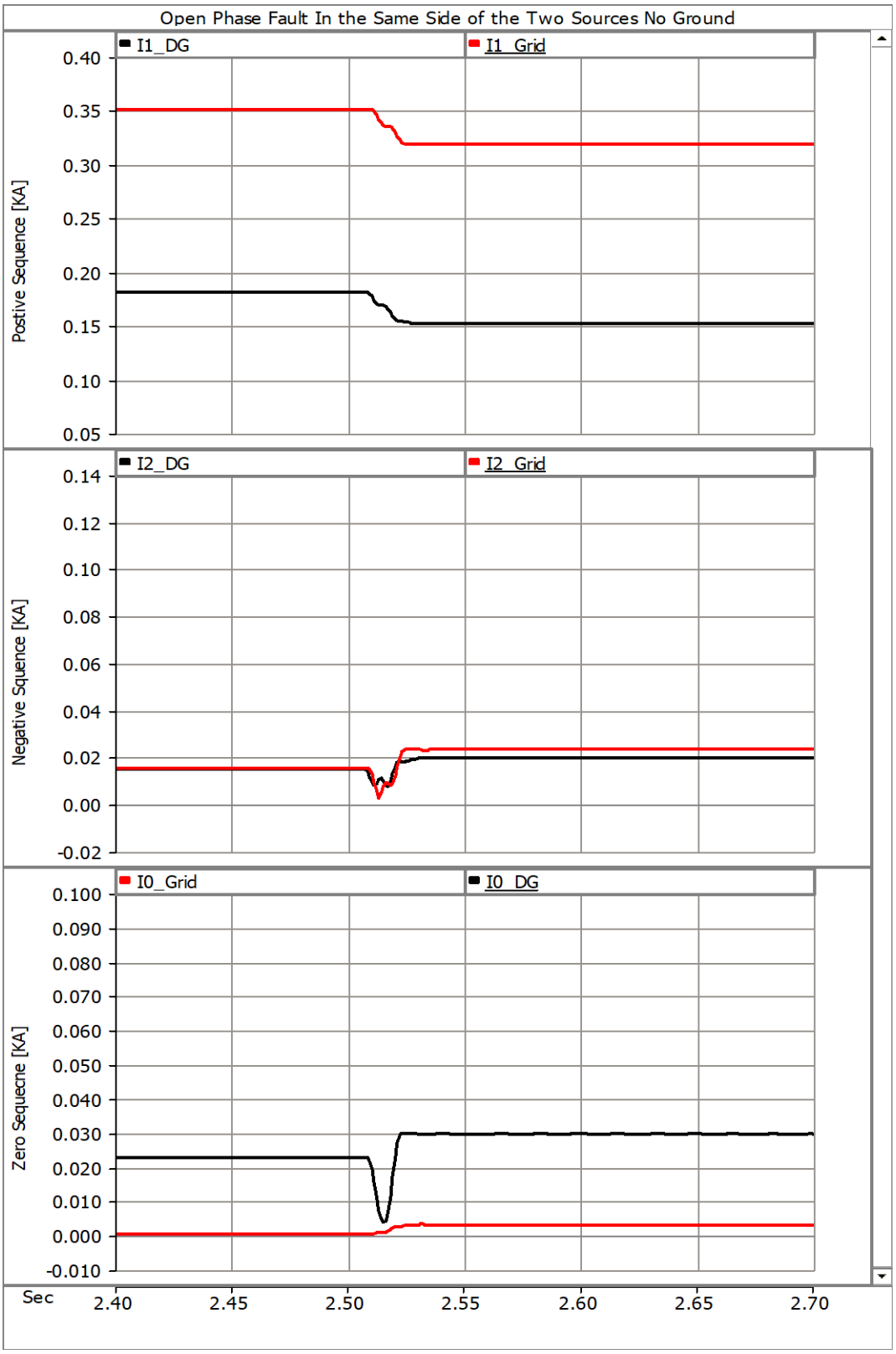

Figure 5.15. Single Open Phase Fault (phase b)- Current

5.8.4 Scenario 2 Case 2

The single open phase fault without ground is simulated at point 2 at $t = 2.5$ second (phase "b" is opened) of the feeder, shown in Figure 5.9. The ground fault with resistance of 200 ohm on the source side is added to the simulation at $\mathrm{t} = 3.00$ sec. The ground fault current measured at the fault is 36 A, which represents the high impedance ground fault (typically less than 50 A) and is caused by a fallen wire. The simulation results are shown in Figure 5.16 and Figure 5.17. The power for the two sources changes in the same direction at the station and at the DG. Both $\mathrm{P_{DG}} \downarrow$ and $\mathrm{P_{Grid}} \downarrow$ decrease due to the loss of portion of the load in the phase "b". The power, voltage, and current measured at PCC and substation and for the time between the open phase and ground fault ($2.5 \leq t \leq 4$) shows an open phase fault signature similar to scenario 2 case 1. (5.19) can be considered for both sources in this simulation:

$$\frac{\Delta \mathrm{P_{Grid}}}{\Delta \mathrm{P_{DG}}} = \frac{-0.75}{-1.22} = 0.61$$

$$\left(\frac{\Delta \mathrm{I1G}}{\Delta \mathrm{t}}\right) = -0.03 \text{ KA} \qquad \left(\frac{\Delta \mathrm{I1DG}}{\Delta \mathrm{t}}\right) = -0.03 \text{ KA}$$

$$\left(\frac{\Delta \mathrm{I2G}}{\Delta \mathrm{t}}\right) = 0.007 \text{ KA} \qquad \left(\frac{\Delta \mathrm{I2DG}}{\Delta \mathrm{t}}\right) = 0.05 \text{ KA}$$

$$\left(\frac{\Delta \mathrm{I0G}}{\Delta \mathrm{t}}\right) = 0.003 \qquad \left(\frac{\Delta \mathrm{I0DG}}{\Delta \mathrm{t}}\right) = 0.007 \text{ KA}$$

$$\left(\frac{\Delta \mathrm{I1G}}{\Delta \mathrm{t}}\right).\left(\frac{\Delta \mathrm{I2G}}{\Delta \mathrm{t}} + \frac{\Delta \mathrm{I0G}}{\Delta \mathrm{t}}\right) < 0 \qquad \left(\frac{\Delta \mathrm{I1DG}}{\Delta \mathrm{t}}\right).\left(\frac{\Delta \mathrm{I2DG}}{\Delta \mathrm{t}} + \frac{\Delta \mathrm{I0DG}}{\Delta \mathrm{t}}\right) < 0$$

The validity of the above inequality shows that the fault is open phase and confirms that it is being fed by the grid.

$$\Delta \mathrm{V1G} = \Delta \mathrm{V1DG} \simeq 0$$

The rate of change of the positive sequence voltage shows that there is no parallel fault in the circuit. After the high impedance ground fault is added to the system, the voltage remains the same, and small changes or perturbations that are observed in the current component does not change the inequality criteria of open phase.

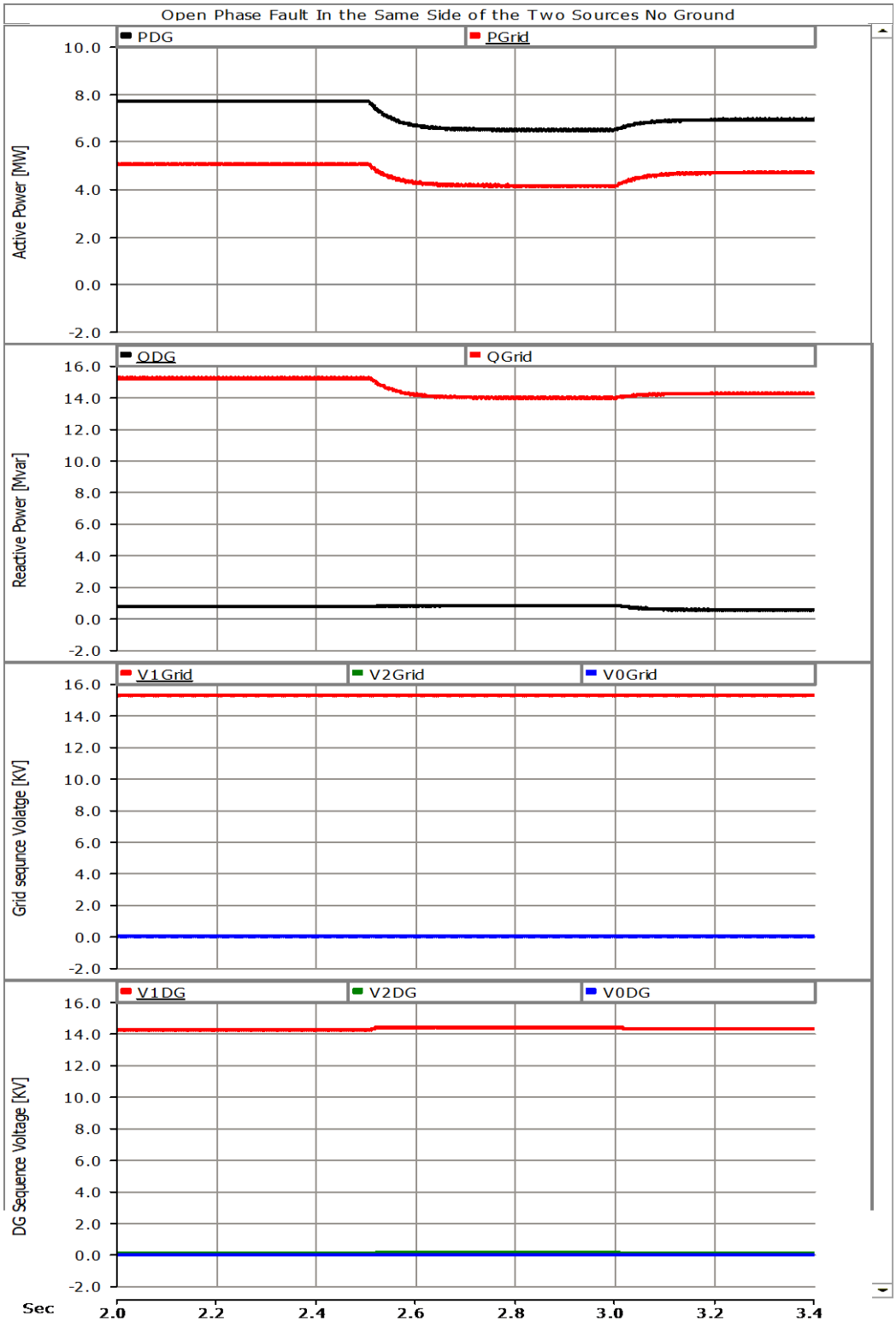

Figure 5.16. Single Open Phase Fault (phase b)- Current

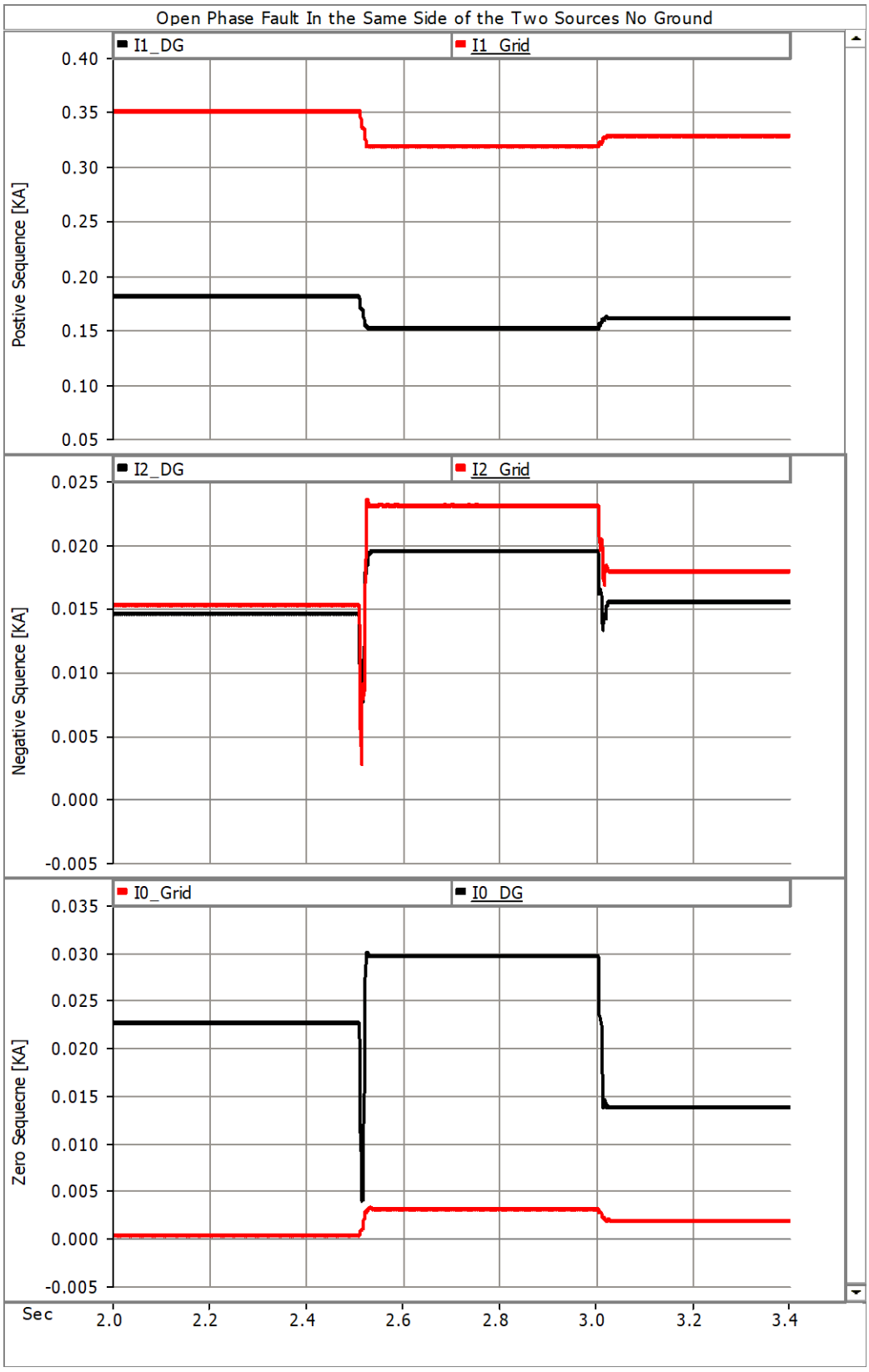

Figure 5.17. Single Open Phase Fault (phase b)- Current

5.8.5 Scenario 2 Case 3

The single open phase fault is simulated at point 2 and at $t = 2.5$ second (phase "b" is opened) of the feeder, as shown earlier in Figure 5.9. The solid ground fault is added to the circuit at $t = 4.0$ sec. The purpose of this simulation is to compare the open phase fault with the solid or low impedance ground fault with the high impedance ground fault. It is interesting to note that one of the major discriminations between the open phase fault and any parallel fault is the rate of change $\frac{dIG1}{dt}$ or $\frac{dIDG1}{dt}$ which is negative opposite to any other fault. Figure 5.18 and Figure 5.19 show the results of this simulation. The detection of a solid ground fault is not an issue for the conventional protection system. After $t = 3.0$ sec, the signature of the open phase fault is totally dissolved by the ground fault protection signature.

The sudden increase in rate of change in all the three-current components $I1, I2, I0$ make the fault easily detectable by any simple or conventional over current protection element. However, it should be noted that the extension of the open phase fault is not a solid ground fault. The concern about the open phase conductor and its consequences is a high impedance ground fault which is not reliably detected by conventional protection system.

It is interesting to note that one of the major discriminations between the proposed solution and parallel fault is at the instance of the open phase fault the rate $\frac{dIG1}{dt}$ for both grid DG are negative. While this is opposite to any parallel fault characteristics.

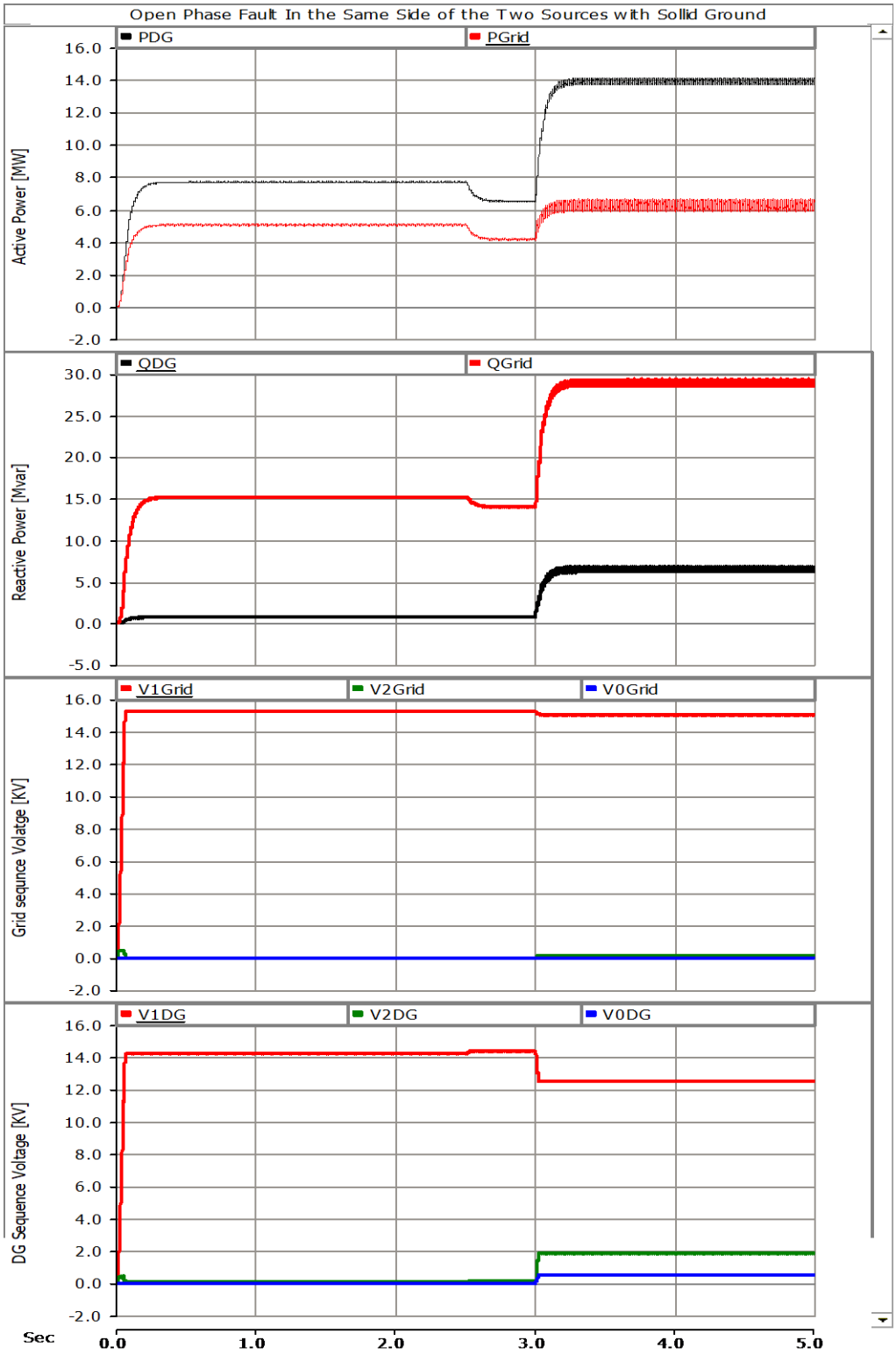

Figure 5.18. Single Open Phase Fault with Solid Ground

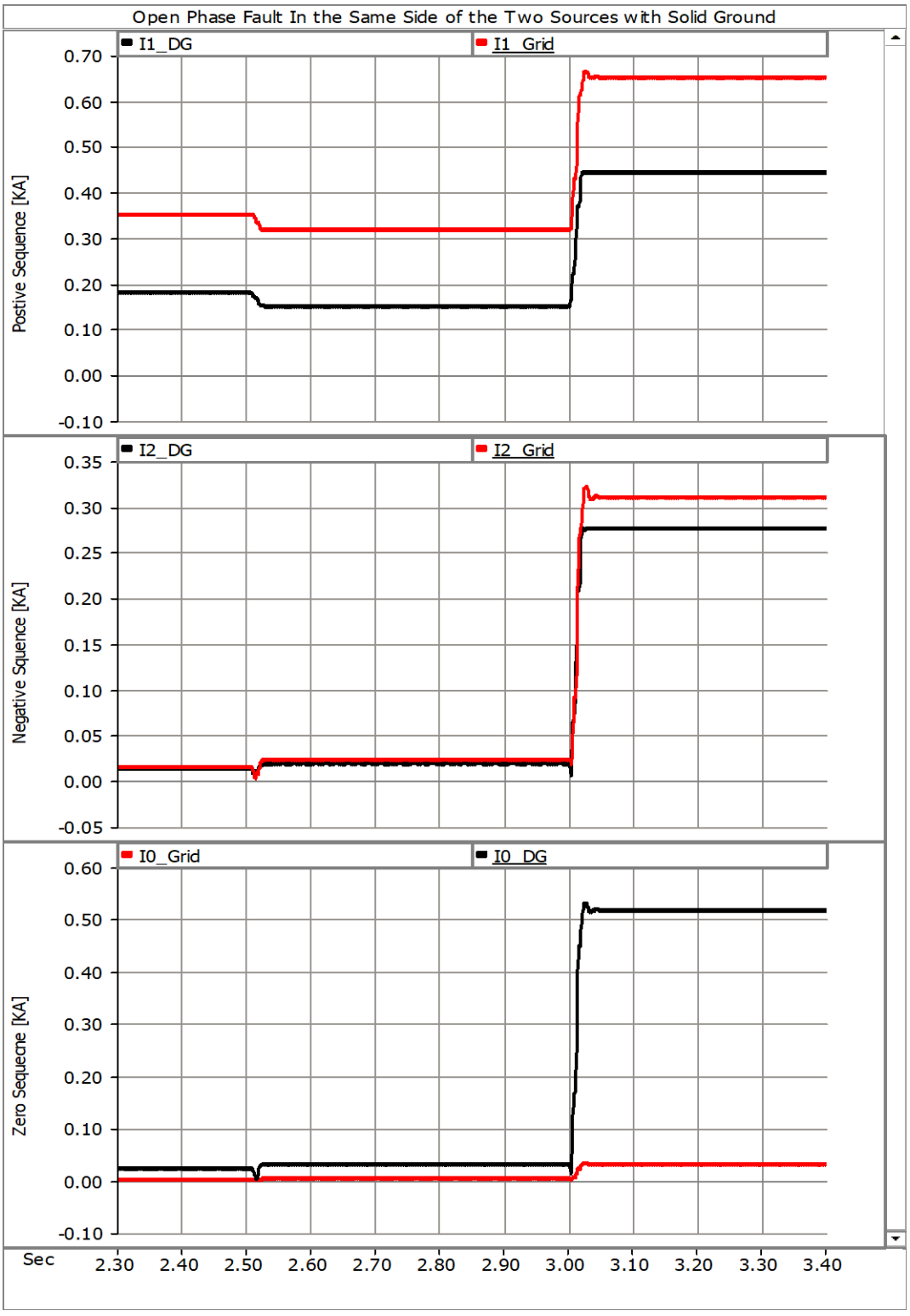

Figure 5.19. Single Open Phase Fault with Solid Ground

5.8.6 Scenario 3 Sensitivity Limitation

The solution presented in this chapter is a current based solution, therefore, in order to detect the open phase fault, the fault should interrupt a minimum amount of the load in the faulty phase. In Figure 5.20, the single open phase fault without ground is simulated at the end feeder in point 2 at “t=2.5” second (phase “b” is opened). The minimum load that is required for the proposed algorithm to detect the open phase is determined by sensitivity analysis and is about 4% of total supplied load at instant of open phase incident. This means that for the solution to work, minimum 4% of the three phase load should be exposed to open phase circuit to leave the signature that is described in (5.18). It important to note that for an ideal balanced feeder with the balanced load, the sensitivity is limited to the ability of measuring the current reliably considering the error of the measurement. However, generally, if prior to the occurrence of an open phase, there is a unbalance load in the circuit in the worst case scenario, the open phase fault will be detectable if the open phase fault disturbs the load which is, at minimum, slightly greater than the current feeder unbalance load. In the current example, the load unbalance is about 2-3 %.

The sensitivity of the proposed solution is not the same among the phases when the feeder supplies an unbalance load. The phase with the highest load represents the least sensitive phase. Figure 5.21. shows the open phase simulated at t=3 sec on the phase with the largest load. The feeder supplies around 15 MVA (1 PU) and phase “C” carries about 5.2 MVA, 1.3% above the average load per phase and has the highest load. The negative sequence component (I2) prior to the open phase incident created by an unbalanced load is around 3.2%. The plotted results show that the open phase in phase C can be detected only if the open phase fault generates more negative sequence current than the unbalance load (3.2%) to leave the detachable signature described in (5.18).

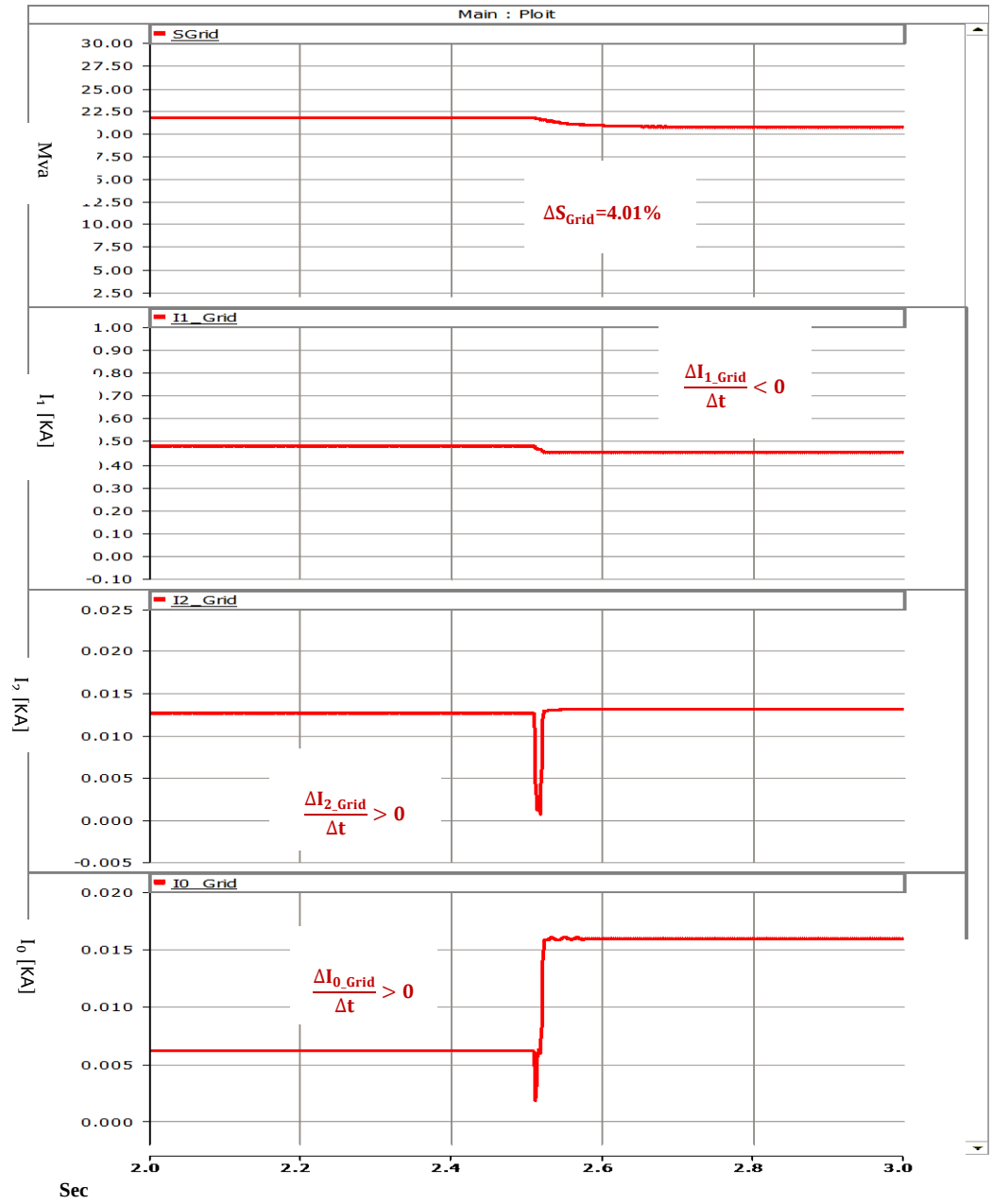

Figure 5.20. Single Open Phase at the End of Feeder with 4% Load

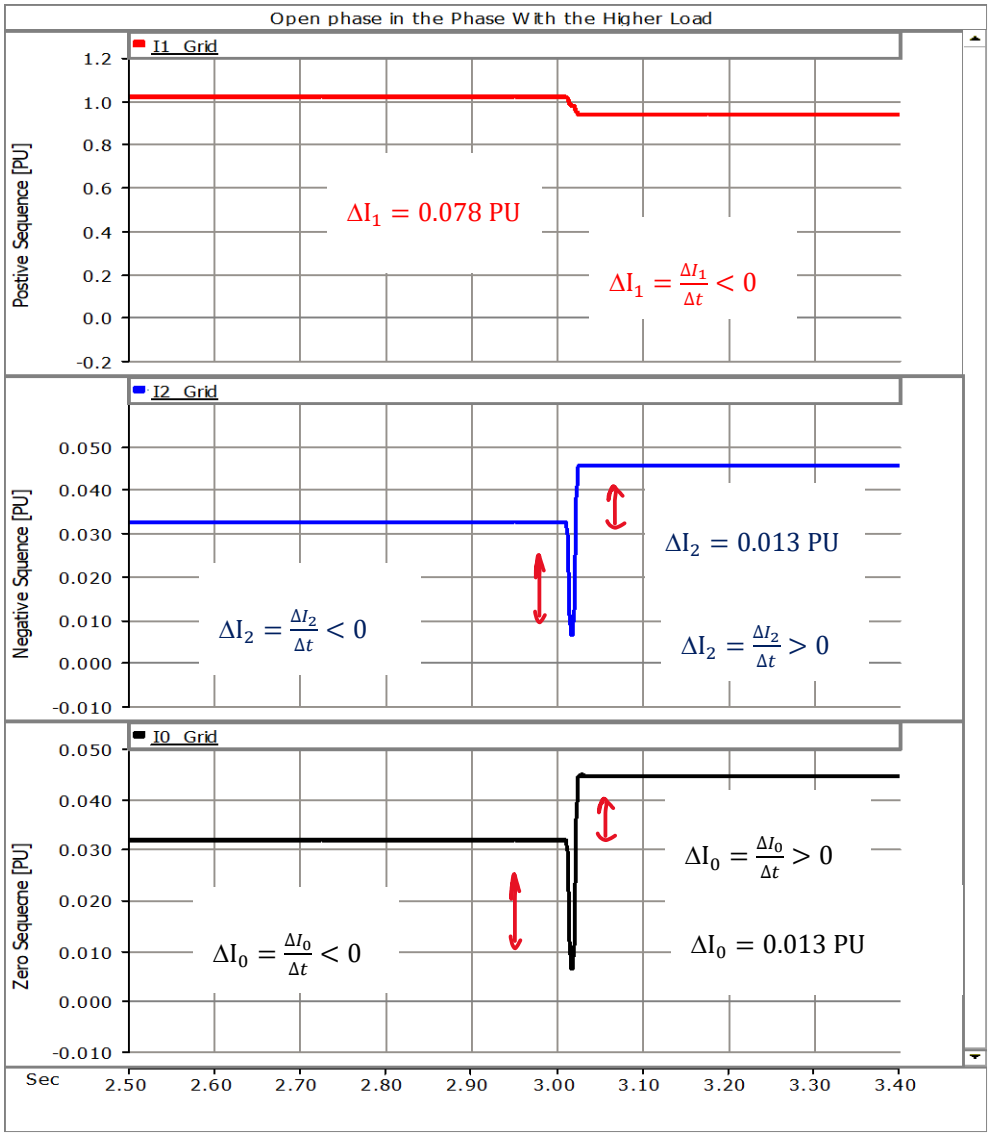

Figure 5.21. Single Open Phase at the End of Feeder with 4% Load

In regard to security of the proposed solution as previously shown in Table 5-1 if a single-phase load connected directly to the primary feeder is switched off by the consumer, not by fault, fuse blown, or feeder operator, this can be seen erroneously as an open phase fault by the proposed sensitive open phase detection algorithm. Figure 5.22 shows that the single-phase load (0.02 PU) is turned off in the completely balanced three-phase system and the dynamic of this switching can be seen by this solution as an open phase. The minim threshold provision in (5.18) is considered to desensitize the algorithm based on the largest single phase load installed at the primary feeder. For example, if the largest single-phase load is 0.02PU installed in the primary

The $\mathrm{Iset1}_{\mathrm{min}}$ must be set at least 3%.

$$\frac{\Delta \mathrm{I1}}{\Delta \mathrm{t}} \geq \mathrm{Iset1}_{\mathrm{min}} \geq 0.03$$

Therefore, the actual sensitivity of the solution is equal to the greater value of the maximum expected unbalance load and the largest installed single-phase load on the primary circuit (one load not a group of loads). With the consideration of the cases discussed in this section the proposed solution can protect 90% to 95% of the feeder-load against the open phase fault if we assume the unbalanced load and the largest installed single-phase load on the primary circuit are somewhat less than 5% to 10% of the feeder rating.

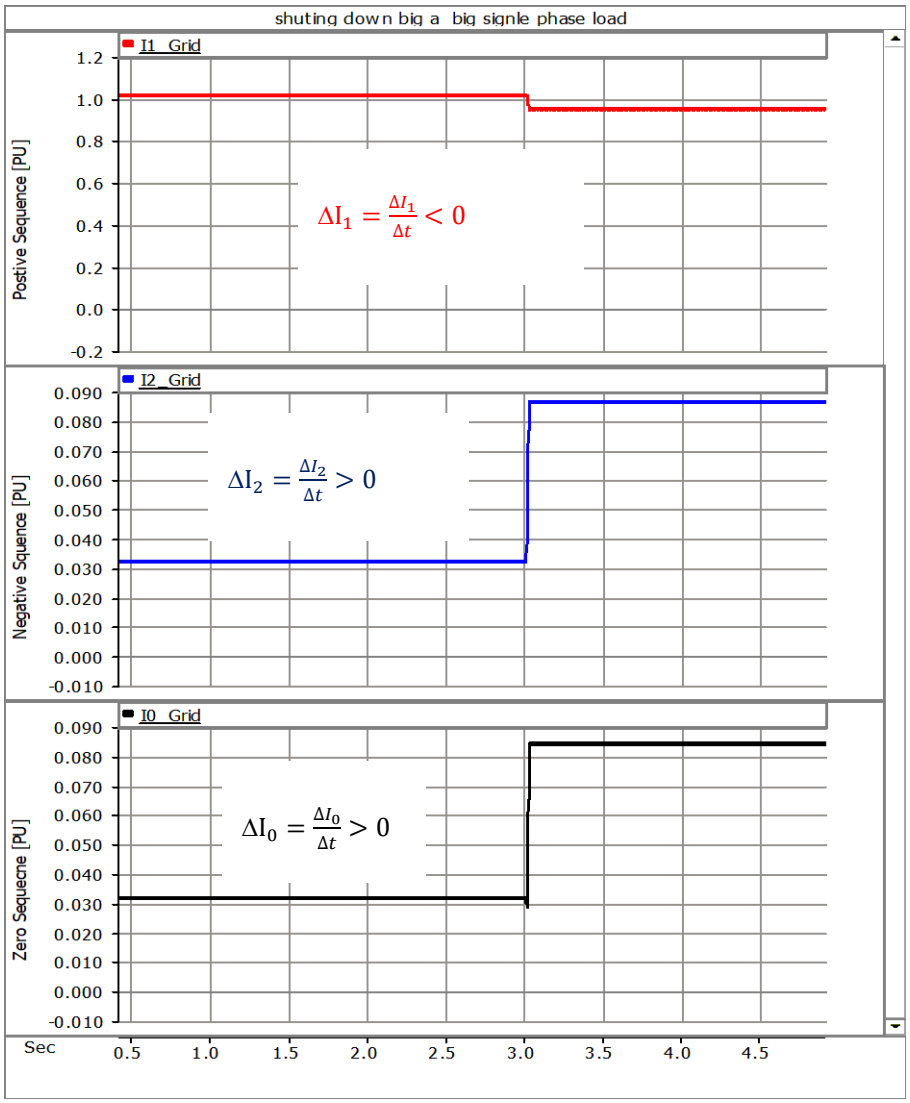

Figure 5.22. Single Open Phase at the End of Feeder with 4% Load

5.9 Conceptual Implementation

The prime PMU application so far has been on the wide area of the power transmission network and bulk energy power system. Although the proposed solution focuses on the open phase fault detection in a distribution network, the same principal can be applied in any network by taking advantage of PMU data stream phasor measurement which makes sets of current and voltage phasors available on a real time basis. The PMU data in the distribution network can serve many applications, such as islanding and fault locations as well as open phase detection scheme. Therefore, capital investment for such a multipurpose device is much easier to justify. The PMU function, as part of integrated IED, is available at negligible additional cost from mainstream IED manufacturers. The communication system architecture for the proposed solution is illustrated in Figure 5.1. The utilization of PDC, particularly for the number of PMUs used in this application, is not essential. Instead, using IEC61850-90-5 standard complaint PMUs, where PMUs connected at the PCC or substation can directly exchange their data in a peer to peer communication relationship by using GOOSE in PDU, can improve the time performance of the application. The main time-consuming tasks in the proposed solution are as follows:

1. PMU response to stream the phasor data
2. Communication time delay
3. Open Phase Detection (OPD) logic task

The communication time delay depends on the type of media and can vary from 5-30 ms. PMU real time performance can take around 10-20 ms, and OPDs logic around 10-20 ms, considering 3 to 5 sample windows for decision making process. The time performance limitation must be taken into consideration when this application is used to block the fast auto-recloser scheme. This chapter presented a novel open phase detection scheme in the distribution feeder with DGs. The application is based on PMU data that are available in substation and PCCs. The solution is examined based on analysis carried on PSCAD/EMDC modeling and calculations.

The open conductor with the ground is modeled as a two-step event which starts with the breaking the conductor and a time delay for it to develop into a ground fault on the bus

side. Detection of open phase fault should be done prior to development of this fault into a ground fault. Symmetrical component characteristics are used as the chief property of the open phase identifier. Rate of change, both in amplitude and in angle of both current and voltage symmetrical components, proved to be reliable metrics to identify the target fault in a complex feeder with multiple power sources.

5.10 Summary

In this chapter, the second use case to detect the open phase fault using the synchrophasor data was studied. The vulnerability of distribution systems in an open phase fault and a critical review of the reach conducted in this area was presented in this chapter. The problem is formulated by analyzing the single- and two-phase open phase fault, with and without high impedance ground using symmetrical component analysis technique and EMT model development. Based on the fault signature, specific measurable criteria were developed to identify open phase fault by PMUs located at the substation and point of common coupling. The algorithm was further developed for a feeder with the multiple integrated DGs. The high impedance ground fault recognition and impact were added to the existing criteria. Although, it is shown that the high impedance fault impact is predictable following the open phase fault, the open phase fault signature is still recognizable with and without the ground fault.

The test system was developed using PSCAD/EMTDC software and a utility type distribution feeder with the actual parameters was modeled using this software. The test scenario to examine the reliability of the proposed solution was developed with emphasis on dependability and security. From the many simulations that were carried out, select representative results were analyzed and reported. The conceptual implementation for the proposed solution considering the market available hardware and software was proposed.

The next chapter will summarize the work, present the major conclusion of this work, and provide suggestions for future research work.

Chapter 6

6 Summary

The communication technology to create a new generation of protection relays that works not only by sensing an abnormal condition based on local measurements, but also by receiving information from remote devices, is becoming more and more possible. NASPI (North American Synchro Phasor Initiative), which is funded by U.S. Department of Energy, has been focusing on bulk power energy and the wide area network. However, the deployment in this area so far, has been limited to some non-time critical monitoring applications. In this initiative, not much attention has been given to distribution systems.

The topology of a typical distribution feeder is very similar to wide area networks but at a much smaller scale, as it contains many connections and branches. However, no infrastructure is available to provide information from these nodes and branches that can be utilized for protection and control system. For many years, the simplicity of the distribution system as a radial system and a network which is designed to be an interface to the consumers only permitted that utilities operate this system as it is with little need for communication and measuring technologies.

With the technological changes that are coming, the distribution system is at the forefront of smart grid initiatives, DG integration, peak demand management, and the microgrid. These are transforming the distribution network from simple radial systems to the more complex bidirectional flow systems which must manage and protect the local generation and the independent, smaller local grids. In this research, the use of synchrophasor data for the protection of the distribution network has been investigated and it has been shown that the investment in this application, coordinated with other aforementioned initiatives, is underway in the distribution system.

The synchrophasor data can serve many protection and control applications with the same structure, some of which are recommended as future research objectives in this work. This work investigates two protection use cases and shows that more work and research in this area can prepare the distribution system with its transformation to a grid with local generations.

The integration of synchrophasor data to the substation automation infrastructure promoted by IEC61850-90-5, further provides an opportunity for the distribution system to make this into an integrated part of the substation automation application and makes the overall application more economically effective.

6.1 Summary and Conclusion

In Chapter 1, an introduction to power system structure and the need to modernize the power grid due to multiple factors, such as economic, political, environmental and technical, including aging infrastructure, integration of multiple DER (Distributed Energy Resources), other new technologies, security concern and more influence of the end consumer to the local legislation. It is discussed that despite the past power industry investment history which has favorited generation and transmission the need for shift of focus to distribution systems modernization. The synchrophasor technology, its advancement and the prospective of its role is discussed. The objectives of the research were presented. Chapter One also included an introduction to synchrophasor measurement, PMU, and μPMU power system protection relevant to the area of this research.

In Chapter 2, the fundamentals of the distribution system feeder structure relevant to this research was presented. The Principle of protection in distribution and feeder protection specifics were reviewed. Challenges related to the integration of DG and DG characteristics were also verified. Wind turbine type 1 to 4 and PV solar DG short circuit and reactive power production capability were studied. The changes in the regulatory standard, such as IEEE 1547 related to DG integration and islanding, were reviewed and summarized.

In Chapter 3, the fundamentals of synchrophasor measurement, data communication, performance, signal processing, application, and system architecture were presented. The IEC61850 compliant system appropriate for the current research in the area of protection application was discussed. The concept of μPMU and high PMU data resolution for distribution systems is reviewed. The accuracy required for some of distribution application is reviewed.

In Chapter 4, the proposed research solution for islanding detection based on phasor measurement data was presented. The mathematical formulation for the detection

algorithm was provided. The test model was developed in PSCAD-EMTDC and MATLAB based on actual utility feeder data. The mathematical formulation is validated by numerous simulations on a real-world test model. The concept is generalized by developing separate models for the mainstream DERs and concept is tested with real world scale utility feeder.

In Chapter 5, the research-based proposed solution for open phase fault detection with and without a downed wire (ground fault) based on synchrophasor data was presented and discussed. The mathematical formulation for the detection algorithm was also described. The computer-based test model was developed in PSCAD-EMTDS and MATLAB based on utility data. The algorithm was validated with numerous simulations representing many actual cases.

6.2 Contribution of this Work

The following are the major contributions of this work in the subject area of this study and distribution systems:

1. This study has provided a theoretical justification that synchrophasor measurement devices can be successfully utilized to address some of the existing and new challenges faced by distribution systems in relatively smaller applications, such as distribution feeders, where a smaller number of PMUs are used in comparison to typically wide area applications, as demonstrated in the use cases in this work. The integration of PMU data using IEC61850-90-5 communication standard with substation automation system can be addressed. The proposed system architecture as demonstrated in this study can be utilized for many applications which will maximize the return of investment on phasor measurement technology in utilities' network.

2. The proposed solution for the first use case - the islanding detection - has contributed to this subject with the following specific innovative features:

    a. The proposed solution relies on the existing protection infrastructure at substations and points of common coupling.

b. The proposed solution uses the adaptive protection scheme when adaptation is done in non-critical time during feeder normal operation.

c. The proposed solution addresses the weakness of the passive detection schemes, particularly, the non-detection zone, by introducing sensitivity-based constrained detection of islanding, when applicable.

d. The proposed solution is not depending on the type of DG integrated into the feeder.

e. The proposed solution does not rely on the static angle of voltage differences between the PCC and DGs which can be small depending on the location and size of DGs. It is based on monitoring the change of this angle when islanding occurs, and the maximum sensitivity solution is defined based on the IEEE compliance PMU with one degree available in the marketplace.

f. The proposed solution if used for a sizeable DG integration in term of power size 2.00 MW and above does not require the use of high-performance PMU.

3. The proposed solution for the second use case, detecting the open phase fault is a major contribution to this subject since the selective detection of this fault is nonexistent. The proposed solution relies on the waveform properties of the open phase fault to recognize it, and within that framework uses an algorithm based on the available and measurable data in substations and PCCs. The accuracy of the measured quantity is not as important as the changes in the quantity. The voltage phase angle is not used in proposed algorithm. Therefore, in contrast to many protection schemes, the proposed solution is immune to inaccuracies in measurement and is not relying on phase angle measurement.

At the time of publication of this work, two journal papers summarizing the two use cases studied for open phase and islanding detection are under review by the IEEE Power System Access.

6.3 Recommendation for Future Research Work

Some of the potential areas for further research are identified below:

1) There is potential to use synchrophasor data to provide real time visibility and state estimation for the distribution network. [63]

2) There is potential to use synchrophasor data to design the PMU-based adaptive over current protection system for distribution system with DG system [64].

3) There is potential to identify and optimize the number and location of PMU sensors to serve control and protection applications of a distribution network.

4) There is potential to develop a cost-constrained optimal load flow real time operational program based on distribution voltage profile measurements and communicated by PMUs.

5) There is potential to investigate upgrading and optimizing the Distribution Management System with the use of synchrophasor data.

6) There is potential for fault location application using synchrophasor data both in primary feeder and in the secondary underground network [65].

References

[1] United State Dpartment of Energy, "Smart Grid System Report," United State Department of Energy, Washington, DC, November 2018.

[2] T. S. Usten, S. M. Fraooq and M. S. Hussain, "Implementing Secure Routable GOOSE and SV Messages Based on IEC 61850-90-5," *IEEE Access,* vol. 8, Februray , 2020.

[3] North American Synchrophasor Initiative, "Itemizing and Calculating the Benefits From Synchrophasor Technology Use," NASPI, October 2015.

[4] P. Pegorano, K. Brady, P. Castelo and a. A. Meier, "Compensation of Systematic Measurement Errors in a PMU-Based Monitoring System for Electric Distribution Grids," *IEEE Transactions on Instrumentation and Measurement,* vol. 68, no. 10, October 2019.

[5] TR-109178, "Distribution Cost Structure Methodology and Generic Data," EPRI, Feb 1998.

[6] T. A. Short, Electric Power Distribution Hand Book, New York: CRC Press LLC, 2004.

[7] IEEE Working Group on Distribution Protection, "Distribution Line Protection Practices Industry Survey Results," IEEE Power System Relaying Committee, December 2002.

[8] Hydro One Inc., "Distribution Generation Technical Interconnection Requirment 50KV and Below-DT-10-015 R3," Hydro one Inc, Toronto , 2013.

[9] C. Chen, J. Wang, F. Qiu and D. Zhao, "Resilient Distribution System by Microgrids Formation After Natural Disasters," *IEEE Transaction on Smart Grid,* vol. 7, no. 2, March 2016.

[10] H. Farzin, M. F. Firuzabad and M. Moeini-Aghtaie, "Role of Outage Management Strategy in Reliability Performance of Multi-Microgrid Distribution Systems," *IEEE Transactions on Power Systems,* vol. 33, no. 3, May 2018.

[11] M. Khederzadeh and S. Zandi, "Enhancement of Distribution System Restoration Capability in Single/Multiple Faults by Using Microgrids as a Resiliency Resource," *IEEE Systems Journal,*, vol. 13, no. 2, June 2019.

[12] R. . F. Arritt and R. C. Dugan, "Distribution System Analysis and the Future Smart Grid," *IEEE Transactions on Industry Applications,* vol. 47, no. 6, December 2011.

[13] North American Electric Reliability , "Bulk Electric System Definition Reference Document," NERC, April 2014.

[14] North American Electrics Reliablity , "Distributed Energy Resources Connection Modeling and Reliability Considerations," NERC, February 2017.

[15] IEEE PES WG Wind Plant Collector System Design, "Characteristics of Wind Turbine Generators for Wind Power Plants," *IEEE PES, Power & Energy Society,* Aug 2016.

[16] Power System Relaying Committee, "IEEE Standard for Synchrophasor Data Transfer for Power Systems-IEEE Std C37.118.2™-2011,," IEEE, 2011.

[17] A. G. Phadke, "Sychronized Phasor Measurement a Historical Overview," IEEE, Virginia Tech, Blacksburg, Virginia, USA, 2002.

[18] M.Paolone, "Synchrophasor from Computation to Implemantaion," in *IEEE PES General Meeting,* Vancouver, July 2013.

[19] I. P. s. R. &. C. Commitee, "IEEE Standard Profile for Use of IEEE 1588 Precision Time Protocol in Power System Applications," IEEE, 2016.

[20] "http://w3.siemens.com," Siemense, 2014. [Online]. Available: http://w3.siemens.com/mcms/industrial-communication/en/rugged-communication/technology-highlights/ieee-1588-precision-time-synchronization-solution-for-electric-utilities/pages/i. [Accessed 5 11 2014].

[21] A. Papoulis, The Fourier integraland its application, New York: McGrawHill, 1962.

[22] B. Jafarpisheh, S. M. Madani and S. Jafarpisheh, "Improved DFT-Based Phasor Estimation Algorithm Using Down-Sampling," *IEEE Transactions on Power Delivery,* vol. 33, no. 6, December 2018.

[23] P. Banerjee and S. C. Srivastava, "An Effective Dynamic Current Phasor Estimator for Synchrophasor Measurements," *IEEE Transactions on Instrumentation and Measurement,* vol. 64, no. 3, March 2015.

[24] S. Vejdan, M. Sanaye-Pasand and P. Malik, "Accurate Dynamic Phasor Estimation Based on the Signal Model Under Off-Nominal Frequency and Oscillations," *IEEE Transactions on Smart Grid,* vol. 8, no. 2, March 2017.

[25] S. Affijulla and P. Tripathy, "Development of Phasor Estimation Algorithm for P-Class PMU Suitable in Protection Applications," *IEEE Transactions on Smart Grid,* vol. 9, no. 2, March 2018.

[26] M. D. Zadeh and P. S. Bains, "Enhanced Phasor Estimation Technique for Fault Location in Series-Compensated Lines," *IEEE Transactions on Power delivery,* vol. 30, no. 4, August 2015.

[27] J. A. Serna, "Reducing the Error in Phasor Estimates From Phasorlets in Fault Voltage and Current Signals," *IEEE Transactions on Instrumentation and Measurement,* vol. 56, no. 3, June 2007.

[28] Power System Society Relaying Committee , "IEEE Standard for Synchrophasor Measurement for Power Systems-IEEE Std C37.118.1™-2011," IEEE, 2011.

[29] K. E. Martin, G. Brunello, M. G. Adamiak, G. Antonova, M. Begovic , G. Benmouyal, P. D. Bui and . A. Zahid, "An Overview of the IEEE Standard C37.118.2 Synchrophasor Data Transfer for Power Systems," *IEEE Transactions On Smart Grid,* vol. 5, no. 4, JULY 2014.

[30] Working Group 10-TC57, "Communication networks and systems for power utility automation - Part 90-5: Use of IEC 61850 to transmit synchrophasor information according to IEEE C37.118-IEC/TR 61850-90-5 ED. 1.0," IEC, 2012.

[31] Working Group 10-10, IEC Technical Comitte 57 , "Communication Networks and Systems in Substations-Part 8-1: Specefic Communication Service Mapping (SCSM) Mapping to MMS and to ISO/IEC 8802-3-Second Editioin," IEC, 2012.

[32] Working Group 10- Technical Committe 57, "IEC 61850-9-2-Communication networks and systems for power utility automation - Part 9-2: Specific communication service mapping (SCSM) - Sampled values over ISO/IEC 8802-3," IEC Publication, 2011.

[33] U.S.-Canada Power System Outage Task Force, "Final Report on the on the August 14, 2003 Blackout in the United States and Canada," U.S. Secretary of Energy & Minister of Natural Resources Canada, April 2004.

[34] UCTE, "Final Report of the 28 September 2003 Blackout in Italy," UCTE, April 2004.

[35] D. L. J. Ree, V. Conteno, J. S. Thorp and A. G. Phadake, "Synchronized Phasor Measurement Applications in Power Systems," *IEEE Transaction on Smart Grid,* vol. 1, no. 1, p. 564, April 2010.

[36] P. Yang, Z. Tan, A. Wiesel and A. Nehorai, "Power System State Estimation Using PMUs With Imperfect Synchronization," *IEEE Transactions on Power Systems,* vol. 28, no. 4, 2013.

[37] NASPI Engineering Team,Analysis Task, "Integrating Synchrophasor Technology into Power System," North American Synchro Phasor Initiative (NASPI), 2016.

[38] N. N. A. S. Initiative, "Synchrophasor Monitoring for Distribution Systems," NASPI, January 2018.

[39] A. V. Meier, E. Stewart , A. McEachern and . M. Anderson, "Precision Micro-Synchrophasors for Distribution Systems," *IEEE Transactions on Smart Grid,* vol. 8, no. 6, November 2017.

[40] W. Xu and K. Mauch, "An Assessment of Distributed Generation Islanding Detection Methods and Issues in Canada," CANMET Energy Technology Centre– Varennes CANMET Energy Technology Center (CETEC), 2004.

[41] M. C. Wrinch, "Negative Sequence Impedance Measurement for Distribuated Islanding Detection," PHD Thesis, University of British Columbia, Vancouver, 2008.

[42] A. Etxegarai., P. Eguía. and I. Zamora, "Analysis of Remote Islanding Detection Methods for Distributed Resources.," in *European Association for the Development of Renewable Energies,Environment and Power Quality (FA4EPQ)- International Conference on Renewabl,* Spain, 2011.

[43] A. Etxegarai, P. Eguía and I. Zamora, "Analysis of Remote Islanding Detection Methods for Distributed Resources," in *Renewable Energy and Power Quality (ICREPQ 11),* Spain, April 2011.

[44] W. Wang, J. Kliber, G. Zhang, W. Xu and B. Howell, "A Power Line Signaling Based Scheme for Anti-Islanding Protection of Distributed Generator Part II: Field Test Results," *IEEE Transactiosn on Power Delivery*, vol. 22, no. 3, pp. 1758-1766, July 2007.

[45] W. Wang., J. Klibe. and W. Xu, "A Scalable Power-Line Signaling- Based Scheme for Islanding Detection of Distributed Generator," *IEEE Transactions on Power Delivery*, vol. 24, no. 2, April 2009.

[46] B. Liu, "Advanced ROCOF Protection of Distribution Systems," PhD thesis, University of Nothingham,, Nothingham, March 2012.

[47] S. NiKolovski, H. R. Baghaee and D. Mlaki´, "Islanding Detection of Synchronous Generator-Based DGs using Rate of Change of Reactive Power," *IEEE System Journal*, vol. 13, no. 4, December 2019.

[48] H. R. Baghaee, D. Mlakic, S. Nikolovski and T. Dra, "Anti-Islanding Protection of PV-Based Microgrids Consisting of PHEVs Using SVMs," *IEEE Transaction on Smart Grid*, vol. 11, no. 1, Januery 2020.

[49] Y. Zhang, "Anti-islanding modeling of grid-tied inverters," in *IEEE Conference-GE (China) Research and Development Center*, 2014.

[50] S. Patra, S. Agrawal, S. R. Mohanty, V. Agarwal and M. Basu, "ESPRIT based Robust Anti-Islanding Algorithm for Grid-tied Inverter," in *Proceedings of the 2016 IEEE Students' Technology Symposium*, 2016.

[51] S. Ozturk and I. Cadırcı, "A Generalized and Flexible Control Scheme for Photovoltaic Grid-Tie Microinverters," *IEEE Transactions on Industry Application* , vol. 54, no. 1, April 2018.

[52] M. Mitolo , R. Musca and G. Zizzo, "A Cost-Effective Solution for Clearing High-Impedance Ground Faults in Overhead Low-Voltage Lines," *IEEE Transactions on Industry Applications*, vol. 55, no. 2, pp. 1208 - 1213, April 2019.

[53] O. Brien , U. William , G. Eric and K. Haes , "Catching Falling Conductors in Midair – Detecting and Tripping Broken Distribution Circuit Conductors at Protection Speeds," *IEEE Conference*, pp. 1 - 11, Febaruery 2016.

[54] Aaron Kalyuzhny, "Analysis of Temporary Overvoltages During Open-Phase Faults in Distribution Networks With Resonant Grounding," *IEEE Transactions on Power Delivery*, vol. 30, no. 1, pp. 420 - 427, Feberuary 2015.

[55] R. A. Walling , R. K. Hartana and W. J. Ros, "Self-Generated Overvoltages Due to Open-Phasing of Ungrounded-Wye Delta Transforemr Banks," *IEEE Transactions on Power Delivery*, vol. 10, no. 1, pp. 526 - 533, January Jaunuary 1995.

[56] B. Gustavsen and J. Å. Walseth, "A Case of Abnormal Overvoltages in a Petersen Grounded 132-kV System Caused by Broken Conductor," *IEEE Transactions on Power delivery*, vol. 18, no. 1, pp. 195 - 200, January 2002.

[57] B. Wang, X. Dong, Z. Bo and A. Klimek, "Negative-Sequence Pilot Protection With Applications in Open-Phase Transmission Lines," *IEEE Transactions on Power Delivery*, vol. 25, no. 3, pp. 1306 - 1313, July 2010.

[58] E. C. Senger , W. Kaiser, J. C. Santos and P. S. Burt, "Broken Conductors Protection System Using Carrier Communication," *IEEE Transactions on Power Delivery*, vol. 15, no. 2, pp. 525 - 530, April 2000.

[59] C. L. Benner and B. D. Russell, "Practical High-Impedance Fault Detection on Distribution Feeders," *IEEE Transactions On Industry Applications*, vol. 33, no. 3, pp. 635 - 640, June 1997.

[60] J. A. Momoh, L. G. Dias and D. N. Laird, "An implementation of a hybrid intelligent tool for distribution system fault diagnosis," *IEEE Transactions on Power Delivery*, vol. 12, no. 2, pp. 1035 - 1040, April 1997.

[61] H. Calhoun, M. T. Bishop, C. H. Eichler and R. E. Lee, "Development and Testing of an Electro-Mechanical Relay to Detect Fallen Distribution Conductors," *IEEE Transactions on Power Apparatus and Systems*, Vols. PAS-101, no. 6, pp. 1643 - 1650, 1982.

[62] D. R. Smith , "Digital Simulation of Unbalances Involving Open and Faulted Conductors," *IEEE Transactions On Power Apparatus and Systems,* Vols. PAS-89,, no. 8, pp. 1826 - 1835, November 1970.

[63] J. Song, E. Dall'Anese, A. Simone and H. Zhu , "Dynamic Distribution State Estimation Using Synchrophasor Data," *IEEE Transactions on Smart Grid,* vol. 11, no. 1, 2020.

[64] M. Ghalei , M. Zanjani , K. Mazlumi and I. Kamwa, "A2018pplication of μPMUs for adaptive protection of overcurrent relays in microgrids," *IET Generation, Transmission & Distribution,* vol. 12, no. 18, 2018.

[65] M. Gholami , A. Abbaspour, M. Moeini-Ag, M. Fotuhi-Firuzabad and M. Lehtonen, "Detecting the Location of Short-Circuit Faults in Active Distribution Network Using PMU Based State Estimation," *IEEE Transactions on Smart Grid,* vol. 11, no. 2, 2020.

Appendix A: Network Model Information

Figure A1 shows the distribution system one-line diagram which is used for Anti-Islanding and open phase study test system. For the open phase study, the location of DGs and AR is changed as per cases requirement as per what is described in chapter 5

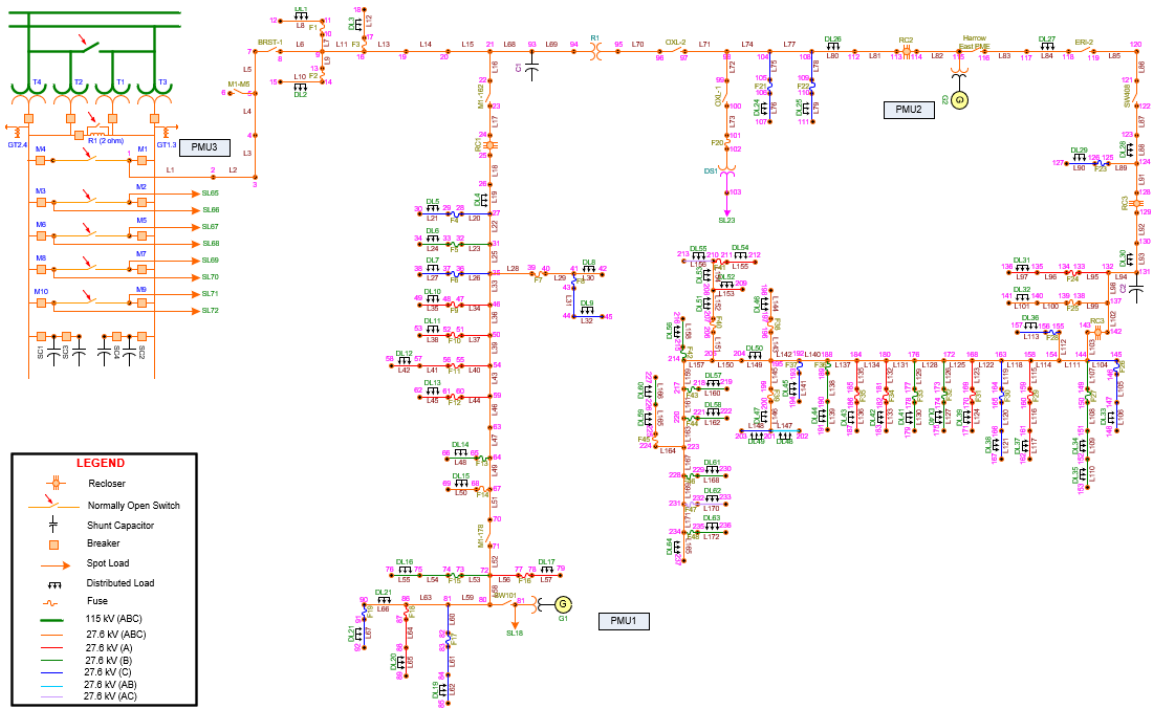

Figure A1. One-line Diagram of Modeled Distribution Feeder

Table A1 is presents the type of conductor which is used in the model with thire electrical characteristics.

Table A1. Conductor Type and Data Used in the Model

Conductor Type	R1 (ohm/km)	X1 (ohm/km)	R0 (ohm/km)	X0 (ohm/km)	B1 (µS/km)	B0 (µS/km)	Ampere Rating (Summer)	Ampere Rating (Winter)
556AL427	0.1021	0.4037	0.2765	1.0946	4.1588	0	777	1022
40ASR427	0.2765	0.4586	0.6307	1.3125	3.828	0	422	553
U20AL1428	0.8199	0.6554	0.8199	0.6554	51.096	51.0957	355	539
336AL427	0.1691	0.4182	0.4441	1.1899	3.954	0	564	740
10ASR427	0.5523	0.4852	0.9644	1.4641	3.6035	0	273	356
30ASR427	0.3481	0.4685	0.7023	1.3224	3.7571	0	365	478

Table A2 presents the length of the conductor used in the model.

Table A2. Conductor Length Used in the Model

PSCAD Label	Phase	From Node	To Node	Conductor Type	Length (km)
L1	ABC	1	2	556AL427	0.1142
L2	ABC	2	3	556AL427	0.1337
L3	ABC	3	4	556AL427	0.1998
L4	ABC	4	5	556AL427	1.2202
L5	ABC	5	7	556AL427	1.1214
L6	ABC	8	9	40ASR427	1.5665
L7	ABC	9	10	40ASR427	0.0192
L8	ABC	10	11	U20AL1428	0.1144
L9	ABC	9	13	40ASR427	0.0294
L10	ABC	14	15	U20AL1428	0.239
L11	ABC	9	16	40ASR427	0.1327
L12	ABC	17	18	U20AL1428	0.1077
L13	ABC	16	19	40ASR427	0.4252
L14	ABC	19	20	40ASR427	0.4185
L15	ABC	20	21	40ASR427	5.6039
L16	ABC	21	22	336AL427	0.1406
L17	ABC	23	24	336AL427	0.856
L18	ABC	25	26	336AL427	0.1068
L19	ABC	26	27	336AL427	0.3571
L20	C	27	28	10ASR427	0.059
L21	C	29	30	10ASR427	0.1475
L22	ABC	27	31	336AL427	0.0814
L23	B	31	32	10ASR427	0.058
L24	B	33	34	10ASR427	0.14
L25	ABC	31	35	336AL427	0.0771
L26	C	35	36	10ASR427	0.0493
L27	C	37	38	10ASR427	0.1429
L28	ABC	35	39	40ASR427	0.0986
L29	ABC	40	41	40ASR427	0.1201
L30	ABC	41	42	40ASR427	0.35
L31	C	43	44	10ASR427	0.3132
L32	C	44	45	10ASR427	0.4135
L33	ABC	35	46	336AL427	0.0805
L34	A	46	47	10ASR427	0.0567
L35	A	48	49	10ASR427	0.1242
L36	ABC	46	50	336AL427	0.0772
L37	A	50	51	10ASR427	0.0524
L38	A	52	53	10ASR427	0.1176
L39	ABC	50	54	336AL427	0.0755
L40	A	54	55	10ASR427	0.0474
L41	A	56	57	10ASR427	0.2411
L42	A	57	58	10ASR427	0.1486

L43	ABC	54	59	336AL427	0.0749
L44	A	59	60	10ASR427	0.0224
L45	A	61	62	10ASR427	0.1693
L46	ABC	59	63	336AL427	0.1622
L47	ABC	63	64	10ASR427	0.7655
L48	B	65	66	10ASR427	0.2213
L49	ABC	64	67	10ASR427	1.452
L50	ABC	68	69	10ASR427	0.3347
L51	ABC	67	70	10ASR427	1.1306
L52	ABC	71	72	10ASR427	0.6802
L53	B	72	73	10ASR427	0.0229
L54	B	74	75	10ASR427	0.107
L55	B	75	76	10ASR427	0.2811
L56	A	72	77	30ASR427	0.0259
L57	A	78	79	30ASR427	1.194
L58	ABC	72	80	10ASR427	0.145
L59	ABC	80	81	10ASR427	0.3988
L60	C	81	82	10ASR427	0.0346
L61	C	83	84	10ASR427	0.1773
L62	C	84	85	10ASR427	0.118
L63	ABC	81	86	10ASR427	0.2321
L64	A	87	88	10ASR427	0.2086
L65	A	88	89	10ASR427	0.091
L66	ABC	86	90	10ASR427	0.5296
L67	C	91	92	30ASR427	3.3797
L68	ABC	21	93	40ASR427	6.4518
L69	ABC	93	94	40ASR427	0.3972
L70	ABC	95	96	40ASR427	0.9648
L71	ABC	97	98	40ASR427	0.6654
L72	ABC	98	99	10ASR427	0.3629
L73	ABC	100	101	10ASR427	2.7921
L74	ABC	98	104	40ASR427	0.9303
L75	C	104	105	10ASR427	0.0273
L76	C	106	107	10ASR427	0.8709
L77	ABC	104	108	40ASR427	0.0305
L78	C	108	109	10ASR427	0.0363
L79	C	110	111	10ASR427	0.9992
L80	ABC	108	112	40ASR427	0.2213
L81	ABC	112	113	40ASR427	0.2939
L82	ABC	114	115	40ASR427	0.4083
L83	ABC	116	117	40ASR427	0.2026
L84	ABC	117	118	40ASR427	0.9115
L85	ABC	119	120	40ASR427	0.3926
L86	ABC	120	121	336AL427	0.6663
L87	ABC	122	123	336AL427	0.1252
L88	ABC	123	124	336AL427	0.3863
L89	ABC	124	125	40ASR427	0.3102
L90	C	126	127	40ASR427	0.5507

L91	ABC	124	128	336AL427	0.5321
L92	ABC	129	130	336AL427	3.1889
L93	ABC	130	131	336AL427	0.4304
L94	ABC	131	132	336AL427	0.1002
L95	A	132	133	10ASR427	0.0479
L96	A	134	135	10ASR427	0.0599
L97	A	135	136	10ASR427	0.1086
L98	ABC	132	137	336AL427	0.2634
L99	ABC	137	138	10ASR427	0.0488
L100	ABC	139	140	10ASR427	0.1686
L101	ABC	140	141	10ASR427	0.1573
L102	ABC	137	142	336AL427	0.0495
L103	ABC	143	144	336AL427	0.237
L104	C	144	145	10ASR427	0.0387
L105	C	146	147	10ASR427	0.3133
L106	C	147	148	10ASR427	0.1727
L107	B	144	149	10ASR427	0.0579
L108	B	150	151	10ASR427	0.5248
L109	B	151	152	10ASR427	0.2227
L110	B	152	153	10ASR427	0.0869
L111	ABC	144	154	336AL427	0.3137
L112	ABC	154	155	10ASR427	0.3412
L113	C	156	157	10ASR427	1.0307
L114	ABC	154	158	336AL427	0.1389
L115	A	158	159	10ASR427	0.0747
L116	A	160	161	10ASR427	0.3018
L117	A	161	162	10ASR427	0.1781
L118	ABC	158	163	336AL427	0.147
L119	C	163	164	10ASR427	0.0815
L120	C	165	166	10ASR427	0.3683
L121	C	166	167	10ASR427	0.1981
L122	ABC	163	168	336AL427	0.2334
L123	A	168	169	10ASR427	0.0728
L124	A	170	171	10ASR427	0.1993
L125	ABC	168	172	336AL427	0.2485
L126	B	172	173	10ASR427	0.0506
L127	B	174	175	10ASR427	0.2067
L128	ABC	172	176	336AL427	0.1787
L129	B	176	177	10ASR427	0.0314
L130	B	178	179	10ASR427	0.1254
L131	ABC	176	180	336AL427	0.2469
L132	A	180	181	10ASR427	0.0583
L133	A	182	183	10ASR427	0.1569
L134	ABC	180	184	336AL427	0.0717
L135	A	184	185	10ASR427	0.0364
L136	A	186	187	10ASR427	0.1284
L137	ABC	184	188	336AL427	0.1187
L138	B	189	190	10ASR427	0.1111

L139	B	190	191	10ASR427	0.0674
L140	ABC	188	192	336AL427	0.1595
L141	C	193	194	10ASR427	0.0698
L142	ABC	192	195	336AL427	1.2174
L143	ABC	195	196	30ASR427	0.0585
L144	ABC	197	198	30ASR427	1.7426
L145	ABC	195	199	30ASR427	0.1552
L146	ABC	200	201	30ASR427	0.4701
L147	AB	201	202	30ASR427	0.2865
L148	C	201	203	30ASR427	0.1988
L149	ABC	195	204	336AL427	0.7638
L150	ABC	204	205	336AL427	0.6184
L151	ABC	205	206	10ASR427	0.078
L152	ABC	207	208	10ASR427	0.3467
L153	A	208	209	10ASR427	0.2129
L154	ABC	208	210	10ASR427	0.0552
L155	A	211	212	10ASR427	0.2583
L156	AC	210	213	10ASR427	1.0601
L157	ABC	205	214	336AL427	0.1752
L158	B	215	216	10ASR427	0.2127
L159	ABC	214	217	336AL427	0.0945
L160	B	218	219	10ASR427	0.2007
L161	ABC	217	220	336AL427	0.0945
L162	B	221	222	10ASR427	0.2496
L163	ABC	220	223	336AL427	0.8372
L164	ABC	223	224	10ASR427	0.0646
L165	ABC	225	226	10ASR427	0.2907
L166	B	226	227	10ASR427	0.1214
L167	ABC	223	228	336AL427	0.1568
L168	B	229	230	10ASR427	0.1338
L169	ABC	228	231	336AL427	0.2139
L170	AC	232	233	10ASR427	0.123
L171	ABC	231	234	336AL427	0.164
L172	B	235	236	10ASR427	0.1835
L173	ABC	234	237	336AL427	0.4795

Table A3 presents the installed load in the feeder.

Table A3**.** Distribution Feeder Installed Load

PSCAD Label	From Node	To Node	Type	Balanced / Unbalanced	Phase	Connected kVA (A)	pf (A)	Connected kVA (B)	pf (B)	Connected kVA (C)	pf (C)
DL1	11	12	Distributed	U	ABC	150	0.919	150	0.8977	150	0.917
DL2	14	15	Distributed	U	ABC	300	0.919	217.49	0.8977	343.45	0.917
DL3	17	18	Distributed	B	ABC	150	0.913	150	0.9126	150	0.913
DL4	26	27	Distributed	U	ABC	765	0.919	835	0.8977	285	0.917

DL5	29	30	Distributed	U	C	0	0	0	0	50	0.917
DL6	33	34	Distributed	U	B	0	0	50	0.8977	0	0
DL7	37	38	Distributed	U	C	0	0	0	0	0	0
DL8	41	42	Distributed	U	ABC	167	0.919	192	0.8977	142	0.917
DL9	44	45	Distributed	U	C	0	0	0	0	510	0.917
DL10	48	49	Distributed	U	A	50	0.919	0	0	0	0
DL11	52	53	Distributed	U	A	50	0.919	0	0	0	0
DL12	57	58	Distributed	U	A	100	0.919	0	0	0	0
DL13	61	62	Distributed	U	A	100	0.919	0	0	0	0
DL14	65	66	Distributed	U	B	0	0	125	0.8977	0	0
DL15	68	69	Distributed	U	BC	0	0	50	0.8977	120	0.917
DL16	75	76	Distributed	U	B	0	0	250	0.8977	0	0
DL17	78	79	Distributed	U	A	45	0.919	0	0	0	0
SL18			Spot								
DL19	84	85	Distributed	U	C	0	0	0	0	225	0.917
DL20	88	89	Distributed	U	A	100	0.919	0	0	0	0
DL21	86	90	Distributed	U	ABC	330		70		20	
DL22	91	92	Distributed	U	C	0	0	0	0	215	0.917
SL23	103		Spot	U	ABC	1114	0.919	1186	0.8977	1195	0.917
DL24	106	107	Distributed	U	C	0	0	0	0	120	0.917
DL25	110	111	Distributed	U	C	0	0	0	0	120	0.917
DL26	108	112	Distributed	U	ABC	175	0.919	340	0.8977	155	0.917
DL27	117	118	Distributed	U	ABC	25	0.919	25	0.8977	25	0.917
DL28	123	124	Distributed	U	ABC	60	0.919	360	0.8977	135	0.917
DL29	126	127	Distributed	U	C	0	0	0	0	45	0.917
DL30	130	131	Distributed	U	ABC	175	0.919	200	0.8977	185	0.917
DL31	135	136	Distributed	U	A	125	0.919	0	0	0	0
DL32	140	141	Distributed	U	ABC	150	0.919	50	0.8977	100	0.917
DL33	147	148	Distributed	U	C	0	0	0	0	275	0.917
DL34	151	152	Distributed	U	B	0	0	350	0.8977	0	0
DL35	152	153	Distributed	U	B	0	0	250	0.8977	0	0
DL36	156	157	Distributed	U	C	0	0	0	0	375	0.917
DL37	161	162	Distributed	U	A	250	0.919	0	0	0	0
DL38	166	167	Distributed	U	C	0	0	0	0	100	0.917
DL39	170	171	Distributed	U	A	100	0.919	0	0	0	0
DL40	174	175	Distributed	U	B	0	0	225	0.8977	0	0
DL41	178	179	Distributed	U	B	0	0	50	0.8977	0	0
DL42	182	183	Distributed	U	A	150	0.919	0	0	0	0
DL43	186	187	Distributed	U	A	50	0.919	0	0	0	0
DL44	190	191	Distributed	U	B	0	0	175	0.8977	0	0
DL45	193	194	Distributed	U	C	0	0	0	0	100	0.917
DL46	197	198	Distributed	B	ABC	50	0.919	50	0.9126	50	0.913
DL47	200	201	Distributed	U	ABC	185	0.919	175	0.8977	185	0.917
DL48	201	202	Distributed	U	AB	10	0.919	10	0.8977	0	0
DL49	201	203	Distributed	U	C	0	0	0	0	75	0.917
DL50	195	204	Distributed	U	ABC	320	0.919	295	0.897	260	0.917
DL51	207	208	Distributed	B	ABC	25	0.919	25	0.9126	25	0.913
DL52	208	209	Distributed	U	A	362	0.919	0	0	0	0

DL53	208	210	Distributed	U	ABC	0	0	125	0.8977	0	0
DL54	211	212	Distributed	U	A	25	0.919	0	0	0	0
DL55	210	213	Distributed	U	AC	0	0	0	0	325	0.917
DL56	215	216	Distributed	U	B	0	0	100	0.8977	0	0
DL57	218	219	Distributed	U	B	0	0	150	0.8977	0	0
DL58	221	222	Distributed	U	B	0	0	25	89.77	0	0
DL59	225	226	Distributed	B	ABC	25	0.919	25	0.9127	25	0.913
DL60	226	227	Distributed	U	B	0	0	275	0.8977	0	0
DL61	229	230	Distributed	U	B	0	0	50	0.8977	0	0
DL62	232	233	Distributed	U	AC	0	0	0	0	275	0.917
DL63	235	236	Distributed	U	B	0	0	100	0.8977	0	0
DL64	234	237	Distributed	U	ABC	275	0.919	160	0.8977	150	0.917

Table A4 presents the transformer data in the feeder.

Table A4. Transformer Data

From Node	To Node	Phase Type	MVA Rating	Primary kV	Secondary kV	Z1 (%)	X1/R1	Z0 (%)	X0/R0	Configuration
94	95	3-ph	25	27.6	27.6	3.6	22	3.6	22	Yg/Yg
102	103	3-ph	3.6	27.6	8.32	5.92	10	5.92	10	D/Yg
-	-	3-ph	25/33/42	110	28.4	7.035	18.63			YD
-	-	3-ph	25/33/42	110	28.4	6.889	18.54			YD
-	-	3-ph	25/33/42	115.5	28.4	8.665	28.87			DY
-	-	3-ph	25/33/42	110	28.4	6.734	26.6			YD

Table A5 presents the transformer tap changer data of the feeder.

Table A5. Transformer Tap Changer Data

General				Tap changer 1			Tap changer 2		
From Node	To Node	Phase Type	Phase Shift	Max Buck (%)	Max Boost (%)	No. of taps	Max kV	Min kV	No. of taps
94	95	3-ph	YNyn0	5	15	16	-	-	-
102	103	3-ph	Dyn1	-	-	-	-	-	-
-	-	3-ph		-	-	-	2.84	-2.84	16
-	-	3-ph		-	-	-	2.84	-2.84	16
-	-	3-ph		-	-	-	5.68	-5.68	32
-	-	3-ph		-	-	-	2.84	-2.84	16

Appendix B: IEC61850 Communication Service Interface

Figure B1 shows the Abstract Communication Service Interface (ACSI) defined in IEC61850 standard. Thee time critical communication service in IEC61850 comprises a peer-to-peer (publisher-subscriber) model or GOOSE (General Object-Oriented Substation Event) used for time-critical purposes, such as fast and reliable transmission of data between protection IEDs, from one IED to many remote IEDs and periodic sampled value services for transmissions. The peer-to-peer communication is a multicast type of communication and uses the only first two layers of the communication and bypass the others.

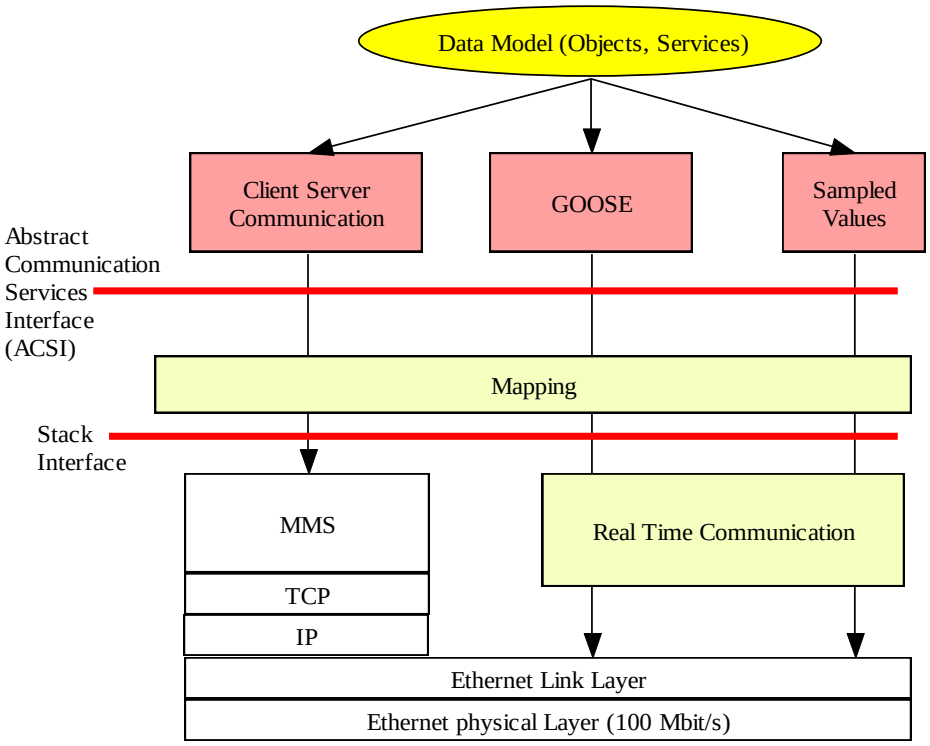

Figure B1. Abstract Communication Services Interface in IEC61850 (Courtesy of ABB Substation Automation)

This communication should be fast, and, for this reason, it cannot pass through all the seven layers of the OSI communication model. In addition to the periodical data transfer from the publisher to the subscriber for the GSE service, the GOOSE message will be sent

instantly upon the occurrence of any changes in the value or state of GOOSE dataset members. In order to increase the reliability of GOOSE message in comparison to client-server type communication model, the GOOSE message is repeated after each trigger of transmission from the minimum time interval (Tmin). This could be as fast as 2 ms after the original event and can be increased up to Tmax (order of seconds), which will be set by the user in the GOOSE control block. The current status of the GOOSE data will be transmitted continuously every Tmax. This feature could be utilized to define an action for subscriber for supervising the connectivity of the GOOSE message if no message is detected by the subscriber after the Tmax interval.

Appendix C: Wind Turbine Model Type 3

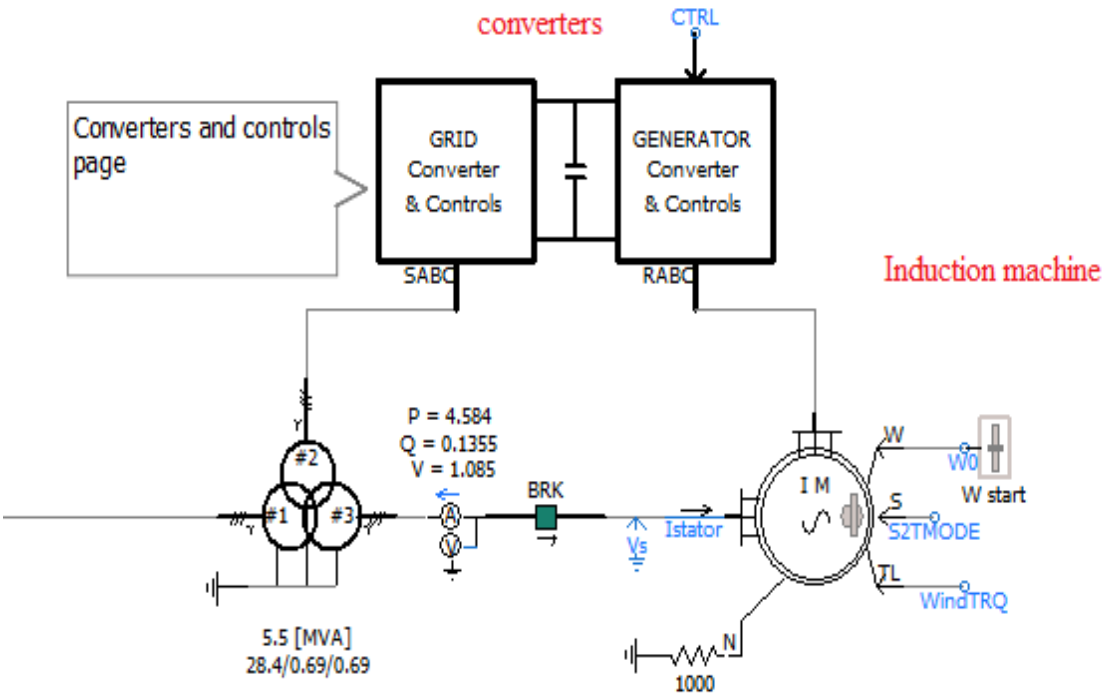

Figure C1. Wind Turbine Model Type 3 Used in this Study

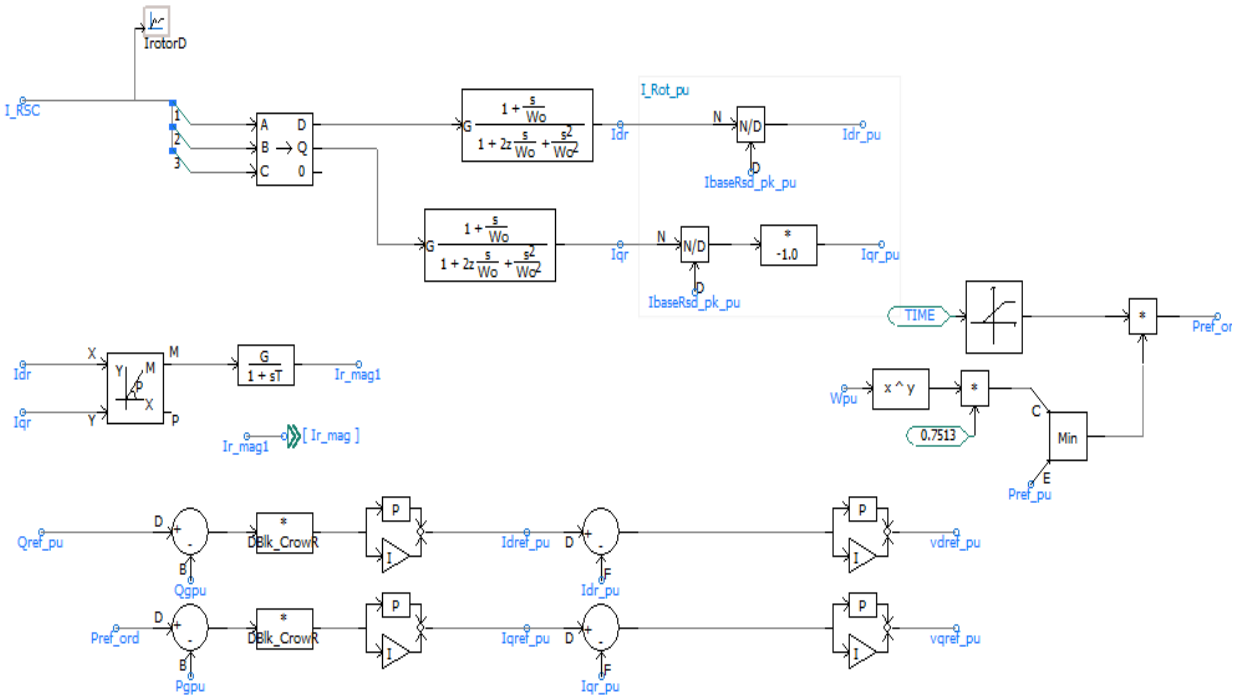

Figure C2. Machine Side Converter Control “dq” Value Transformation

Appendix D: Wind Turbine Model Type 4

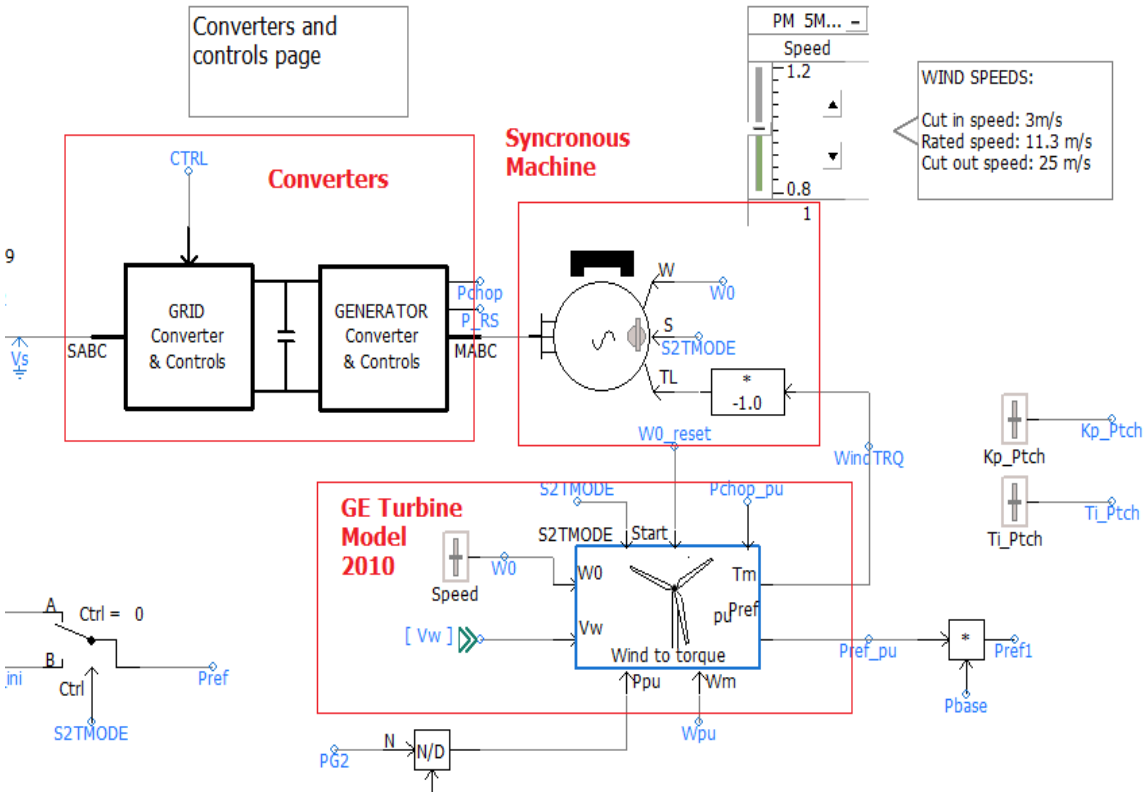

Figure D1. Wind Turbine Model Type 4 Used in this Study

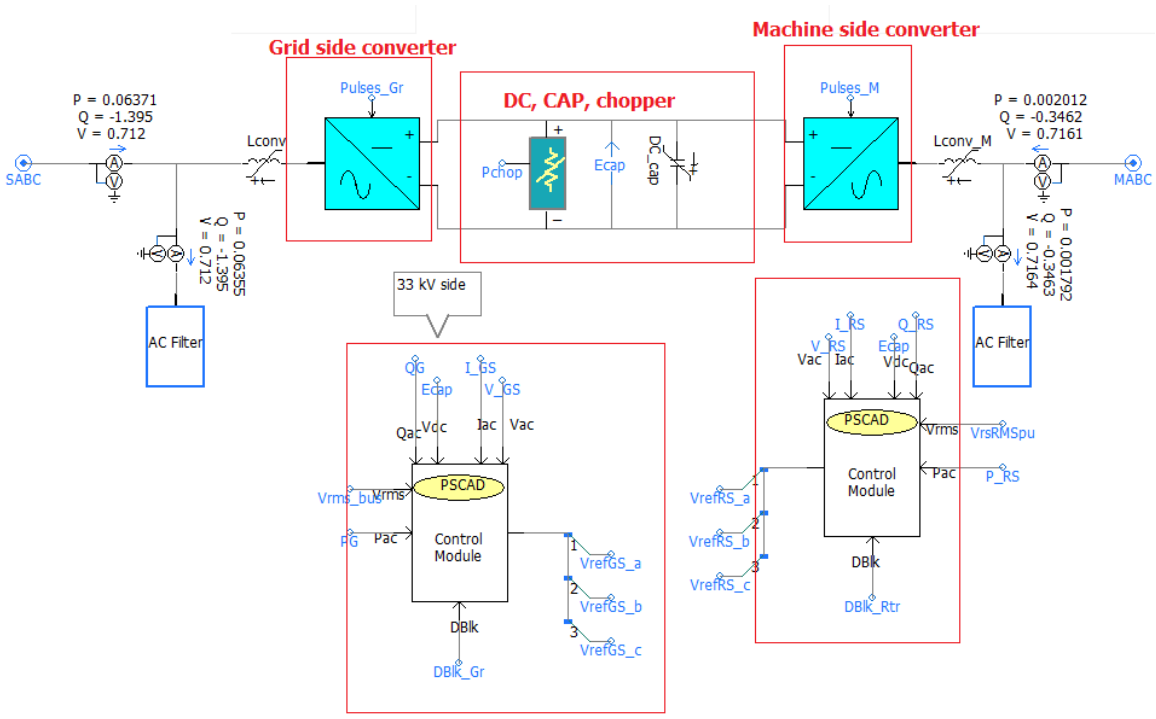

Figure D2. Converters, DC link, Grid, and Machine Side Control I/O

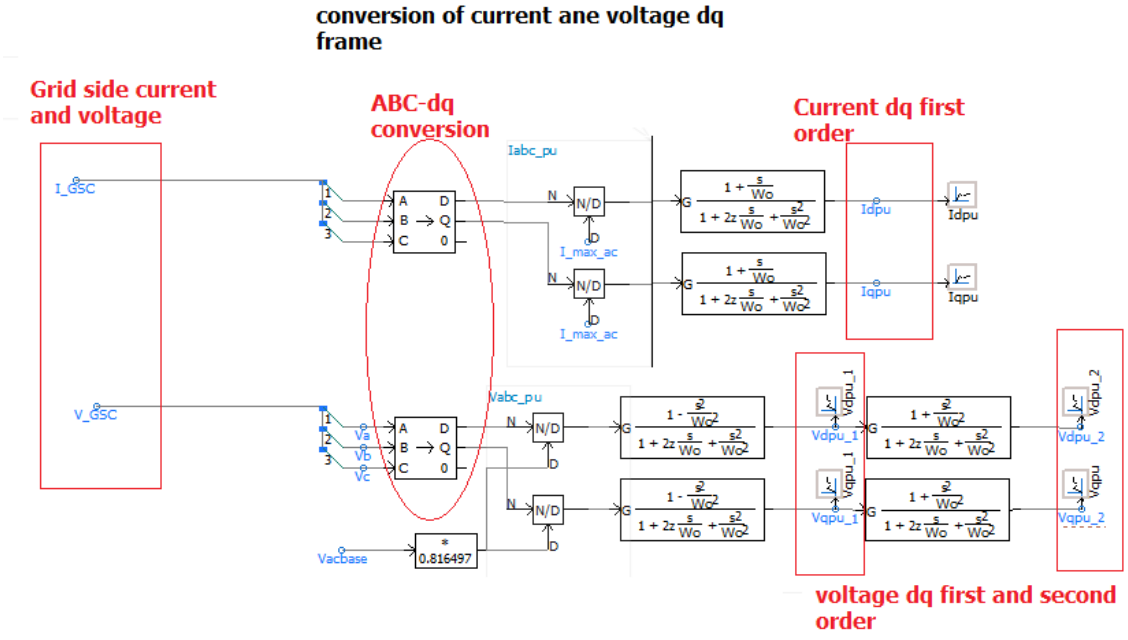

Figure D3. Grid Side control, Identification of Current and Voltage Component

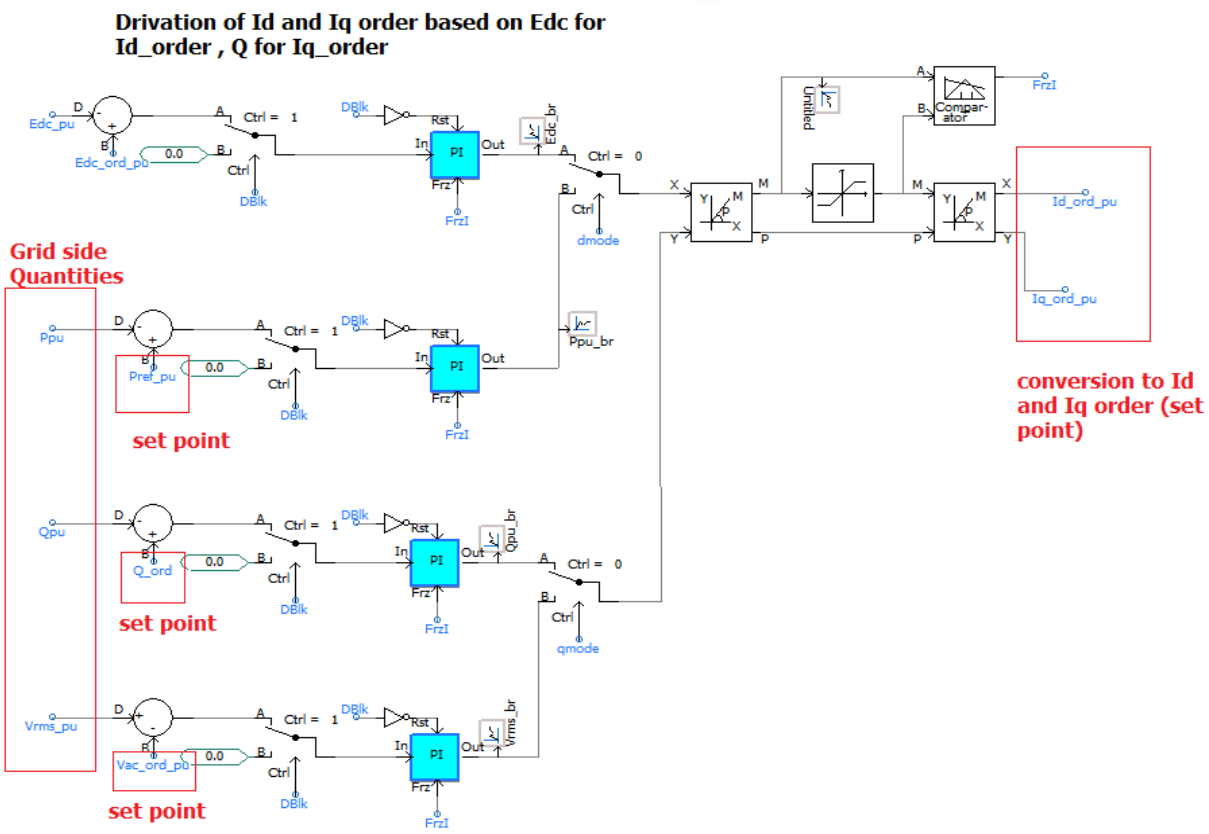

Figure D4. Grid side Control, Calculation of Id, and Iq Current

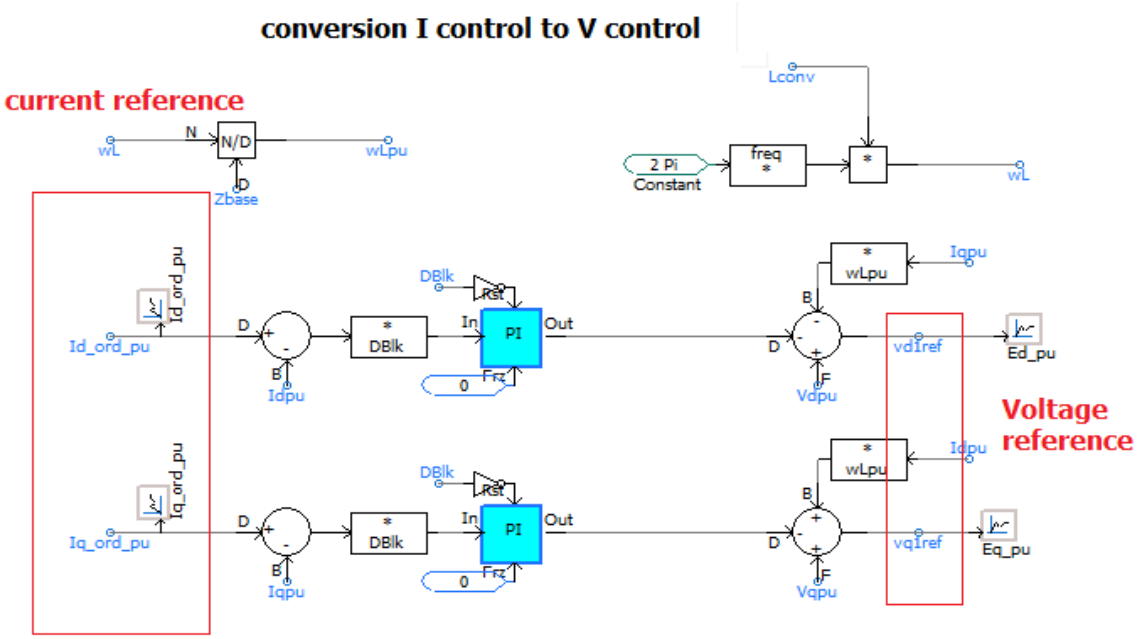

Figure D5. Grid side, Decoupled Control

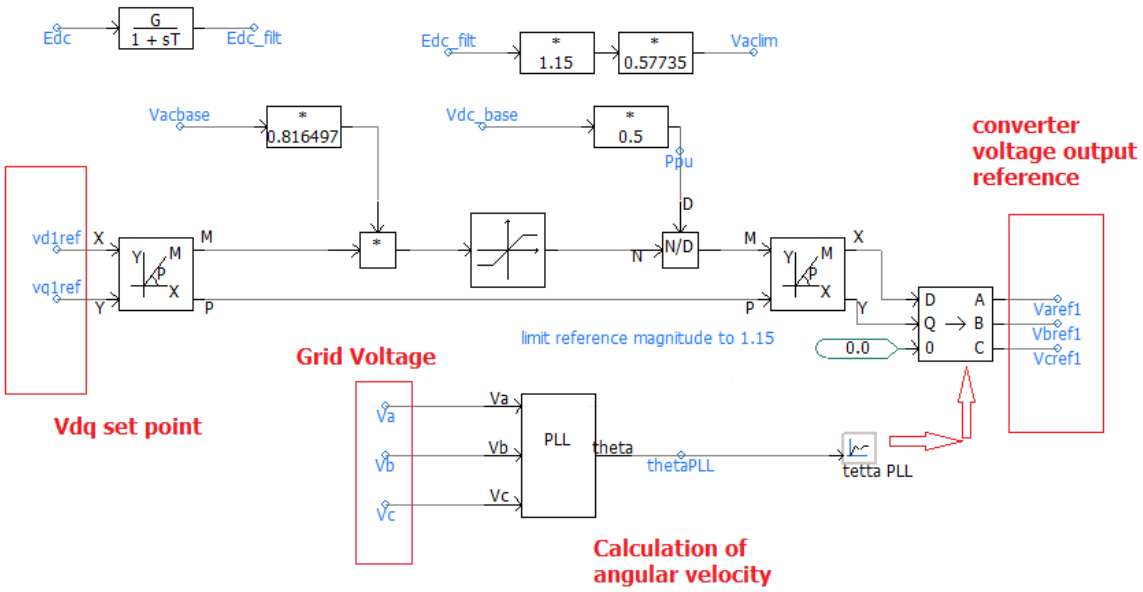

Figure D6. Grid Side, Transformation of Grid Side Voltage

Appendix E: Open Phase fault Additional Simulations

Additional simulation in this section covers the different types of fault, switching operation, and double open phase fault. The list simulation and thire results are shown in Table E1. The different types of fault and switching operation simulation serves to demonstrate how the proposed algorithm for the open phase fault can be discriminated from any parallel faults and switching operation. The plus sign means that the ratio is greater than zero. Thus, the quantity of the current component in the table increases after the instance of the fault while the negative sign represents a decrease in the quantity after the fault. The double sign represents the intensity of increase or decrease compared to the single sign.

Table E1. Rate of the Change of Current Symmetrical Components

No.	Fault or switching type	$\frac{\Delta I1}{\Delta t}$	$\frac{\Delta I2}{\Delta t}$	$\frac{\Delta I0}{\Delta t}$	$\frac{\Delta V1}{\Delta t}$	Figure No.
1	Three phase fault	++	NA	NA	-	Figure E1
2	Two phase fault	++	++	NA	-	Figure E3
3	Two phase to ground	++	+	+	-	Figure E5
4	Ground fault	++	++	++	-	Figure E8
5	Energizing unbalance load	+	+	+	NA	Figure E9
6	De-energizing unbalance load	-	-	-	NA	Figure E12

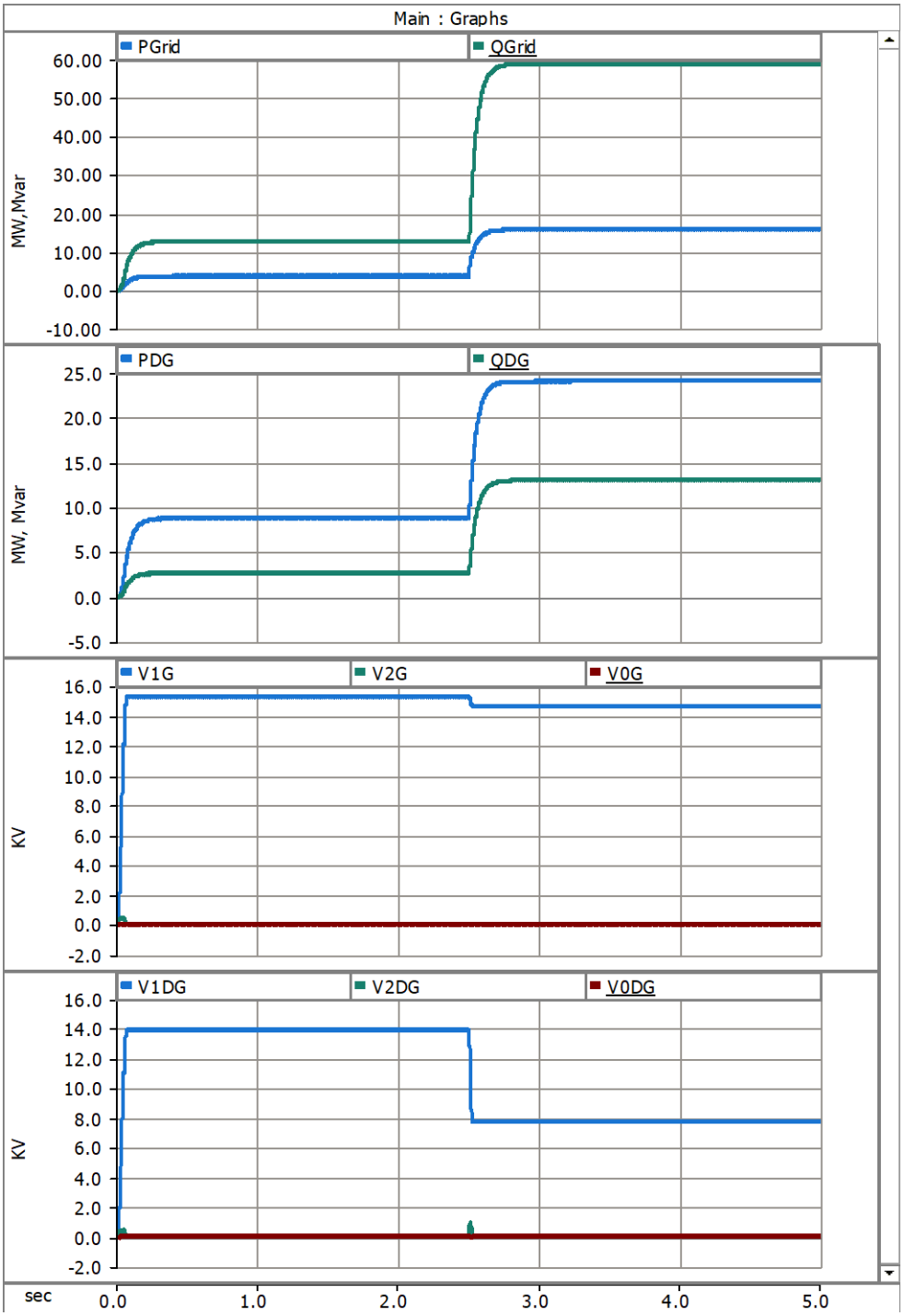

Figure E1. Three phase Fault (ABCG) Power and Voltage

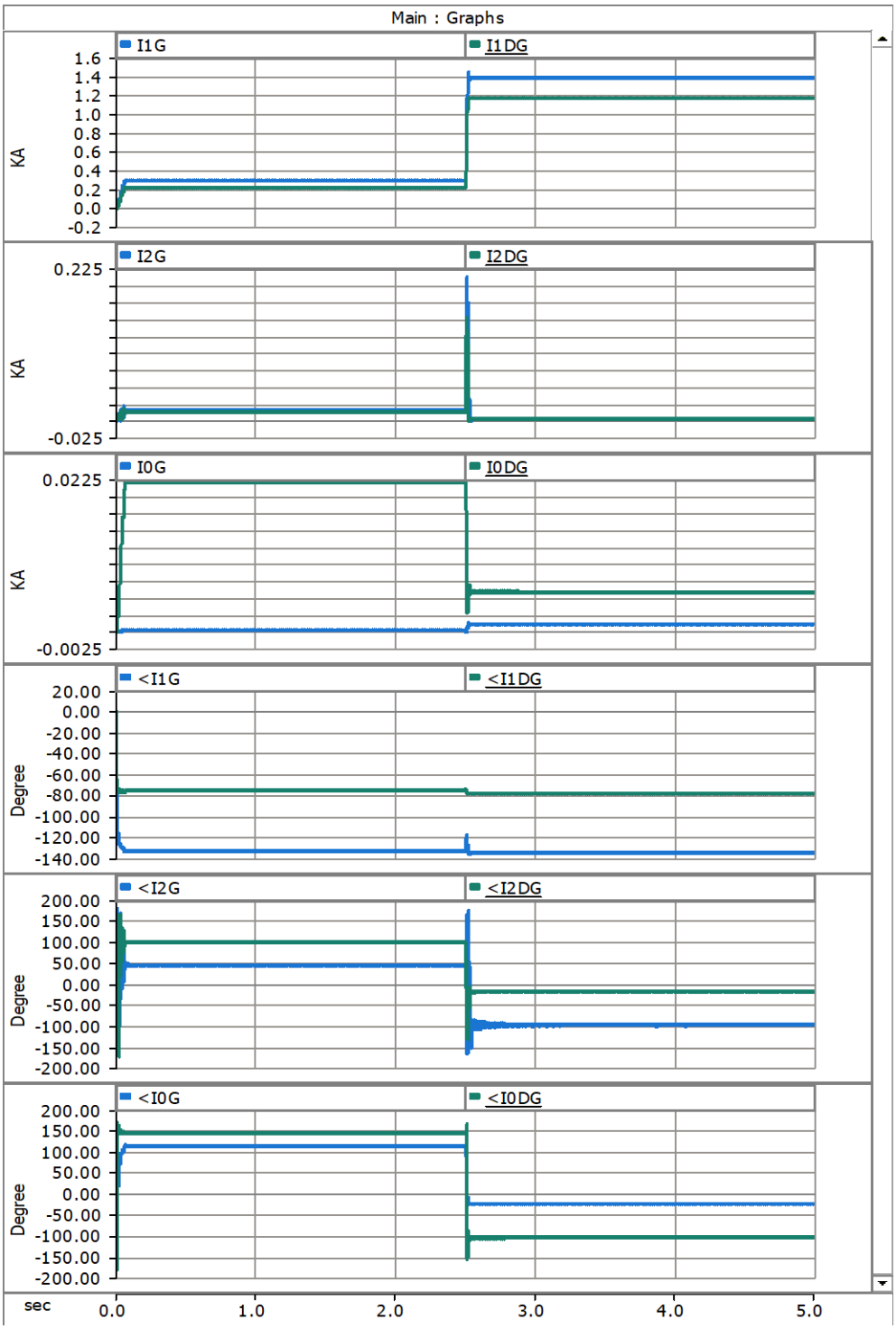

Figure E2. Three Phase Fault (ABC) Current

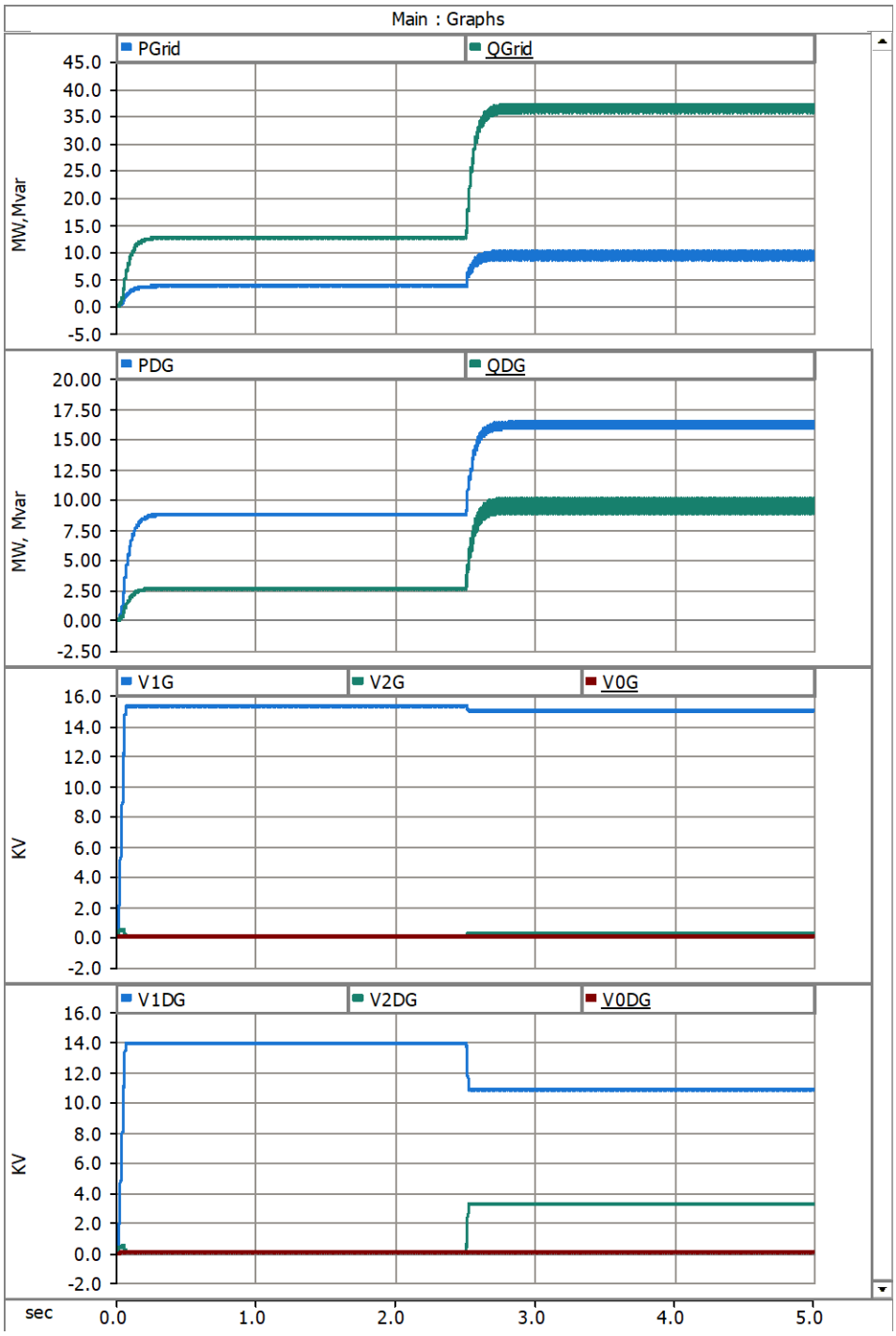

Figure E3. Two Phase Fault (BC) Power and Voltage

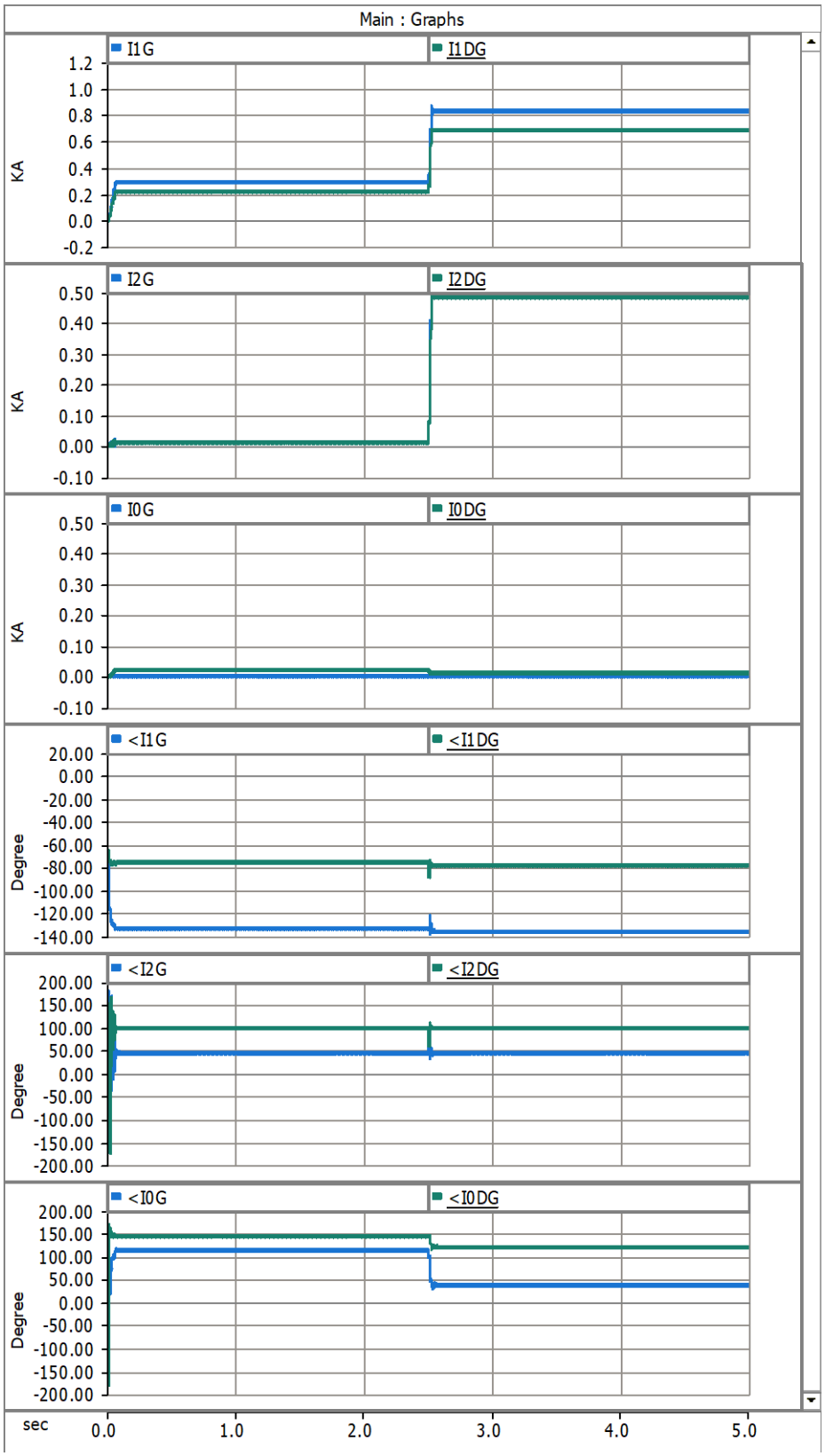

Figure E4. Two Phase Fault (BC) Current

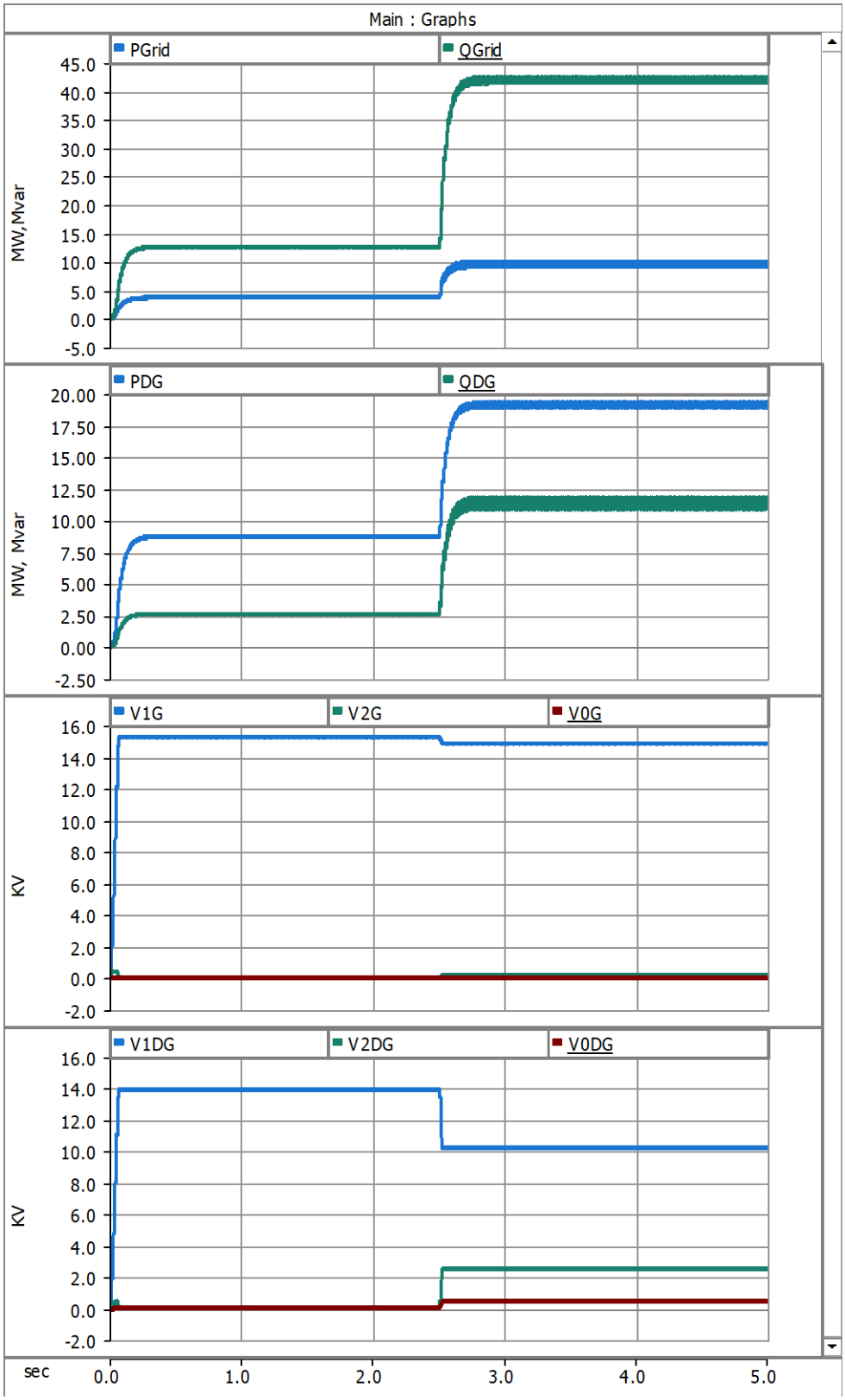

Figure E5. Two Phase to Ground Fault (BCG) Power and Voltage

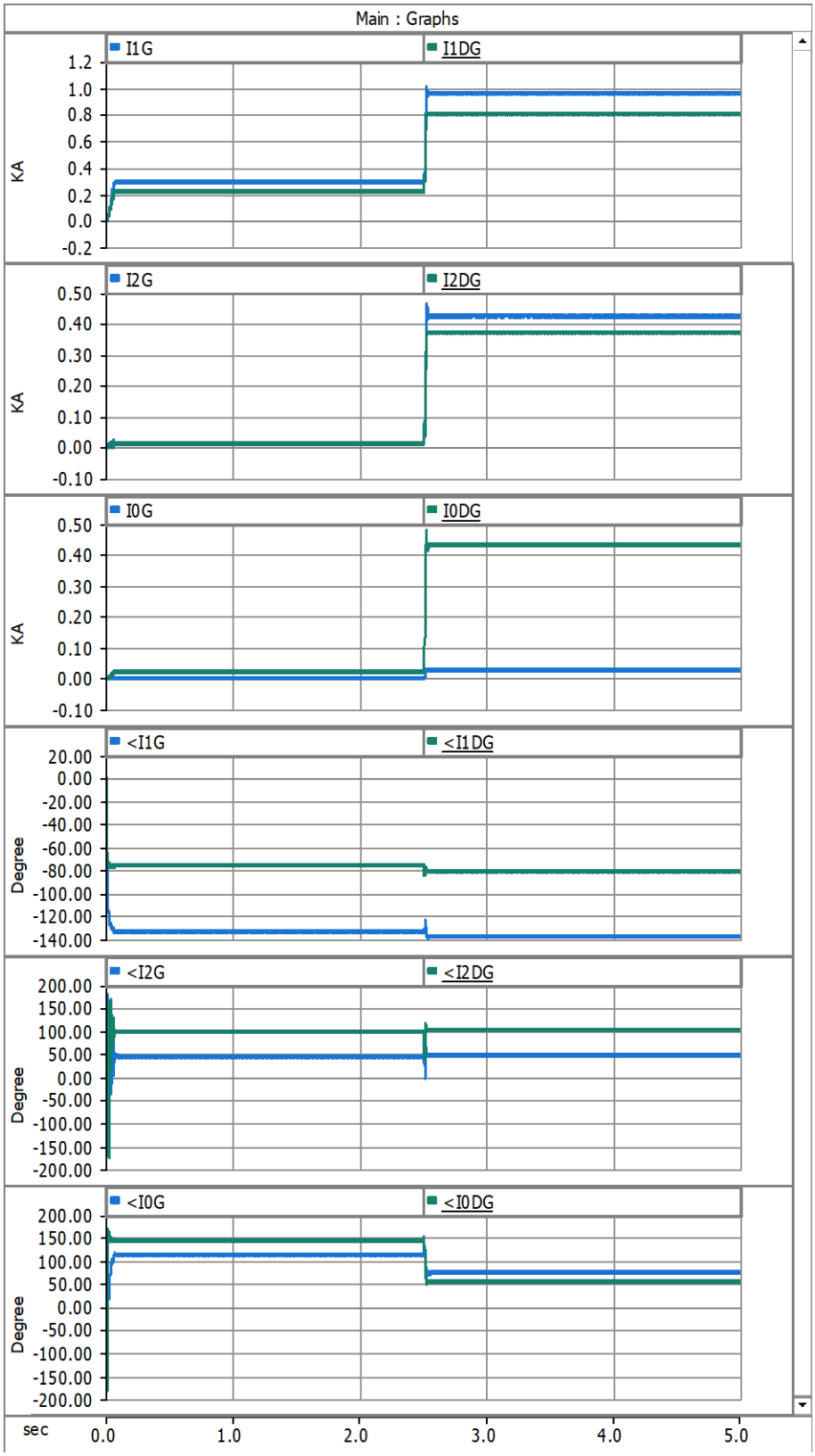

Figure E6. Two Phase to Ground fault (BCG) Current

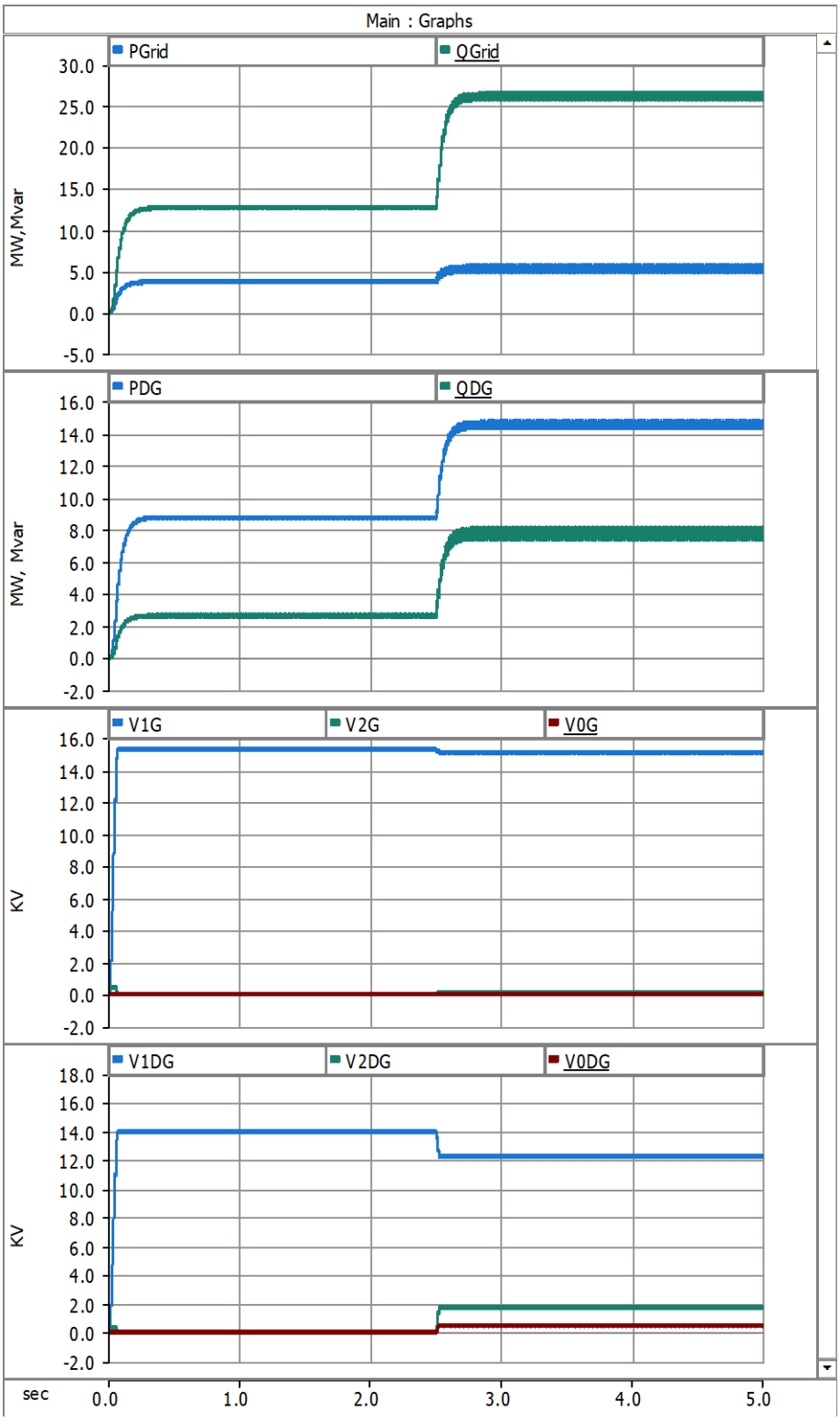

Figure E7. Ground Fault (BG) Power and Voltage

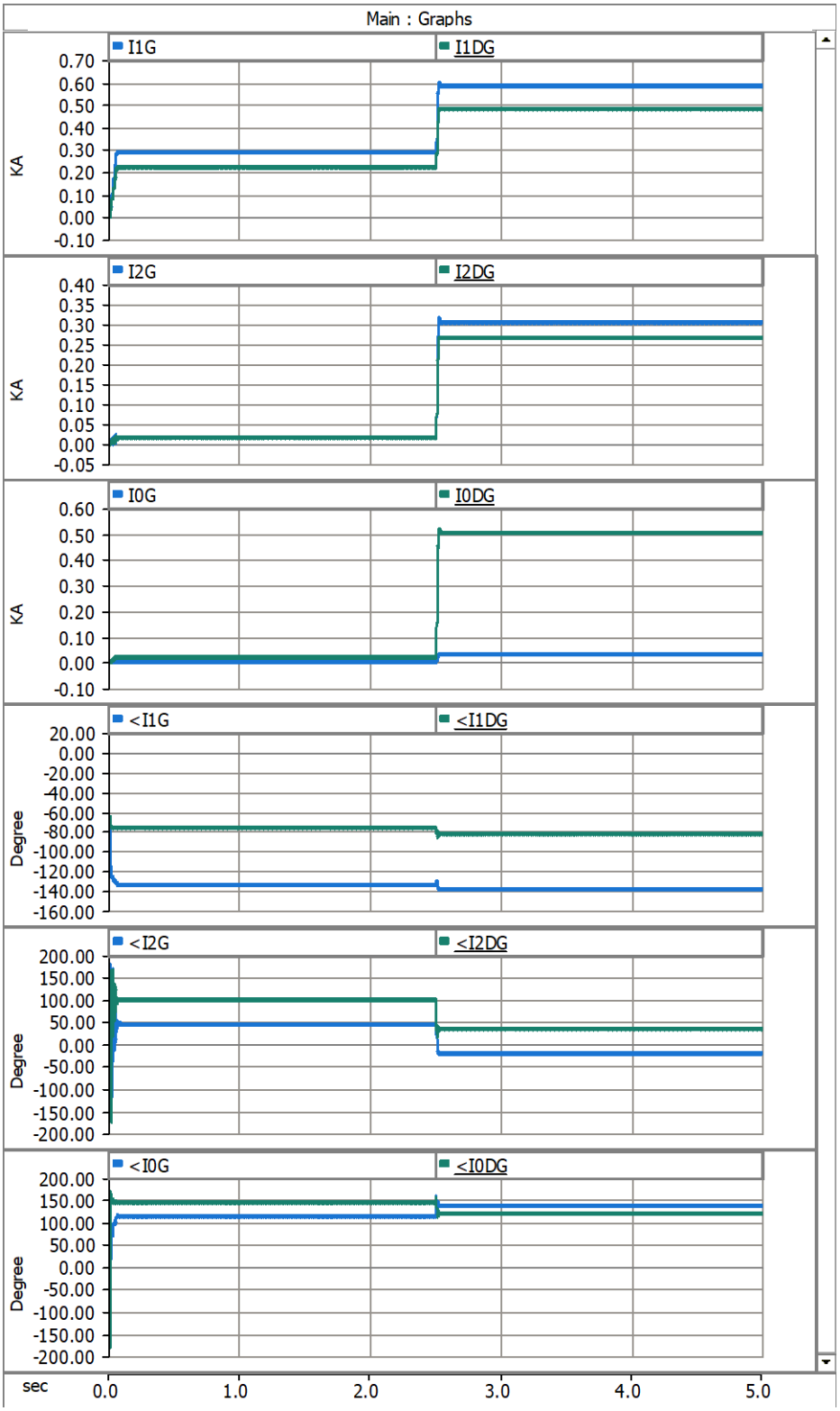

Figure E8. Ground Fault (BG) Current

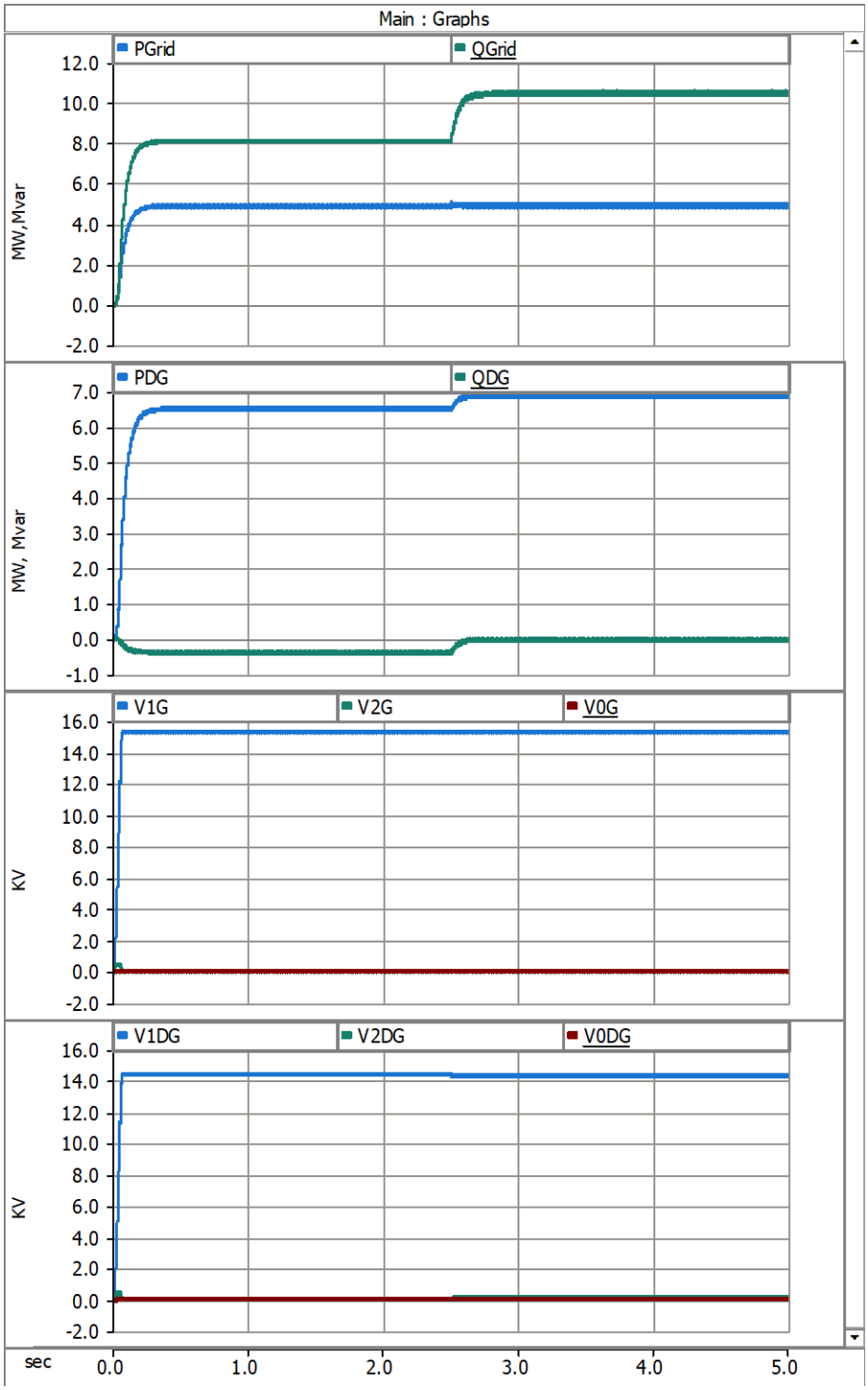

Figure E9. Energizing Unbalance Load Power and Voltage

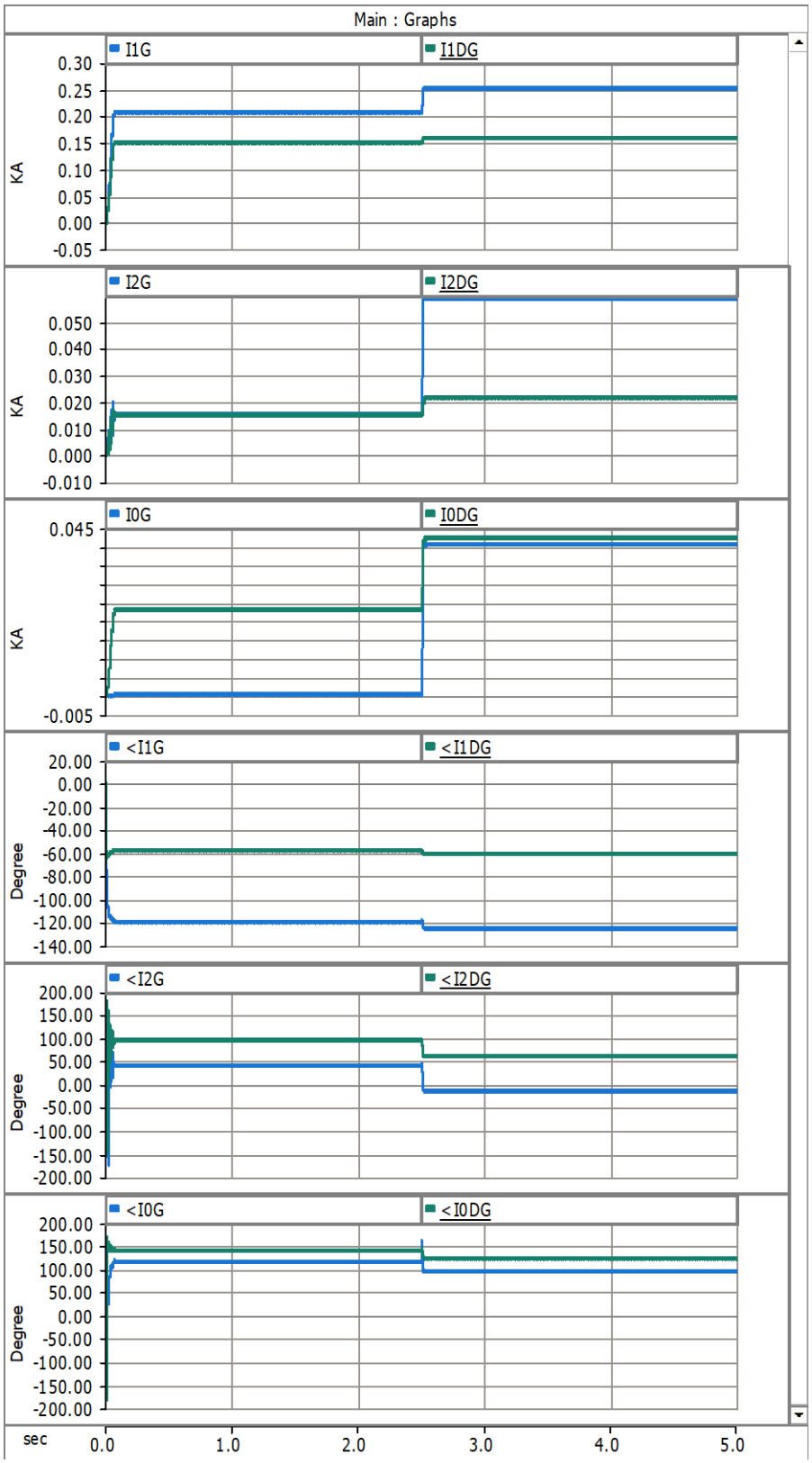

Figure E10. Energizing Unbalance Load Current

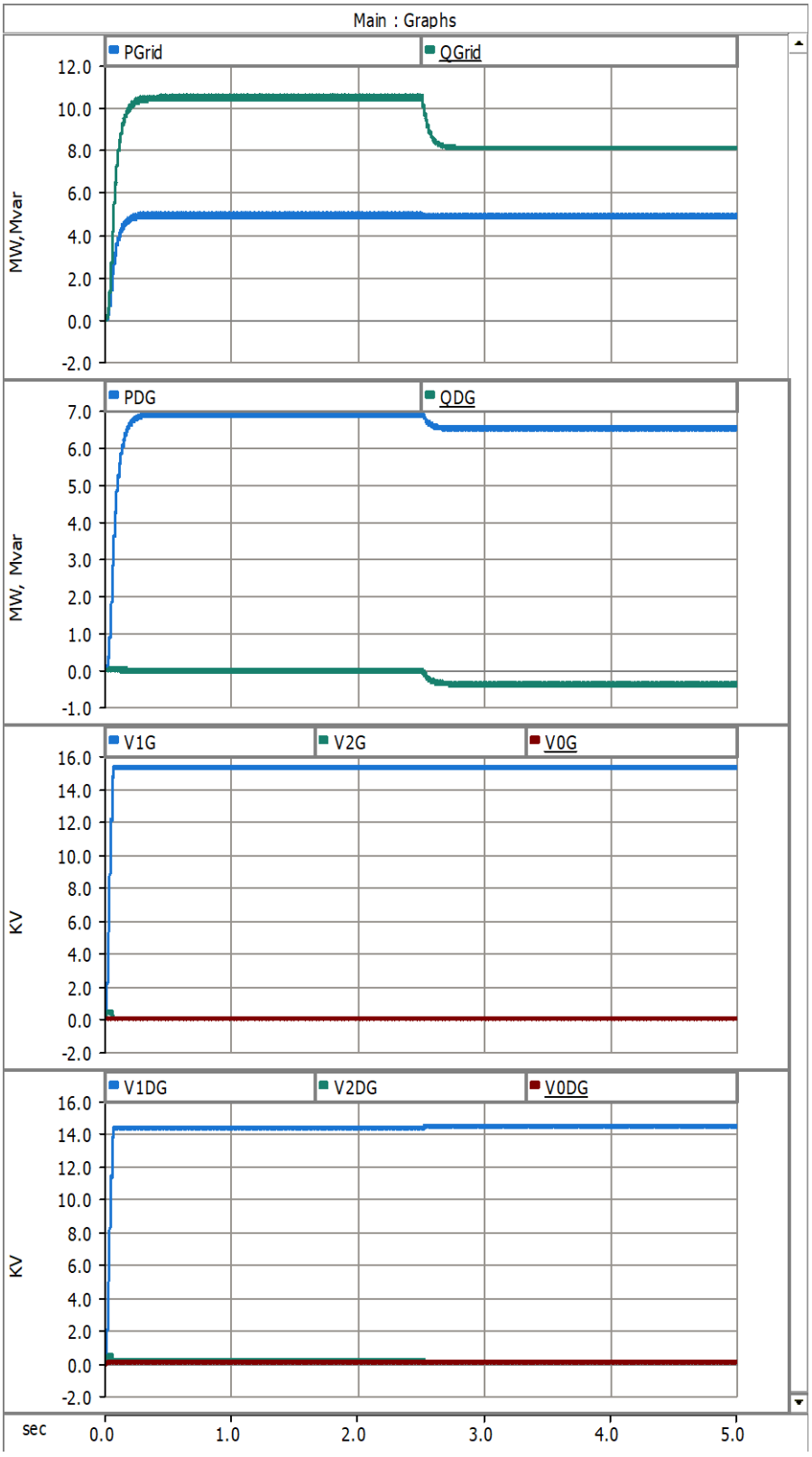

Figure E11. De-energizing Unbalance Load Power and Voltage

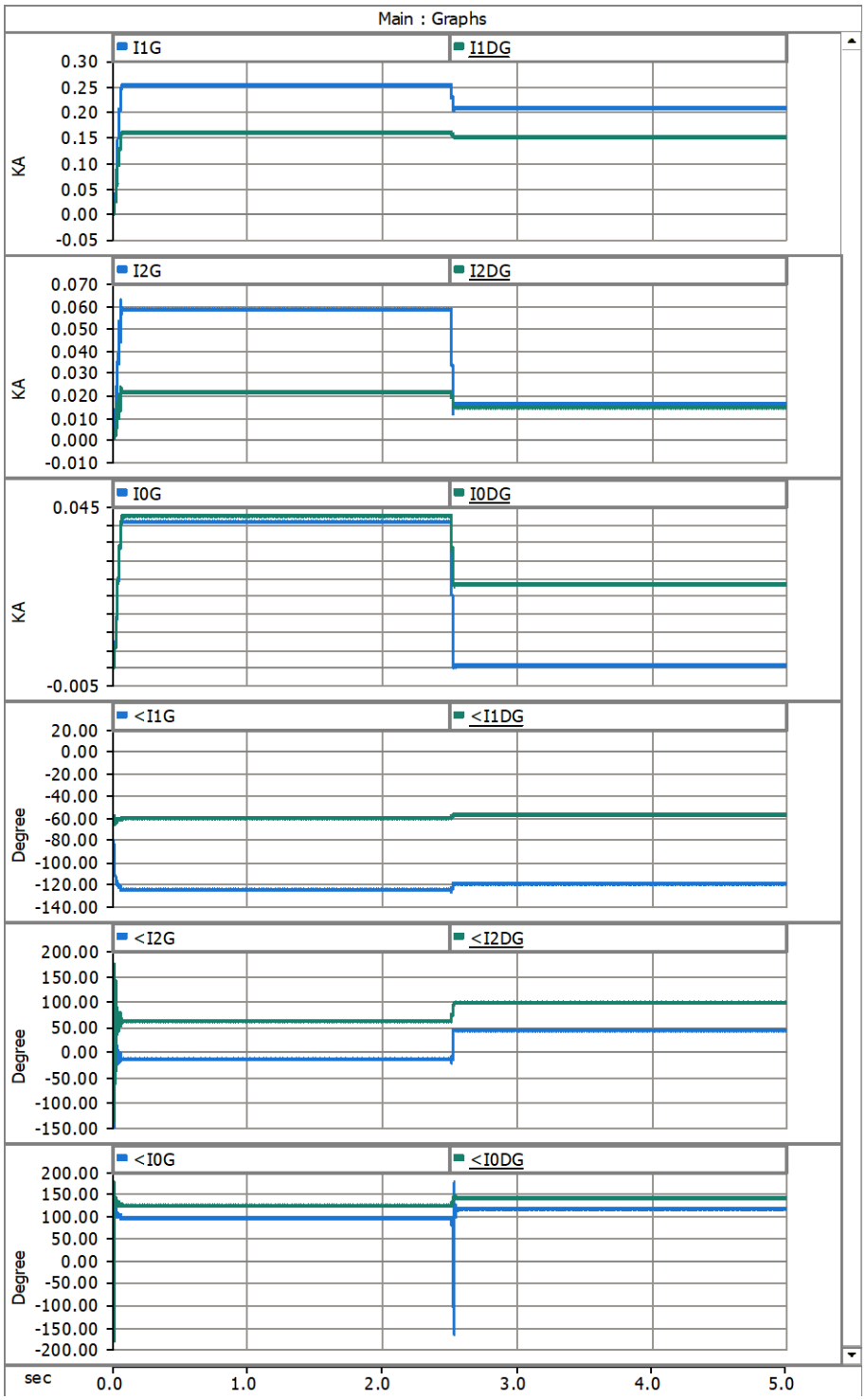

Figure E12. De-energizing Unbalance Load Current

Figure E13 and Figure E14 presents the double open phase fault at the point where both sources of DG and grid are feeding the fault on the opposite side. The first open phase occurs at t=2.5 second and the second open phase occurs at 3.5 s. Figure E15 and Figure E16, however, show the open phase fault at point 2 where the fault is on the same side of substation and DG. The current sequence component rate of the change at t=2.5 second and t=3.5 sec, respectively, and for both simulations represent the signature of the open phase, which is discussed in chapter 5, where sequence positive current decreases while negative and zero components are increasing.

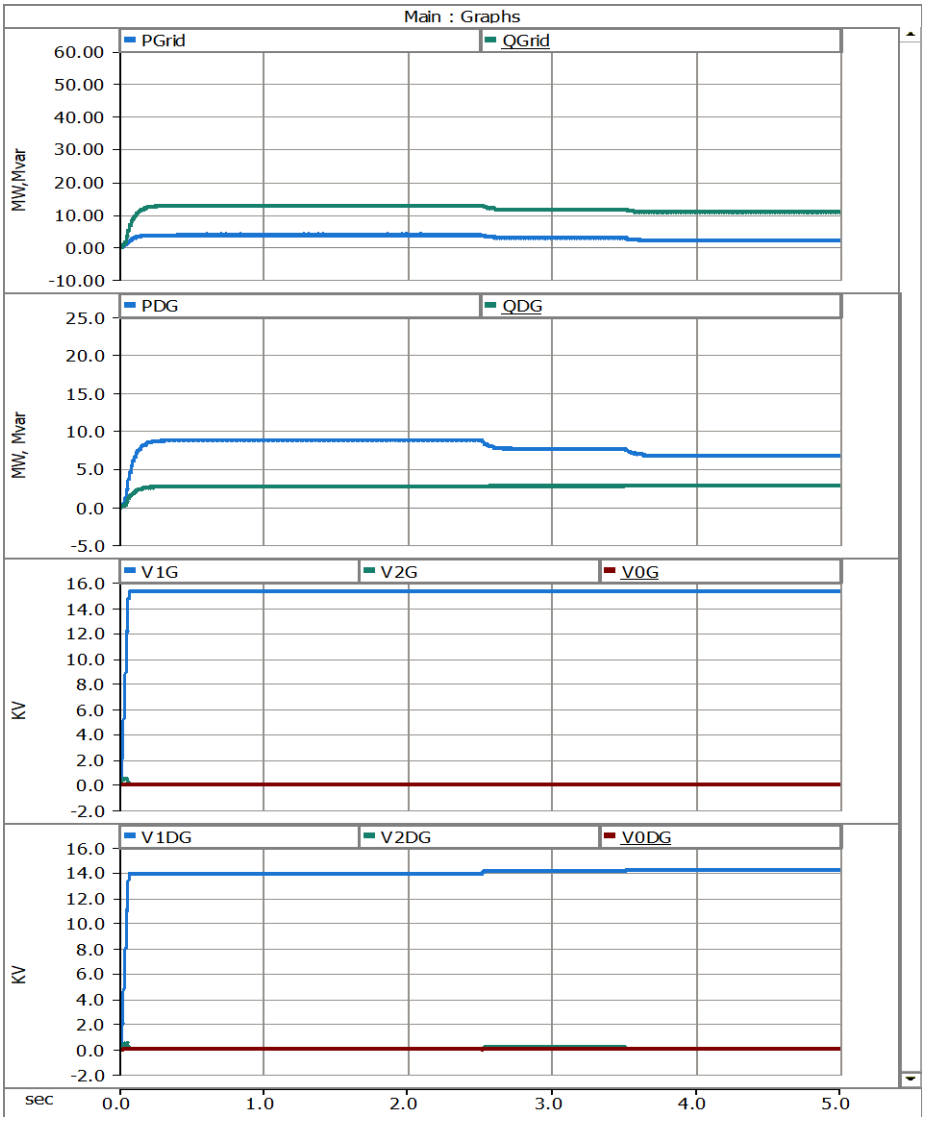

Figure E13. Two Open Phase Fault (BC) Power and Voltage (point 2)

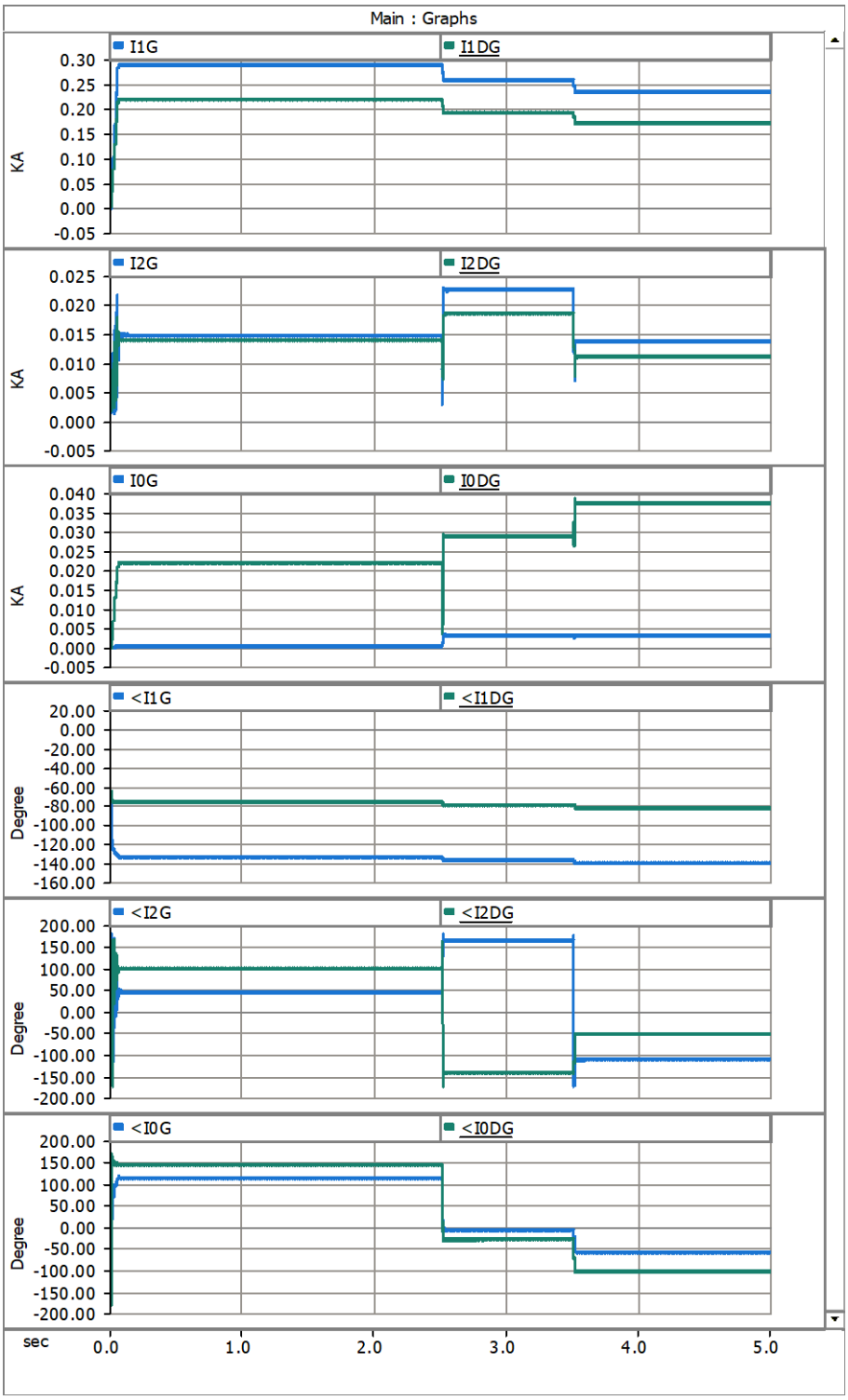

Figure E14. Two Open Phase Fault (BC) Current (point 2)

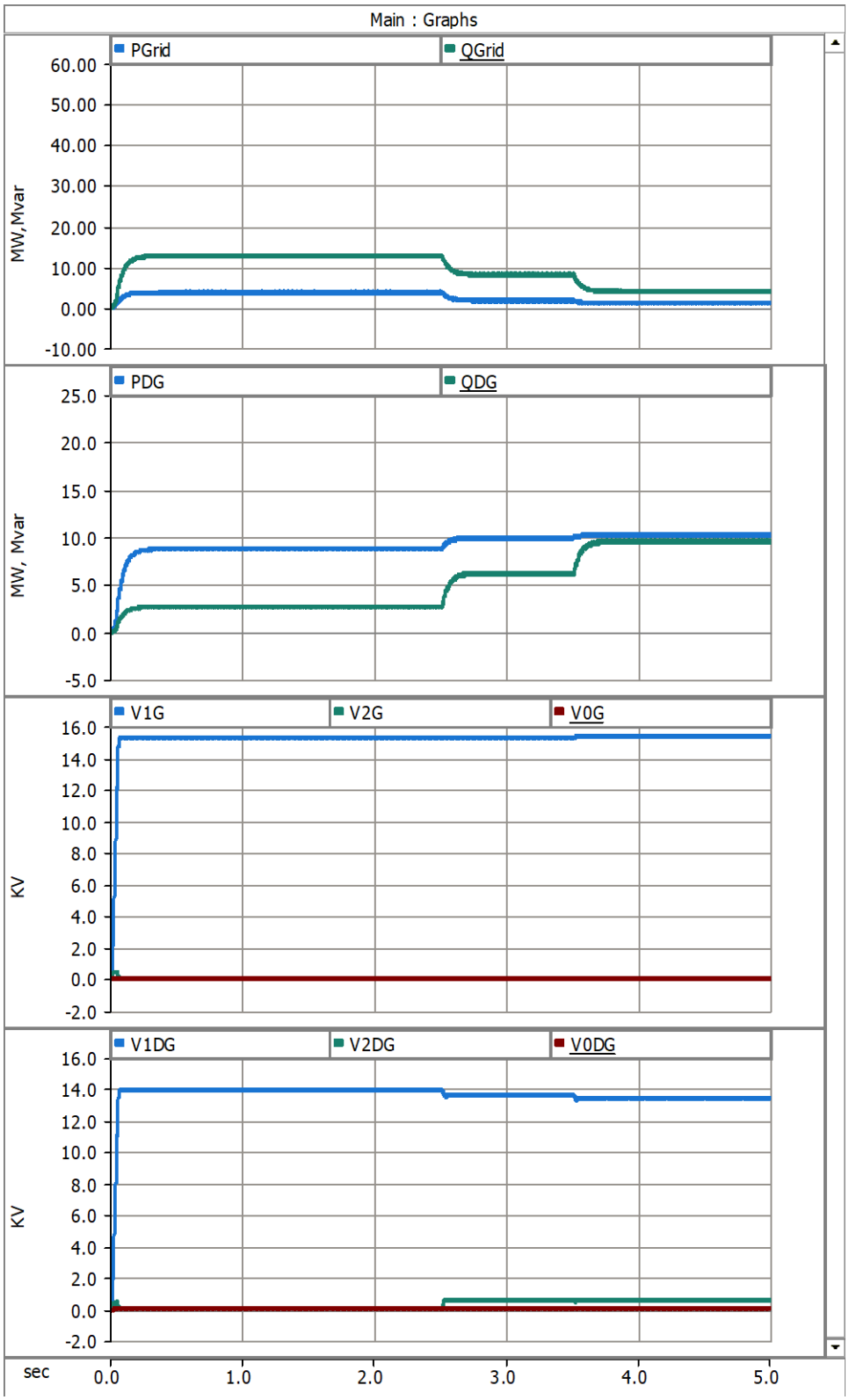

Figure E15. Two Open Phase Fault (BC) Power and Voltage (point 1)

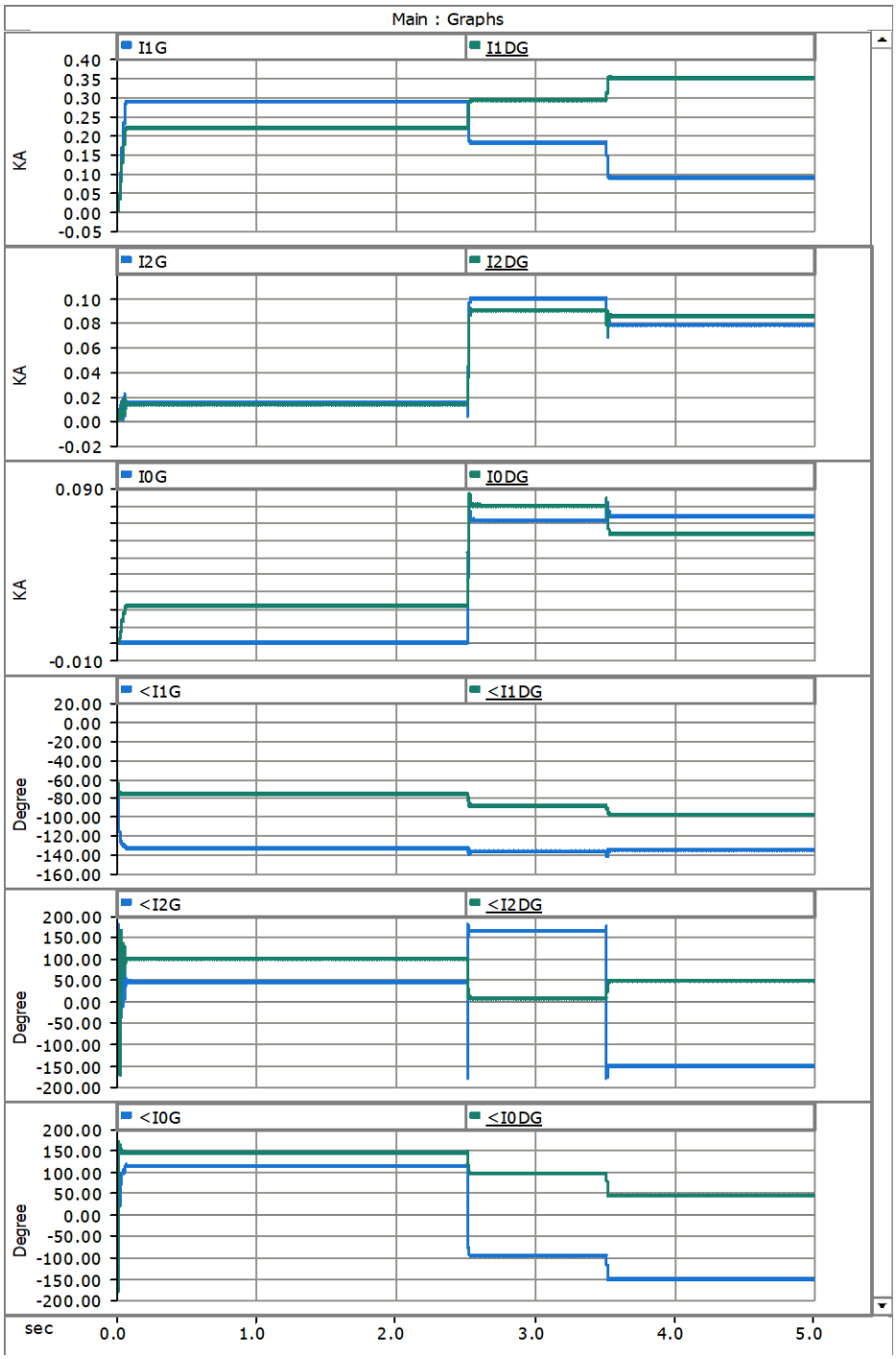

Figure E16. Two Open Phase Fault (BC) Current (point 1)

Curriculum Vitae

Name: **Mansour Jalali**

Post-secondary Education and Degrees:

Iran University of Science and Technology-IUST
Tehran, Iran
Bachelor's in Electrical Engineering - Power
Thesis Title: Designing the variable frequency drive for the induction motors
1985-1989

University of Waterloo
Waterloo, Ontario, Canada
Master of Applied Science in Electrical & Computer Engineering
Thesis Title: Contribution of DFIG type wind turbine in primary Frequency regulation
2008-2011

University of Western Ontario
London, Ontario, Canada
Ph.D. in Electrical and Computer Engineering
Thesis Title:
2012-2019

Related Work Experience

Principal Engineer Kinectrics (Ex Ontario Hydro Research)
RTDS LAB, EMT Modeling, System Study
2011-Present

ABB Inc. Substation Automation
Last position- Chief Engineer
1995-2010

Recent Publications:

M. Jalali, S. Cress, A. Zamani, Over current protection for underground Distribution system- Chapter for EPRI Bronze Book-2016

M. Jalali, NERC PRC-005 Best Practices for Compliance, CEATI International -2019

M. Jalali, Guide for IEC61850 Application, CEATI International -2019